The Role of actin-based Protrusions in 2D *vs* 3D Migration

Von der Fakultät für Lebenswissenschaften

der Technischen Universität Carolo-Wilhelmina zu Braunschweig

zur Erlangung des Grades eines

Doktors der Naturwissenschaften

(Dr. rer. nat.)

genehmigte

D i s s e r t a t i o n

von Aleks Guledani
aus Mestia / Georgien

1. Referentin: Professorin Dr. Theresia Stradal
2. Referent: Professor Dr. Reinhard Köster
eingereicht am: 31.08.2018
mündliche Prüfung (Disputation) am: 17.12.2020

Druckjahr 2021

Vorveröffentlichungen der Dissertation

Teilergebnisse aus dieser Arbeit wurden mit Genehmigung der Fakultät für Lebenswissenschaften, vertreten durch die Mentorin der Arbeit, in folgenden Beiträgen vorab veröffentlicht:

Posterbeiträge

Aleks Guledani, Kathrin Ladwein, Tanja Bosse, Manfred Rhode, Klemens Rottner & Theresia Stradal. Circular dorsal versus peripheral membrane ruffling: why Cdc42 matters. International Meeting of the German Society for Cell Biology on Actin Dynamics, Regensburg (2012).

Aleks Guledani, Kathrin Ladwein, Tanja Bosse, Manfred Rhode, Klemens Rottner & Theresia Stradal. Circular dorsal *versus* peripherial membrane ruffling: of webs and struts. International Joint Meeting of the German Society for Cell Biology (DGZ) and the German Society for Developmental Biology (GfE), Heidelberg (2013).

Vorträge

Role of Actin-based Protrusions in 2D vs 3D cell migration. (Presentation within series: Live Imaging of Cells, Tissue and Bacteria). 5th Public Retreat HZI Graduate School, Golsar Hahnenklee (2014).

Content

Summary

Both, the highly motile cancer cells and slower migrating fibroblasts utilize similar movement patterns and use comparable sets of actin-based protrusions in the course of their migration on 2D surfaces. These actin protrusions can be thin, sheet-like structures filled with a branched actin network called lamellipodia and finger-like filopodia that consists of bundled parallel actin filaments. Additionally, cancer cells often additionally can display dot-like structures, so-called invadopodia. Invadopodia are considered as protrusive, degradative and adhesive actin structures.

Cells that are embedded in a 3D extracellular matrix (ECM) are considered to be closer reflecting to the *in vivo* situation such as in a connective tissue compared to cells that are plated on 2D surfaces. In a 3D setting cancer cells and fibroblasts (MEFs) show significant differences in their migration style and mode. Depending on the cell to ECM interactions, cells in 3D can move in an adhesion- and a degradation-dependent mode called mesenchymal migration- or an adhesion- and degradation-independent mode termed amoeboid migration mode. Some cell types like cancer- or immune cells can switch between these migration-modes or use a mixed mode of migration. Some cell types can migrate on 2D surfaces, but cannot efficiently move in a 3D environment, the reason for which is currently not fully understood. Moreover, actin-based protrusions of cells in 3D are less well characterized, appear morphologically different and somewhat more complex than the protrusions of cells in 2D environments. This fact has raised debates on the existence of classical lamellipodia and filopodia in 3D environments.

This work is about the differential contributions of actin-based protrusions to the different modes of 2D and 3D migration. An additional aim was to shed more light on the conditions which facilitate cells to switch between amoeboid and mesenchymal types of cell migration. In particular, the present work analyzes the contribution of lamellipodia, circular dorsal ruffles, and filopodia to 2D-chemotaxis of fibroblasts and macrophages and the role of actin-based protrusions termed as pseudopodia in 3D migration of cancer cells.

In this work, cell migration on 2D and in 3D was studied under conditions when specific actin-based protrusions were suppressed. These conditions were achieved by using established cell lines, mouse embryonic fibroblasts or primary mouse cells isolated from mice lacking specific

genes or by application of specific inhibitors on cells. Here I address the roles of prominent actin-based protrusions in several well-defined and context-specific experimental setups as models for *in vivo* processes such as:

1) In 2D: the role of lamellipodia in chemotaxis of macrophages towards C5a and role of CRs and filopodia in chemotaxis of MEFs towards PDGF-BB.
2) In 3D: migration and protrusions of highly invasive HT1080 cells

The Hem1 deficient macrophages showed approx. 60% reduced chemotaxis compared to WT cells. Simultaneously, the Hem1 knockout cells displayed no detectable lamellipodia, suggesting these structures as a significant contributor to macrophage 2D chemotaxis towards C5a.

In MEFs, *Cdc42* knockout coincided with a reduced rate of filopodia formation, the formation of CDRs and loss of chemotaxis towards PDGF-BB. These cells also showed significantly reduced speed and partly loss of their polarity. The formin inhibitor smiFH2 had a similar effect to loss of Cdc42 on MEFs regarding the reduced numbers of filopodia accompanied with loss of CDR formation and diminished polarity. Moreover, the knockdown of fascin, which crosslinks actin filaments within filopodia, also resulted in a simultaneous decrease in filopodia numbers and CDR formation. Based on these findings the present work suggests that CDR formation is dependent on intact filopodia formation. Furthermore, these both actin structures are critically involved in chemotaxis of MEFs towards PDGF-BB.

This work shows that filopodia and lamellipodia are formed at the leading edge during the migration of HT1080 cells in a 3D collagen matrix. However, the presence of filopodia in HT1080 cells increases in 3D environments as compared to 2D environments, suggesting an important role for filopodia in 3D migration. Based on matrix degradation assays and treatments of cells with GM6001, which interferes with matrix degradation, newly formed filopodia in HT1080 cells turned out not to be degradative structures. The inhibition of filopodia formation in 3D using the smiFH2 formin inhibitor leads to severe reduction of cell velocity in 3D-random migration and to loss of 3D chemotaxis. Furthermore, smiFH2 treated cells show increased blebbing, which indicates a shift from a mesenchymal to an amoeboid migration mode during migration in 3D collagen. The knockdown of fascin in HT1080 cells led to the disorganized formation of filopodia, a reduced directness and velocity of HT1080 cells in 3D collagen supporting the results of smiFH2

treatment. These findings are supportive for a role of filopodia in contributing to cell velocity and chemotaxis of HT1080 cells in 3D collagen.

List of figures

1 Introduction

1.1 Cytoskeleton

Many motile eukaryotic cells are able to adopt a variety of shapes or to move through different tissue barriers. This morphological plasticity greatly depends on the cell's cytoskeleton. Unlike a rigid, skeleton, for example in mammals, the cellular cytoskeleton is highly dynamic and is continuously reorganized during cell division, movement, and other vital processes which require shape changes such as macropinocytosis or phagocytosis. Besides providing mechanical support to a cell, the cytoskeleton is involved in the intracellular movement of its organelles or vesicles loaded with different types of cargos. The cytoskeleton of a mammalian cell is composed of three types of protein filaments: actin filaments, microtubules and intermediate filaments.

The basic structure of each filament-type is made of a specific protein. Actin filaments are composed of actin molecules, microtubules are made of tubulin and intermediate filaments are composed of approx. 70 cell type specific fibrous proteins. Typical examples of these are vimentin and lamin (Eriksson et al. 2009). Filaments that compose the cytoskeleton are generally made upon polymerization of many identical proteins into helical polymers. These filaments are supported by accessory proteins which can link them to each other or to other cell components, provide motors for filament movement, or regulate the filament assembly at certain times and locations within the cell. Furthermore, adaptor proteins enable filaments to selectively interact with each other and with the plasma membrane.

Microtubule filaments are on one end embedded and stabilized in a structure termed as a centrosome. On the other end (the plus end) filaments can grow or shrink in size by polymerizing or depolymerizing dynamically. The monomers of microtubule are α- and β-Tubulin heterodimers. Thirteen of these filaments are bundled in one microtubule (Wade and Hyman 1997). Organelles, proteins and vesicles are transported, dependent on hydrolysis of adenosine triphosphate (ATP), along microtubules via motor proteins. Microtubules are major components of the spindle apparatus, which is formed during cell division and mediates the positioning and separation of the

chromosomes during mitosis. Microtubules are critically involved in correct positioning of cell organelles like endoplasmic reticulum (ER) and Golgi apparatus. These are supposed to align with the microtubule network (Vale 2003; Gelfand and Bershadsky 1991; Sandoval et al. 1984). Based on their supportive role in many vital processes the microtubules are rather indirectly involved in cell migration.

Intermediate filaments are 8-10nm thick, stable protein fibers mostly organized in a network around the nucleus and extending to the cell periphery. Attached to the inner membrane of nuclear envelope intermediate filaments form nuclear lamina. Intermediate filaments are formed by elongated fibrous proteins which align and form coiled-coil dimers and further tetramer subunits, which can bind to each other to form filaments. Intermediate filaments can be formed by seven subgroups of proteins that are grouped in subclasses such as desmins, vimentins or lamins. The major role of intermediate filaments is to provide mechanical stability of a cell and embedded organelles (Alberts et al. 2002a; Schoumacher et al. 2010; Eriksson et al. 2009).

The actin cytoskeleton is composed network of actin filaments. Actin filaments can be bundled and / or assembled into several different higher order actin structures such as stress fibers, lamellipodia, filopodia, dorsal ruffles, podosomes and invadopodia. The actin cytoskeleton plays a key role in cell motility, shape changes, exo-and endocytosis and cell to substrate adhesion (Chhabra and Higgs 2007b; Blain 2009).

1.1.1 Actin polymerization

Actin isoforms show high sequence similarities and comparable dynamics in actin polymerization assays. Based on their different isoelectric points mammalian actins were grouped in six types. Actin isoforms are tissue specific. Muscle cells harbor α-actin isoform whereas β- and γ-actins are found in non-muscular cells (Alberts et al. 2002a). Cytoplasmic free actins are bound to ATP which is tightly associated with actin monomers. ATP-bound actin monomer has a globular shape and is therefore termed G-actin. The actin polymerization reaction does not occur spontaneously and needs factors to overcome the kinetic barrier (Thomas D Pollard and Cooper 2009; Rouiller et al. 2008).

The polymerization of G-actin is dependent on mono- and divalent cations, which are in most cases K^+ and Mg^{2+} ions, and on ATP. This reaction has to overcome, the energetically unfavorable assembly of a trimer of actin molecules. After overcoming this barrier the core structure (trimer) can rapidly polymerize by addition of G-actin molecules to the trimer one after another. The orientation of actin subunits within a trimer and the resulting polymer allows the actin filament to grow faster on one end than on the other end of the filament. The slow-growing end was termed as a "pointed" or the minus end due to the orientation of myosin heads on the filament as it was imaged via electron microscopy. Subsequently the faster-growing end was termed as "barbed" or the plus end of the polymer. The concentration of non-polymerized actin in a cell is much higher than the concentration of free actin monomers at which actin polymerization would stop. Or in other words, the critical concentration of free actin at which polymerization stops is much lower than the concentration of polymerized actin in a cell. To favor the polymerization reaction this process is tightly controlled. The formation of a nucleating core and further actin polymerization is a thermodynamically unfavorable reaction, therefore cells use modulatory proteins to increase the reaction rates leading to temporally and spatially regulated polymerization. (T. Pollard 1986; Thomas D. Pollard and Weeds 1984; T D Pollard and Cooper 1984).

Actin polymerization goes together with the hydrolysis of ATP whereas adenosine diphosphate (ADP) stays incorporated into the polymer. The interaction of the terminal actin subunit of an actin filament with G-actin leads to a conformational change of the latter which triggers the hydrolysis of its bound ATP. This leads to increased interactions of new terminal F-actin to the next G-actin molecule which favors the further polymerization of the filament. The addition of G-actin monomers to the plus end is several times the rate of monomer addition at the minus end. This is due to conformational changes of G-actin during its polymerization to F-actin and hydrolysis of ATP that is bound to G-actin. As a consequence of this the affinity of actin monomers at the minus end is much lower than at the plus end. The filament growth, where subunits are added at the plus- and lost at the minus end is also termed as treadmilling. In this case filaments retain their net length, but move towards the direction of the barbed end (or forward) during the process. One of the proposed roles of ADP in F-actin filaments is to loosen interactions of actin subunits within a filament. This enables easy depolymerization of F-actin when this is required.

.

1.1.2 Regulation of actin polymerization

The fact that the critical concentration of free actin in a eukaryotic cell is low (1≤μM), whereas approx. 50% of actin is in a monomeric- and 50% is in a polymeric state, indicates that other mechanisms (and proteins) are involved in regulation of actin polymerization. In fact, the regulation of actin polymerization is accomplished by actin-binding proteins which can engage during actin polymerization at distinct stages (or states). Actin-binding proteins can influence the F-actin polymerization and depolymerization rates, they can associate with G-actin or cap the filament ends to interfere polymerization or promote actin nucleation (Stovold, Millard, and Machesky 2005).

1.1.2.1 Receptor tyrosine kinases (RTKs)

RTK are activated due to binding of growth factors to their extracellular receptor domains. This leads to dimerization of these receptors and induces autophosphorylation of tyrosine residues on the cytoplasmic side of the receptors. This event creates among others the binding sites for PI3 kinase, which consists of catalytic (p110) and regulatory (p85/p55) subunits (Vanhaesebroeck and Waterfield 1999; Carpenter and Cantley 1996). The p85 subunit interacts via its SH2 domain with the phosphorylated tyrosine residues of RTKs and the p100 subunit phosphorylates its substrates. PI3 kinase catalyzes the generation of PIP_3 at the inner leaflet of the cell membrane, which in concert with other second messengers, is involved in recruitment and activation of GTPases at the cell membrane (Insall and Weiner 2001). In this manner the platelet-derived growth factor PDGF activates its specific platelet-derived growth factor receptor (PDGFR) at the membrane leading to recruitment of small GTPases of the Rho family. These GTPases can recruit and activate the actin polymerization machinery at the membrane thus initiating formation of actin-based protrusions (Figure 1).

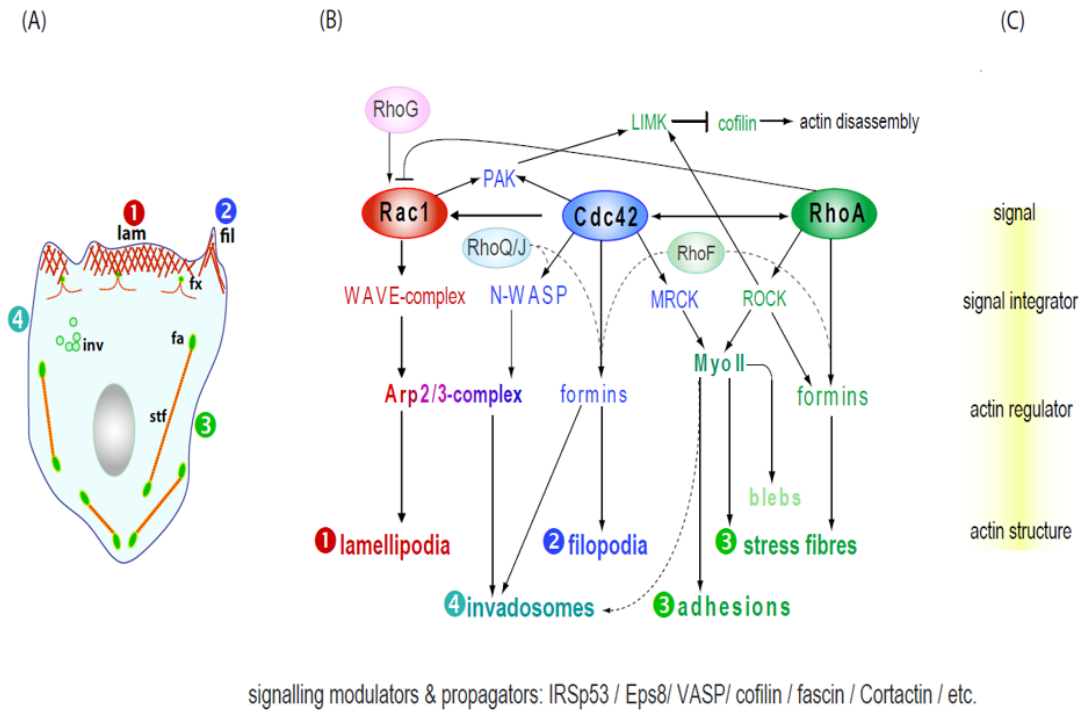

Figure 1: Regulation of 2D cell migration and related actin structures. (Modified From Rottner and Stradal 2011c). (A) During migration on 2D cells form actin-based protrusions such as lamellipodia (1) and filopodia (2) to project their body in a specific direction. Stress fibers (3) are anchored in focal adhesions (fa) and are used for cell retraction. Invadopodia and invadosomes possess both degradative and adhesive properties. (B) Formation of each actin-based structure is regulated by Rho GTPases most prominently by Rac1, Cdc42 and Rho A. Activation of Rac1 leads to the formation of lamellipodia via activation of WAVE and Arp2/3 –complexes subsequently. Cdc42 activates formins which leads to the formation of filopodia. Rho A regulates dynamics of stress fibers and focal adhesions involving formins, ROCK and myosin II downstream of this GTPase. (C) Steps of signal propagation that lead to the formation of actin structures. The incoming signal activates Rho GTPase (signal) that can activate signal integrator proteins such as WAVE-complex, which in turn activates actin regulator proteins (Arp2/3 complex) which activity can generate final actin structures such as lamellipodia.

As presented in Figure 1, in mammalian cells, activation of small GTPases such as Rac, Cdc42 and Rho at the cell membrane leads to actin reorganization and subsequent formation of actin-based protrusions at the cell edges. In fibroblasts, activation of PDGFR by a gradient of PDGF-BB and subsequent signaling to GTPases induces chemotaxis towards this growth factor (Kundra et al. 1994a).

1.1.2.2 PI3 kinase and phospholipids

Class I PI3 kinases are activated downstream of RTKs and mediate the transduction of extracellular growth factor signals leading to cellular actin reorganization and cell survival. At the cell membrane, PI3 kinase, consisting of P85 and p110 subunits is recruited to the tyrosine phosphorylated site of activated RTKs. After association with RTK, PI3 kinase phosphorylates its substrates. The subsequent recruitment of Ras GTPase to p110 subunit of PI3 kinase leads to full catalytic activation of PI3 kinase (Cantrell 2001). The activity PI3 kinase leads to enrichment of PIP_3 and related phosphoinositides at the membrane. In this manner several sites for recruitment and activation of regulatory proteins of actin polymerization such as Rho GTPases are created. To facilitate the recruitment of GTPases the enrichment of guanine nucleotide-exchange factors (GEFs) at the membrane has to take place. GEFs act as specific activators of Rho GTPases promoting the exchange of guanosine diphosphate (GDP) to guanosine triphosphate (GTP) which activates the GTPase. PI3 kinase activity and PIP_3 can recruit Rac specific GEFs such as Vav, Tiam1, Swap70 and SOS-1 at the membrane (J. Han et al. 1998a; Nimnual, Yatsula, and Bar-Sagi 1998; Shinohara et al. 2002; Soisson et al. 1998). The PI3 kinase is important for the generation of a intracellular gradient of signaling molecules such as PIP_2 and PIP_3, but appears not to be the only pathway that leads to the formation of intracellular gradients of molecules and proteins leading to chemotaxis as shown in soil amoeba *Dictyostelium discoideum* cells (Merlot and Firtel 2003).

1.1.2.3 Rho-GTPases

Rho-GTPases are a subgroup of the Ras-superfamily of GTPases and represent a subfamily of proteins relatively small in size (approx. 20 kDa) that share over 50% sequence identity. Most of Rho-GTPases are expressed ubiquitous and are represented by 22 members in mammals. The distinguishing property of these GTPases from other small GTPases is an alpha-helical domain of approx. 13 amino acids termed Rho-insert domain. The insert domain appears to be important for negative regulation of Rho GTPases (D. I. Johnson 1999). Rho-GTPases are activated downstream of membrane receptors such as RTKs and act as molecular switches which control signal transduction to pathways that regulate cell migration. Rho-GTPases cycle between inactive GDP-

bound and active GTP-bound conformations (Figure 2). The GTP-bound (active) Rho-GTPase can elicit a variety of cellular responses by interacting with their downstream targets. One of such responses can be a rearrangement of actin cytoskeleton, protrusion formation and cell migration. Studies of fibroblasts utilizing constitutively active or dominant negative forms of Rho GTPases indicated that Rho was involved in regulation of actin stress fibers, while Rac and Cdc42 were regulating the formation of actin-based protrusions at the cell periphery (C D Nobes and Hall 1995; Hall 1992).

To perform their tasks as regulators in the formation of actin-based protrusions Rho GTPases have to be activated and localized at cellular membranes. To associate to membranes Rho-GTPases typically bear a specific CAAX motif at their C-terminus. CAAX stands for Cysteine, A is for an aliphatic and X stands for any other amino acid. The CAAX motif can be prenylated, which can enhance the localization of Rho-GTPases at the plasma membrane or other lipid bi-layers (Hrycyna and Clarke 1993; Michaelson et al. 2001; Wennerberg and Der 2004a). The Iso-prenylation of the CAAX motif is important, but not sufficient for membrane association of Rho-GTPases. C-terminal palmitate modification immediately upstream of the CAAX motif is re-quired for proper membrane localization of these proteins (Raftopoulou and Hall 2004c; G. a Murphy et al. 2001; Michaelson et al. 2001). In the absence of specific extracellular signals Rho GTPases can reside in an inactive state in the cytoplasm, stabilized by specific proteins termed GDIs (Guanine nucleotide dissociation factors). In this inactive state the lipid moiety of GTPase is masked by the GDI and cannot interact with the cell membrane.

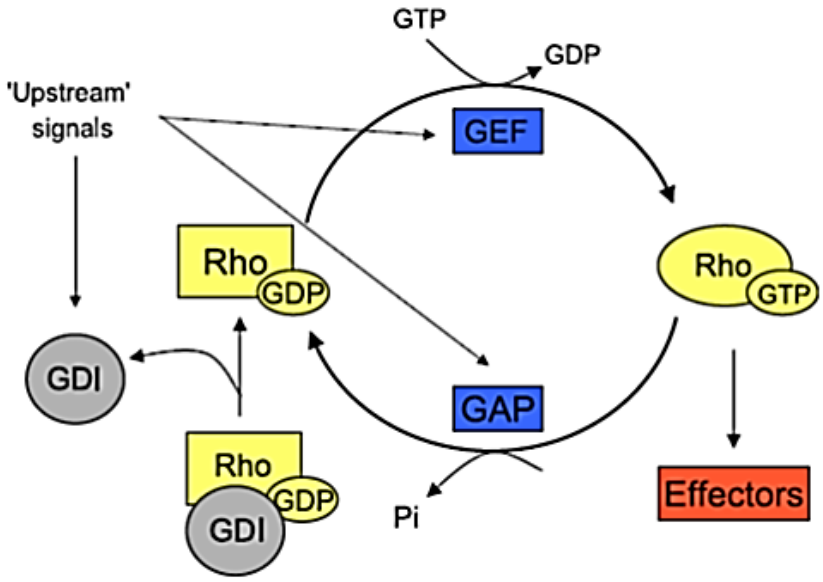

Figure 2: Activation and inactivation cycle of Rho GTPases (Modified from Raftopoulou & Hall, 2004). GTPases act as molecular switches cycling between their active (GTP-bound) and inactive (GDP-bound) states. This cycle is regulated by proteins that modulate binding of either GTP or a GTP to a GTPase. Interaction of GTPase with GEFs promotes the exchange of GDP to GTP thus activating the GTPase. GTPase activating proteins (GAPs) enhance the GTPase activity which leads to shifting from GTP-bound to GDP-bound inactive GTPase. Guanine nucleotide exchange factors (GDIs) block the exchange of GDP to GTP thus maintaining the inactive state of GTPase.

To date, Rho-family GTPases are grouped in six subfamilies based on their amino acid sequence, structural- and functional similarities. These subfamilies are 1. Rho (with RhoA, RhoB, and RhoC); 2. Rac (with splice variants of Rac: Rac1, Rac1b; Rac2 and Rac3) and RhoG; 3. Cdc42 subfamily with Cdc42; G22K-brain expressed version of Cdc42, TC10, TCL, Chp/Wrch-2 and Wrch-1; 4. Rnd subfamily; 5 RhoBTB subfamily and 6. Miro subfamily. In addition atypical Rho GTPases RhoD, Rif and TTF/RhoH were discovered that are structurally different and possess additional domains compared to other Rho family members (Aspenstrom, Fransson, and Saras 2004; Wennerberg and Der 2004b).

The Rho A, B and C GTPases are highly identical (approx. 85% sequence identity) and interact supposedly with the same GEFs and effectors, but due to their C-terminal divergence are supposed to localize at distinct subcellular locations. All of the Rho GTPases are thought to stimulate actin-myosin contractility required in different cellular processes such as endomembrane vesicle transport or cell proliferation (Wennerberg and Der 2004b). Whereas only RhoA is involved primarily in retraction during cell migration. Classical 2D models of cell migration support the idea that Rho was involved in cell retraction at the rear of the migrating cell. Although, FRET-based

analysis showed RhoA involvement in the protrusive process also at the leading edge of the cell (Pertz et al. 2006).

Rac related proteins share sequence identity of approx. 88 percent. Rac subfamily members diverge in their 15 C-terminal residues at highest, similar to the divergence observed within Rho subfamily. The exception in this case is RhoG, which shows higher divergence to all other three Rac isoforms. Rac1 is ubiquitously expressed. Rac2 is expressed only in the hematopoietic lineage (Didsbury et al. 1989) and is thought to be involved in regulation of production of reactive oxygen species (ROS) in these cells (Werner 2004). Rac3 is specifically expressed in the nervous system and apparently regulates actin dynamics during axonal branching (Spillane and Gallo 2014).

Rac is activated downstream of growth factor stimulation in cells and is recruited at the cell membrane where this GTPase activates actin machinery proteins to induce actin polymerization (Hall 1998; Kundra et al. 1994b). During this process actin-based protrusions are formed to mediate cell migration towards chemoattractant. Rac1 regulates mainly the formation of lamellipodia and dorsal ruffles, but is also involved in regulation of other types of actin protrusions which are used in different kinds of cell migration (Rottner and Stradal 2011a; Steffen et al. 2004a; Sandrine Etienne-Manneville 2006; Sixt 2012).

Two isoforms of Cdc42 are present in mouse and in humans due to alternative exon splicing of the same gene. Both proteins are composed of 191 amino acids and prominently differ at residue 163 and their C-terminal residues from each other. The most studied form Cdc42p (also termed Cdc42Hs or Cdc42a) is ubiquitously expressed, whereas the second isoform is restricted to the brain (Cdc42b or G25K or brain Cdc43p).

Cdc42 and further members of this subfamily are supposed to regulate the formation of filopodia. Overexpression of Cdc42 prominently induces the formation filopodia. It was also suggested that overexpression of subfamily member Tc10 could induce filopodia, although putative Tc10 induced filopodia were longer in size (G. a Murphy et al. 2001; Neudauer et al. 1998; Kawamura et al. 2004). Furthermore, GTPases Wrch-1, RhoD and Rif could induce the formation of filopodia when activated (Aspenstrom, Fransson, and Saras 2004). Additionally, the interaction of Rif with formin mDia2 was responsible for induction of filopodia (Pellegrin and Mellor 2005). Therefore,

genetic removal of Cdc42 does not lead to loss of filopodia in fibroblasts (Mains, Sulston, and Wood 1990; Faix and Rottner 2006a).

1.1.2.3.1 Regulation of Rho GTPases

The difference between the affinities of Rho GTPase to effector molecules can be 100-fold, dependent on GTP or GDP-bound states. To achieve this distinction, the active and inactive state of Rho GTPase is tightly regulated by several protein families. GEFs promote the exchange of GDP to GTP and activate the GTPase. GTPase activating factors (GAPs) negatively regulate the GTPase by enhancing its intrinsic GTPase activity and shifting the equilibrium to the inactive, GDP-bound state of the GTPase. The nucleotide exchange can be also inhibited by sequestering the GDP-bound form of the GTPase. This is accomplished by GDP dissociation inhibitors (GDIs) (Schmidt and Hall 2002). Both, GEFs and GAPs utilize the same binding interfaces of Rho-GTPases (switch I/switch II region).

To date two families of GEFs are identified. These are Dbl- and Dock family of GEFs. Dbl family GEFs are characterized by the presence of GTPase activating Dbl region in their sequence. Dock family of GEFs has eleven members that share two conserved domains which are dock homology region (DHR)-1 and-2 The DHR-1 enables Dock proteins to associate with membranes whereas the DHR-2 region possesses GEF activity. Because of their later discovery compared to Dbl GEFs and the differences in activating domains of GTPase, Dock GEFs were termed atypical GEFs or unconventional GEFs (Laurin and Côté 2014). Furthermore, Dock family GEFs apparently activate exclusively Cdc42 or Rac, but no other Rho GTPases (Côté and Vuori 2002; J.-F. Cote 2006).

GEFs can bind to phosphatidylinositides with their PH-domain. This enables their enrichment at the membrane in response to the local increase of products of PI3 kinase activity. The interaction between PIP_3 and GEFs is thought to unmask the catalytic domains of a GEF. The catalytic subunit can induce the exchange of GDP to GTP and thus activate the GTPase. In a next step Rac-GTP can interact with WAVE-complex (via Abi1) and mediate its recruitment and activation at the membrane (Miki, Suetsugu, and Takenawa 1998; Steffen et al. 2004a). The interaction of GEFs with the switch region of a GTPase induces structural changes of the GTPase that lead to

displacement of Mg^{2+} and release of GDP in exchange for GTP. Binding of a GAP on the other hand, leads to insertion of a water molecule into the catalytic pocket of GTPase which enhances the hydrolysis reaction of GTP to GDP up to approx. 400 fold over the intrinsic GTPase activity (Donnelly, Bravo-Cordero, and Hodgson 2014). *Dbl* was identified as the transforming gene from diffuse large B-cell-lymphoma cells which showed homology to regions of Cdc24, a specific GEFs of Cdc42 in *Saccharomyces cerevisiae (S. cerevisiae)* (Eva et al. 1988). This homologous region is composed of a 200 residues long region (termed Dbl homology region) and its adjacent 100 residues long PH domain (pleckstrin homology region). Later it was shown that Dbl was a specific GEF for human Cdc42 (Hart et al. 1991). The PH domain was first described in the hematopoietic protein Pleckstrin and named thereafter. Generally, PH domains contain approx. 100-200 amino acids and are present in many proteins involved in cellular signaling and cytoskeletal reorganization (Ingley and Hemmings 1994). The major feature of these domains is the ability to associate with membranes via their binding capacity to phosphoinositides. PH domains are divided into either high- or low-affinity class towards 3'-phosphorylated phosphoinositides. High-affinity PH domains show strong specificity towards 3'-phosphorylated phosphoinositides and simple alteration of membrane composition (such as an increase in PIP_3 concentration) is considered sufficient to drive membrane localization of associated proteins (Metello Innocenti et al. 2003).

GDIs bind to Rho proteins and thereby block the nucleotide exchange and thus binding of effectors and GAPs to GDP-bound Rho-GTPase (Olofsson 1999). Binding to GDI blocks accessibility to lipid moiety of Rho GTPases which is needed for recruitment of GTPase to the cell membrane. Therefore this interaction maintains the Rho-GTPase in an inactive / (soluble) conformation in the cytosol. Of note, GEFs and GAPs outnumber GTPases by more than 3 to 1, whereas only three Rho GDIs are known that show different Rho binding specificities (Adra et al. 1997; Zalcman et al. 1996; G. a Murphy et al. 2001; Behnia and Munro 2005).

When released from the GDIs Rho-GTPases associate with membranes by insertion of their isoprenylated C-terminal domain into the membrane bilayer and are activated by membrane-associated GEFs. GTP hydrolysis of Rho-GTPases leads to re-association of GDIs with the GTPases and therefore to their recycling to the cytosol. This cycling between membrane and cytosol mediated by GDIs is a further step in Rho-GTPase regulation. The affinity of GDIs and

Rho-GTPases towards each other is thought to be regulated by phosphorylation (Cherfils and Zeghouf 2013). For instance protein kinase A (PKA) mediated phosphorylation of GDI negatively regulates RhoA (Qiao et al. 2008). Src binds and phosphorylates Rho GDI at Tyr156 which leads to negative regulation of Rho (Spiering and Hodgson 2011; DerMardirossian and Bokoch 2005).

1.1.2.4 WASP and WAVE family proteins

Wiskott-Aldrich syndrome protein (WASP) is produced exclusively in the hematopoietic system and was identified as a gene product linked to the autoimmune disease termed Wiskott-Aldrich syndrome (WAS) (Zhu et al. 1997; Kajiwara et al. 1999; Ochs and Notarangelo 2005). It has been shown that the *WAS* gene in dendritic cells and macrophages of affected patients carries several mutations. This apparently causes severe functional deficiencies in affected cells that perform immune tasks. Based on these immune defects, WAS patients develop severe immunodeficiency, eczema and thrombocytopenia also referred to as a clinical triad (Zhu et al. 1997). The mutation of the *WAS*-gene is associated with defective chemotaxis of macrophages and impaired motility of dendritic cells (Binks et al. 1998; Zicha et al. 1998). Furthermore, scanning electron microscopy of lymphocytes from WAS patients revealed that the number of actin-based microvilli on the surface of these cells was reduced (microvilli of lymphocytes from WAS patients were also short and blunt) (Kenney et al. 1986). Further research led to the discovery of a ubiquitous version of WASP, N-WASP (Neural WASP) and finally, a functional role of WASP could be identified as a downstream effector of Cdc42 and an activator of the Arp2/3 complex. WASP mediated activation of the Arp2/3 complex was reported to lead to actin reorganization (Miki, Miura, and Takenawa 1996; Laura M. Machesky and Insall 1998; Rohatgi et al. 1999a). The biochemical characterization of WASP protein revealed a direct interactions with Cdc42- and in less extent with Rac (Kirchhausen and Rosen 1996).

Furthermore, it was found that WASP and N-WASP possess common regions termed VCA (V: C-terminal verprolin-homology domain or WH2 (WASP homology domain 2); C: cofilin homology domain; A: acidic domain). Based on sequence homology to the VCA region of WASP,

other proteins of this family were identified such as mammalian brain-enriched WAVE1 (WASP-family verprolin-homologous protein-1) and Scar (Suppressor of the car)-a homolog of WAVE in *Dictyostelium*. Thereafter ubiquitously expressed mammalian WAVE2 and brain-enriched WAVE3 were discovered (Miki, Suetsugu, and Takenawa 1998). *Scar* was identified as a causative gene for the restoration of tip formation in *Dictyostelium* cells depleted of *carB* gene. The *carB* gene product is a CAR2 receptor which is a seven transmembrane G-protein coupled receptor for cAMP. The cAMP molecule acts as a chemoattractant and the morphogenic signal for *Dictyostelium* cells inducing rearrangements of the actin cytoskeleton, chemotaxis and tip-formation. The protein encoded by the *Scar*-gene showed similarities with WASP, but was grouped to WAVE proteins, because of much higher sequence similarity in humans and *Caenorhabditis elegans (C. elegans)* WAVE, rather than being considered as a homolog of WASP (S Linder et al. 1999b).

WASP and WAVE proteins have a modular structure. Characteristic of both proteins is a very similar poly-proline domain followed by a C-terminal VCA domain (Figure 3). WASP and WAVE proteins prominently differ in the presence of GBD (GTPase binding domain) and the N-terminal WH1 (WASP homology 1) domains that are both present in WASP and N-WASP. WAVE1-3 lack a GBD domains and, in contrast to the WH1 of WASP/N-WASP, harbor an N-terminal WH (WAVE homology)-domain. VCA-domains of WASP and WAVE can bind to Arp2/3 complex and actin monomer which activates Arp2/3 complex and creates an actin nucleation core (Yamazaki, Kurisu, and Takenawa 2009a). Because of the common ability of WASP/WAVE proteins to activate Arp2/3 complex these proteins were termed nucleation promoting factors (NPFs). The activated Arp2/3 complex is able to bind to a side of a pre-existing actin filament and initiate actin polymerization at those sites. This generates side branches of actin polymers (R. Dyche Mullins, Stafford, and Pollard 1997; L M Machesky et al. 1999; Takenawa and Miki 2001; Thomas D. Pollard and Borisy 2003).

Different domains of WASP and WAVE proteins enable direct interactions with a set of regulatory proteins which define the place and timing of activation of these NPFs. WASP and WAVE proteins are found *in vivo* as protein complexes being intrinsically inactive due to their conformation (Figure 4). They can be activated by direct or indirect interactions with Rho GTPases leading to conformational changes and thereby unmasking the VCA region of WASP/WAVE

proteins which activates these. The N-terminal WH1 domain of WASP interacts with adaptor protein WIP (WASP-interacting protein) in a 1:1 molar ration. This interaction stabilizes the inactive conformation of WASP (Elkhal et al. 2007). On the other hand this interaction is thought to protect WASP from degradation. (Yamazaki, Kurisu, and Takenawa 2009a). The WH1-domain is followed by a short "basic" region and a GBD, also known as a Cdc42/Rac-interactive binding domain (CRIB) domain. In an inactive state (WASP-WIP complex) intermolecular interactions between the CRIB and the VCA-region of WASP occur. In this way, the VCA region is masked and cannot interact with the Arp2/3 complex and actin (Yamazaki, Kurisu, and Takenawa 2009a). The basic region of WASP is thought to bind to PIP_2 (Rohatgi et al. 1999b). PIP_2 binding, together with association of GTP-bound active Cdc42 to CRIB domain, promotes the activation of WASP. These both interactions mediate unfolding of WASP, which reveals the VCA-region and thereby fully activates WASP (Aspenström, Lindberg, and Hall 1996; S Linder et al. 1999a; Miki, Suetsugu, and Takenawa 1998; Rudolph et al. 1998; Kirchhausen and Rosen 1996). Furthermore, the activity of WASP can be regulated by tyrosine phosphorylation after activation via Cdc42 (Cory et al. 2003; Seth, Otomo, and Rosen 2006; Haein Park and Cox 2009).

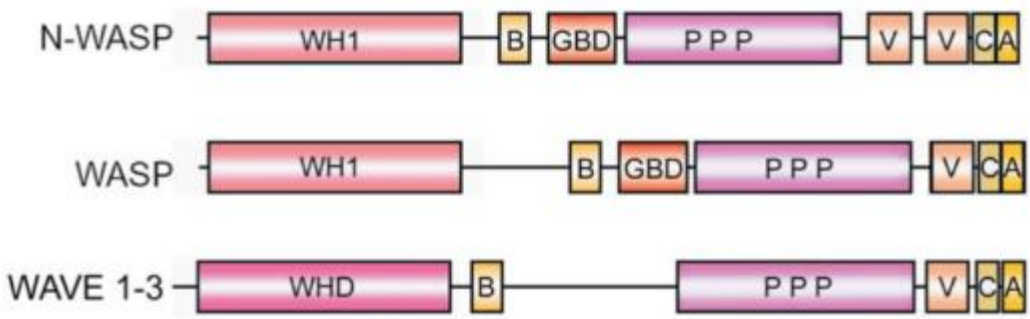

Figure 3: Modular domain structure of WASP- and WAVE-proteins (modified form Stradal & Wehland, 2005). WASP, neural (N)-WASP and WASP family verprolin-homologous (WAVE) proteins have a modular structure. WASP and N-WASP harbor conserved WASP homology 1 domain (WH1) followed by a short basic region which mediates binding to F-actin and PIP_2. GBD, also known as CRIB (Cdc42/Rac-interactive binding domain) mediates binding to the activated GTPase Cdc42. The polyproline-domain (PPP) enables the interaction with SH3 domain-containing proteins and profilin due to harboring binding sites. The C-terminal VCA region contains verprolin homology domain (V), cofilin homology domain (C) and a short acidic region (A). The VCA region can bind to the Arp2/3 complex and G-actin simultaneously, which in turn activates the Arp2/3 complex. The WAVE isoforms harbor WAVE homology domain (WHD) instead of the WH1 domain.

Possibly proline-rich regions (PPP) of WASP and WAVE proteins enable interactions with adaptor proteins during signal transduction at the cell membrane. The proline-rich region of WASP is

able to bind SH3 domain-containing adaptor proteins such as Nck or Grb2 and profilin (Steffen et al. 2004b; Gomez-Cambronero 2011; Miki, Suetsugu, and Takenawa 1998). The polyproline domain is followed in case of N-WASP by the VVCA domain. The VVCA domain harbors two WH2 domains (or V-domains). In contrast, WAVE1-3 and WASP harbor only one WH2 domain at the similar location. Once WASP/N-WASP is activated, the exposed (V)VCA domain can bind to the Arp2/3 complex and G-actin simultaneously. The proximity of G-actin and Arp2/3 complex leads to activation of the Arp2/3 complex. The activated Arp2/3 complex can bind to sides of pre-existing actin filament branches (Kurisu and Takenawa 2010b; Rottner and Stradal 2011a; Thomas D. Pollard and Borisy 2003). The side branching preferably occurs near the barbed end of the actin filament, which indicates the importance of the availability of free barbed ends in this process (Le Clainche and Carlier 2008b). The VCA or VVCA region is sufficient to stimulate actin nucleation via the Arp2/3 complex *in vitro*. Structural and biochemical data of the VCA region suggest that due to interaction with the Arp2/3 complex and G-actin, VCA places Arp2, Arp3 and G-actin in proximity to each other. This stimulates the formation of the nucleation core (Yamazaki, Kurisu, and Takenawa 2009a).

WAVE proteins, in contrast to Cdc42 mediated activation of WASP, are activated downstream of Rac GTPase and are thought to be major activators of the Arp2/3 complex in the process of lamellipodia formation (Ridley 2001; Rottner and Stradal 2011a; Miki, Suetsugu, and Takenawa 1998). WAVE proteins lack the GBD domain and thus cannot interact directly with Rac. In an inactive conformation, WAVE proteins are complexed with four other proteins, forming a stable multiprotein complex. This interaction masks the VCA domain of WAVE. The constituents of this complex include Nap1 / Hem1 (Nck associated protein 1 / hematopoietic protein-1), PIR121/Sra-1 (p53 inducible mRNA), HSPC300 (hematopoietic progenitor cell 300) and Abi1 (Abl interactor 1) (Eden et al. 2002; T. Stradal et al. 2001a; Stovold, Millard, and Machesky 2005). *In vivo,* the pre-formed inactive WAVE complex is activated by direct interaction of Rac1 with Nap1/Sra1 constituents of the complex. After this interaction the active complex and Arp2/3 are rapidly translocated to the cell membrane at the site where lamellipodia will be formed (Steffen et al. 2004b).

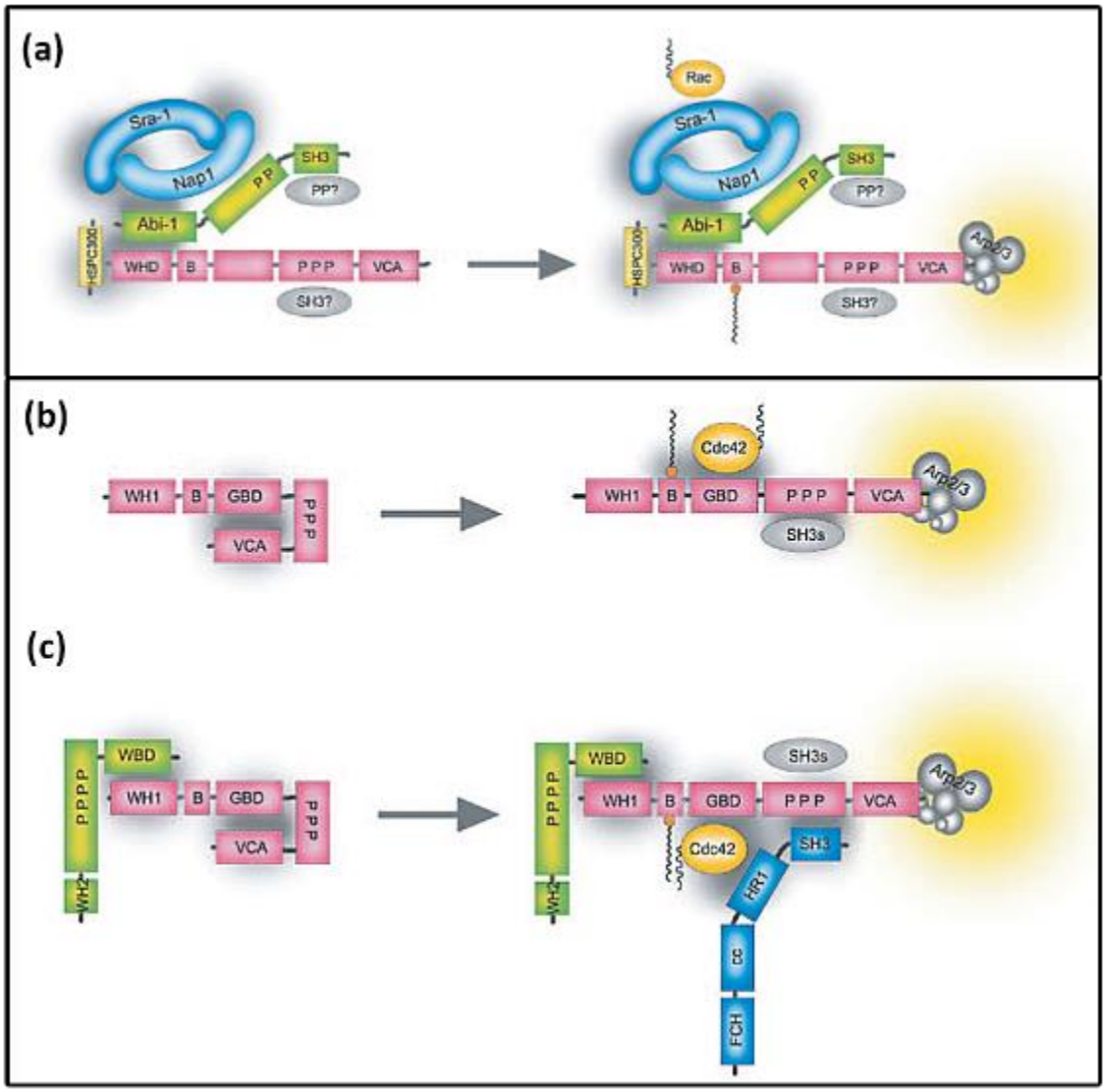

Figure 4: Proposed mechanisms of activation of WASP and WAVE proteins (modified from Stradal & Wehland, 2005). (**a**) WAVE forms a constitutively inactive complex in the cytoplasm consisting of Sra-1, Nap1, Abi proteins and HSPC300. As a consequence of the interaction of Sar-1, activated by Rac1 GTPase, the entire WAVE complex is recruited to the membrane and activated locally. Activated WAVE complex can bind and locally activate the Arp2/3 complex leading to the formation of a branched actin filament network which is the driving force in protruding lamellipodia. (b) and (c) demonstrate two proposed models of WASP/ N-WASP activation. WASP is intrinsically inactive due to its closed conformation. This is apparently due to the intermolecular interaction of GBD- and VCA domains of WASP. (**b**) Inactive WASP is activated by simultaneous binding of active Cdc42 and PIP_2 its GBD and basic regions respectively. (**c**) WASP was found to be in an inactive complex with WIP proteins. Interaction of N-terminal WH1 domain of WASP with the adaptor protein WIP apparently supports inactive conformation and protects WASP from degradation. SH3 domain-containing proteins (such as Nck1 and GRB2) together with Cdc42 /PIP_2 are also involved in full activation of WASP.

It is proposed that native WAVE complex is inactive and for its activation a simultaneous interactions with prenylated Rac1-GTP, acidic phospholipids and serine/threonine phosphorylation,

most likely at the cell membrane is required (Dubielecka et al. 2011; Lebensohn and Kirschner 2009). WAVE proteins are constitutively active in contrast to the WAVE complex. To activate the WAVE complex, activated Rac binds to the WHD domain of WAVE or to Sra1, which then binds to Nap1/Hem1. Interaction of Nap1/Hem1 with Abi1/2 leads to binding of Abi1/2 to HSPC300 and to the WHD domain of WAVE. This leads to a conformational change of WAVE making its VCA domain available for Arp2/3 binding and activation. The activation is believed to take place already at the membrane initiating local actin polymerization (Gautreau et al. 2004; Heon Park, Chan, and Iritani 2010a; Steffen et al. 2004b; Small et al. 2002a). This was supported by bleaching and photo-activation experiments that indicate that Arp2/3 is activated at the lamellipodia tip, where the WAVE complex already resides when Rac1 is activated. As a consequence of Arp2/3 activation, the Arp2/3 complex is incorporated into the F-actin network exclusively at the tips of lamellipodia (Lai et al. 2008).

Despite the fact that both WASP and WAVE activate the Arp2/3 complex in a similar manner, it is believed that these proteins are involved in regulation and formation of different F-actin-based substructures needed for various cellular processes. In macrophages WASP is involved in podosome formation. N-WASP is involved in endocytic transport and formation of invadopodia in cancer cells (Stefan Linder, Wiesner, and Himmel 2011; Benesch et al. 2005). WAVE1 and WAVE3 are expressed predominantly in neuronal tissue and are less well studied so far. WAVE2 is expressed ubiquitously and is thought to stimulate the formation of lamellipodia and dorsal ruffles in various cell types (Yamazaki, Kurisu, and Takenawa 2009a; Steffen et al. 2004b; Dubielecka et al. 2011).

1.1.2.5 ADF / Cofilin

Actin-depolymerizing factor (ADF), also known as cofilin, can bind to actin filaments and cause structural changes at the binding sites of the filament. These changes induce severing of cofilin bound actin filament and enhance the overall depolymerization rate of the pointed end of actin filaments *in vitro* (Carlier et al. 1997; Laurent et al. 1999; Andrianantoandro and Pollard 2006).

Thus the concentration of G-actin increases, thereby allowing on the other hand, the polymerization rate of newly formed free barbed ends to increase. *In vitro* studies indicate that at low concentrations cofilin favors depolymerization of actin filaments. In contrast, at higher concentrations of cofilin, the nucleation of filaments is induced (Andrianantoandro and Pollard 2006). It has been assumed that the severing activity of cofilin towards actin filaments increases the number of free barbed ends hence to increase branching of filaments and the actin nucleation rate (Ghosh et al. 2004). Cofilin is constitutively active in cells. The activity of cofilin is regulated by phosphorylation downstream of Rac, Rho and Cdc42 GTPases. It has been shown that Lim kinase and phosphatase Slingshot can inactivate or reactivate cofilin by phosphorylation and dephosphorylation respectively (Arber et al. 1998; Niwa et al. 2002; Rottner and Stradal 2011b). Cofilin localizes at the leading edge of a cell, but is excluded from lamellipodia tips, indicating a possible role in actin depolymerization (Svitkina and Borisy 1999a).

1.1.2.6 Barbed end capping proteins

Barbed ends of actin filaments are capped by capping proteins. These have higher affinity to the barbed end of actin filament compared to other actin-binding proteins. Besides antagonizing activity to Arp2/3 complex and filament nucleation, capping promotes the higher degree of branching of actin filaments (Rottner and Stradal 2011b). This is essential for actin network formation in lamellipodium (S. Kojima, Vignjevic, and Borisy 2004). Moreover, capping proteins are thought to control and regulate the rate of lamellipodia protrusion indirectly. One possibility of such regulation is the increase of G-actin concentration as a consequence of capping of actin filaments, which can drive the polymerization of other uncapped filaments (Le Clainche and Carlier 2008b). Another regulatory mechanism for actin nucleation by filament capping is supposedly the inhibitory effect of PIP_2 on this process. Thus an increase in PIP_2 levels can support actin polymerization this way. The inhibitory effect of PIP_2 on filament capping was demonstrated *in vitro* (Schafer, Jennings, and Cooper 1996). Capping of filaments also appears to be essential for the formation of longer actin filaments (Chhabra and Higgs 2007a).

Different capping proteins are utilized in various cellular processes that lead to the formation of distinct actin structures. The heterodimeric capping protein (CP) controls protrusion of lamellipodia. Gelsolin family proteins (gelsolin, Capping protein gelsolin like (CapG)) are generally involved in cell migration. Tensin, a large modular protein displays capping activity in focal adhesions. Esp8 is an autoinhibited CP which is activated by Abi1 and is involved in lamellipodia formation and also supports motility of *Listeria monocytogenes* in host cells (Croce et al. 2004; Disanza et al. 2004). It is thought that capping function is redundant which was indicated by double knockout of *gelsolin* and *capg* in mice. The affected animals showed no vast defects or abnormalities (Witke et al. 2001; Le Clainche and Carlier 2008b).

1.1.2.7 Nucleators in actin polymerization at the leading edge

1.1.2.7.1 Arp2/3 complex

To drive the unfavorable reaction of actin filament nucleation, special proteins are required. So called actin nucleators can directly catalyze the actin polymerization reaction. Additionally, actin nucleators balance the effect of ADF/cofilin and the capping proteins that favor actin depolymerization. Actin nucleators are currently grouped in three classes: Arp2/3 complex, formins and spire (Figure 5).

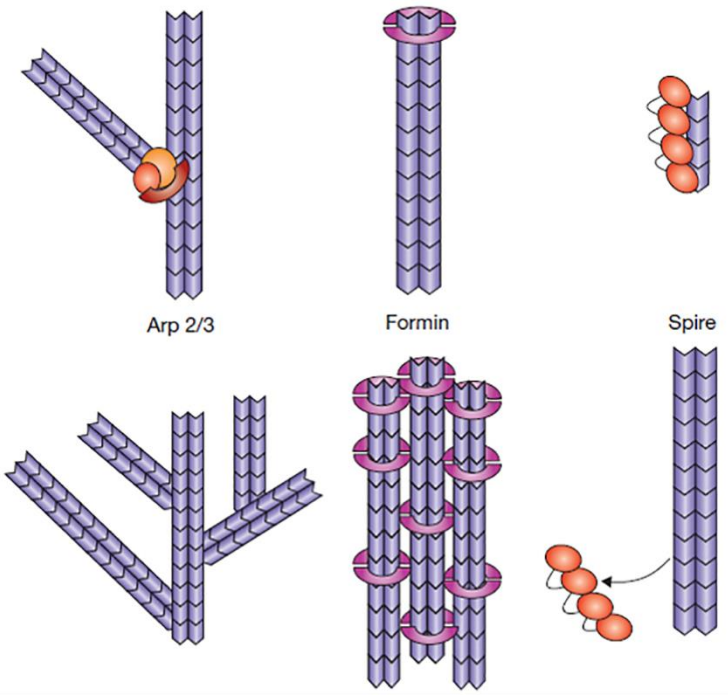

Figure 5: Schematic illustration of the mode of action of major actin nucleators and resulting actin structures. (Modified from Chhabra & Higgs, 2007). The Arp2/3 complex binds to sides of pre-existing actin filaments at an approx. 70° degree angle and induces actin nucleation at these sites. The extensive repeating of this process gives a rise of branched actin network that is found in lamellipodia. Formins nucleate actin filament and stay attached to the tip or the barbed of the growing filament. Some Formins, can also bundle actin filaments. These processes can give rise to actin structures where unbranched actin filaments are majorly observed such as filopodia. Spire is able to stabilize the formation of actin tetramer, thereby overcoming the energetic barrier and starting the polymerization process. Spire apparently dissociates from the growing filament as the polymerization proceeds.

The Arp2/3 complex was the first actin nucleator to be identified. It is composed of seven subunits (ARPC1-5; Arp2 and Arp3). Arp2 and Arp3 are thought to mimic an actin dimer within the activated Arp2/3 complex (M. D. Welch, Iwamatsu, and Mitchison 1997; R D Mullins et al. 1998; Laura M Machesky et al. 1994; Kelleher, Atkinson, and Pollard 1995). Being able to bind to sides of pre-existing actin filaments, the Arp2/3 complex serves as a nucleation site and induces branch formation by recruiting free actin monomers (Blanchoin et al. 2000; Goley and Welch 2006; R. Dyche Mullins, Stafford, and Pollard 1997). It has been shown that the angle between pre-existing and newly induced branch is around 70°, thereby providing the structure of the actin network in lamellipodia. The result of Arp2/3 complex-mediated actin polymerization is a network of short branched actin filaments that grow successively. Another model of actin filament branching describes branching from the barbed ends of the existing filaments. This model assumes that the activated Arp2/3 complex is incorporated and integrated into growing filaments at their barbed ends instead of binding the filaments from the side (Boujemaa-Paterski et al. 2001; Le Clainche and Carlier 2008a).

Arp2/3 complex is recruited and activated to induce actin polymerization at various locations of a cell. Most prominently this happens at the lamellipodium during cell spreading or migration on a 2D surface. The Arp2/3 complex is apparently essential for eukaryotic cells. The complex functions at very low concentrations making the RNA targeted knockdown experiments difficult to analyze and interpret (Thomas D Pollard and Cooper 2009). Also the pathogenic bacterium *Listeria monocytogenes* can activate the hosts Arp2/3 complex and thereby support its own locomotion within an infected mammalian cell. The force for propulsion of bacteria is apparently generated by host Arp2/3 complex-mediated F-actin polymerization at the surface of this pathogen (M. D. Welch et al. 1998a).

1.1.2.7.1.1 *Effects of Arp2/3 complex depletion*

Due to lethality caused by genetic removal of Arp2/3 complex subunits in yeast, *Dictyostelium* or in mice (knockouts which lead to preimplantation lethality in mice), it was assumed that the Arp2/3 complex is essential in eukaryotes(Schwob and Martin 1992; Yae et al. 2006; Zaki et al.

2007; C. Wu et al. 2012). RNAi mediated downregulation of the Arp2/3 complex is difficult to interpret because the Arp2/3 complex can induce actin polymerization at very low concentrations (Thomas D Pollard and Cooper 2009). Although, it has become possible to generate viable ES-derived cells with stable knockdown of Arp2/3 or *ARP3* knockout ES-derived cells(C. Wu et al. 2012; Suraneni et al. 2012). Also the transient knockdown of ARPC3 and ARP3 in B16 cells could be provided and could successfully interfere with lamellipodia formation without compromising cell viability (Steffen et al. 2006).

1.1.2.7.1.2 *Mechanism of Arp2/3 complex activity and its inhibitors*

As described in the previous chapter on the nucleating promoting factors, WASP/Scar-WAVE family members bind the Arp2/3 complex and lead to its full activation. The VCA domain of WASP/Scar proteins binds to monomeric actin with its V-domain and Arp2/3 complex with CA-region (central and acidic regions) inducing the conformational changes in the complex leading to actin nucleation. The Arp2/3 complex nucleation process, requires additionally to binding WASP/WAVE proteins, binding of Arp2/3 to the pre-existing filament, ATP and free actin monomers. The exact mechanistic explanation how all these factors interact in this process is still elusive (S. L. Liu et al. 2013). The Arp2/3 complex activation involves the conformational changes within the complex so that its subunits Arp2 and Arp3 are placed 25A closer to each other, presumably to mimic an actin dimer within an actin filament (Rouiller et al. 2008). This conformation of both Arp subunits is termed as a short pitch conformation. The transformation of Arp2 and Arp3 subunits within the Arp2/3 complex into the short pitch conformation can be blocked by specific small molecule inhibitors such as CK666 and CK588. Thus blocking the nucleation of new filaments (Nolen et al. 2009a). This was demonstrated by results of *in vitro* assays as well as *in vivo*. In mammalian cell culture these inhibitors could successfully block Arp2/3 dependent generation of listeria comet tails, the formation of podosomes or the formation of the endocytotic actin patches in yeast (S. a Rizvi et al. 2009a; Nolen et al. 2009b).

The inhibitor molecule CK666 acts presumably as an allosteric inhibitor that stabilizes the inactive conformation of the Arp2/3 complex by blocking the movement of Arp2 closer to Arp3 during activation of the complex. The crystal structure of CK666 bound to Arp2/3 complex suggested that binding of CK666 to the pocket at the interface between Arp2 and Arp3 may disrupt

the short pitch conformation of these subunits. Another Arp2/3 complex inhibitor CK548 is supposed to bind to Arp3 subunit and presumably destabilizes the active configuration of the whole Arp2/3 complex. Binding of CK-548 to Arp3 doesn't block binding sites of NPFs or the ability of the Arp2/3 complex to bind to pre-existing actin filament (Baggett et al. 2012).

1.1.2.7.2 Formins

Formins were first identified as gene products that were important for the development of limb in mice. Later, another protein of this family, a product of Drosophila homologous diaphanous-gene, was found to be critically important in cytokinesis in this organism (Mass et al. 1990; Castrillon and Wasserman 1994). Next, Bni1 a protein from *S. cerevisiae* was shown to possess two homologous regions to previously identified formins in *Drosophila melanogaster* and in mice (Kühn and Geyer 2014). These two regions were depicted as proline-rich, formin homology 1 (FH1) domain followed by formin homology 2 (FH2) domain (Castrillon and Wasserman 1994). Further studies, revealed the third homology domain-FH3, which was identified within the protein Fus1 from *Schizosaccharomyces pombe (S. pombe).* To date, the existence of a highly conserved FH2 domain of approx. 400 amino acids is the defining feature of formins (Figure 6 A) (Y. Xu et al. 2004).

There are fifteen known formin genes in mammals, whereas six genes are known in *Drosophila* and two in yeast. Isoforms of formins display different roles in cellular functions, although they all are known to be directly related to dynamics of the actin cytoskeleton. Some formins that appear to have very similar domain structure and high sequence identity, can still significantly differ in their potency to elongate actin filaments. Rho-GTPases are the major activators of formins (Higgs and Peterson 2005).

The formin and diaphanous are most widely studied formins and became founding members of formin family proteins, termed as FMN and Dia. The studies on Bni1 in yeast showed for the first time, the involvement of formin in remodeling and formation of the actin cytoskeleton (M Evangelista 1997). Shortly thereafter, the involvement of Rho-GTPases in activation of formins in mammalian cells was described (M Evangelista 1997; Naoki Watanabe et al. 1997). Further

research showed that formins are intrinsically autoinhibited and are activated by interaction with activated Rho-GTPases. Activated Rho-GTPases can bind to a specific domain termed the GBD domain within formins. This interaction relieves the FH2 domain, which is sterically hindered as a result of the autoinhibited conformation of formins. The autoinhibited conformation of formin is maintained due to interactions of C-terminal Dia autoregulatory domain (DAD) with the N-terminal diaphanous inhibitory domain (DID) of a formin dimer (Figure 6 B).

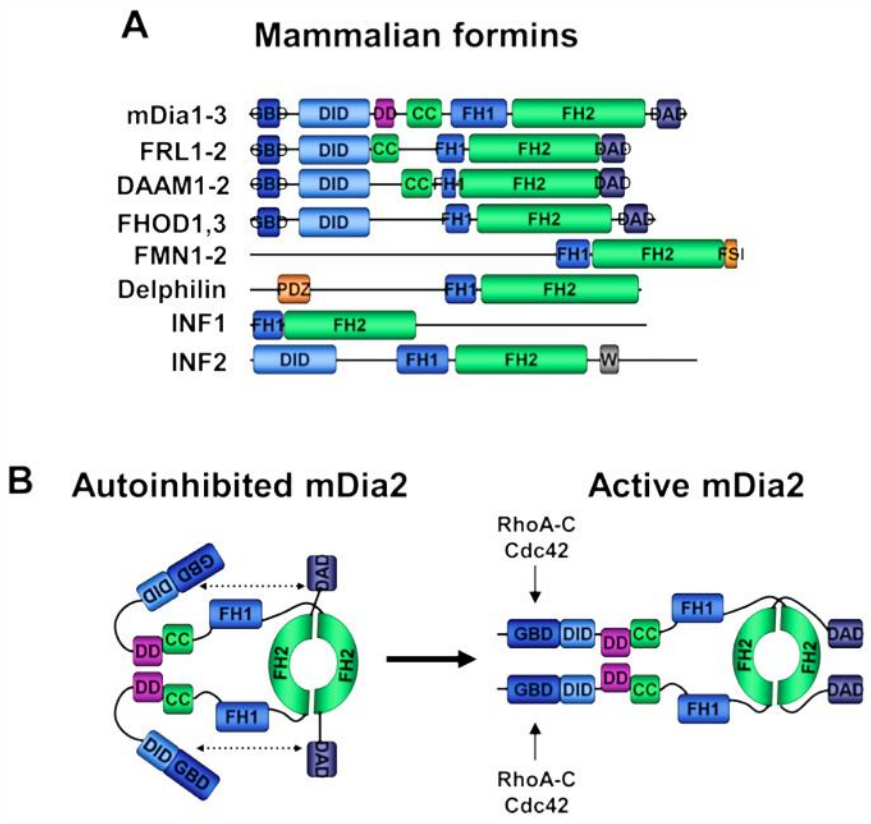

Figure 6: Modular structure and common activation mechanism of mammalian formins. (modified form (Campellone and Welch 2010)) (A) Mammalian formins generally possess similar domain structure with a characteristic conserved FH1-FH2 domain which is mainly responsible for actin nucleation. GBD domain serves as an interaction site with GTPases. Coiled-coil (CC) region and dimerization domain (DD) apparently support dimerization of formins (Otomo et al. 2005; Lammers et al. 2005). PDZ domains generally recognize specific short sequences at C-terminus of numerous proteins and are thought to serve as scaffolds to generate multiprotein complexes at specific cellular locations (B. Z. Harris and Lim 2001). In case of delphilin its PDZ domain can interact with the glutamate receptor in Purkinje cells possibly linking this receptor to actin cytoskeleton at the postsynaptic site of these cells. (B) Formins such as mouse diaphanous-related formin 2 (mdia2) are dimeric and intrinsically inactive due to autoinhibition. Upon binding to GTPases autoinhibition is resolved and formins change conformation to their active state which enables actin polymerization.

The FH2 domain of formin can enhance an actin nucleation reaction by stabilizing an actin dimer (Kovar and Pollard 2004a; Zigmond 2004). Additionally, the FH2 domain can simultaneously bind to a barbed end of an actin filament. Based on structural data derived from formin Bni1P, the FH2 domains of a formin dimer form a donut-shaped structure around an actin filament and thereby bind the terminal subunits of the filament (Otomo et al. 2005). Apparently, FH2 domains of both formin polypeptides align in an antiparallel orientation to each other within a dimer (Y. Xu et al. 2004). After binding to the barbed end of an actin filament, formin recruits profilin-actin via its FH1 domain. In a further step, profilin-actin is added to an actin filament in an elongation reaction (Marie Evangelista, Zigmond, and Boone 2003). Profilin bound to an actin monomer is thought to be highly important for the elongation reaction and can accelerate the reaction up to 15-fold *in vitro*, This was shown in a polymerization assay utilizing beads coated with formin mDia (Josephine C Adams et al. 2004a). The FH1 domain is followed by a linker sequence that helps to maintain flexibility of both FH2 domains in a dimer. This flexibility supposedly allows formins to move along the filament stepwise (Y. Xu et al. 2004). The linker sequence between FH1 and FH2 domains is also important for- and mediates the dimerization of formins. Furthermore, due to its essential role in the flexibility of FH2 domains, the linker sequence appears to be essential for the nucleation activity of formin. Without the linker sequence formins act as capping proteins of barbed ends (Josephine C Adams et al. 2004b).

Based on their biochemical properties formins, besides Arp2/3 complex, form another family of actin nucleators. Additionally to their nucleating and elongating activities, formins can even bundle actin filaments. Therefore, in contrast to Arp2/3 complex derived branched F-actin network, formin-mediated actin polymerization results in a formation of unbranched actin filaments *in vitro* and most likely *in vivo*. In the process of filament elongation formin dimer binds to free barbed end of the actin filament, remains associated to and moves along the filament during the elongation process. Binding of formin to the barbed end blocks the capping proteins from filament binding, thereby facilitating the elongation reaction (Higgs and Peterson 2005).

1.1.2.7.2.1 *Isoforms and functional roles of formins*

In yeast, two formins participate in an assembly of unbranched actin filaments such as cytokinetic rings and actin cables. In mammalian cells fifteen formin genes and their products are involved in assembly of various actin structures such as filopodia, stress fibers and are involved in construction of cytoplasmic actin networks which are apparently used for long rage transportation of vesicles across the cell (Leader et al. 2002; Schuh 2011), or assembly of cytokinetic rings and phagocytic cups. Apparently, formin activity at the leading edge also indirectly promotes assembly of lamellipodia (Brandt et al. 2007; Breitsprecher and Goode 2013).

Fifteen mammalian formins are identified so far. They are divided into seven different subclasses based on their FH2 domain sequence divergence: Diaphanous (Dia), Formin-related proteins in leukocytes (FRL), Dishevelled-associated activators of morphogenesis (DAAM), Formin-homology-domain proteins (FHOD), (Formin) FMN, Delphilin and inverted formin (INF).

From fifteen isoforms of mammalian formins the largest subset are the so-called DRFs (Diaphanous-related formins). DRFs are highly modular proteins and can be divided into three functional regions, N-terminal, GBD and DID domains, central DD domain and C-terminal FH1-FH2 domain followed by DAD domain. Three isoforms of Dia (mDia 1-3) were found in mammalian cells which are also widely expressed throughout the tissues. Based on gene knockout analysis in mice the mDia1 is important in polarization and chemotaxis of T cells and neutrophils and in trafficking of these to secondary lymphoid organs (Gupton et al. 2007; Sakata et al. 2007).

From Rho GTPase subfamily only Rho isoforms were reported to bind to GBD-DID domain and activate mDia1 *in vitro* (Lammers et al. 2008). This interaction leads to actin polymerization in *in vitro* assays. Cdc42 is known to signal to mDia2 (also termed DRF3) and activate this formin via binding to its CRIB-motif, which leads to translocation of mDia2 to the leading edge of a cell, apparently to lamellipodia and tips of filopodia. On the other hand, the antibodies against mDia2 interfere Cdc42 induced formation of filopodia in ES-derived cells (Peng et al. 2003). Reportedly, mDia2 can also be activated by Rac1, whereas mDia1 can only be activated by Rho GTPases (A, B and C) *in vitro* (Lammers et al. 2008). Proteins harboring SH3-domain (such as

Src-family kinases) can interact with DRFs, suggesting the link between these formins and tyrosine kinase signaling (Young and Copeland 2010a).

Beyond of their participation in the formation of many actin-based structures such as stress fibers, dorsal ruffles and in cytokinesis rings, DRFs localize at the tips of protruding filopodia and lamellipodia. Further, the overexpression of DRFs positively correlated with the number of filopodia per cell (Pellegrin and Mellor 2005; Pruyne et al. 2007; Peng et al. 2003). DRFs also were shown to be involved in assembly of F-actin at focal adhesions during cell migration. Furthermore, this subfamily of formins is also involved in phagocytosis, which was indicated by their presence in phagocytosis cups. FH2-domains of DRFs can also trigger serum response factor-induced transcription. DRFs can interact with- and bind to microtubules and to other proteins which are capable of interacting with microtubule plus end (Bartolini et al. 2008; Young and Copeland 2010b).

Formin like proteins (FMNL1-3) and disheveled-associated activator of morphogenesis (Daam1-2) are reminiscent of DRFs, structurally related to each other and similarly regulated formins. These subclass of formins, besides their actin nucleation activity, also possesses the ability to bundle actin filaments. FMNL1 can be activated via Cdc42 in *in vitro* assays. The activation of FMNL1 leads to relocation of this formin of to the cell membrane and phagocytic cups during phagocytosis (Seth, Otomo, and Rosen 2006). FMNL2 is recuired and supports the formation of filopodia and lamellipodia downstream of Cdc42 during cell migration (Jennifer Block et al. 2012). FMNL2 and FMNL3 were shown to be involved in force generation during protrusion of lamellipodia of migrating mammalian cells downstream of Cdc42 (Kage et al. 2017a). FMNL3, in contrast to the autoinhibited isoforms (1 and 2), is apparently constitutively active in cells. This formin was reported to be involved in the formation of cell to cell adhesions (Gauvin, Young, and Higgs 2014; E. S. Harris et al. 2010).

Formin (FMN-1/2) and formin homology domain 2 containing (FHOD1/3) possess markedly distinct N-terminal sequences than Dia, FRL and Daam formins suggesting a difference in autoinhibition and activation of these formins compared to formins from other subfamilies. Reportadly, FHOD1 binds to Rac via its GBD domain (Schonichen et al. 2006). This interaction supposedly recruits FHOD1 to the plasma membrane and activates the formin (Gasteier et al. 2003). The ex-

pression of constitutively active FHOD lacking a DAD domain leads to extensive stress fiber formation which is dependent on ROCK, RhoA and Rac (Schonichen et al. 2006). ROCK GTPase interacts with FHOD1 (which is majorly expressed endothelial formin) and can phosphorylate the DAD region of the formin *in vitro*. This relieves autoinhibited conformation of FHOD1 and probably leads to activation and inducting stress fiber formation in endothelial cells after treatment of these with thrombin (Takeya et al. 2008; Schonichen et al. 2006).

FMN1 is reportedly involved in the formation of adherence junctions and focal adhesions. Depletion of this formin affects cell migration and manifests in abnormalities in the formation of focal adhesions. In knockout and knock in models of FMN1 in mice could be observed that depletion of FMN1 resulted in less focal adhesions and slight negative effect on migration during wound healing in cells. Formin FMN1 co-localizes with microtubules, but no co-localization was detected at focal contacts or adherence junctions (Dettenhofer, Zhou, and Leder 2008). FMN2 was suggested to play a role in cytokinesis, particularly in correct positioning of the spindle apparatus as well as in chromosomal movements during this process. This was observed in meiosis of oocytes of FMN2 deficient mice (Leader et al. 2002).

Delphilin and INF 1-2 proteins, in contrast to typical formins, lack GBD, DID or DAD domains. The F-actin assembly mediated by these formins is not well understood. Delphilin plays apparently a role in F-actin assembly in mammalian neuronal tissue due to its high expression profile in this tissue. INF1 induces stress fiber formation when transfected into cells, however it localizes to microtubules. INF2 can additionally to polymerizing activity can severe or depolymerize actin filaments *in vitro* (Chhabra and Higgs 2006).

Sipre, cordon-bleu, Cobl and Leimonin (Lmod) represent a group of actin nucleators which have characteristically three or more G-actin-binding motifs. In addition they harbor WH2-domains. Apparently, the WH2-domains of these proteins are promoting the formation of an actin trimer, although the high resolution structural data confirming this assumption is currently not available (Campellone and Welch 2010).

It is still not well understood how formins are activated leading to the formation of filopodia and which formins exactly are involved in this process. In mammalian cells DRFs (2 and 3) and

FMNL1 and 3 are most likely involved in the formation of filopodia and can be activated downstream of Cdc42. DRFs also localize to tips of filopodia.

1.1.2.7.2.2 *Effects of formin depletion*

Formins are important, if not essential, in tissue invasion of cancer cells. Furthermore, apparently different formins are utilized by different types of cancer cells to accomplish invasion related tasks into artificial 3D tissue (Matrigel). This was demonstrated by analyzing three different cell lines in their ability to invade into Matrigel when different formin proteins were downregulated by shRNA approach. In HT1080 cells shRNA approach targeting either DAAM1, Dia1 or FMNL1 showed 80%, and 50% decreased invasion whereas downregulation of FMNL2 had no negative effect in the same assay. In contrast, in MDA-MB-231 cells shRNA mediated knockdown of DAAM1 or FMNL2 had no negative effects on cell invasion (Kitzing et al. 2010). In B16 cells FMNL2 but not FMNL1 localizes to the tips of lamellipodia and filopodia and interacts specifically with Cdc42. The localization of this formin to the cell periphery is dependent on the presence of activated Cdc42. Also the N-terminal myristyolation is apparently an important factor for FMNL2 activation. The shRNA mediated knockdown of FMNL2 led to reduced (approx. 70%) overall protrusion rates and decreased velocity in these cells (Jennifer Block et al. 2012).

Macrophage specific DRF, FRLα (Formin related gene in leukocytes α) is activated specifically downstream of active Cdc42, but not of activated RhoA or Rac. In this case also such as in case of FMNL2 in B16 cells, the activation of formins defines its localization at the cell periphery. The downregulation of *FRLa*-gene leads to severe defects in Fc-y mediated phagocytosis in macrophages (Seth, Otomo, and Rosen 2006).

The highly aggressive breast cancer cell line MDA-MB-231 expresses all three DRFs (1-3) which were shown to be critically involved in the invasion of these cells by forming invadopodia and degrading extracellular matrix (ECM) substrate beneath of these structures. The silencing of one of the *DRF* genes had a critical impact on cell invasion, matrix degradation and invadopodia formation. Additionally, knockdown of Cdc42 or RhoA also reduced the formation of invadopodia in these cells (Lizárraga, Poincloux, Romão, et al. 2009; Sakurai-Yageta et al. 2008).

1.1.2.7.2.3 *Inhibition of formins*

Besides RNAi mediated silencing or genetic knockout approach, direct inhibition of formin proteins is another way to study the function and mechanisms of action of formins. This is achieved by a small molecule inhibitor termed smiFH2 (small molecule inhibitor of formin homology 2 domains). The inhibitory properties of this molecule on formins were identified by screening of large numbers of commercially available small molecules for their ability to inhibit actin polymerization *in vitro*. SmiFH2, is a 2-thiooxodihidropyrimidie-4, 6-dione derivative that inhibited mDia mediated actin assembly in a concentration dependent manner with IC_{50} of 15µM. Further experiments identified the FH2 domain of formins as the target of the inhibitor. This was confirmed by inhibition of formins from diverse organisms such as *C. elegans* (CYK-1), *S. pombe* (Cdc12) or form *S. cerevisiae* (Bni1). Due to blocking of both, nucleation and elongation reactions of actin polymerization by smiFH2 authors concluded that this inhibitor generally decreases the affinity of formins to barbed ends of actin filaments. Furthermore, the binding of smiFH2 is apparently reversible and the molecule undergoes cellular breakdown after some time. The selectivity of smiFH2 towards formins, but not to Arp 2/3 complex was demonstrated by its inhibitory effect on assembly of formin dependent actin cables and cytokinetic rings and not of Arp2/3 dependent endocytic actin patches in yeast.

3T3 fibroblasts treated with 10µM smiFH2 showed 50% reduced velocity of migration which additionally involved non-apoptotic blebbing in 20% of cells. SmiFH2 also induced switch form lamellipodia based to the blebbing associated motility when applied for several hours. Of note, smiFH2 had a negative effect on assembly of stress fibers (S. a Rizvi et al. 2009b). Other studies involving smiFH2 treatments of cancer cells showed that mDia2, but not mDia1 or mDia3 were downregulated after smiFH2 treatment (Isogai, Kammen, and Innocenti 2015). Also in human glioma samples and glioblastoma cell lines the upregulation of DIAPH1 (mDia1) and DIAPH3 (mDia2) was observed. The upregulation of these formins was prominent from stage I to stage 4 gliomas compared to expression of these formins in normal brain tissue. Inhibition or downregulation of these formins using smiFH2 or siRNA approaches led to decreased invasion capacity of glioblastoma cell line in 3D (Arden et al. 2015a). Still the data on exact mechanism how smiFH2 binds to formins and which formins are affected is not available and needs further clarification.

To summarize, from fifteen mammalian formin proteins, most likely only a few are involved in the formation of actin-based protrusions in fibroblasts or HT1080 cells. Interesting candidates could be DRFs (DRF2 and DRF3) and FMNL1/ FMNL3. These formins can be activated by Cdc42 which is known to induce filopodia. Reportedly mDia2 localizes at the tips of filopodia that are induced by Cdc42. Furthermore, increased expression of Drf3 (mDia2) is associated with increased numbers of filopodia in murine ES-derived cells. Also in 3T3 fibroblasts, filopodia formed downstream of Cdc42 and Drf3 which localized at the tips of these structures. Furthermore, blocking of Drf3 with antibodies in the presence of active Cdc42 still led to decreased filopodia numbers in cells (Peng et al. 2003; Pellegrin and Mellor 2005).The formin mDia1 was shown to be involved in the formation of filopodia downstream of RhoA in mtLn3 cells which is a rat mammary cancer cell line (Philippar et al. 2008a).

FMNL1-3 can be essential candidates for formation of filopodia downstream of Cdc42 besides DRFs. Moreover, these formins can also bundle actin filaments. Rho GTPase Cdc42 was shown to specifically bind and activate formin FMNL2. This interaction leads to translocation of this formin to the leading edge in migrating cells (Jennifer Block et al. 2012; Kühn et al. 2015; Kage et al. 2017a).

1.1.2.7.3 Ena/Vasodilator-stimulated phosphoprotein (VASP) proteins in cell migration

Smooth muscle cells coat veins and arteries externally and depending of their contractile state can control the diameter of blood vessels. Due to this mechanism, it is possible to adjust the diameter of blood vessels to match blood flow rates. Application of vasodilator drugs leads to relaxation of smooth muscle cells thereby increasing the diameter of blood vessels. This is a established treatment of several heart diseases (Walter, Waldmann, and Nieberding 1988). Research on the molecular mechanism of vasodilator drugs showed that these substances, besides their effect on smooth muscle cells, can also inhibit the aggregation of platelets. This effect goes together with activation of cGMP or cAMP kinases followed by increase of intracellular levels of cAMP or cGMP in these cells. Vasodilator-stimulated phosphoprotein (VASP) was discovered as 46 kDa

membrane associated protein which was specifically phosphorylated in response to vasodilators (Ulrich and Biochem 1990).
In fibroblasts as well as in platelets that were adhered on glass coverslips, endogenous VASP was localized at the ends of stress fibers, cell periphery and ruffling areas of protruding cell edge (Reinhard et al. 1992). VASP is enriched at intracellular loci that are rich in F-actin such as focal adhesions, cell-cell contacts, filopodia tips and edges of lamellipodia (Rottner et al. 1999a; Chesarone and Goode 2009). In line with these findings, VASP can bind both G-and F-actin (Barzik et al. 2005; Reinhard et al. 1992). Moreover, ActA (Actin Assambly-inducing Protein) a bacterial activator of the Arp2/3 complex, was shown to bind and recruit VASP at the bacterial membrane. At the membrane VASP in concert with the hosts Arp2/3 complex, promotes bacterial movement within the cytosol of infected cells by actin polymerization on the bacterial surface (Lommel et al. 2001; Temm-Grove et al. 1994; M. D. Welch et al. 1998b). These findings suggested that VASP could act either as a nucleator or elongation enhancer of actin filaments (Chesarone and Goode 2009).

1.1.2.7.3.1 *Structure and localization of VASP*

Mammals possess three versions of closely related Ena/VASP proteins- Mena, VASP and EVL. The common structure of these proteins shows a proline rich core domain, flanked by amino terminal EVH1 and C-terminal EVH2 domains (Ena/VASP homology domains 1 and 2). The proline-rich core domain is important for the interaction of VASP with profilin. The EVH1 domain is thought to localize Ena/VASP proteins to focal adhesions, whereas EVH2 domain can bind F- and G-actin and is supposedly important for Ena/VASP mediated elongation of actin filaments (Franke 2004; Lai et al. 2008; Breitsprecher et al. 2011; Barzik et al. 2005). Furthermore, the C-terminal EVH2 domain of VASP mediates tetramerization of VASP (Bachmann et al. 1999; Hu et al. 1999; Lai et al. 2008).

The EVH1 domain of Ena/VASP proteins is responsible for subcellular targeting of these proteins to focal adhesions (Bear et al. 2000). This is achieved through the ability of VASP to bind proteins that harbor the consensus motif of D/E FPPPPXD (Gertler et al. 1996; Bear et al. 2000). This motif was also found in both, focal adhesion proteins, vinculin and zyxin (Jockuschb and

Walter 1996). It was shown that vinculin interacts with VASP *in vitro* and both proteins co-localize at nascent adhesions (Huttelmaier et al. 1998). VASP is also recruited to terminal ends of stress fibers apparently by binding to vinculin and zyxin via its EVH1 domain (Steffen et al. 2006; Jockuschb and Walter 1996).

Structural data of regions of VASP bound to G-actin or profilin actin suggest that VASP is linked with the EVH1 domain to its ligands, binds actin monomers with its central proline rich region and interacts with F-actin with its C-terminal EVH2 domain (Chereau and Dominguez 2006).

VASP was shown to localize at tips of filopodia and lamellipodia during the protrusion phase of these structures. The rate of recruitment of VASP at these sites positively correlated with protrusion rates of these structures (Rottner et al. 1999b). Based on these studies and on the promoting role of Ena/VASP proteins in bacterial movement, it has been proposed that these proteins can promote cell migration (Rottner et al. 1999b). Although, Ena/VASP depleted fibroblasts showed increased motility on 2D (Bear et al. 2000). Further studies showed that VASP is required for the formation of filopodia in murine neurons and *Dictyostelium* (Schirenbeck et al. 2006; Faix and Rottner 2006b; Kwiatkowski et al. 2007; Lebrand et al. 2004; Applewhite et al. 2007).

Depletion of one of the VASP isoforms in mice leads to only subtle defects in affected animals. Removal of all three VASP isoforms results in embryonic lethality. Affected embryos show severe morphogenetic and cardiovascular defects (Riquelme et al. 2015). Depletion of VASP in *Dictyostelium* led to reduced numbers of filopodia and showed inefficient chemotaxis compared to wildtype cells (Y. H. Han et al. 2002; Schirenbeck et al. 2006).

1.1.2.7.3.2 *Mechanism of action of Ena/VASP*

Data from *in vitro* actin polymerization assays indicate that VASP bundles- and processivly elongates actin filaments (Lai et al. 2008; Bachmann et al. 1999; Breitsprecher et al. 2011; Hu et al. 1999; Laurent et al. 1999). Although, it is still controversially discussed whether Ena/VASP proteins are nucleators of actin filaments or act indirectly by their anti-capping activity (Chesarone and Goode 2009).

Studies on VASP from mammalian cells show formation of protein complex between VASP and mDia1 (Grosse et al. 2003). Also VASP form *Dictyostelium* (DdVASP) showed interaction with Dia2 *in vitro* and apparently *in vivo* acting as a protein complex during the formation of filopodia in *Dictyostelium* cells (Schirenbeck et al. 2006). Furthermore, DdVASP can directly nucleate F-actin and does not possess the anti-capping activity. Reportedly, VASP proteins can additionally bundle actin filaments involving F-actin-binding site of VASP. Mutation within this site of VASP severely affected the bundling activity, but did not affect the polymerization of F-actin by VASP. VASP is thought to capture several actin filaments at once and directly add actin monomers and elongate these filaments. Apparently the tetramerization of VASP proteins leads to binding and tethering of actin filaments. Thereafter G-actin is directly bound by VASP and transferred to F-actin filament (Breitsprecher et al. 2011). This study also showed that different isoforms of VASP display considerably distinct actin nucleation rates both, in solution and when immobilized on beads (Breitsprecher et al. 2011). The higher rates of actin nucleation of immobilized VASP compared to VASP in solution is probably due to multimerisation or clustering of VASP on the surface of beads (Lai et al. 2008).

1.1.2.7.3.3 *VASP at invadopodia*

The metastasis of mouse mammary breast cancer has been linked to a paracrine loop between carcinoma cells that secrete colony-stimulating factor (CSF)-1 and tumor-associated macrophages that in turn secrete EGF (Wyckoff et al. 2004). In this scenario, a subpopulation of cancer cells responds to EGF signal by invasion into surrounding tissue and blood vessels (Philippar et al. 2009; Yamaguchi et al. 2005; Josephine C Adams et al. 2004b). EGF on the other hand, similar to some other growth factors, can induce the formation of invadopodia (Yamaguchi, Pixley, and Condeelis 2006). Apparently, EGF mediated formation of invadopodia enables cancer cells to protrude into ECM and secrete proteases focally to degrade the extracellular matrix and move further into the surrounding tissue (Condeelis and Segall 2003; Buccione, Orth, and McNiven 2004; Stefan Linder 2007) (Philippar et al. 2008b). The formation of invadopodia and thus invasiveness of these cells is attributed to Mena upregulation, which is a murine member of the Ena/VASP family proteins (Di Modugno et al. 2004; Stefan Linder, Wiesner, and Himmel 2011).

A specific splice isoform of Mena is overexpressed in motile mammary cancer cells and is involved in stabilization of invadopodia in these cells. This Mena version potentiates the degradation of underling matrix by invadopodia and increases the lifetime of these structures when overexpressed. Furthermore, Mena co-localized with cortactin in protrusions formed during the invasion into collagen I gel of rat mammary cancer cell line MTLn3. Also when MTLn3 cells were plated on fibronectin / gelatin coated dishes endogenous Mena was concentrated in dot-like structures and co-localized with cortactin at those locations. These structures were presumably invadopodia (Philippar et al. 2008b).

1.2 Actin-based protrusions

1.2.1 Lamellipodia

Lamellipodia are sheet like, thin, actin-based protrusions consisting of F-actin filaments that are organized in a criss-cross pattern. This structure was first characterized by Abercrombie as 0.2 µm thin layer of cytoplasm formed by migrating cells at the leading edge. Lamellipodia which curled upwards in a perpendicular direction to the substrate were termed as “ruffles” and the process was referred as “ruffling” (Small et al. 2002b). Later the formation of lamellipodia was shown to be a dynamic process where actin molecules are polymerized to actin filaments at the plasma membrane to form a branched network (Rottner and Stradal 2011c). The key step in the formation of branched F-actin pattern is the binding or incorporation of the Arp2/3 complex at pre-existing filaments. The Arp 2/3 complex can bind to pre-existing actin filaments at an angle of around 80° and initiate the formation of daughter filaments at the attachment site (R. Dyche Mullins, Stafford, and Pollard 1997; R D Mullins et al. 1998).

1.2.2 Filopodia and microspikes

Filopodia are finger-like actin-based protrusions which are produced by various cell types prominently during their migration on 2D substrates. Their major role can be found in contributing to cell protrusion and probable environmental sensing (Faix and Rottner 2006c; Rottner and Stradal 2011a). Additionally filopodia are also thought to be involved in formation of stress fibers (Nemethova, Auinger, and Small 2008; Catherine D Nobes and Hall 1995b). The aligned and tightly bundled actin filaments inside filopodia are oriented with their barbed ends towards the direction of migration (schematic illustration in (Figure 7)) (Faix and Rottner 2006b)(Svitkina and Borisy 1999b). Often filopodia and lamellipodia emerge simultaneously, although they are regulated distinctly and are assembled by different actin machinery proteins (C D Nobes and Hall 1995; Chhabra and Higgs 2007a; Rottner and Stradal 2011c).

The convergent elongation model of filopodia assembly proposes the existence of a so called tip complex. Residing at the tips of growing filopodia the tip complex elongates filopodia that emerge from the lamellipodial dendritic network. The tip complex apparently contains VASP, formins, Vav1, Abi and myosin X (Danijela Vignjevic et al. 2006a; Svitkina et al. 2003). Due to the convergent elongation model, filopodia are thought to be assembled from precursor filaments within the lamellipodia. These precursor filaments are clustered and processivly elongated at their barbed ends by Ena/VASP proteins. Actin filaments in filopodia are bundled by the cross-linking protein fascin (Mellor 2010a). Cross-linking of filopodia was proposed to be a key step of formation of functional actin structure, stiff enough to push forward against the cell membrane (Alex Mogilner 2006; Alexander Mogilner and Rubinstein 2005).

The tip-nucleation model is another convenient model of filopodia formation that suggests formins as central actors in the formation of these structures. This model was initiated by the discovery of formin mDia2 at the tips of filopodia downstream of Cdc42 activation (Peng et al. 2003). Supposedly, Cdc42 activates mDia2, which than can bind to filament barbed ends and initiate elongation of filaments from their tips. Elongation of filaments by mDia2 generates a force of 1.3 pN per actin filament (Kovar and Pollard 2004b). Apparently, a bundle of approx. 20 filaments could produce a force, strong enough to deform the cell membrane (Peskin, Odell, and Oster 1993). Supposedly, mDia2 at the tip of filopodia is able to produce such a force to deform

the cell membrane (Schirenbeck et al. 2006). Finally, in contrast to the convergent elongation model the tip nucleation model proposes the formation of filopodia from the top down and not as emerging from the base of filopodium (Mellor 2010b).

Another protein prominently involved in the formation of filopodia and microspikes is fascin. Fascin can bundle actin filaments *in vitro* (Otto, Kane, and Bryan 1979; Yamashiro-Matsumura and Matsumura 1986). In a number of cell types fascin specifically localizes to filopodia (Sasaki et al. 1996; Yamashiro et al. 1998; Yamashiro-Matsumura and Matsumura 1986; Svitkina et al. 2003). Fascin is highly expressed in cells that possess numerous filopodia. Whereas, other proteins are also able to cross link parallel actin bundles such as α-actinin (stress fibers), espin, fibrin and vilin only fascin among those, exclusively localizes along the entire length of filopodia. The shRNA mediated knockdown of fascin markedly reduced filopodia per cell in B16 mouse melanoma cells. Moreover, the number of filopodia per cell positively correlated with the expression of active, dephosphorylated fascin and vice versa (Danijela Vignjevic et al. 2006b).

1.2.3 Podosomes and invadopodia

Podosomes and invadopodia are structurally related actin-based protrusions, which are primarily formed by cells that have to move through different tissues and/or across the existing tissue barriers (Buccione, Orth, and McNiven 2004). A typical characteristic feature of these two related actin structures is an actin-rich core region. Furthermore, both structures are able to degrade ECM and its components and their presence is considered to be one of the main hallmarks of invasive cells (Stefan Linder, Wiesner, and Himmel 2011). In cells plated on 2D surfaces podosomes and invadopodia are induced at the ventral surface of cells and appear as actin-rich dots in fluorescence microscopy (Kurisu and Takenawa 2010a). Typically, N-WASP/WASP, Arp2/3 complex and cortactin as well as fascin are often found in podosomes and invadopodia and are enriched (or localize in proximity in case of fascin) in F-actin-rich core regions of these structures (Li et al. 2010a; Stefan Linder 2009). Invadopodia typically are observed in many cancer cell types and are considered as major degradative protrusions of these cells. Podosomes are primarily formed by cells from myeloid linage. Podosomes are supposed to stabilize or mediate the adhesion of a cell

to the underlying substrate and additionally can degrade the underlying ECM. The inhibition of formation or functionality of podosomes impairs the migration of macrophages in 3D Matrigel, but not on 2D glass coverslip surfaces (Cougoule Véronique Poincloux, Renaud Al Saati, Talal Mège, Jean-Louis Tabouret, Guillaume Lowell, Clifford A. Laviolette-Malirat, Nathalie Maridonneau-Parini, Isabelle 2009). Whereas numerous reports show that the inhibition podosome formation has a dramatic effect on migration of immune cells on 2D and apparently also *in vivo* (Jones et al. 2002b; S Linder et al. 1999a).

Besides many structural and functional similarities, there are also a key differences between podosomes and invadopodia. For example, the actin-rich core of podosomes is often surrounded by a ring of proteins that are usually associated with adhesive structures, such as vinculin, paxillin or talin. Yet, no other prominent adhesion associated proteins are found around actin-rich cores of invadopodia except talin. Furthermore, podosomes are not considered as protrusions, in contrast to invadopodia which can protrude several microns into the underlying substrate. Moreover, invadopodia differ from podosomes by size, temporal appearance and their special organization. Single podosomes are approx. 1µm in diameter and 0.4 µm in depth. They can appear organized in podosome rings. Invadopodia can form clusters up to 8 µm in diameter and 5 µm in depth. Moreover, lifetimes of invadopodia and podosomes differ significantly from each other. Invadopodia can persist for more than an hour, whereas podosome-lifetime is limited to several minutes (D. A. Murphy and Courtneidge 2011a).

Majority of actin filaments in both, podosomes and invadopodia are thought to consist of a branched actin network (because of presence and the essential role of the Arp2/3 complex). Formins are also involved in the formation of invadopodia. Therefore, the existence of unbranched actin filaments within the core region of this structure is being discussed. These unbranched actin filaments are apparently radially oriented to the core region in case of podosomes, or are successively polymerized at the tips of invadopodia. (Schoumacher, Louvard, and Vignjevic 2011; Lizárraga, Poincloux, Romao, et al. 2009). NPFs such as N-WASP or WASP, but not WAVE, are essential for the Arp2/3 complex dependent formation of the core region of podosomes (Kurisu and Takenawa 2010c). WASP is considered to be essential in the formation of podosomes in myeloid cells. Although in macrophages, N-WASP can reportedly compensate WASP in case of podosome formation (Jones et al. 2002b; Isaac et al. 2010). Formins also play a

significant role in the formation of podosomes. In particular, formin FMNL1 was shown to decorate the core region of podosomes in a cap like manner in macrophages. Furthermore removal of this formin reduced the adhesive capability of macrophages (Mersich et al. 2010).

Fascin an actin-bundling protein has been shown to localize in the proximity of podosomes of mouse dendritic cells and is thought to be involved in the turnover of these structures. Although, no data of co-localization of fascin with podosomes has been reported so far (Yamakita et al. 2011). Still few study reports are available that address the role of fascin in formation of podosomes and requirement and recruitment of fascin in core regions of podosomes in THP-1 cells or to podosome rosettes in smooth muscle cells suggesting an involvement of fascin in turnover of these structures (Quintavalle et al. 2010; Jayo and Parsons 2010; Yamakita et al. 2011).

A typical disease involving defects in podosome formation is WAS. In this disease the *WAS* gene in macrophages and dendritic cells carry several mutations. Interestingly, these cells cannot form podosomes (S Linder et al. 1999b). The absence of podosomes correlates with defective migration and chemotaxis in effected immune cells (Jones et al. 2002b).

Formins from DRF subfamily play an essential role in the formation of F-actin core region in invadopodia of breast cancer cell line. The siRNA-mediated knockdown of these formins caused severe defects in degradation of underling gelatin matrix and invasion capability into the Matrigel substrate (Lizárraga, Poincloux, Romão, et al. 2009). Fascin, an actin-bundling protein involved in the formation of filopodia and podosomes, was also shown to be enriched in invadopodia formed by cells plated on 2D gelatin. The knockdown of fascin severely reduced the number of invadopodia- (counted as cortactin rich dots) and additionally the number of filopodia per cell. The degradation area per cell was reduced to 60% of wildtype cells. Moreover, the ability of cells to invade into collagen I / Matrigel substrate was markedly affected (Li et al. 2010b).

Formins supposedly facilitate elongation of invadopodia due to the formation of longitudinal unbranched actin fibers in their tips after (or in the process) ECM has been degraded. The degradation of ECM in the proximity of invadopodia is accomplished by microtubule dependent recruitment of matrix metalloproteinases such as MT1-matrix metalloproteinase (MT1-MMP) at the matrix facing surface of invadopodia (Schoumacher, Louvard, and Vignjevic 2011).

Many cancer cell lines have a characteristic ability to form invadopodia. Fascin is considered to be a typical marker candidate of these structures being additionally essential for the formation of filopodia (Hashimoto, Skacel, and Adams 2005). Fascin also localizes in the invasive front of colorectal cancer and downregulation of this actin modulator decreases the invasiveness of the mentioned cells (Danijela Vignjevic et al. 2007a). Thus it can be speculated that upregulation of fascin in certain cancer types supports invadopodia formation which is followed by the increased invasiveness of those cancers. Therefore, the formation of invadopodia can be one of the steps in the progression of cancer to a more invasive grade (Li et al. 2010a).

1.2.4 Circular dorsal ruffles: One structure, multiple functions?

When cultured cells are stimulated with growth factors, either globally or in the form of chemical gradient, they form actin-based protrusions at cell periphery such as lamellipodia with embedded microspikes and filopodia and begin to migrate. In a case of stimulation of mouse embryonic fibroblasts (MEFs) with PDGF-BB, within 2-5 minutes after stimulation, these cells display transient actin-based protrusions termed as circular dorsal ruffles besides lamellipodia and filopodia. These transient circular actin-based protrusions are formed on the dorsal surface of cells. Within 5-20 minutes post stimulation this dynamic actin structure constricts and collapses back into the dorsal surface of a cell (Rottner and Stradal 2011c; Buccione, Orth, and McNiven 2004).

Microspikes and filopodia are enriched in circular dorsal ruffles. Consequently fascin, an actin-bundling protein in filopodia, is also localized and enriched in circular dorsal ruffles. The knock-down of fascin significantly decreases the rate of circular dorsal ruffle formation in MEFs (Schloen, K,. PhD thesis; Guledani, A. unpublished Data). Furthermore, the formation of circular dorsal ruffles requires almost similar actin machinery proteins as it is required for formation of peripheral ruffles. Besides active Rac, additionally active Cdc42 is essential for the formation of CRs whereas Cdc42 is dispensable for formation for the formation of lamellipodia. Inhibition of PI3 kinase or Akt kinase isoforms and subsequent inhibition of Rac GTPase diminishes both, dorsal ruffles and formation of lamellipodia in MEFs (Schloen, K,. PhD thesis).

1.2.4.1 Putative roles of CRs

Although decades have passed since the discovery of CRs, the functional role of these structures still remains elusive. It is possible that these dynamic actin structures harbor multiple functions (Buccione, Orth, and McNiven 2004). These functions could lead to a cumulative effect of the mobilization and reorganization of actin to prepare cells for migration. It has been proposed and experimentally shown that beneath circular ruffles stress fibers are actively dissembled. CR formation site also positively correlates with the area of subsequent lamellipodia formation (Krueger et al. 2003). Formation of circular dorsal ruffles is associated with several cellular processes, where extensive actin reorganization is required. These processes include receptor internalization, actin reorganization during cell migration, macropinocytosis and macropinocytosis mediated integrin redistribution and recovery during migration (Gu et al. 2011; Orth and McNiven 2006b). Although, it has already been shown that formation of CRs can support-, but is not essential in macropinocytosis (Suetsugu et al. 2003).

Circular dorsal ruffling was implicated in mediating selective internalization of EGF-Receptor independent of clathrin-coated pits. The engulfed receptors and ligands were shown to localize within dynamic tubules moving towards central areas of the cells. Therefore, authors assigned CRs to another distinct and clathrin-independent form of pinocytosis which is stimulated by growth factors (Orth and McNiven 2006b). It is still unclear, whether circular dorsal ruffling is another mechanism of pinocytosis or if pinocytosis is one of several functions of CRs.

It has been reported that during PDGF-BB stimulated cell migration, integrin-ß3 relocates form focal adhesions sites to circular dorsal ruffles. Form dorsal ruffles, integrins are reportedly internalized through macropinocytosis and enter endosomal compartments. From these compartments integrins are recycled to participate in the formation of new focal adhesions on the ventral surface of the cell (Gu et al. 2011). In contrast to that, reportedly during the random unstimulated- or basal cell migration the turnover of integrins always requires clathrin mediated endocytosis (Chao and Kunz 2009; Ezratty et al. 2009).

1.2.4.2 Endocytosis

Cells can take up extracellular material in a process termed endocytosis. Depending on physical state and size of the extracellular material to be internalized, this process is further divided in phago- and pinocytosis. Uptake of solid material (diameter < 250 nm) by cells is termed phagocytosis. On the contrary, uptake of liquid (diameter < 150 nm) is referred as pinocytosis. The endocytic vesicles formed during pinocytosis have a uniform shape in contrast to phagocytic vesicles, of which size and shape are determined by the geometry of the engulfed particle. Phagocytosis can be initiated by activation of membrane anchored receptors, given corresponding ligands are presented on the surface of the particle to be engulfed. If receptors on a cell surface recognize and bind to those ligands residing on a particle surface the cell subsequently activates phagocytic machinery. Pinocytosis in contrast to phagocytosis, occurs continuously during the lifetime of a cell at the specialized regions of the cell membrane. These regions are prominently coated with a protein termed clathrin and therefore are referred as clathrin-coated pits. Clathrin can form a characteristic basket around the invaginated cell membrane. During this process the extracellular fluid is taken up by cells for the further processing. During clathrin mediated endocytosis specific membrane bound receptors are activated by extracellular stimuli. This apparently ensures, selective enriching and ingesting of biomolecules at the membrane and from the extracellular space. A model example of this process is EGF mediated pinocytosis during which EGF binds and activates EGF-receptors at the extracellular surface of a cell membrane. This is followed by the accumulation of the EGF-receptors (EGFR) in clathrin-coated pits and their ingestion. Engulfed receptor-ligand complexes are thought to be degraded in lysosomes. This might be a mechanism of receptor downregulation at the cell surface. The higher the concentration of ligand such as EGF, the more intensely cells reduce the number of receptors on their surfaces (Alberts et al. 2002b).

Despite several implications of functional roles of CRs in cell migration no studies have been yet performed directly on cell migration or chemotaxis of cells lacking the ability to form these structures. Therefore, the present work addresses this issue using Cdc42 knockout MEFs that lack the ability to form CRs in response to PDGF-BB. Nevertheless, these cells can form filopodia and lamellipodia and show no growth defects or morphologically defective actin cytoskeleton.

1.3 Protrusion adhesion and retraction-three phases of cell migration

In contrast to 3D environments where cells display several modes and strategies of migration, on 2D surfaces most of the motile mammalian cells show one morphologically distinct mode of migration. This migration mode generally consists of cycles of protrusion formation, adhesion to the substrate and a retraction at the rear of the cell (figure 7) (Rottner and Stradal 2011c).

1.3.1 Protrusion

Protrusion phase of mammalian cells is accomplished by polymerizing actin into the filaments or polymers at the plasma membrane and in this way "pushing" the membrane with the resulting force in the specific direction (figure 7). The actin polymerization is a tightly controlled process involving Rho-GTPases as main regulatory switches. The GTPases, in dependence on extracellular stimuli, can activate a supporting machinery for the actin polymerization. These machines can either induce branched- or/and unbranched actin polymerization. As a consequence of branched, Arp2/3 dependent actin polymerization thin, sheet like protrusion termed lamellipodium emerges. Another type of actin protrusion that can co-occur- and is often embedded in lamellipodium is referred as microspike or filopodium- if it extends over the edge of the lamellipodium. A filopodium is a finger-like protrusion consisting of bundled unbranched actin filaments (figure 7). When cells are cultured on 2D surfaces that are coated with constituent proteins of ECM, some cell types can develop dot-like actin-based protrusions on their ventral side that can degrade ECM. This actin-based structure is termed as invadopodium or a podosome in case of macrophages. Podosomes and invadopodia are capable of degradation of the underlying substrate. The outer surface of invadopodia and podosomes can display ECM degrading enzymes such as metalloproteinases and degrade the underlying substrate. These enzymes on the other hand can be also secreted by invadopodia into the adjacent surroundings.

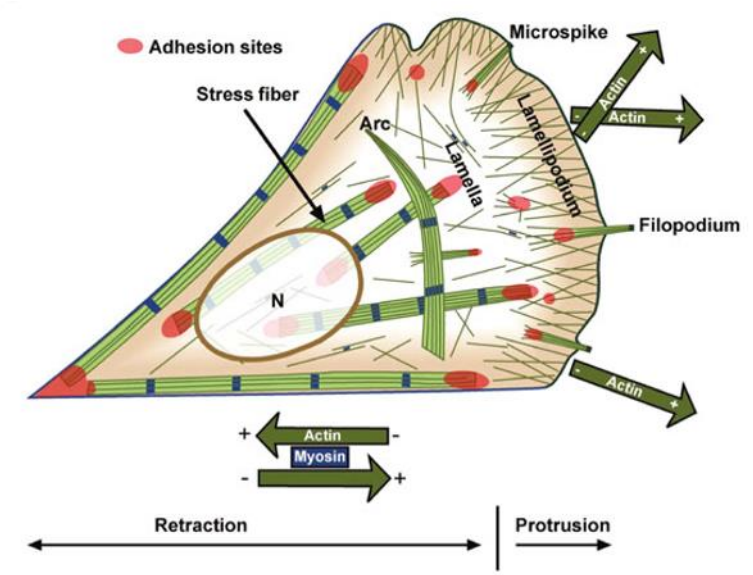

Figure 7: Schematic illustration of cell motility and corresponding actin-based structures in 2D migration (Adopted form Small and Rottner 2010). The lamellipodium is a major protrusive structure in a polarized migrating cell that is produced at the cell edge due to the activity of the Arp2/3 complex. This highly dynamic branched actin network grows in the direction of filament elongation. It produces the protrusive force for translocation. The filopodium is another prominent protrusive structure of migrating cells. Actin filaments are not branched in filopodia and are generated by nucleating activity of formins at the leading edge. In the course of migration cells also need to adhere to the substratum and retract their rear part of the body. This is achieved by contractile actin fibers termed stress fibers. Stress fibers are connected to cell-substratum adhesion sites (red) which link actin cytoskeleton to ECM enabling the force transmission. The repletion of protrusion, adhesion and retraction results in continuous cell movement observed on 2D substrates.

One of the major forces in cell movement is thought to be the force resulting from the formation of actin-based protrusions at the leading edge of a cell. The network of actin filaments at the leading edge can be divided into two distinct areas. A peripheral highly dynamic actin network which is poorly connected to the substrate (lamellipodium) and the cytoplasmic actin network of a cell. The cytoplasmic actin network is a "deeper" actin network and is termed as lamella. The lamella is thought to more tightly adhere to the substrate (via focal adhesions) than the lamellipodium. Some reports suggest that the resulting protrusive force is first generated when actin monomers are added to the filaments that are mechanically linked to the substrate (Stephens, Milne, and Hawkins 2008).

1.3.2 Adhesion

The cell-substrate adhesion on the 2D surface is accomplished by specialized adhesive structures called nascent adhesions that can evolve in focal contacts and focal adhesions. Contractile actin fibers, decorated with myosin II are anchored in these adhesion sites and constrict during the retraction of cell rear thus facilitating this process (Rottner and Stradal 2011c). Nascent adhesions are assembled near the leading edge of a moving cell. These structures are first initiated and can later undergo maturation into the focal contacts or disassemble rapidly. Focal adhesions are complex multiprotein structures which are organized in a layered architecture of specialized signaling or adaptor proteins and actin filaments as shown by super-resolution microscopy (Schwartz 2011). This architecture shows distal integrin layer decorated with protein layer which directly interacts with actin filaments. In this way the ECM is indirectly coupled with the cytoskeleton.

The question, which actin nucleators are involved in the nucleation of actin filaments in the focal adhesions still remains unanswered. Formin mDia1 is implicated in this process, nevertheless the fact that its deletion did not substantially influence the formation of stress fibers and focal adhesions (Peng et al. 2003). Also Arp2/3 complex is thought to play a role in actin nucleation events during nascent adhesion formation, but the clear evidence of this mechnism is still missing (Rottner and Stradal 2011c).

The early stage of formation of focal contacts involves integrin binding to the extracellular cues (ligands) usually beneath the protruding edge of a cell. At this stage the adhesive structures are termed nascent adhesions, which then can either disappear or evolve into more stable and strong focal adhesions. During the maturation of nascent adhesion, integrins are clustered to this structure. Clustered integrins can recruit signaling/adaptor proteins and actin filaments and to their cytoplasmic domains (Hynes 2002). As adhesions are still in the process of formation, they are termed as focal adhesions. After maturation into larger protein complexes they are referred as focal complexes (Brakebusch and Fa 2003).

1.3.2.1 Integrins

Integrins are transmembrane heterodimeric glycoprotein receptors, which mediate cell adhesion and linkage of the cytoskeleton to extracellular environments. The integrin heterodimers consist of extracellular ligand binding domain, a transmembrane domain and cytoplasmic domain which can bind to an adaptor and signaling proteins. Integrin heterodimers are composed of α- and β-subunits that are non-covalently attached to each other. These adhesion proteins are presented either in an inactive- or activated state on the cell surface. While most of the heterodimers are widely expressed- they can be as well specifically expressed by certain cell types (Takada, Ye, and Simon 2007).

The activation of integrins also involves the binding of talins and kindlins on the intracellular domain and extension of extracellular domains of integrins. In an active state α- and β-subunits change their spatial orientation to each other as well as their intracellular conformation. These changes lead to the unfolding of the extracellular domain which can bind to ECM proteins. In this open conformation extracellular binding of ECM-proteins to integrins can occur. The binding to ECM is followed by clustering of activated integrins, which is a necessary step for evolving of nascent adhesions into stronger focal adhesions.

One of the key steps in the formation of focal adhesion is the recruitment of vinculin to integrins, which can bind to talin and actin, supposedly acting as an adaptor protein. It has been reported that vinculin also binds to Arp2/3 complex and promotes in this way the actin nucleation at focal adhesions (Srichai and Zent 2010). This might serve to strengthen the linkage of the actin cytoskeleton to adhesion sites and thus to ECM.

1.3.3 Retraction

1.3.3.1 Contractile actin bundles in cell migration

The retraction phase of cell movement is thought to be a result of the activity of bipolar contractile arrays of actin filaments with incorporated myosin II at the rear of the cell (Small and Rottner 2010). Stress fibers (SF) represent such bundled contractile actin filaments. Stress fibers are often

formed by stationary cells in response to mechanical tension on the cell exterior. These structures are visible in cultured cells in fluorescence microscopy on the ventral surface of the cell. Usually stress fibers are anchored at one or both ends to focal adhesions. The bundled actin filaments in stress fibers are cross-linked via α-actinin, which is the major cross-linking protein found in these structures. The α-actinin is periodically distributed on stress fibers and is followed by myosin II, a distribution reminiscent of muscle sarcomere. Several types of stress fibers have been described so far. Besides ventral stress fibers also dorsal stress fibers and "transverse arcs" were detected. Dorsal stress fibers are reportedly anchored only at their one end in focal adhesion and are perceived as precursors of ventral SFs. "Transverse arcs" are formed at the base of lamellipodia. These contractile stress fibers have a convex shape and are not anchored in focal adhesions (Burridge and Wittchen 2012; Le Clainche and Carlier 2008a).

Cells can apparently assemble stress fibers using various mechanisms. Although, generally the formation SFs is controlled by RhoA GTPase and occurs majorly by aggregation of pre-existing actin filaments rather than *de novo* actin polymerization. Besides RhoA, myosin II plays a major role in this process (Chrzanowska-wodnicka and Burridge 1996). Myosin II is activated by ROCK downstream of RhoA and is involved in the bundling of SFs, additionally to its role in the contraction of these structures (N Watanabe et al. 1999). RhoA GTPase can mediate assembly of stress fibers reportedly also by activation formins of mDia family. These formins appear to be important in normal dorsal SF assembly by increasing the F-actin density at the focal adhesions (Oakes et al. 2012; Hotulainen and Lappalainen 2006). Although, SFs can be still induced in the absence of mDia and simultaneous overexpression of ROCK. Under such conditions stress fibers appear thicker than in control cells in fluorescence microscopy (N Watanabe et al. 1999).

SFs are also assembled by transformation of dorsal SFs and "arcs" into the ventral SFs. Also two dorsal SFs can fuse and form a ventral SF (Hotulainen and Lappalainen 2006). Additionally, contractile actin bundles are formed by recycling of filopodia from the leading edge back to lamella region of the migrating cell where they are bundled to form contractile fibers. This process is myosin II-dependent. The contractile actin fibers that are assembled by this pathway are oriented parallel to the leading edge (Nemethova, Auinger, and Small 2008).

Contrary to the claims that stress fibers are only formed in 2D cell culture, SFs were detected in myofibroblasts of *in vivo* wound granulation tissue where they probably play a role in wound

contraction and closure. Moreover, the formation of SFs can be induced in endothelial cells grown under shear stress similar to that in arteries which indicates their functional role *in vivo* processes (Tomasek et al. 2002).

In contrast to prominent stress fibers of cells cultivated on 2D surfaces, in cells grown in 3D collagen or other 3D matrices stress fibers are rarely observed. Only when these 3D gels are firmly attached to a supporting surface, in contrast to free-floating gels, the embedded cells tend to develop microscopically visible stress fibers (Contraction and Grinnell 1994).

Although cell migration without contractile actin arrays is unlikely, still the role of SFs in cell migration is controversially discussed. One of the reasons for that was reduced appearance of these structures in many highly motile cell types during their migration process. Conversely, the possible role of these actin structures in cell migration could be the force generation required to detach adhesions at the rear thus contributing to release of the cell rear during the migration (Crowley and Horwitz 1995). But studies involving inhibition formation of stress fibers downstream of Rho GTPase resulted in markedly increased cell motility during wound closure. This led authors of the study to the conclusion that stress fibers are not necessary for cell migration and even can counteract this process (C D Nobes and Hall 1999). Another report showed that cell contraction at the trailing edge doesn't involve stress fibers at all (Small and Resch 2005; Pellegrin and Mellor 2007). Cell contraction at the cell rear therefore is assigned to contractile actin arrays or assemblies with incorporated myosin II that connect traction points on the cell surface with one another (Small and Rottner 2010).

1.3.4 Random migration and chemotaxis

Chemotaxis is termed a process of cell migration in the direction of a special cue often provided in the form of a gradient of chemoattractant molecules. Pro- and eukaryotic cells are able to sense and interpret chemical gradients by utilizing diverse mechanisms. Bacterial cells can follow such gradients by a trial and error process which involves periodical sensing of surroundings for a higher concentration of chemoattractant. This is followed by movement of the bacterium in the direction higher concentrations for statistically longer time periods than towards an environment

presenting a lower chemoattractant concentration. Lower chemoattractant concentration causes quicker changes in cell trajectory of moving bacteria. In this manner there is a higher chance of bacteria moving up the gradient (D. Wu 2005). Eukaryotic cells have more complex mechanisms to interpret and respond to chemical gradients. These processes involve "measuring" the gradient presumably at two rear points of a cell periphery and transforming this information into a much steeper intracellular biochemical gradient. Mammalian cells are undergoing chemotaxis in different situations during their life cycle. Macrophages are attracted to sites of inflammation during the invasion of bacteria. Neuronal- and embryonic cells migrate and perform chemotaxis during their specific development stages. Epithelial cells and fibroblasts migrate into the wound during the wound healing process. In tumorigenesis cancer cells brake through tissue barriers and metastasize into certain tissues, which involves at certain stages chemotactic migration towards chemoattractant gradients. The ability to translate the extracellular gradient of the chemotactic ligand into intracellular gradients of molecules such as products of PI3 kinase activation is essential for chemotaxis. As a consequence of this translation, highly motile eukaryotic cells such as *Dictyostelium* or neutrophils acquire polarized morphology oriented towards chemoattractant gradient during their chemotaxis (Stephens, Milne, and Hawkins 2008).

In mammalian cells chemotaxis is generally trigged by chemoattractant molecules that bind to their specific cell surface receptors, which activates latter. This is followed by activation of membrane-adjacent signaling proteins such as of PI3 kinase. These processes contribute to a polarization of the cell towards the gradient of specific chemoattractant. Thereafter, actin polymerization and formation of F-actin-rich protrusions in the direction of increasing chemical gradient takes place. The presence of chemical gradient leads to stabilization of cell polarization and continuously stimulates actin polymerization during the cell protrusion.

In a polarized cell many intracellular proteins also show polarized distribution and in many cases one of the initial steps to accomplish this polarization is a synthesis of phospholipid PIP_3 by the PI3 kinase. In this reaction activated PI3 kinase converts PIP_2 into PIP_3. PIP_3 can bind to proteins harboring pleckstrin homology domain (PH-domain) thereby mediating the recruitment of these proteins to the plasma membrane. In this way the activity of recruited proteins can be regulated directly at the membrane (D. Wu 2005). In the majority of studied chemotactic processes the

chemoattractant induces accumulation of 3'-phorsphorylated phosphoinositide lipids (PI) predominantly at the cell periphery that faces chemoattractant (Hall 1998; Kundra et al. 1994b). Accordingly, proteins harboring PH domains of high class specificity towards PI3 kinase products tend to locate at the leading edge of chemotactic cells (Parent and Devreotes 1999a). Protein Kinase B (PKB/Akt) is one of such proteins containing high affinity PH domain and also localizes to the leading edge (Parent and Devreotes 1999b). It is also required by *Dictyostelium* during polarization (formation of F-actin protrusions) towards chemoattractant (Funamoto et al. 2001). In *Dictyostelium* PhdA is PH domain containing protein which enriched at the membrane when cells are stimulated with cAMP. PhdA is thought to serve as a scaffolding protein to recruit other actin machinery proteins to the leading edge (Metello Innocenti et al. 2003).

Signaling in chemotaxis

Besides *Dictyostelium*, also subtypes of leukocytes such as neutrophils respond to chemoattractant gradients mainly via activation of heterotrimeric G-protein coupled receptors (GPCRs). In leukocytes chemotactic motility can be induced by various ligands such as C5a, fMLP and IL-8 that mediate immune responses. These ligands bind to GPCRs and resulting signals are mostly transduced by pertussis sensitive $G\alpha_i$ family of G-proteins. The βγ subunits of these G-proteins are thought to propagate chemotactic signals in similar ways (Shefcyk et al. 1985; Goldman et al. 1985).

Activation of G-proteins engages a large number of intracellular effectors, which are reportedly important in chemotaxis such as Ras- and Rho-family of GTPases, PI3 kinase, Phospholipase C and Phosphatase A_2 (PLA_2). In leukocytes, chemoattractants bind to their corresponding GPCRs leading to activation associated heterotrimeric G-proteins (consisting of α, β, γ-subunits). Activated GPCR promotes the exchange of GDP to GTP in Gα subunit of the G-protein. This leads to dissociation of Gα- from G-βγ subunit. In case of chemotactic signals in leukocytes, specific $G\alpha_i$ subunit inhibits adenylate-cyclase thus reducing the intracellular cAMP level, whereas βγ-subunit can activate several chemotaxis relevant effectors such as Phospholipase C, PI3 kinase and ion channels. However, also $G\alpha_{12/13}$ was reported to activate Rho-GTPases leading to chemotaxis (J. Xu et al. 2003; Stephens, Milne, and Hawkins 2008).

The activity of PI3 kinase greatly contributes to the polarization of the cell towards a gradient of chemoattractant. This process leads to the final stage of cell polarization which is the formation of F-actin-rich protrusions towards the chemical gradient. From different classes of PI3 kinases (PI3Ks), PI3K class I are the most prominently involved in chemotaxis. PI3Ks can phosphorylate phosphoinositides (PtdIns), PtdIns4P and PtdIns (4, 5) P2 at the 3' position. PI3K can be activated by many types of membrane receptors to produce PtdIns (3, 4, 5) P3, which are mostly distributed at the inner leaflet of a plasma membrane. Head groups of PIP_3 and PIP_2 can bind selectively to signaling proteins that contain PH domains. These proteins thereafter can transduce the signal to various destinations in a cell (Stephens, Milne, and Hawkins 2008). PIP_3 produced by PI3K is considered to be a part of a compass mechanism of a cell that detects a vector of the extracellular gradient. Although, PI3K signaling appears not to be the main conserved mechanism that guides the chemotaxis as a cellular compass (Ferguson et al. 2007). Besides PIP_3, also polarized distribution of PIP_2 appears to be essential for proper polarization and chemotaxis. Phosphatase and tensin homolog (PTEN) is a phosphoinositide 3' specific phosphatase that dephosphorylates phosphatidylinositol (3, 4, 5)-trisphosphate (PIP_3) to phosphatidylinositol 4, 5-bisphosphate (PIP_2) and PIP_2 to phosphatidylinositol 4-phosphate (PIP). Similar to the kinetics of localization of PIP_2, PTEN is localized to sides and back of the cell and is expelled from the leading edge of a cell during chemotaxis. Apparently, N-terminus of PTEN harbors PIP_2 binding site which is responsible for membrane localization of later. The PIP3/PIP2 gradient produced by the interplay of PI3K and PTEN at the cell periphery represents a conserved mechanism in chemotaxis of eukaryotes (Merlot and Firtel 2003).

1.3.4.1 PI3 kinase effectors in chemotaxis

PI3 kinase and its products can activate signaling and adaptor proteins which are important for chemotaxis. One of the signaling proteins downstream of PI3 kinase is PKB/Akt kinase, which is involved in myosin II assembly and thus retraction at the rear of the cells during chemotaxis of *Dictyostelium* cells and leukocytes (Chung and Firtel 1999). Another prominent effector of PI3K in *Dictyostelium* is PhdA which is involved in F-actin assembly at the cell leading edge, presumably as an adaptor protein and has no clear homologue in mammals (Merlot and Firtel 2003).

Unconventional GEFs such as DOCK180, DOCK2 and zizimin1 are also thought to be regulated by PIP_3 due to their binding specificity to this molecule. Dock 180 is a specific GEF for Rac (E et al. 2002), whereas zizimin1 reportedly is a GEF for Cdc42 (Côté and Vuori 2002; Meller et al. 2002a). These GEFs are likely to be involved in cell polarization, but their roles have not been well studied to date. Furthermore, PIP_3 activates its own positive feedback loop which apparently signals selectively to Rac GTPase (F. Wang et al. 2002; Weiner et al. 2002).

Also PLA_2 activity has been reported as a supportive mechanism to chemotaxis independent of PI3K signaling in *Dictyostelium*. In these cells both pathways, either downstream PI3K or PLA_2, act in a redundant manner, but are not molecular replacements for one another (Van Haastert, Keizer-Gunnink, and Kortholt 2007; Takeda et al. 2007) (Stephens, Milne, and Hawkins 2008).

1.3.4.2 Chemotactic signaling in MEFs

Besides general chemotaxis mechanisms that are activated in response to a broad range of chemoattractant gradients, there are also specialized chemotactic responses that are activated during certain external processes. For example, in wound healing: fibroblasts from adjacent tissue are recruited into the provisional matrix of the wound. In this case PDGF-BB is the chemoattractant which mediates the recruitment of these specific fibroblasts and is thought to be secreted by macrophages and platelets. PDGF-BB activates its specific membrane bound receptor (PDGFR) in fibroblasts leading to recruitment of PI3 kinase to the cytosolic side of receptors and activation of latter. This leads to the generation of PIP_3 at the membrane and to rather polarized recruitment and activation of Rho GTPases Rac and Cdc42 to the leading edge. RhoA GTPase which mediates cell retraction is recruited to the trailing edge of a cell. At those locations the GTPases orchestrate turnover of actin filaments leading to protrusion formation in the front and retraction at the rear of a cell (Hall 1998; Kundra et al. 1994b).

Activation of PI3 kinase appears to be one the most primary events after growth factor stimulation which can induce the PIP_3 gradient at the leading edge. PIP_3 can recruit proteins necessary for actin remodeling that bear PH domains. Simultaneously, PTEN is removed from the leading edge to lateral and posterior of the cell, where it can dephosphorylate PIP_3 to PIP_2 supporting

thereby the formation of PIP_3 gradient at the leading edge. PIP_2 is responsible for localization of PTEN at the rear of the cell where it exhibits its inhibitory effects on cofilin. The Removal of PIP_2 from the leading edge is supposedly due to the activity of PIP_2 specific PLC and not of directly PI3 kinase (Merlot and Firtel 2003).

Due to widely accepted model the stimulation of eukaryotic cells by chemoattractants leads to activation PI3K and PTEN and production and enrichment of PIP_3 at these sites. PIP_3 can recruit GEFs via their PH domain at the membrane and enhance their activation. GEFs can activate GTPases Rac, Rho and Cdc42, in concert with other proteins, at the membrane. These proteins mediate the recruitment and activation of WASP/ WAVE family proteins at these sites, which consequently leads to a burst of actin polymerization by activation of nucleators such as Arp2/3 complex and/or formins at this location (Merlot and Firtel 2003). Furthermore, the F-actin synthesis is supported by cofilin, an F-actin severing protein. Due to its activity cofilin can produce new barbed ends for actin polymerization and thus promote this process (Bailly et al. 2001; Thomas D. Pollard and Borisy 2003).

To achieve the effective migration towards a chemical gradient, stimulated cells have to maintain the continuous formation of protrusions at the leading edge. These protrusions are presented as filopodia, lamellipodia and membrane blebs when cell migration of 2D substrates is considered (Rottner and Stradal 2011b).

1.3.4.3 Signaling downstream of Rac and Cdc42 to actin-based protrusions

Reportedly the growth factor induced the formation of lamellipodia downstream of active Rac is essentially dependent on the constituent of WAVE complex, Nap1 (Hem2) protein. In line with this, the knockdown of Nap1 leads to the breakdown of WAVE complex and marked interference of lamellipodia formation in melanoma cells (Steffen et al. 2004b). Supposedly, assembly of actin polymerization machinery takes place at the membrane where WAVE complex is recruited and activated (T. Stradal et al. 2001a).

Activated Cdc42 and PIP_2 can bind to CRIB and basic domains of WASP/N-WASP respectively, leading to release of VCA domain and thus activation of WASP. The active WASP is an activator of Arp2/3 complex inducing the actin polymerization (Theresia EB Stradal and Scita 2006; Heon Park, Chan, and Iritani 2010b; Kurisu and Takenawa 2010c). Cdc42 mediated activation of WASP leads to the formation of podosomes in macrophages. In fibroblasts, this interaction leads to actin reorganization required for endocytosis or vesicle trafficking (Theresia EB Stradal and Scita 2006). Similarly, Cdc42 mediated activation of the Arp2/3 complex by N-WASP might be important of not essential for formation of invadopodia in cancer cells and transformed fibroblasts that can form these structures (Kurisu and Takenawa 2010a). The activation of Cdc42 GTPase also prominently induces filopodia (C D Nobes and Hall 1995). This was thought to be caused by Cdc42 induced activation of WASP/N-WASP and subsequent Arp2/3 complex activation. Additionally, deletion of N-WASP disrupted formation or generation of filopodia in murine fibroblast cells (Snapper et al. 2001). However, further research showed that Arp2/3 complex was absent from microspikes and from tips of filopodia. Subsequently a tip-nucleation model was developed that suggests formins as major actin nucleators during formation of filopodia. In line with these formins are located at the tips of growing filopodia. Cdc42 and its related GTPase Rif can bind to Drf3 (or murine mDia2) and this interaction induces reportedly the formation of filopodia (Pellegrin and Mellor 2005). Although, the deletion of Cdc42 did not lead to loss of filopodia in murine ES-derived cells (Mains, Sulston, and Wood 1990). However, in Swiss 3T3 fibroblasts dominant negative expression of Cdc42 led to abrogation of the formation of filopodia (C D Nobes and Hall 1995). Furthermore, active Cdc42 was reported to bind to ISPR53 (Insulin Receptor Substrate of 53 kDa) which can also bind to PIP_2 lipids and induce negative curvatures in cell membranes. This interaction apparently recruits VASP to sites of formation of filopodia indicating that this mechanism, in concert with formin driven actin nucleation, could be an important pathway in the formation of filopodia (Disanza, Bisi, Winterhoff, Milanesi, Ushakov, Kast, Marighetti, Romet-Lemonne, et al. 2013).

1.3.4.4 Roles of Cdc42 and downstream actin protrusions in chemotaxis *vs* random migration

During their migration, cells that are plated on 2D surfaces, use several kinds of actin-based protrusions such as lamellipodia, filopodia and membrane blebs to protrude in a certain direction. These protrusions are apparently formed downstream of distinct Rho GTPase signaling pathways, which are coordinated to each other due to their cross-talk. Whereas, the assembly of these actin-based structures is well understood, the relative contribution of different actin protrusions to different migration scenarios such as chemotaxis or random migration still has to be elucidated.

The roles of actin-based protrusions of mammalian cells were studied most widely *in vitro* using 2D migration assays of macrophages, in the migration of fibroblasts and in protrusion of neurons. The first cues indicative of the roles of actin protrusions in cell migration came from identification of the major cause of Wiskott-Aldrich syndrome as the mutation in *WASP* gene. This mutation resulted in defective podosome formation in macrophages of WAS patients. The affected macrophages showed defective chemotaxis, polarization and cell migration, which could be reversed by expression of full length *WASP* gene in these cells (Jones et al. 2002b; S Linder et al. 1999b).

In fibroblasts, expression of Cdc42 GTPase is known to induce the formation of filopodia. Removal of this protein reduces the numbers of these structures, effects negatively cell polarization towards chemotactic cues and leads to generally reduced cell velocity during 2D migration (Catherine D Nobes and Hall 1995b; Kozma et al. 1995; C D Nobes and Hall 1999; Czuchra, Wu, Meyer, van Hengel, et al. 2005). In macrophages activation of Cdc42, similar to fibroblasts, induced formation of filopodia. Loss of this GTPase is associated with or reduction of filopodia numbers, reduced cell polarization, cell velocity and chemotaxis (Allen et al. 1998). In hemocytes of *Drosophila*, which resemble neutrophils and macrophages form mammals, loss of Cdc42 led to diminished directional persistence, but the increased velocity of these cells during *in vivo* wound closure assay (Stramer et al. 2005b).

It is commonly accepted that Rho GTPases regulate actin polymerization at the leading edge of the cell during chemotaxis or random migration. The generated protrusions such as lamellipodia,

filopodia and invadopodia/podosomes are induced downstream of active Rac1 and Cdc42 respectively. One very common characteristic of Cdc42 activation is that this GTPase induces the formation of filopodia. However, how the signal after activation of Cdc42 is propagated to actin structures is still not fully understood. Furthermore, contributions of lamellipodia and filopodia in different mechanisms of cell migration is not well understood. Thus one of major aims of the present work is to shed more light on these issues.

1.3.5 Role of Cdc42 in cell polarity and migration

Prior to chemotaxis cells tend to acquire polarized morphology which is expressed by the formation of filopodia and lamellipodia towards increasing gradient of specific chemoattractant. Rho GTPase Cdc42 is thought to play an important role in the ability of the cell to adopt polar morphology. This was first indicated by defective budding and rounded shape of *S. Cerevisiae* cells as consequence of Cdc42 gene knockout (A. E. Adams et al. 1990a). In mammalian cells knockout Cdc42 led to the non-polar formation of actin-based protrusions as well as loss of orientation of Golgi apparatus towards the direction of movement. The role of Cdc42 was proposed to locate formation of actin protrusions and on the other hand orchestrate the orientation of Golgi apparatus towards the direction of cell movement during migration (C D Nobes and Hall 1999). Other studies showed that Cdc42 knockout cells could sense directional cues, but could not maintain the directional movement. Apparently, other GTPases of the Cdc42 family could have redundant functions to Cdc42 (Mains, Sulston, and Wood 1990). The role of Cdc42 as a GTPase that mediates the locus of formation of actin-based protrusions is further supported by a study where Hemocytes of *Drosophila* showed the non-polarized formation of lamellipodia, reduced directional movement and increased migration speeds when *Cdc42* gene was removed (Stramer et al. 2005b). Another report showed that in neuronal cells depleted of Cdc42, polarized formation actin protrusions and thus formation of an axon was also lost (Garvalov et al. 2007). In contrast to this reports the defects in cell polarity associated with loss of Cdc42 were primarily assigned to loss of microtubule orientation, which is also important for cell polarization and directional migration. During cell migration the Centrosome and Microtubules are often directed towards the direction of cell motion thereby directing intracellular transport pathways towards the leading

edge to supply the leading edge. This was thought be important for persistent migration. Later, it was reported that Cdc42 is a potent regulator of the reorientation of microtubules and of the centrosome in astrocytes and fibroblasts (C D Nobes and Hall 1999; Palazzo et al. 2001; Sandrine Etienne-Manneville 2006).

1.4 3D cell migration

In contrast to 2D *in vitro* environments, where cells can adhere only at their ventral surface, the majority of mammalian cells *in vivo* are surrounded by a three dimensional ECM. Therefore, cells interact and probably adhere to it, all over the cell surface. There are mainly three types of extracellular matrices in the mammalian organism. These are a dense connective tissue, a lose connective tissue and a tightly packed basement membrane. The Basement membrane is a thin and very dense layer of ECM. The three-dimensionality of ECM supplies the cells with additional information that can trigger typical cell type associated responses to various extracellular stimuli (Even-Ram and Yamada 2005a).

During the migration of cells in the 3D matrix, cell movement is often termed generally as “mesenchymal” or amoeboid” movement. To denote movement as mesenchymal or amoeboid depends on the occurrence of the cell to matrix adhesions and involvement of matrix degradation during cell migration. The “mesenchymal” mode of cell migration in 3D has similarities to cell migration on 2D surfaces, such as a spindle cell shape and a movement composed of cycles of protrusion, adhesion and retraction of the rear. “Mesenchymal” movement is often accompanied by degradation and remodeling of surrounding matrix, which is most prominently observed in cancer cells (Katarina Wolf et al. 2003). On the other hand, the “amoeboid” movement of cells in 3D is characterized by rounded cell shape and quick shape changes during the migration due to rapidly protruding cell projections called pseudopodia and / or membrane blebs. Amoeboid movement is accompanied by weak cell-matrix adhesions and an absence of matrix degradation and remodeling (Katarina Wolf et al. 2003; Renkawitz et al. 2009a). Although, these two migration modes are not sharply defined and represent rather two extreme cases of a spectrum (Renkawitz et al. 2009a). Interestingly, some cells types are able to switch between the migration modes or use

mixed migration mode to adopt to changes in tissue struckture (Katarina Wolf et al. 2009). Invasive cancer cells can invade and migrate into a 3D environment using several strategies (Figure 8). Cancer cells can either migrate collectively or a portion of cells can detach from the primary tumor and migrate as single cells. These single migrating cells can move either in adhesion dependent mesenchymal mode, accompanied by matrix degradation or they can use non-degradative amoeboid mode accompanied by weak cell-matrix adhesions (Katarina Wolf et al. 2003).

Cells that show higher levels of integrin expression and stronger cytoskeletal contractility on 2D substrates tend to adhere and degrade 3D matrix when they encounter such environment (fibroblasts, endothelial cells, many cancer cells). In contrast, smaller cells that express low levels of integrins (T cells, dendritic cells, some tumor cells) use 3D migration strategies which are less- or entirely integrin-independent and does not require matrix degradation. These types of cells rather morphologically adopt to pre-existing matrix gaps (Friedl and Bröcker 2000).

1.4.1 Leading edge in 3D migration

On 2D substrates, many eukaryotic cells protrude with a clearly distinguishable flat leading edge, composed of lamellipodia and filopodia, during their migration. In contrast, same cells when embedded in a 3D environment such as in collagen *or in vivo*, the leading edge of mesenchymal migrating cells is narrow and difficult to visualize in detail. This problem raised the question if protrusions characteristic of 2D migration such as lamellipodia still exist in 3D (Beningo, Dembo, and Wang 2004). A study using electron microscopy reported that cells in 3D collagen matrix possess protrusions, which due to their different and complex morphology compared to protrusions on 2D, were termed as pseudopodium. However, very small sheet like protrusions were observed at the tips of pseudopodium, which could be putative lamellipodia. This indicated the presence of small lamellipodia at the leading edge of cells embedded in 3D collagen (Heath and Peachey 1989; Even-Ram and Yamada 2005a).

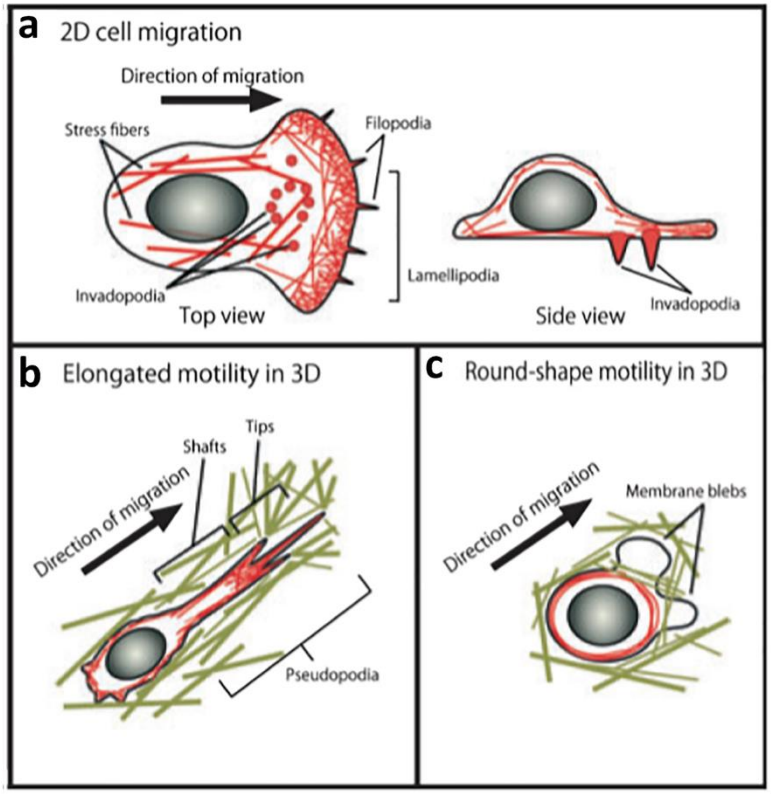

Figure 8: Different modes of cell motility in 3D *vs* 2D environments (adopted and modified from (Kurisu and Takenawa 2010b). a) During 2D migration cells display typical spindle-shaped morphology with leading edge consisting of lamellipodia and filopodia. To degrade underling matrix cells form invadopodia (side view). b) Cells that migrate in 3D often show wedge-shaped morphology with narrow and less defined leading edge. Some cell types in 3D display rounded morphology during their migration that is accompanied by blebbing of the cell membrane.

Because pseudopodia were typically observed in cells migrating in mesenchymal mode, these structures were regarded as protrusions of mesenchymal migrating cells. Further research showed that pseudopodium is basically a cylindrical and relatively long (approx. 1/3 of a cell) actin-based protrusion. According to the previously reported definition, pseudopodium comprises of two components: a shaft which is supported by thick cortical actin bundles and a tip with several filopodia-like protrusions embedded in a very small lamellipodia-like structure. The tip of pseudopodium is in contrast to shaft densely packed with F-actin (Kurisu and Takenawa 2010c).

In a recent study pseudopodia formed by HT1080 cells during 3D migration where classified as protrusions of first, second and third grade, or as mother and daughter protrusions. The daughter protrusions used to emerge from mother protrusion. The formation of mother protrusion was dependent on focal adhesion proteins focal adhesion kinase (FAK), talin or p130Cas, whereas the

formation of daughter protrusions was Arp2/3, WAVE1, N-WASP, cortactin and Cdc42 dependent (Giri et al. 2013b).

Besides pseudopodia, membrane blebs are thought to represent an alternative way to actin-based protrusions to project cell body to another location in the process of cell migration. The blebbing associated cell migration, is preferably grouped to amoeboid movement, which implies weak adhesions to the matrix and its greater dependency on cell contraction. Bleb formation is accomplished by myosin II mediated actin contraction, which results in a local rise in hydrostatic pressure followed by rupture of cortical actin network or local detachment of membrane from the cortical actin. In both cases cytosol flows along the newly generated gradient of hydrostatic pressure. This force protrudes the membrane and forms the bleb. After reaching the pressure equilibrium the cortical actin is re-established in a newly formed bleb and contracts leading to bleb retraction. This process is than restarted again (Blaser et al. 2006; Renkawitz et al. 2009b; Paluch and Raz 2013; Sixt 2012)

Another newly described type of actin-based protrusion associated with migration of fibroblasts in 3D was recently termed as lobopodium. Lobopodia are described as bluntly ended protrusions that develop multiple small blebs on their surface. Typical lamellipodia markers such as active Rac1, Cdc42 or PI3 kinase where not enriched in these structures. Although lobopodia of these cells were sensitive to inhibitors that impair acto-myosin contractility. Furthermore, lobopodia-based 3D migration of fibroblasts was accompanied by formation of focal adhesions by these cells (Sixt 2012; Petrie and Yamada 2012).

1.4.2 Invasion of cells in 3D ECM-the role of invadopodium.

During the invasion of cancer or fibroblast cells in collagen-based ECMs the encountered matrix is usually degraded and/or modified. This is achieved reportedly through invadopodia. Invadopodia, besides their protrusive role, apparently present or secrete zinc-dependent matrix metalloproteinases (MMPs) at their surface. In line with this, elevated MT1-MMP expression coincides with invasive potential of many tumor cells. Apparently, fibroblasts and tumor cells degrade

Type I collagen predominantly utilizing this protease. Depletion of MT1-MMP reportedly affected invasiveness of cells into collagen, but not their migration on 2D collagen coated surfaces (Sabeh et al. 2004). Further, it was shown that MT1-MMP is enriched in invadopodia and is important in matrix degradation at these sites (Nakahara et al. 1997; Caldieri et al. 2009; Stefan Linder 2007).

Form proteins of actin-nucleating machinery, N-WASP, cortactin and Arp2/3 complex reportedly are enriched in invadopodia. N-WASP is apparently essential for the formation of invadopodia as these structures are induced by EGF downstream of Cdc42 and EGFR pathway in highly invasive rat adenocarcinoma cells (mtln3) on 2D (Yamaguchi et al. 2005; Yu et al. 2012). Actin-bundling protein fascin is highly expressed in tumors and is mostly enriched at their invasive front. Fascin also is suggested to be important in the formation of invadopodia. Knockdown of this protein in cancer cells leads to reduced numbers of invadopodia and decreased matrix degradation. In 3D matrix knockdown of fascin led to markedly reduced invasiveness and reduced actin-based protrusions (Li et al. 2010a).

In contrast to migration on a 2D surface, in order to move in 3D some cell types additionally have to modify and degrade collagen matrix. Opinions are divided about the sites of the breakdown of ECM by cells. Several degrading protrusions and sites are being discussed. Macrophages seeded in collagen matrix or Matrigel can display numerous protrusions that can be enriched in F-actin at their tips and degrade collagen at these loci, although the matrix degradation was also detected at the cell rear and periphery in general. (Van Goethem et al. 2010; Van Goethem et al. 2011). Another matrix degrading cell type MDA-MB-231 forms numerous finger-like protrusions during invasion into underlying Matrigel. These finger-like protrusions are enriched in F-actin, cortactin and p-tyrosine containing proteins. Moreover, the location of finger-like protrusions coincide with matrix degradation sites and require recruitment of MT1-MMP on their surface (Lizárraga, Poincloux, Romao, et al. 2009; Poincloux, Lizárraga, and Chavrier 2009). Another report showed cancer cells forming lateral spikes enriched in MT1-MMP when seeded on 2D collagen matrix (Katarina Wolf et al. 2009). Although, which kind of protrusion is responsible for matrix degradation in 3D remains still matter of debate. Furthermore, it is not clear yet at which part of the cell during migration in 3D-matrix the degradation takes part.

1.4.2.1 The role of matrix metalloproteinases in 3D cell migration

Matrix degradation is an important process during migration of cells in 3D environments and is accomplished by proteases. A number of secreted and membrane bound proteases can cleave collagen fibers. Most well studied matrix degrading enzymes are membrane-type matrix metalloproteinases (MMPs) probably due to their vast abundance and clinical relevance. MT1-MMP has been reported to localize predominantly at tumor-stroma borders *in vivo* in highly aggressive tumors. Additionally, MMP-2 was also functionally active at those sites (Hofmann et al. 2000). MT1-MMP was also reported to support the migration of fibroblasts and cancer cells in ECM (Sabeh et al. 2004). This collagenase also apparently plays an important role in sprouting and collagen degradation in endothelial cells (Chun et al. 2004).

Because of the fact that many clinical trials involving treatments with inhibitors of matrix proteases as cancer-drug targets failed, the major debate occupies the question, if the proteases are generally required for cell migration in ECM. Additionally, it was reported that cancer cells still could migrate in ECM when proteases were inhibited in both, *in vitro* and *in vivo* mouse models. The plasticity mechanism of 3D migration was proposed which could explain how cells are able to migrate without matrix degradation. (Katarina Wolf et al. 2003). This model assumes that cancer cells can change the migration mode from integrin dependent mesenchymal, to integrin independent amoeboid mode, similar to leukocytes. Further research showed that cells with rounded morphology don't require proteolytic activity. Rather this mode of migration requires prominently active Rho and ROCK (Sahai and Marshall 2003). Apparently, the 3D architecture of collagen matrix can also influence the mode of cell migration. Cross-linked collagen can even prevent protease dependent migration in some cancer cell types (Katarina Wolf et al. 2003)

Some of the cell types that can form podosomes on 2D ECM can as well dig tunnels when they migrate in a 3D collagen matrix and invade into surrounding ECM collectively or as a single cell. Matrix defects that are produced by 3D migration of cells are termed have been termed single cell invasion tunnels or SCITs (Yu and Machesky 2012). This SCIT producing migration of cells in *in vitro* 3D collagen-based matrix is comparable to the collective invasion of tumor cells shown *in vivo* model. In this case the “leader cells” at the invasive front remodel ECM and generate

paths in the tissue, which are used by follower cells to invade (Katarina Wolf et al. 2003; Even-Ram and Yamada 2005a).

There are basically four types of protrusions that are described in the 2D migration of eukaryotic cells. These are lamellipodia, filopodia, podosomes and invadopodia. In 3D environments these protrusions are not well classified. During cell migration in 3D no strong data of presence of filopodia or lamellipodia-like structures was yet reported. Furthermore, there is a lack of understanding how protrusions in 3D influence parameters of cell migration such as directionality or cell velocity. On 2D surfaces protrusions such as invadopodia lead to invasion of cells in the underling matrix, but the role or appearance of these structures in 3D is yet not clear. This work addresses these issues to shed more light on different actin-based structures during 3D migration of cancer cells. The link between degradation and cell migration in 3D matrices and thus in connective tissue is not well understood yet. To shed more light on the role of matrix degradation during 3D migration of cancer cells general inhibitor of MMPs GM6001 which blocks matrix degradation was used in the present work. Thereby this work addresses questions such as: Which actin-based protrusions are involved in MMP mediated matrix degradation in cancer cells? How matrix degradation influences migration of invasive cancer cells in 3D in terms of cell directionality and cell velocity? And does the inhibition of MMPs have a visible effect on the formation of actin-based protrusions?

2 Materials and Methods

2.1 Chemicals and reagents

2.2 Chemicals

Chemicals that were used in the present work and are not listed detail were purchased from following companies: AppliChem, Biochrom, Bio-Rad, Gibco, Greiner, Hoechst, Invitrogen, Millipore, Merck, Roche, Roth, Sarstedt, Sigma-Aldrich, Serva, Santa Cruz, Thermo Fischer scientific. The used purity grade of used substances was "p.a." The Water used in this work was deionized and purified using Milli-Q-System Advantage A10 Water purification system. Prior to use for cell culture the purified water produced with Milli-Q-System, was additionally autoclaved (cell culture H_20). Plastic ware for cell culture was ordered from Sarstedt, Greiner, Gibco and Thermo Fischer scientific. Cell migration chambers were ordered form Ibidi GmbH.

2.3 Special reagents

Reagent Name	**Supplier**	**ProductNr**
Benzonase	Merck	101695
Collagen I rat tail (20 ml vial at 5 mg⁄ml)	Gibco	A1048301
CK666 (Arp2/3 Inhibitor)	Sigma	SML0006-5MG
C5a	RD Systems	2150-C5-025
DMSO molecular biology grade	Applichem	A3006
DMSO cell culture grade	Applichem	A3672
DMEM (High Glucose (4.5 g/L) with L-Glutamine	GE(PAA)	E15-810
DMEM (High Glucose (4.5 g/L) without phenol red	GE(PAA)	E15-877
EGF lyophilized powder, suitable for cell culture	Sigma	E9644-2MG
Fetal Bovine Serum PAA Clone (Low endotoxin)	GE (PAA)	A15-102-1873
Fetal Calf Serum	Sigma	F7524
FITC	Sigma	F7250-50MG
Fibronectin (pure) 1mg	Roche	1.10451E+11
Gelatin 2% in H_2O; Mr 50-100.000 Da.	Sigma	1393
Glutaraldehyde 25 %	Agar	R1020
GM6001	Millipore	
Ham's F12 (Ham's nutrient mixture F-12)	PAA	E-15-817

HEPES (1M)	GE (PAA)	S11-001
Hoechst 33342	Thermo Sci.	62249
IMDM	Gibco (Life)	21980-032
MEM Non Essential Amino Acids (100x)	GE(PAA)	M11-003
Opti-MEM	Gibco	31985-070
Lipofectamine 2000	Invitrogen	11668-019
L-Glutamine 200 mM	GE (PAA)	M11-004
Paraformaldehyde	Applichem	A3813
PDGF-BB (human) 10 µg	Cell signaling	8912
Phalloidin, CF488A	Biotum	00042 300U
Phalloidin, CF594	Biotum	00045 300U
Phalloidin-Alexa 594	Invitrogen	
Poly-L-Lysin 50ml, 70-150 kDa; sterile filtered 0.01% in Water	Sigma	P4707
PDGF-BB (human) 10 µg	Cell signaling	8912
Penicillin/Streptomycin (100x)	GE (PAA)	P11-010
Trypsin-EDTA (1x) 0.05/0.02% in PBS	GE(PAA)	L11-004
Poly-L-Lysin 50ml, 70-150 kDa; sterile filtered 0.01% (w/v) in Water (PLL)	Sigma	P4707
Sodium Pyruvate Solution (100mM)	GE (PAA)	S11-003
smiFH2 (Formin Inhibitor)	Sigma	S4826-5MG
10 x MEM 500 ml	Invitrogen	21430-020

2.4 Plasmids for transfection

To visualize F-actin in living cells plasmids containing a construct termed as “Lifeact” was used. Lifeact is a 17aa peptide of 140kDa actin-binding protein from *S. cerevisiae* (Abp140) which is fused with GFP or mRFPruby (Fischer et al. 2006) within the pEGFP-N1 plasmid (Riedl et al. 2008). Because the Lifeact was found to bind selectively with low affinity to F-actin within mammalian cells, it is used as a versatile F-actin marker. As control plasmids for non-specific fluorescence, pEGFP-C1 or pEGFP-N1 were used that don’t contain Lifeact and thus cannot label F-actin in cells. Lifeact plasmids were kindly provided by Prof. Dr. Weldich-Söldner (University of Muenster, Germany).

For the knockdown of the *Fascin1* gene in cells of mouse or human origins, used pG-Super plasmid bearing antisense shRNA construct targeting human and or mouse fascin mRNA was used which was kindly provided by Dr. Danijela Vignjevic (Danijela Vignjevic et al. 2006a). To

visualize the localization of VASP, cells were transfected with a pEGFP-hvasp plasmid (Carl et al. 1999).

Construct	**Description**	**Function**	**Re-sistance**	**Origin**
PG-Super Fascin Tc	shRNA	Expression of GFP and knockdown of fascin in human and mouse	Amp	Vignjevic et al., 2006
pG-Super Fascin Tm	shRNA	Expression of GFP and knockdown of fascin in mouse	Amp	Vignjevic et al., 2006
pG-Super Facin Th	shRNA	Expression of GFP and knockdown of fascin in human	Amp	Vignjevic et al., 2006
pG-Super GFP				Clontech
pEGFP-N1	DNA	Control plasmid	Kana	Clontech
pEGFP-C1	DNA	Control plasmid for EGFP expression	Kana	Clontech
GFP-Lifeact	DNA	Expression of life-act insert fused with GFP to visualize F-actin	Kana	Weldich-Söldner
Ruby-lifeact	DNA	Expression of life-act insert fused with mRFPruby to visu-alize F-actin	Kana	Weldich-Söldner
pEGFP-hvasp	DNA	Expression of GFP-VASP for visualiza-tion of VASP	Kana	Carl et al. 1999

2.5 Cell culture methods

2.6 Cells and cell lines

Name	Description	Origin	Growth Medium
390 Cdc42 (fl/-)	Cdc42 (flox/del) mouse fibroblastoid cells	Cord Brakebusch, MPI Martinsried	GM 1
399 Cdc42 (-/-)	Cdc42 (del/del) mouse fibroblastoid cells	Cord Brakebusch, MPI Martinsried	GM 1
HT-1080	Human fibrosarcoma cell line	CLS	GM 2
Bone marrow-derived macrophages (BMM)	Cells were isolated from bone marrow of wildtype-, Hem1 knockout and Wasp-KO mice	WASP KO mice were kindly provided by Dr. Kathrine Siminovitch; Hem1 (-/-) and Wildtype mice were provided by Dr. David deGorter	MM

2.7 Cell culture media and buffers

All cell culture media and buffers were prepared as 500 ml working solution, sterile filtered into sterilized glass bottles and stored at 4°C for maximal 1 Week. Before using all media were pre-warmed at 37°C in water bath. Sera were heat inactivated for at 56°C at least for 40 min.

Media:

Growth Medium for MEFs (GM 1)

DMEM (Dulbecco's modified eagle's medium, Gibco) 4.5 g/L Glucose	
FBS F7524 (Sigma-Aldrich), heat inactivated	10 % (v/v)
L-Glutamine (Gibco)	2 mM
Sodium pyruvate (Gibco)	1 mM
Non-essential amino acids (Gibco)	1 mM
Penicillin/Streptomicin (100x)	1x

Growth Medium for HT1080 cells (GM 2)

Ham's F12 / DMEM (1:1)	
FBS F7524 (Sigma-Aldrich), heat inactivated	10 % (v/v)
L-Glutamine (Gibco)	2 mM
Non-essential amino acids (Gibco)	1 mM
Sodium pyruvate (Gibco)	1 mM
Penicillin/Streptomycin (100x)	1x
HEPES	15 mM

Starvation Medium for MEFs (SM 1)

DMEM (Gibco) 4.5 g/L Glucose	
L-Glutamine (Gibco)	2 mM
Non-essential amino acids (Gibco)	1 mM
Sodium pyruvate (Gibco)	1 mM
Penicillin/Streptomycin (100x)	1x

Starvation Medium for HT1080 cells (SM 2)

Ham's F12 (PAA)	
L-Glutamine (Gibco)	2 mM
Non-essential amino acids (Gibco)	1 mM
Sodium pyruvate (Gibco)	1 mM
Penicillin/Streptomycin (100x)	1x
HEPES	15mM

Differentiation Medium for Macrophages (Bone-Marrow) (MM)

IDMEM (Gibco)	
FBS (PAA)	(10%)
L929 conditioned medium	20 % (v/v)
Penicillin / Streptomycin	1x

PBS solution (Phosphate Buffered-Saline), pH 7.4

NaCl	137 mM
KCl	2.7 mM
Na_2HP0_4	10 mM
KH_2PO_4	2 mM

The pH-value was adjusted to pH 7.4 by adding HCl solution. Finally, solution was autoclaved and sterile filtered using sterile filter (500 ml) with 0.2 µm pore size and poured into sterile glass bottles.

2.8 Cultivation of cells

MEFs were grown in 10 cm cell culture dishes supplied with 10 ml GM1 at 37 °C in humid cell culture incubator with 5% CO_2 and split every two or three days at 70 %- 80 % confluence levels. Cells were split into 1:5 or 1:10 ratio. To harvest cells were rinsed with pre wared PBS (37 °C), 1ml Trypsin-EDTA solution was added to the dish for 1-2 min at 37°C for cells to detach. To suppress trypsin activity, 9 ml growth medium was added to the cell suspension, and detached cells were placed in 10 ml falcon tube and centrifuged at 400 x g at RT. After discarding supernatant, the pellet was dissolved in fresh pre-warmed medium and split into new dishes at 1:5 or 1:10 ratios. HT1080 cells were cultivated and split every two days in 1:4 or 1:8 rations in the same manner as MEFs, however for HT1080 cell GM2 growth medium was utilized.

2.9 Freezing and thawing of cells

Cells were grown to 80-90 % confluence in 10 cm cell culture dish and were harvested in 1 ml medium after trypsinization. In a separate tube, 3 ml medium was supplemented with 10 % DMSO. Finally, cells were re-suspended with medium with 10% DMSO and distributed in three

cryovials. Cells were placed in isopropanol filled freezing chamber in -80 °C fridge overnight. Next day, cells were placed in a fluid nitrogen tank.

For thawing cells were slowly lifted from liquid nitrogen tank and placed in isopropanol chamber. Subsequently vails with cells were transferred to 37°C water bath and after 2 minutes transferred to 15 ml falcon tube. Next, 13 ml growth medium was added cells were centrifuged 4min at 1000 rpm. The supernatant was discarded, and cells were resuspended in 10 ml pre-warmed growth medium. Finally, cells were seeded in 10 cm cell culture dish and incubated at 37°C, 5% CO_2.

2.10 Transfection of cells

For live imaging experiments or shRNA knockdown cells were transfected with various plasmids (s. list of plasmids). For transfection experiments, cells were seeded in 6-well plates and grown to 80-90% confluence. For every single transfection the transfection mixture was made as follows: first in a sterile Eppendorf vail 250µl Opti-MEM was gently mixed with 10µl Lipofectamine 2000 and incubated for 5 min at RT. Simultaneously 0.5-1 µg plasmid DNA was added to 250µl Opti-MEM in a separate 1.5ml Eppendorf vail. Both mixtures were gently mixed (3x) with a Gilson P1000 pipette incubated 45 min at RT. After the incubation, the transfection reaction mixture was added into the well to cells. The transfection mixture was pipetted slowly, dropwise into the well with cells followed by incubation of cells in a cell culture incubator for 2-12 hours depending on the toxicity of the construct. After that, the supernatant was discarded, and fresh growth medium was added to cells. For double transfection of cells, 0.25 µg of each plasmid per transfection was used.

2.11 shRNA mediated gene knockdown

Eukaryotic cells possess posttranscriptional gene regulation mechanism that generates short double-stranded RNA (dsRNA) complementary to the mRNA of the gene to be downregulated. These dsRNAs are processed to 21-22 nucleotide small interfering RNAs (siRNAs) that bind to mRNA of their complementary sequence and lead to their breakdown (Fire et al. 1998; Elbashir et al. 2001). This information led researchers to development of artificial dsRNA sequences to downregulate specific genes of interest. The dsRNAs that are complementary and can bind to target mRNA. Finally, this short RNA-mRNA molecule is degraded by the cell which leads to downregulation of the target gene expression.

For gene knockdown experiments in present work, constructs based on plasmid pG-Super were used. This plasmid was developed by integrating the sequence of GFP into the p-Super vector and expresses GFP and target shRNA sequence in transfected cells simultaneously, which enables more convenient detection of transfected cells (Brummelkamp, Bernards, and Agami 2002; S. I. Kojima, Vignjevic, and Borisy 2004). The pG-Super vector served as a backbone to incorporate antisense sequences to either human, mouse or combined antisense sequence for human and mouse fascin mRNA termed as fascin shRNA-Th, fascin shRNA-Tm, and fascin shRNA-Tc respectively (Danijela Vignjevic et al. 2006c). These constructs were used in present work to suppress the expression of *fascin1* in MEFs or HT1080 cells.

2.11.1 ShRNA mediated knockdown of fascin in MEFs

For transfection of MEFs, $8*10^5$-$10*10^5$ cells per well were seeded in three wells of a 6-well plate in 2ml DMEM / well one day prior the transfection. On the each of the following days 0.5-1 µg shRNA construct per transfection was prepared as described and added to non-transfected cells. This was followed by incubation 10-12h of cells with transfection mixture as described. After that, medium with transfection mixture was exchanged with fresh growth medium. Finally, cells were lysed using 50-100µl SDS lysis buffer, and lysates were subjected to further analysis or frozen at -20 °C.

2.12 SDS PAGE

In SDS-PAGE proteins are separated based on their molecular weight. Sodium dodecyl sulfate binds and denatures proteins by adding the negative charge to proteins which leads to maintaining of the constant mass-charge ratio of proteins. After application of electrical field negatively charged proteins travel towards the cathode dependent of their molecular mass. During the passage through the pores of polyacrylamide, matrix proteins are separated due to their size.

To prepare SDS-Gels first 10 x separating gels were poured in custom-made chambers at once and overlaid with isopropanol for 30 minutes. After that isopropanol was discarded, and gels were washed extensively with water. This was followed by pouring of stacking gels on the top of separation gels. Quickly after that, a gel comb was inserted into separation gels to create pockets for the probe. After 30 minutes polymerization is over and gels are either processed or stored at 4°C.

To subject to SDS-PAGE cells were washed with PBS. Finally in the ¼ volume of the suspension was filled with 4x SDS buffer. To break down the cellular DNA, 0.5µg Benzonase was added to the probe. After mixing with a pipette, the probes were heated to 95°C for 5min and processed or frozen at -20°C. As protein ladder, PageRuler protein Ladder and PageRuler pre-stained Protein Ladder were used.

To perform SDS-PAGE, SDS gel was mounted in a custom-made SDS chambers which were inserted into SDS-running buffer. Protein samples and protein ladders were loaded into pockets of stacking gel and gels were run at 120 V to focus proteins at the edge of stacking gel. After that voltage was increased to 160-180V for 2h. After SDS-PAGE, the polyacrylamide gels were stained with Coomassie or subjected to western blotting.

4x Sample Buffer:

4ml	10% (w/v) SDS-solution
0.6 ml	0.5 M Tris-HCl (pH 6.8)
4.0 ml	Glycerin
0.4 ml	ß-Mercaptoethanol
0.2 ml	5% (w/v) Bromphenolblau
2.8 ml	H_20

Electrophoresis buffer:

25 mM	Tris-Base
192 mM	Glycin
0.1 %	SDS (w/v)

Acrylamide solution:

30 %	Acrylamide (w/v)
0.8 %	N,N-Methylenbisacylamide (w/v)

Stacking Gel (5%)

1.8 ml	H_2O
0.320 ml	0.5 M Tris-HCl (pH 6.8)
0.330 ml	Acrylamide solution
0.025 ml	10 % SDS solution
0.0125 ml	TEMED
0.0125 ml	25 % APS (w/v)

Separation Gel:

7.5 %	10%	
3 ml	2.5 ml	H2O
1.5 ml	1.5 ml	1.5 M Tris-HCl (pH 8.8)
1.5 ml	2 ml	Acrylamide
0.06 ml	0.06 ml	10% SDS
0.008ml	0.008 ml	25% APS (w/v)

2.13 Western blot

In Western blot proteins for SDS-gel were transferred to PVDF membrane (Millipore) using a "semi-dry" method. PVDF membrane and Whatman-paper were pre-cut to the size of the SDS gels. Before protein transfer, the PVDF membrane was activated in methanol. After activation PVDF membrane and Whatman-paper, together with SDS gel were equilibrated in blotting buffer. Two pieces of blotting paper were placed on the cathode followed by SDS gel, PVDF membrane and final two pieces of blotting paper. The transfer took place for 2 hours at 100mA per gel. After protein transfer was completed PVDF membrane was blocked in 10 % milk/TBS-T for 1h. As a first antibody polyclonal rabbit anti-Fascin1 antibody (sc-28265, Santa Cruz) was diluted 1:200 /1:400 in 1% milk / TBS-T (w/v) and the PVDF membrane was incubated with the first antibody overnight at 4°C. Next day, PVDF membrane was washed 3 x 15min in TBS-T and incubated with second antibody 1:2000 (goat-anti-rabbit polyclonal antibody coupled with horse-radish peroxidase; dianova 111-035-045) for 1h at RT. The membrane was rewashed 3 x for 15 min in TBS-T and H_2O_{dd} and incubated with 8ml LumiLight substrate (Roche) and placed in Geliance 600 imaging system (Perkin Elmer) to detect the activity of peroxidase coupled to the second antibody. Images were saved as TIF files and processed using ImageJ and Adobe Pho-toshop CS6 software.

Blotting buffer:

50mM	Tris-Base
39mM	Glycin
0.037%	SDS (w/v)
20%	Methanol (v/v)

TBS-T solution

200 mM	Tris base
1.37 M	NaCl
pH	7.6 (HCl)
(0.1 % (v/v)	Tween-20)

2.14 Preparation of coverslips

For the use in cell culture and fluorescence microscopy, 100 coverslips (12-15 mm, 0.17 mm thick) were gently shaken overnight in a glass bottle with Ethanol/HCl solution (60 % Ethanol / 40 % HCL, v/v) at RT. To remove residual ethanol/HCL coverslips were 10x washed and additionally boiled 3-5 times with MiliQ-H_20. This was followed by drying of coverslips between two layers of Whatman-paper in a fume hood. Dried coverslips were placed in a glass Petri dish and sterilized in dry heat sterilizer at 220°C.

2.15 Coating of coverslips with ECM and ECM-proteins

To coat coverslips with either fibronectin, laminin, or PLL, the 30µl drops of either 25 µg/ml fibronectin (stock 1mg/ml in 2M Urea) in PBS or 25 µg/ml laminin or 0.1 mg/ml PLL are placed in sterile Petri dish. Later coverslips are let float on these drops for 1h. Afterwards coated coverslips are washed 3 x with 2 ml PBS to remove the rests of stock solutions.

Coating of coverslips with collagen was done by adding 100 µl freshly prepared 1mg/ml collagen to coverslips precooled (0-4°C) plate or on ice and collagen was gently spread with pipet tip to approximate size of the coverslip. Next coverslips with collagen were incubated at 37°C in a humid chamber within an incubator to allow polymerization of collagen at least 30 min. The effect of successful polymerization was visually checked as the consistency of polymerized collagen changes from transparent to opaque.

Coverslips were coated with 0.2% Gelatin (diluted in cell culture H_20) before dilution gelatin stock solution (2% Gelatin) was pre-warmed at 37°C to make pipetting possible. For coating of coverslips, 100µl of gelatin was incubated on the top of coverslip for 1h at RT under sterile conditions. After 1h gelatin was gently aspirated from the coverslip using Gilson pipette and coverslips were washed with 2ml DMEM or PBS. This was followed by seeding of cells on coated coverslips and incubation at 37°C, 5% CO_2 cell culture incubator.

2.16 Staining of fixed cells on 2D coverslips and in 3D collagen drops

Fixed cells on coverslips were stained for F-actin using Alexa-594 conjugated phalloidin. To extract soluble proteins, coverslips were incubated with 0.1 % Triton-X in PFA-PBS solution for 1min. Coverslips were then washed gently with 3 ml PBS three times and placed on 30µl drops of phalloidin-Alexa 594 (1:50 diluted in PBS-1%BSA solution) for 45 min in the dark at RT. Coverslips were carefully removed from the phalloidin-Alexa 594 drops and washed by dipping them into the glass with PBS of the solution. After last wash, the rest of buffer was removed from the coverslip by touching its edge to Whatman-paper. Finally, coverslips were mounted on slides

with a 10-15µl drop of Mowiol containing 2.5 mg/ml n-propyl gallate as an anti-bleaching agent. The coverslips were kept at 4°C overnight and subjected to fluorescence microscopy.

2.17 Quantification of CDRs and filopodia numbers

The cells were seeded and grown on glass coverslips in 6-well or 12-well cell culture plates. After 18- 24-hour incubation growth medium was exchanged to starvation medium. After 16-18 hours incubation plate with cells was placed on a Styropor-plate within cell culture hood. The starvation medium was exchanged with pre-warmed, 20 ng/ml PDGF-BB containing DMEM for 5-10 minutes. Cells were fixed with pre-warmed (37°C) 4% Paraformaldehyde-PBS solution for 20 minutes at RT and stained for F-actin. Cells were imaged by fluorescence microscopy at 60-90x magnifications. Filopodia were counted when these structures originated from within lamellipodia and were crossing the edge of lamellipodia.

2.18 Inhibitor treatments

2.18.1 SmiFH2 treatment of MEFs in circular ruffling assay

MEFs were seeded on coverslips and incubated for 24hours. Next, cells were washed twice with PBS (1x) and incubated in starvation medium for 16-18 hours. For the treatments with either smiFH2, PDGF or both, cells were placed on Styropor-plate and starvation-medium was substituted with fresh starvation medium with 15µM smiFH2 for 30 minutes at 37°C 5% CO_2. In case of PDGF-BB treatment, smiFH2 containing medium was exchanged with starvation medium containing 20ng/ml PDGF-BB for 5-7 minutes at 37°C. After 5min of incubation cells were fixed with pre-warmed 4% PFA-PBS solution and stained for F-actin using phalloidin-Alexa 594.

2.19 Adhesion assay

For adhesion assays, cells were harvested as usual. Coverslips were prepared and coated if desired with 25µg/ml fibronectin as described previously. For adhesion assays on gelatin and collagen, the appropriate concentrations of these substances were plated on coverslips, placed in humidity chambers and incubated on RT or 37° incubator. Immediately after coating coverslips were washed 3x with PBS and growth medium (2.5ml) was added to each well with coverslips.

Cells at a final concentration of 10^5 cells /ml were added to each well of 6-well plate. Cells were let adhere for 40min at 37°C in a cell culture incubator. After adhesion on the substrate, cells were washed 2x with 2ml PBS, overlaid with 2ml DMEM-full and pictured with 4x magnification on EVOS fl digital cell culture microscope equipped with Sony ICX285AQ CCD camera.

2.20 Matrix degradation assay

Materials:

Glutaraldehyde 25% (Agar, R1020, EM-Grade)

Poly-L-Lysine (Sigma, P4707, 0.01% in water, sterile filtered)

FITC (Sigma, F7250), working solution is diluted in DMSO (1mg/ml)

Gelatin 2% in H2O (Sigma, 1393). Working solution is diluted in sterile water (0.2%).

0.1M sodium-carbonate pH 9.0, sterile filtered.

Dialysis tubing: Spectator 7; MWCO 1000; Lot 1232103.

The preparation of FITC conjugated gelatin and of coverslips was done according to published protocols with some modifications. (Anderl, Ma, & Armstrong, n.d.; Artym, Zhang, Seillier-Moiseiwitsch, Yamada, & Mueller, 2006; “Gelatin degradation assay – Buccione Lab .,” 2003; Wang & McNiven, 2012).

Day1

Coupling of FITC to gelatin was performed according to manufacturer's protocol (Sigma) with some modifications. Gelatin was diluted 1:20 in 1 ml of 0.1M sodium-carbonate buffer. 50 µl of 1mg/ml FITC solution was added dropwise under simultaneous inverting. The solution was inverted overnight in darkness under 4°C. Dialysis tubing with MWCO 1000 was prepared according to manufacturer's manual.

Day2:

FITC-gelatin mixture was dialyzed against 5L 1x PBS twice, for 4h each at 4°C in the dark room. After the dialysis, FITC-Gelatin was sterile filtered with syringe filters of 0.2µm pore size and stored at °4°C.

Degradation Assay:

Short before:

-Cell culture medium with supplements (without FCS) for the quenching reaction.

-warm up media for cell harvesting.

-prepare sterile hood.

-dilute 0.01% PLL in sterile MilliQ-water to 0.05 %.

-dilute 25% Glutaraldehyde in sterile 1 x PBS to 0.5 %.

Coverslips were placed in 12 well cell culture plate under the sterile hood and coated with 200µl 0.05% Ply-L-lysine per well, for 20min at RT. This was followed by 3x 1ml PBS wash for each well. Coverslips were then overlaid with 150µl 0.5 % Glutaraldehyde drops for 15 min, at RT, followed by 3x 1ml PBS wash. Unconjugated 0.2 % gelatin was mixed with FITC-gelatin at a ratio of 8:1 and coverslips were inverted on 20µl drops of this solution for 10min, RT, in the darkness. The coverslips coated with FITC-gelatin were placed in a new 12-well plate and very carefully washed with 3x 1ml PBS. Free aldehyde groups were quenched with 1ml medium with supplements (without FCS) for 1h, 37°C incubator, in darkness. After the medium exchange approx. $1.5*10^5$ cells per well were added to each well and incubated for 5h in presence or absence of inhibitors. Cells were fixed with warm 4% PFA in PBS for 20min at RT. Afterwards, cells

were either permeabilized with 0.1 % Tween in PBS for 20min and stained with phalloidin-Alexa 594 or stored at 4°C in PBS for further processing.

Day 3:

Fixed cells were permeabilized with 0.1% Tween in PBS for 1 min. Cell were washed 3x with 1ml PBS. Phalloidin-Alexa 594 was diluted in 1% BSA-PBS to 1:50. Coverslips were inverted on phalloidin-Alexa 594 drops for 1h at RT in darkness. After the incubation in phalloidin Alexa 594, coverslips were washed with PBS and embedded in Mowiol on a coverslip.

Quick protocol:

1) Place coverslips in a 12-well cell culture plate.
2) Dilute PLL stock in a sterile miliQ water to 0.05 %
3) Overlay with 200µl 0.05% PLL per coverslip for 20min RT.
4) Wash 3x with 1ml sterile PBS.
5) Fix with 0.5% glutaraldehyde drops for 15min RT.
6) Prepare 10cm cell culture dish with FITC-gelatin drops, 20µl per coverslip, and store in the dark.
7) Wash coverslips to remove glutaraldehyde, 3x with 1ml PBS.
8) Invert coverslips on 20µl FITC-gelatin drops on 10cm cell culture dish for 10min, RT, in the dark.
9) Place the coverslips in the new 12-well plate and overlay with 1ml Medium with supplements to quench the free aldehyde groups for 1hour, 37°C in an incubator.
10) Harvest the cells.
11) Exchange the quenching medium to the cell growth medium and add 50.000-150.000 cells per well, add inhibitors if needed.
12) Incubate for 5 hours.
13) Fix the cells with 4% warm PFA in PBS.

2.21 2D random migration assay

2D random migration assays were performed in 6-chamber µslide $6^{0.1}$ (Ibidi 80666). The channel was pre-incubated in a cell culture incubator prior to injecting of cells. When desired, individual channels of the chamber were coated with 25µg/ml fibronectin. To coat channel fibronectin solution was pipetted into the channel and the chamber was incubated at 1h RT in a humid chamber. The channel with fibronectin solution was washed with PBS, and residual fluid was removed by cell culture aspirator. Finally, the cell suspension was injected into channels into channels according to manufacturer's instructions. For migration assay of MEFs, initial cell concentration was adjusted to $1*10^6$ cells/ml medium. For migration assay of HT1080 cells approx. 150-200.000 cell/ml medium was injected into each chamber of the µslide. Reservoirs of migration channels were left empty during the cell adhesion and spreading stage. The evaporation of fluid form µslide channels was prevented by placing the µslide in custom made humid chamber within cell culture incubator. Prior to migration assay cells were let adhere and spread for at least 2h-4h at 37°C, 5% CO_2. If desired after adhesion and spreading, cells were starved using SM2 supplied with 10mM HEPES for 16-18h. To stimulate cells with growth factors or inhibitors, appropriate concentrations of these chemicals were freshly prepared, and SM2 was substituted with growth factor or inhibitor containing media for desired durations and incubated at 37°C, 5% CO_2. Finally, stimulation/inhibition medium was exchanged to a microscopy medium (SM2+10µM HEPES), and reservoirs of channels were covered with sterile Parafilm pieces to avoid evaporation. The µslide 6 with cells was mounted on the motorized xy-table in a heating system 6 (Ibidi). Cell migration was acquired using phase contrast brightfield microscopy at 2.5 x or 5x magnifications on Axiovert 135 microscope. Pictures were taken every 5-10 minutes when imaging MEFs or HT1080 cells using idea spot 1.3 camera and VisiView software. Images and corresponding movies were processed as described (s. 2D chemotaxis assay).

2.22 2D Wound healing assay

The 2D wound healing assay was performed in a multi-well slide with miniaturized wells for cell growth referring to the protocol from Dr. Kees Straatman form the University of Leicester with modifications (Feb, Cell, and Nikon 2008). For multi-scale experiment approach by µ-Slide Angiogenesis (Ibidi 81506) was used. This slide incorporates 12 wells letting to perform twelve experiments simultaneously. MEFs were seeded in chambers of µlsilde as follows. The cell suspension was adjusted to 180.000 cells/ml in GM1, and 30µl of this suspension were pipetted per well. The µslide with cells was incubated in custom made humid chamber within cell culture incubator for 18-24h. At the cell confluency of above 90% scratch wound was induced using 20µl pipette tip in each well. If desired, inhibitors such as smiFH2 or GM6001 were introduced to cells prior to the wounding of the cell monolayer. For the treatment of cells with inhibitors, growth medium was exchanged to microscopy medium containing an appropriate concentration of the inhibitor. Prior to microscopy wells of µslide were sealed using sterilized pre-cut Parafilm to prevent evaporation of fluid and were additionally covered with a provided plastic lid. Finally, µ-Slide Angiogenesis was mounted on Zeiss Axiovert 135 microscope equipped with automatized xy-table and Ibidi heating system 6 which maintained the temperature of cells at 37°C. The wound healing process was acquired for 8-12 hours, and cell migration data was processed as described in previous chapters. To assess cell migration parameters such as velocity and directness cells from the leading edges of the wound were tracked. Images and corresponding movies were processed as described (s. 2D chemotaxis assay).

2.23 2D Chemotaxis assay

For 2D chemotaxis assays, cells were harvested and concentrated in growth medium to 800.000 cells/ml for MEF cells, or 600.000 cells/ml for macrophages. Migration was performed using µslide 2D chemotaxis slide (Ibidi, CatNo: 80306). Prior to seeding of cells, µslide was incubated in a cell culture incubator for 2h. The cell suspension was drawn in migration channels according to manufacturer's manual. The chamber with cells was placed in a custom-made humid chamber within a humidified cell incubator for 2h at 37 °C to let cells adhere and suppress evaporation.

Cells were washed twice and incubated with a starvation medium for 16-18h. After starvation, chemoattractant was diluted in a starvation medium containing 25 mM HEPES and was applied in one of the reservoirs. The 2D chemotaxis chamber was immediately placed in a heating stage (Ibidi) mounted on automatized xy-table on the Zeiss Axiovert 135 microscope. Cells were imaged at 2.5x magnification using brightfield phase contrast microscopy. Images were acquired using CMOS camera "Spot idea 1.3mp" (Diagnostic Instruments) every 3 minutes for 12-16h at several locations simultaneously. Acquired sets of images were combined with corresponding movies using ImageJ software. Migrating cells within movies were tracked with manual tracking plugin of ImageJ. The resulted cell migration paths were stored as overlay movies and as an excel tables of xy-coordinates and corresponding time points of each tracked cell. For the analysis of cell migration parameters such as forward migration index, cell velocity or directness the data were imported to migration tool 2.0 (Ibidi). This tool enables the mathematical transformation of cell migration paths and according to coordinates and timepoints of each cell to the cell velocities, directness and forward migration index. These parameters were calculated for each tracked cell and finally imported into Sigma plot 13 software for statistical analysis. The statistical analysis Mann-Whitney rank sum test by using Sigma plot 13 software.

2.23.1 2D chemotaxis of macrophages

For 2D chemotaxis experiments BM-derived macrophages from wildtype, Hem1 (-/-) or Wasp (-/-) mice were harvested at 600.000 cells/ml and injected into three separate channels of µSlide 2D chemotaxis chamber (Ibidi; 80306) as described previously with modifications (Isfort et al. 2011b). Cells were incubated overnight in a growth medium. On the next day, C5a was added to one of the reservoirs and chambers (150 nM final concentration). For the imaging slide was placed on preheated stage on Axiovert 135 microscope equipped with motorized xy-stage. Images were recorded every 3 minutes for 8-16h. The migration of cells was tracked using ImageJ manual tracking plugin as described in the previous chapter. The results were analyzed with chemotaxis tool (Ibidi). The statistical analysis was performed using Sigma plot 13 software via Mann-Whitney Rank Sum Test. BM-derived macrophages were kindly provided by Dr. David de Gorter (University of Munester).

2.24 3D collagen gels

The ECM consists of a network of mainly collagen type I (collagen I) fibrils and fibers and contains additionally various cross-linking proteins. To form such structures collagen molecules bear intrinsic self-assembly mechanism which is apparently entropy driven (Self-assembly 1981). Initially, collagen molecules are secreted by fibroblasts as collagen monomers (consisting of the triple helix of three molecules). The collagen monomers possess non-helical ends termed as telopeptides. In a further step, cell-derived stromal lysyl-oxidase modifies lysyl- or hydroxylysyl residues within the telopeptides to aldehyde groups, which react to amino-groups of neighboring collagen monomer and forming an aldimine bond. This reaction leads to cross lining of collagens to fibrils, fibers and finally to 3D collagen network found in various tissues.

Collagen can be extracted from several tissues such as rat tails by treatment of these with acids, which reversibly breaks the aldimine bond between collagen monomers. Thus, the monomers dissociate and become soluble at low pH values, specific salt conditions, and low temperature. Thus, by raising of pH value and temperature of solubilized collagen, the self-assembly of collagen monomers can be reinitiated (Katarina Wolf et al. 2009). The principle of self-assembly reaction of collagen is used to fabricate artificial 3D collagen scaffolds, which reportedly have advantages over 2D cell culture by the closer mimicking of the situation *in vivo* (Even-Ram and Yamada 2005a).

There are several commercial-kits for *in vitro* collagen assembly available. However, most of these kits require the addition of 3-5 components to collagen to achieve fibrillogenesis of collagen monomers. Most of these substrates are several times concentrated solutions and are probably not adequately dissolved at storage and working temperature of 0-4°C. Additionally, the critical step for cell viability, however, was the neutralizing the acidic collagen solution with 5N NaOH solution. Due to many components of collagen assembly, kits and many pipetting steps it is difficult to achieve reliability and reproducibility of collagen assembly. In present work, this circumstance led to the formation of gels which were either detaching from the surface of coverslip or less were less viable for embedded cells. Therefore to increase the reproducibility and simplify assembly of collagen the collagen matrix was prepared by using HEPES as a neutralizing agent with modifications (Sung et al. 2009). By mixing of collagen stock solution (5mg/ml)

with HEPES and growth medium and cells, the final concentration of the collagen-cell mixture of around 1mg/ml collagen-I was achieved. This collagen concentration is common in 3D cell culture studies (Isfort et al. 2011a; Katarina Wolf et al. 2009; K. Wolf 2003; Sung et al. 2009; Helary et al. 2012).

2.25 Embedding of cells in 3D collagen

For imaging of cells in 3D collagen or 3D migration assays, cells were embedded in the collagen matrix. To prepare cell-collagen mixture following steps were done on the ice. 75µl of GM1 or GM2 were pipetted in a 1.5ml Eppendorf vail, 5µl HEPES (1M Gibco) was added GM, which was followed by pipetting of 20µl of Collagen I solution (5mg/ml, Invitrogen) into the vail. Finally, 10 µl of cell suspension was added to the solution. The cell-collagen mixture was gently mixed 2 times with Gilson P100 pipette and placed as 30µl drops on the sterile coverslip or injected into the 3D chemotaxis chamber (IBIDI). For the polymerization of collagen, the coverslip or chemotaxis chamber was placed in a custom-made humid chamber within a cell culture incubator for 30-40 minutes at 37°C. Within first 10 minutes of incubation at 37°C chambers with collagen-cell mixture were inverted every 2 minutes to prevent cells from sedimentation and attachment on the surface of the coverslip. This step ensures that most of the cells stay embedded in 3D collagen.

2.26 3D random migration assays

The freshly prepared cell-collagen mixture was injected into each channel of 6-channel µSlide $4^{0.4}$ (form Ibidi, 80606, incorporates six channels for max. six parallel assays simultaneously) according to manufacturer's instructions. The µslide was pre-incubated in a cell culture incubator before injecting cell-collagen mixture. For HT1080 cells approx. 7-8*10^6 cells/ml collagen were injected into each chamber of the µslide. Collagen was polymerized at 37°C at 5% CO_2 as described previously. The evaporation fluid from the channels was prevented by placing the µslide in custom made humid chamber within cell culture incubator. After polymerization of collagen

reservoirs were filled with 70µl medium and cells were incubated at least for 18-24h in collagen to spread and adapt to the 3D environment at 37°C and 5% CO_2 in a humid chamber within a cell culture incubator.

If desired, cells were starved using SM2 supplied with 10-25mM HEPES for 16-18h. To stimulate cells with growth factors or treat with inhibitors, appropriate concentrations of these chemicals were freshly prepared, and SM2 was substituted with growth factor or inhibitor containing media for desired durations and incubated at 37°C, 5% CO_2. (Cells were incubated with inhibitors smiFH2 or GM6001 overnight. For live microscopy medium was exchanged with microscopy medium with appropriate inhibitors). Finally, stimulation/inhibitor-medium was exchanged to microscopy medium (SM2+10µM HEPES), and reservoirs of channels were covered with precut sterile Parafilm pieces to avoid evaporation. The µslide 6 with cells was mounted on the motorized xy-table in a heating system 6 (Ibidi). Cell migration was acquired using phase contrast brightfield microscopy at 2.5 x or 5x magnifications on Axiovert 135 microscope. Images were acquired every 5-10 minutes when imaging MEFs or HT1080 cells using idea spot 1.3 camera and VisiView software. The migration parameters were calculated and processed as described previously (s. 2D chemotaxis assay).

2.27 3D chemotaxis assay

This assay based on the principle that gradient of molecules can be formed within a narrow channel which connects two greater sized reservoirs. In the case of filling one reservoir with molecule A, a gradient of A will form within the channel. The 3D chemotaxis assay was performed in the µSlide chemotaxis-3D slide which incorporates three separate chambers and thus max. three parallel assays on one slide can be performed. Before migration assay, the µslide was pre-incubated in a cell culture incubator for 2h before injecting the cell-collagen mixture into the channels. For HT1080 cells at $8*10^6$ cells/ml collagen was injected into each of three channels of the µslide. All silicon plugs were inserted into the openings of reservoirs, but not of the channels Collagen was polymerized at 37°C at 5% CO_2 for 20min. The evaporation fluid from the channels was prevented by placing the µslide in custom made humid chamber within cell culture incubator. After polymerization of collagen reservoirs were filled with GM2 according to manufacturer's instructions and cells were incubated

at least for 18-24h in collagen to spread and adapt to the 3D environment at 37°C and 5% CO_2 in a humid chamber within a cell culture incubator. Next day, media in every reservoir was exchanges to SM2 and cells were starved for 8-10h. After starvation one of the reservoirs of each chamber was filled with DMSO in GM2, or 30µM smiFH2 in GM2 or only GM2 as a positive control for chemotaxis.

The reservoirs and channels were sealed with provided silicone plugs to avoid evaporation. The filled µslide 6 was mounted on the automated motorized XY-table and a heating system 6 (Ibidi) which were installed on Axiovert 135 (Zeiss) microscope. Images were taken using phase contrast brightfield microscopy at 2.5 x or 5x magnifications (Objective Zeiss 5x/0.15). Pictures were taken on several locations simultaneously every 5-10 minutes using IdeaSpot 1.3 CMOS camera and VisiView software. Three conditions of the experiment (treatments with DMSO; 30µM smiFH2 and only GM) were acquired simultaneously. The resulting data were processed as described previously (s. 2D chemotaxis assay).

2.28 Visualization of F-actin in live cells

Visualization of F-actin was in living cells was achieved by expression of Lifeact containing plasmids in cells. Lifeact was developed based on findings, which showed that an actin-binding protein of 140 kDa (ABP140) from *S. cerevisiae* was able to bind to to F-actin and was absent in other organisms. Reportedly, the loss of this protein did not affect actin filament formation in yeast. However, a slight actin bundling activity of ABP140 was also detected (Asakura T. 1998). Later, another group reported visualization of F-actin by expression of ABP140-GFP fusion constructs in yeast (H.-C. Yang and Pon 2002). Based on this reports the F-actin-binding motif of ABP140 was identified as the first 17aa of ABP140, which was cloned and fused to either GFP or mRFPruby to visualize F-actin in mammalian cells (Riedl et al. 2008; Fischer et al. 2006). Biochemical studies indicated that the weak binding of lifeact to F-actin did not have an adverse effect on actin polymerization *in vitro* or cells. However, the effect of expression of Lifeact-plasmids on cells probably depends on a number of plasmids that are transfected into cells. In this work, several transfected cells showed altered morphologies compared with non-transfected cells,

showing several dendritic protrusions (not shown). Of note, also many cells retained normal morphology, and thus these type of transfected cells were chosen to for further studies. The cell morphology was considered as normal when it matched to the morphology of non-transfected cells in collagen (s. Figures 28; 29).

2.29 Spinning disc laser confocal microscopy

For confocal imaging of live cells, cells were transfected with corresponding plasmids. The transfection rate was estimated in fluorescent microscopy by assessing the expression of GFP within cells. Transfected cells were embedded in 3D collagen as described. For live laser confocal microscopy cell-collagen mixture was injected into µslide $6^{0.4}$ (Ibidi, 80606) or pipetted as 20-30 µl drops on 3.5 cm glass-bottom imaging chambers (Ibidi, 81156) and were let adjust to 3D collagen for 18-24 h. For live cell imaging, all reservoirs of µslide $6^{0.4}$ were filled with microscopy medium and sealed with custom cut sterilized Parafilm.

2.30 Imaging of fixed cells embedded in 3D collagen

If desired, the cell-collagen mixture was cultivated on glass coverslips in 6-well plates or 3.5 cm cell culture dishes for 18-24 h at 37°C and 5% CO_2 in a humid cell culture incubator. This was followed by fixation and staining for F-actin using Phalloidin-Alexa 594 as described in the previous chapter. Finally, the coverslips were mounted in a 10µl drop of Mowiol on microscope slides and subjected to laser confocal microscopy.

2.31 Random migration of fascin1 knockdown HT1080 cells in 3D

Before 3D random migration assay, HT1080 cells were subjected to fascin knockdown experiment as described, by using 0.5 µg fascin shRNA-Th and fascin shRNA-Tc constructs. From these experiments, the most effective knockdown of fascin combined with expression of GFP was achieved by using fascin shRNA-Th construct at day 3 of transfection. Corresponding cells from 6-well plate were harvested in 1ml medium to approx. 600.000 cells/ml which were embedded in collagen as described in the previous chapter for following fixation and confocal microscopy (Figure 48). The rest of suspension was centrifuged at 400 x g at RT and suspended in 50 µl GM2 at $12*10^6$ cell/ml. 5µl of this cell suspension was mixed with 50 µl of freshly prepared collagen solution and pipetted as 20 µl drops on glass coverslips for live cell imaging in laser confocal microscopy (Figure 49). The rest of cell suspension was centrifuged and lysed with SDS lysis buffer and frozen for later SDS-Page and western blot analysis (Figure 47). Collagen was polymerized 30min at 37°C in a humid chamber within cell culture incubator as described. The cells were incubated for 16-18 h to adapt to 3D collagen environment. Next, the medium was exchanged to microscopy medium and cells embedded in 3D collagen were subjected to live spinning disc confocal microscopy.

2.32 Microscopes

- EVOS fluorescence digital cell culture microscope (AMG)
- Olympus IX71/IX51 Inverted Microscope equipped with Lei HXP-120 Light source (Visitron Systems) and Spot Insight monochrome 2.0mp camera (Diagnostic instruments). High magnification images were taken with 60x objective lens UPLDLN60XOI (Olympus).
- Zeiss Axiovert 135 equipped with high precision motorized XY table and controller (Visitron systems). Ibidi Heating System 6 comprising of Heated Lid (524082), Heat Controller HAT 200 (262016) and Heated stage (524083). Image acquisition was made with CMOS camera "Spot idea 1.3mp VisiView software (Visitron systems). Objective Zeiss 5x / 0.15

- Axiovert 200 with a pE-2LED excitation system (CoolLED) as a light source and "sennsicam qe" cooled digital 12-bit camera. Higher magnification images were taken with Zeiss 63x or 100x objectives (Plan Neofluar).

- Laser confocal spinning disc microscope

  For imaging cell in confocal microscopy, Ultra View Vox 3D live cell imaging system was used (Perkin Elmer). The system comprises of Nikon Eclipse Ti inverse microscope with Yokogawa CSU-XI spinning disc scanner, C9100-50 EM-CCD camera (Hamamatsu) and Volocity 6.0 software. For high magnifications and imaging of cells within collagen matrix, a Nikon CFI Apo TIRF 60x (NA 1.49) oil immersion objective lens with coverslip corrected working distance of 120 µm was used. The system was additionally equipped with temperature controlled incubator (Okolab) and motorized xy-table controlled by Volocity software.

2.33 Statistical analysis

Statistical analysis of cell migration data was perfumed using Sigma plot 13 software by application of Mann-Whitney Rank Sum test algorithm to data sets of velocities, FMIs and Directness of two different treatment groups. Mean values of data sets were compared to each other for the significance of differences and were considered as statistically significant if $p<0.05$.

3 Results

3.1 2D Migration and protrusions: Effects of *Cdc42* knockout on actin protrusions in MEFs

During migration on 2D substrates, many cell types display actin-based protrusions such as circular dorsal ruffles, filopodia, lamellipodia and invadopodia to protrude their cell body in a certain direction. During movement, cells can degrade ECM if required. At least *in vitro* cells migrate randomly or they show chemotaxis towards a range of specific chemoattractants. While actin protrusions are studied in detail regarding their biochemical composition and dynamics of their formation, their roles in different types of cell migration remain less well understood.

Cells rapidly respond to stimulation with growth factors of the PDGF family by a massive reorganization of their actin cytoskeleton that is followed by formation of actin-based protrusions which can lead to cell migration. Stimulation of fibroblasts *in vitro* with PDGF-BB, that reportedly is responsible for recruitment of fibroblasts from the deeper tissue into a wound, leads to the display of different kinds of known actin-based protrusions. Furthermore, stimulation of fibroblasts with PDGF-BB induces prominent actin-based protrusions on the dorsal surface termed circular dorsal ruffles (CDRs or CRs) (Rottner and Stradal 2011a; Buccione, Orth, and McNiven 2004). The role of these actin-based structures in cellular processes induced by PDGF-BB is not well understood.

3.1.1 Cdc42 knockout MEFs are unable to form PDGF-BB induced CDRs

Cdc42 and Rac GTPases are both essential for formation CDRs. Previous work from our lab showed that Cdc42 deficient MEFs lose the ability to form these structures in response to PDGF-BB. Furthermore, it was shown that dorsal ruffles are composed of lamellipodia-like structures with embedded filopodia and microspikes reminiscent of peripheral lamellipodia. Whereas Cdc42 is dispensable for formation of lamellipodia, it is essential for the formation of CDRs. Further analysis of downstream effectors of Cdc42 and Rac1 showed that WAVE but not WASP-induced

activation Arp2/3 complex is essential for the formation of CDRs. Actin-bundling protein fascin and intact microtubules are also important for the formation of CDRs (Schloen, K,. PhD thesis). Of note, fascin is not essential for the formation of lamellipodia (Danijela Vignjevic et al. 2006b).

3.1.2 Cdc42 knockout MEFs show defects in the formation of filopodia in response to PDGF-BB

To date, there are several contradicting reports regarding the role of the small GTPase Cdc42 in the formation of filopodia (Catherine D Nobes and Hall 1995b; Kozma et al. 1995; Pellegrin and Mellor 2005; Czuchra, Wu, Meyer, Hengel, et al. 2005; L. Yang, Wang, and Zheng 2006). Although, it is well established that overexpression this GTPase induces the formation of filopodia (Kozma et al. 1995; Pellegrin and Mellor 2005; L. Yang, Wang, and Zheng 2006). Previous work form our lab (performed by Katrin Schloen) showed that filopodia and microspikes are enriched in CDRs. Therefore, possibly loss of CRs in Cdc42 knockout MEFs might be due to defective formation of filopodia in these cells.

To test whether Cdc42 knockout MEFs are affected in their ability to form filopodia, CDC42 (fl/-) and Cdc42 (-/-) MEFs were treated with PDGF-BB and stained for F-actin to visualize and count filopodia in each genotype (Figure 9).

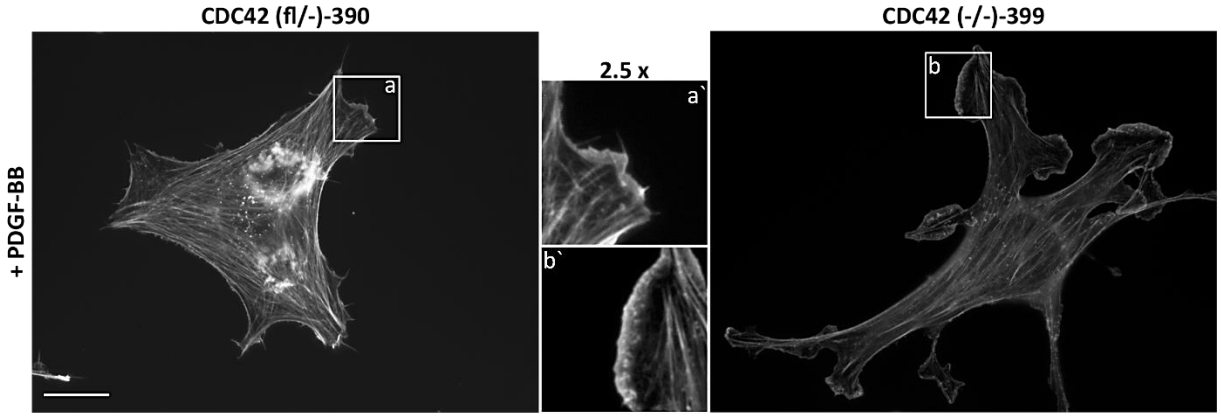

Figure 9: Effects of *Cdc42* knockout on the formation of filopodia in MEFs. MEFs (390 and 399) were seeded on glass coverslips and cultivated for 18-24 hours at 37°C in cell culture incubator. The medium was changed to starvation medium (without FCS) and cells were starved for 16-18 hours. After starvation cells stimulated with 20nM PDGF-BB. Finally cells were fixed in 4% PFA and actin cytoskeleton was stained using Alexa594-conjugated phalloidin. Cells were visualized by fluorescence microscopy. Scale bar 20µm. (a, a') control treatment with CDC42 (fl/-) MEFs; (b, b'): CDC42 (-/-) MEFs.

Figure 9 shows representative images of Cdc42 (fl/-) and Cdc42 (-/-) cells treated with PDGF and stained for F-actin. Cdc42 (fl/-) cells show lamellipodia and embedded filopodia at the leading edge whereas Cdc42 knockout cells show no visible filopodia, but can produce normal lamellipodia. To quantify these results, filopodia from random groups of Cdc42 (fl/-) and Cdc42 knockout cells were counted and results were statistically evaluated (Figure 10).

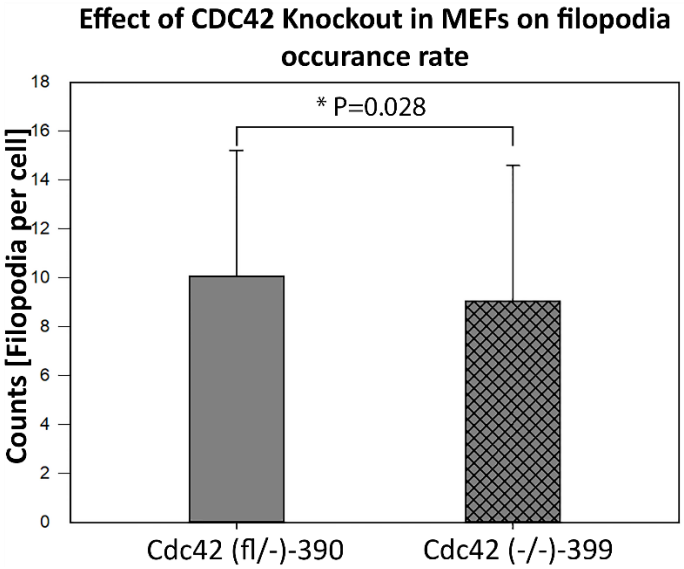

Figure 10: Cdc42 knockout MEFs show reduced numbers of filopodia in response to PDGF-BB. MEFs were plated on glass coverslips and cultivated for 18-24 hours at 37°C in cell culture incubator. The medium was changed to starvation medium (without FCS) and cells were starved for 18 hours. After starvation 20nM PDGF-BB was applied to cells for 10 min. Finally cells were fixed in 4% PFA and stained using Alexa594-conjugated phalloidin. A number of filopodia per cell for each treatment group were counted in ImageJ and statistically analyzed using Sigma plot 13 software. Statistical analysis was performed using Mann-Whitney Rank Sum Test. Error bars show one standard deviation of the mean value form two independent experiments with sample size of 169 cells.

The evaluation of the results showed an approx. 13 % reduction in the numbers of filopodia in Cdc42 knockout MEFs. This is in line with another study showing that Cdc42 is important, but not essential for the formation of filopodia in MEFs. Furthermore, the study showed that the dynamics of the formation of filopodia was not altered in Cdc42 knockout MEFs *vs* control cells (Czuchra, Wu, Meyer, Hengel, et al. 2005). In contrast, here we induced the formation of filopodia using chemoattractant PDGF-BB and showed that the number of filopodia per cell is slightly, but significantly reduced in Cdc42 knockout cells.

3.1.3 Cdc42 knockout MEFs show defective polarity in response to PDGF-BB

It is well accepted that Cdc42 plays an important role in regulating cell polarity in many organisms and cell types from yeast to mammals (D. I. (University of M. Johnson and Pringle 1990; Catherine D Nobes and Hall 1999; S. Etienne-Manneville 2004; A. E. Adams et al. 1990b). There is although still an ongoing discussion whether Cdc42 regulates cell polarity due to its modulating activity of actin cytoskeleton at the leading edge or by its essential role in the reorientation of microtubules and/or Golgi apparatus towards the direction of movement. (Bartolini et al. 2008; Palazzo et al. 2001).

To gain more insight in the role of Cdc42 in cell polarity, I compared the Cdc42 (-/-) with Cdc42 (fl/-) MEFs in their ability to polarize their actin cytoskeleton after treatment with a global PDGF-BB stimulus (Figure 11 a; a`). The results were quantified by counting and comparing numbers of polarized and non polar cells within the PDGF-BB treatment group (Figure 11 b)

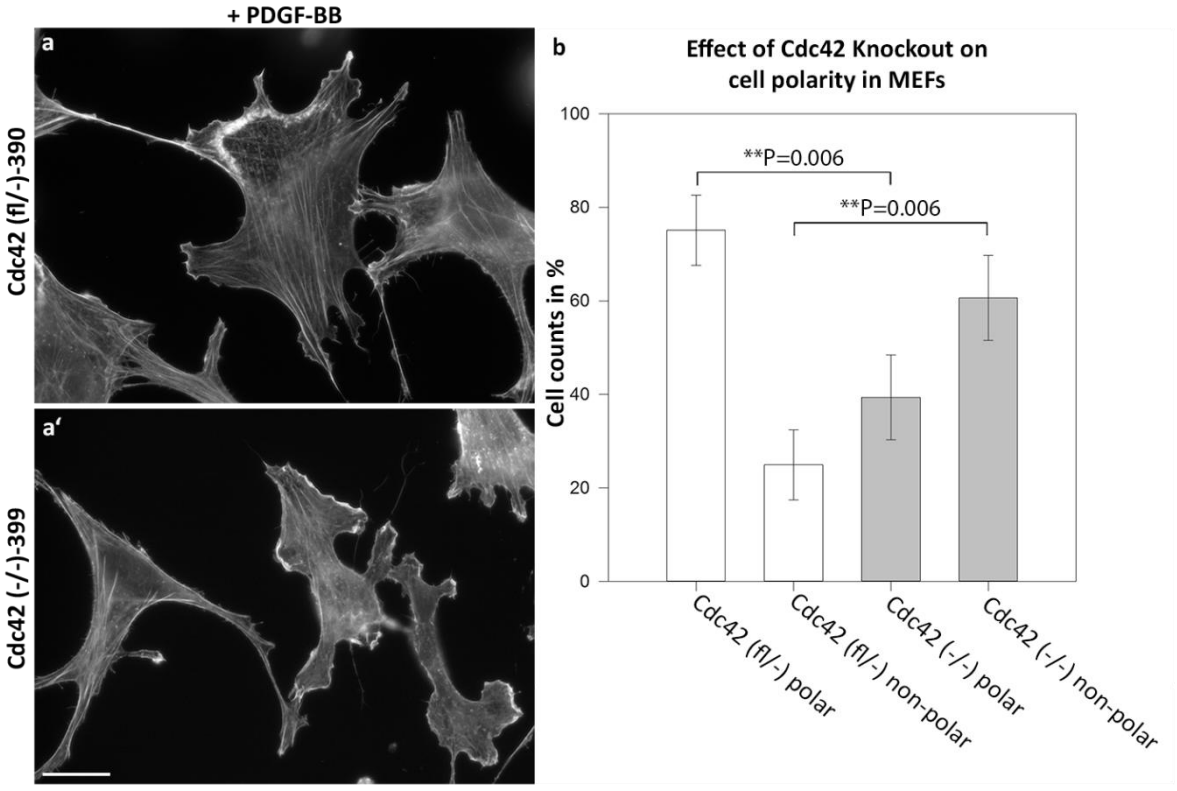

Figure 11: *Cdc42* knockout leads to reduced polarity in MEFs. (a;a'): 390 and 399 MEFs were plated on glass coverslips and cultivated for 18-24 hours at 37°C in cell culture incubator. Medium was changed

to starvation medium (without FCS) and cells were starved for 18 hours. After starvation 20nM PDGF-BB was applied to cells. Finally cells were fixed in 4% PFA and stained using Alexa594-conjugated phalloidin. Cells were visualized by fluorescence microscopy. Scale bar 20µm. (b): Numbers of polar cells for PDGF-BB treated Cdc42 (fl/-) and Cdc42 (-/-) MEFs were counted using ImageJ and statistically analyzed with Sigma plot 13 software. Statistical analysis was performed using student's t-test. Error bars show one standard deviation of the mean value form three independent experiments with sample size of 242 cells

A global PDGF-BB treatment caused Cdc42 (fl/-) MEFs to polarize their cytoskeleton predominantly in one direction as shown in Figure 11a. In contrast, in the majority of the Cdc42 knockout cells lamellipodia were induced in a scattered pattern around cell perimeter (Figure 11 a'). The Figure 11b shows that approx. 75% of control MEFs show a polar morphology whereas only 40 % of Cdc42 (-/-) cells can develop polar morphology in response to PDGF-BB. In Cdc42 (-/-) MEFs the fraction of non-polar cells is increased from approx. 40 % - to 60% of cells compared to control.

3.1.4 *Cdc42* knockout has a negative effect on PDGF-BB induced 2D chemotaxis

Several reports point out the important role of Cdc42 GTPase in polarization of cells and suggest its role in chemotaxis of macrophages and fibroblastoid cells, while other studies claim the role of Cdc42 in chemotaxis is less important (Catherine D Nobes and Hall 1999; Mains, Sulston, and Wood 1990; Stramer et al. 2005a; Allen et al. 1998; Monypenny, Zicha, Higashida, Oceguera-yanez, et al. 2009). It is rather well established that Cdc42 is not essential for 2D migration per se.

In our study Cdc42 knockout MEFs show slightly reduced numbers of filopodia. Furthermore, the Cdc42 knockout MEFs have defects in the formation of the polarized actin cytoskeleton in response to PDGF-BB, which is a specific chemoattractant for these cells. Next, I assessed whether Cdc42 knockout MEFs are affected in chemotaxis towards PDGF-BB. The 2D chemotaxis assay was performed in a 2D µslide chamber (Ibidi) (Isfort et al. 2011b). Representative images of chemotaxis assay and cell migraton plots are displayed in the following Figure 12.

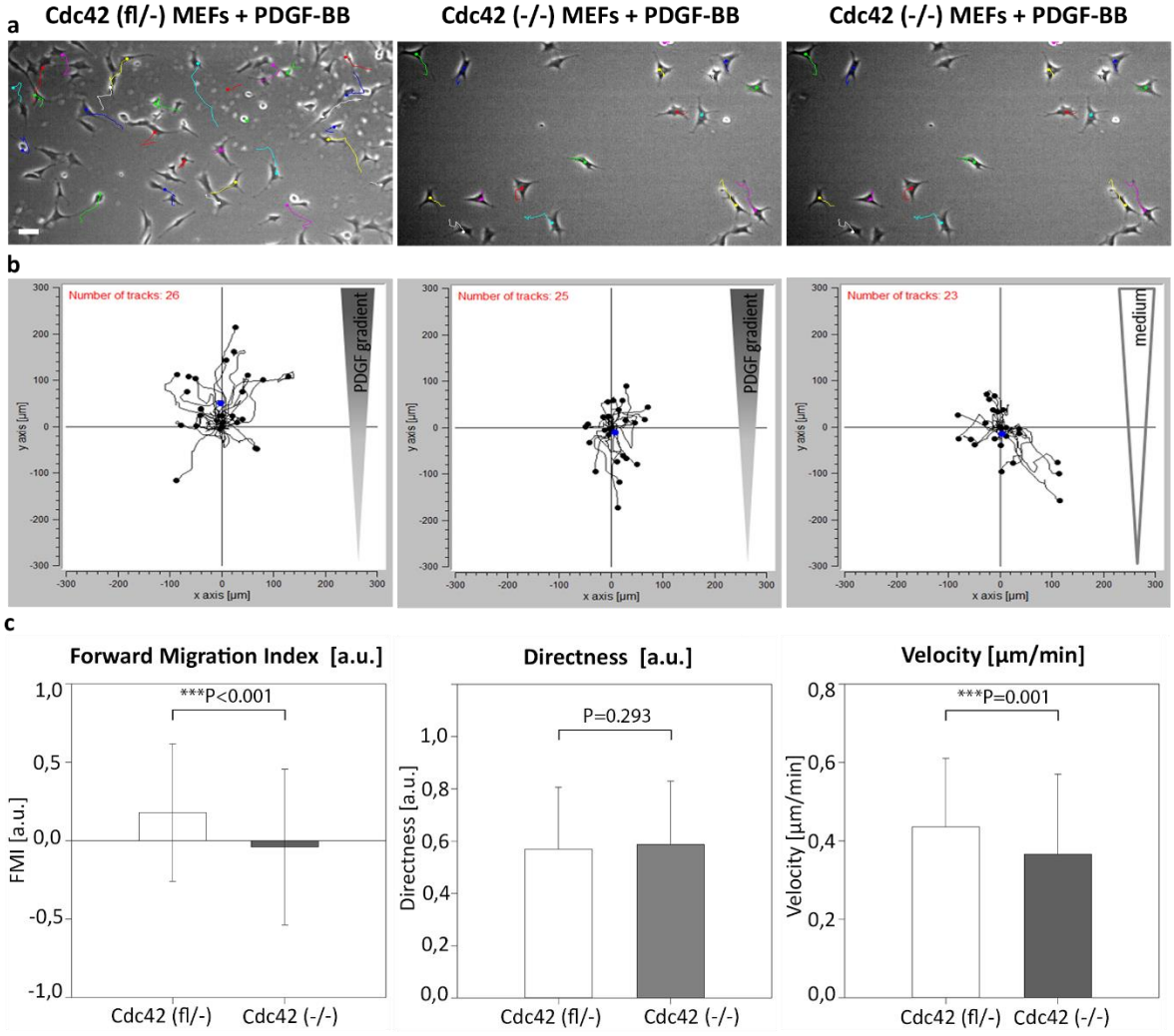

Figure 12: Effect of *Cdc42* knockout on 2D chemotaxis of MEFs. MEFs were injected into 2D µslide chemotaxis chamber (Ibidi) and incubated for 18-24h. Thereafter cells were starved for 16-18 hours. After starvation 20 ng/ml PDGF-BB (final concentration) was added to one of the reservoirs of chemotaxis slide. In one of chambers starvation medium was applied to Cdc42 (-/-) MEFs as a negative control. Next, the 2D chemotaxis slide was placed in an environmental chamber (Ibidi) mounted on the microscope equipped with motorized XY-table. Live cell imaging was performed using VisiView software (visitron systems). Pictures were taken every 5 minutes at 5x magnification in brightfield illumination for 8-12 hours. (a): Videos of different treatment groups were imported and tracked using ImageJ manual tracking plugin. (b): The resulting Datasets of XY coordinates of migrating cells were imported into chemotaxis tool 2.0 (Ibidi) and plotted on an XY coordinate system representing each individual chemotaxis chamber. (c): The forward migration index (FMI), directness and velocities of cells in chemotaxis chamber were calculated. The results were exported for statistical analysis to Sigma plot 13 software. Statistical analysis was performed using Mann-Whitney Rank Sum Test. Scale bar 50µm. Error bars show one standard deviation of the mean value form three independent experiments with sample size of 971 cells.

Figure 12a shows overlays of tracked videos of 2D chemotaxis experiments of MEFs that either harbour floxed version of *Cdc42* gene (left image) or are deficient in this gene (middle and right

images). As visible form the plots of cell-paths, the majority of Cdc42 (fl/-) MEFs migrate towards PDGF-BB (+Y direction in Figure 12b). In contrast, Cdc42 (-/-) cells don't migrate towards PDGF-BB gradient reminicent of negative controle. Figure 12c shows statistical quantification of chemotaxis results. MEFs deficient of Cdc42 show defiective chemotaxis which is expressed in close to zero FMI of the whole cell population in Cdc42 (-/-) cells comapred to Cdc42 (fl/-) cells. The directness of cell movement is not altered after PDGF-BB treatement of both, Cdc42 (fl/-) and Cdc42 knockout cells, which means that cell traectories in both treatment groups are much alike. Furthermore, the mean velocity of Cdc42 knockout MEFs in PDGF-BB gradient is approx. 20% reudced compared to Cdc42 (fl/-) cells.

3.1.5 CDR-formation coincides with more efficient chemotaxis

PDGF-BB is a prominent chemoattractant of fibroblasts triggering chemotaxis in these cells when a gradient of PDGF-BB is applied (Jackson, Stephens, and Hawkinsq 1992). CDRs were often implicated to play a role in several cellular processes such as reorganization of actin cyto-skeleton, micropinocytosis or degradation of surface receptors (Krueger et al. 2003; Suetsugu et al. 2003; Alberts et al. 2002b). In contrast to filopodia and lamellipodia that are generally formed in response to chemoattractants, CDRs are specifically formed in MEFs after treatment with PDGF-BB. MEFs perform chemotaxis towards a gradient of PDGF-BB. This raises the question whether the CR formation is an important part of PDGF induced chemotactic process in MEFs.

When MEFs are stimulated with PDGF-BB approx. 60-80 % of the cells form CDRs within the first 10 minutes. In this 2D chemotaxis assay I assessed if cells that form CRs extensively during the chemotaxis experiment differ in migration pattern from cells that do not show visible CRs. Therefore, cells from the same population and treatment group were assessed. CRs are visible when 10x magnification in brightfield phase contrast microscopy is applied. This way, cells which clearly formed CRs during 2D chemotaxis assay could be identified and tracked to com-pare them with cells which displayed no visible CRs under the exact same conditions (Figure13).

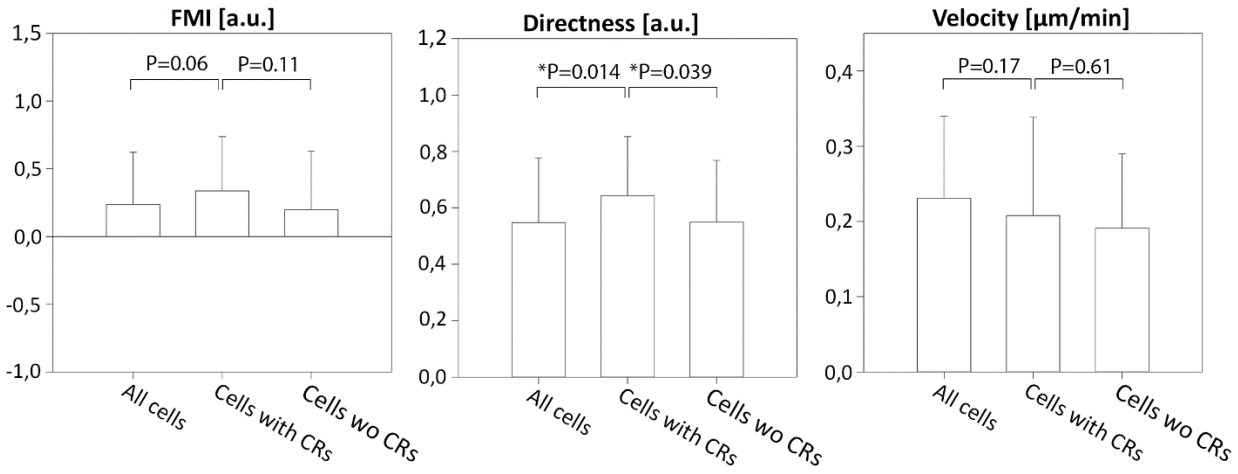

Figure 13: Cells that frequently form CRs are slightly more efficient than the whole subpopulation of MEFs in chemotaxis. MEFs were injected into 2D µslide chemotaxis chamber (Ibidi) and incubated for 18-24h. Thereafter cells were starved for 16-18 hours. After starvation 20 ng/ml PDGF-BB (final concentration) was added to one of the reservoirs of chemotaxis slide. In one of chambers starvation medium was applied to Cdc42 (-/-) MEFs as a negative control. Next, the 2D chemotaxis slide was placed in an environmental chamber (Ibidi) mounted on the microscope equipped with motorized XY-table. Live cell imaging was performed using VisiView software (Visitron systems). Pictures were taken every 10 minutes at 10x magnification in brightfield illumination for 8-12 hours. Videos were imported and tracked using ImageJ manual tracking plugin. The resulting Datasets of XY coordinates of migrating cells were imported into chemotaxis tool 2.0 (Ibidi) and plotted on an XY coordinate system representing each individual chemotaxis chamber. The FMI, directness and velocities of cells in chemotaxis chamber were calculated. The results were exported for statistical analysis to Sigma plot 13 software. Statistical analysis was performed using Mann-Whitney Rank Sum Test. Error bars show one standard deviation of the mean value form three independent experiments with sample size of n = 159 cells.

Whereas, no significant differences could be detected in Velocity or FMI between CR positive and negative cells, the directness of CR positive cells was approx. 20 % higher as of that of CR negative and of the whole cell population**.**

3.1.6 Cdc42 knockout MEFs show reduced velocity in various setups

To test, if reduced velocities of Cdc42 knockout cells in the chemotaxis assay were assay-independent results, I used different setups of cell migration conditions such as fibronectin coating and treatment of cells with global PDGF stimulus (s. methods). Velocities of cells per well/condition were measured and plotted as described previously. Figure 14 illustrates the results of this assay.

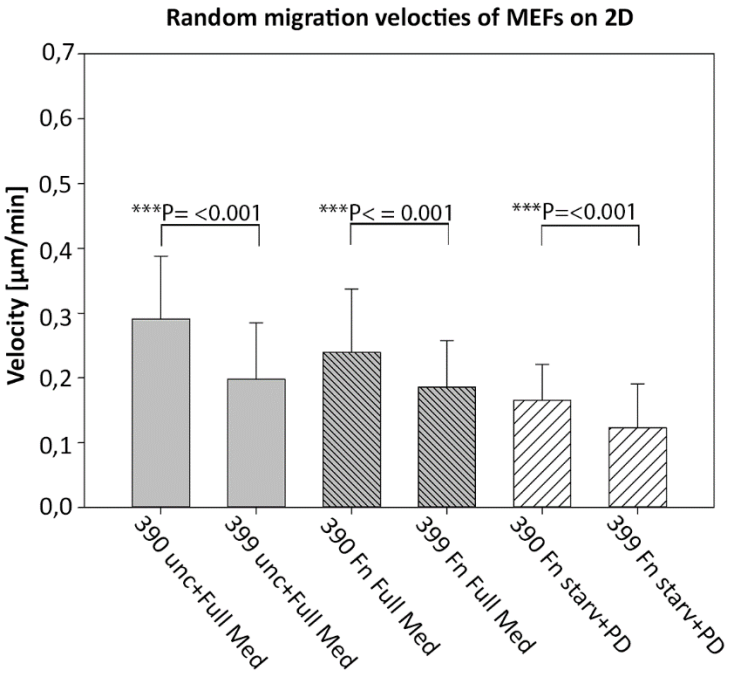

Figure 14: *Cdc42* knockout leads to reduced velocity in MEFs. MEFs were injected to pre-coated or uncoated wells in µslide 6 (Ibidi) and let to adhere for 24h. After adhesion in several wells medium was exchanged to starvation medium for additional 18-16 hours. Thereafter starvation medium was exchanged with medium with 20ng/ml PDGF and the µslide was placed in an environmental chamber (Ibidi) and live cell migration from each well was recorded using VisiView software. Pictures were taken every 5 minutes at 5x in brightfield illumination. Videos of different treatments were imported and tracked using ImageJ manual tracking plugin. These XY coordinates of cells were imported to chemotaxis tool 2.0 (Ibidi) and the velocities cells in each well were calculated. The results were exported for statistical analysis to Sigma plot 13 software. Statistical analysis was performed using Mann-Whitney Rank Sum Test. Unc: uncoated well; Fn: fibronectin coated well; starv: starved cells; +PD: PGDF-BB treatment of cells; Full Med: Medium with supplements (s. methods). Error bars show one standard deviation of the mean value form three replicates per condition with sample size of n = 79-218 cells per condition.

As shown in Figure 14 in all utilized 2D migration setups, Cdc42 knockout cells showed consistently reduced velocity compared to Cdc42 (fl/-) cells across different substrates such as fibron-

ectin, culture dish or glass. Generally, velocities of Cdc42 (-/-) cells were approx. 20-30% reduced compared to Cdc42 (fl/-) cells in each setup (uncoated wells with medium treated cells, in fibronectin-coated wells with medium treated cells and also in fibronectin-coated wells with PDGF-BB treated cells).

3.1.7 Effects of knockdown of fascin on actin protrusions in MEFs

3.1.7.1 *Fascin1* knockdown leads to reduced formation of CDRs and filopodia

The previous work from our lab showed that knockdown of fascin negatively affects the ability of MEFs to form dorsal ruffles in response to PDGF-BB. To confirm the effect of fascin knockdown on the ability of cells to induce CDRs MEFs were treated with shRNA constructs targeting mouse or human fascin mRNA and after treatment of cells with PDGF the CRs were quantified (Figure 15).

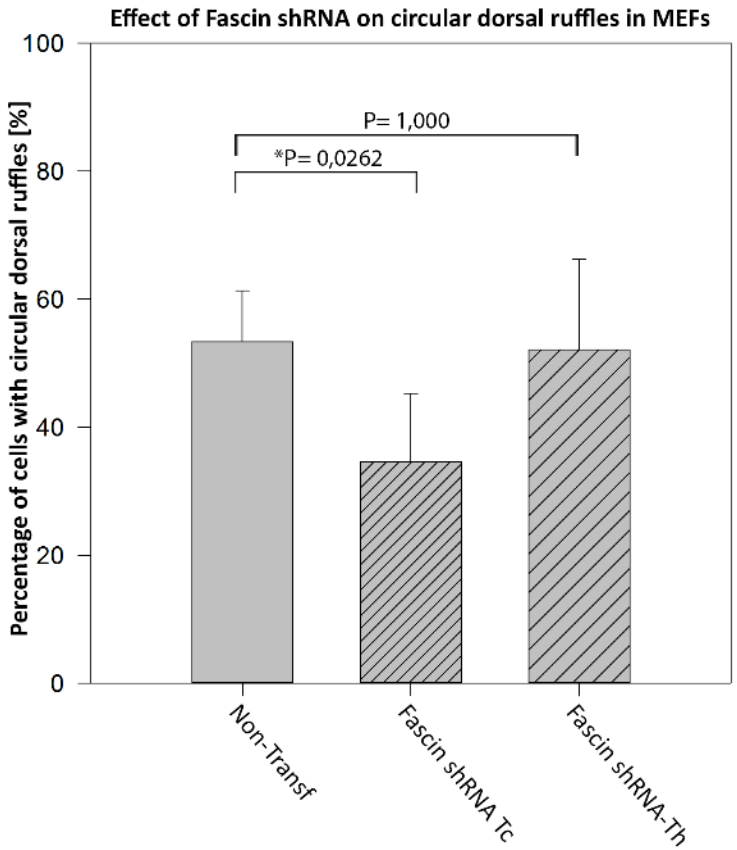

Figure 15: Fascin knockdown leads to reduced formation of CDRs in MEFs. Prior to transfection MEFs were cultured to approx. 70-80% confluency. Cells were transfected with plasmids containing GFP-

fascin RNA containing constructs for downregulation of fascin gene of human origin (shRNA-Th) or of mouse and human origins (shRNA-Tc). Post 18-20 hours transfection cells were rescued with fresh medium containing FCS and further cultivated for 8-12 hours. Thereafter cells were seeded on coverslips and adhered overnight. This was followed by a starvation phase for 16-18 hours. Finally cells were stimulated with PDGF-BB to induce the formation of CDRs. After 5-10 minutes of stimulation with PDGF-BB cells were fixed with 4% PFA and stained for F-actin using phalloidin alexa-594. Fixed and stained cells were imaged by fluorescence microscopy. CDRs were counted from random samples of n = 74-157 cells per each treatment. Results were exported for statistical analysis to Sigma plot 13 software. Statistical analysis was performed using Mann-Whitney Rank Sum Test. Error bars show one standard deviation of the mean value form three independent experiments with sample sizes of n = 409-433 cells per condition.

Figure 15 shows that MEFs treated with fascin shRNA construct against both mouse and human *fascin1* (shRNA-Tc) have markedly reduced ability to form dorsal ruffles compared to non-transfected cells or to cells treated with shRNA construct targeting human fascin specifically which serves as a control. To detect whether fascin shRNA treated cells had additionally a reduced number of filopodia, treated cells were fixed and filopodia from cells expressing fascin shRNA-GFP constructs were counted (Figure 16).

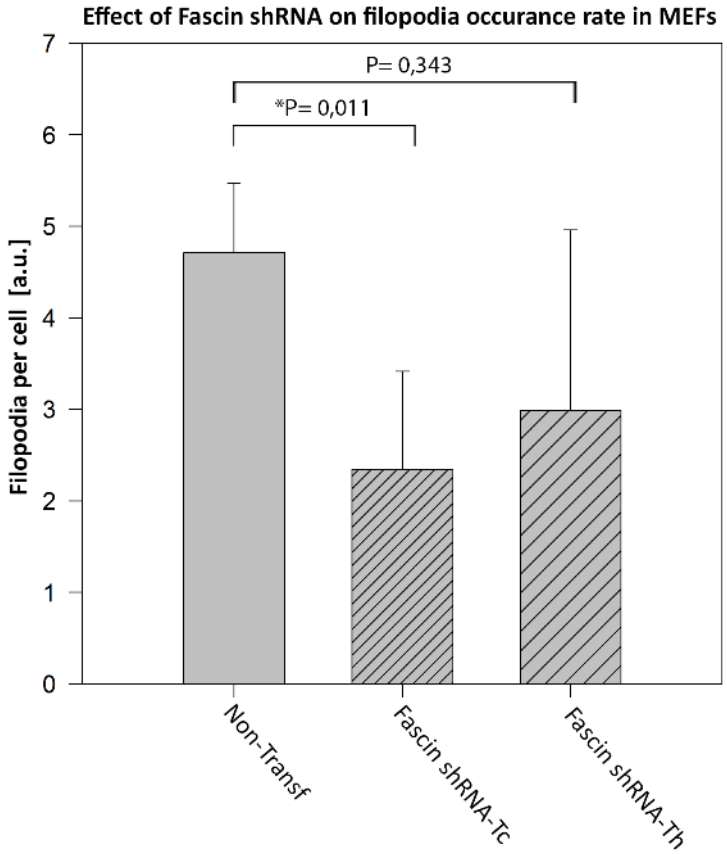

Figure 16: Fascin knockdown leads to reduced formation of filopodia in MEFs. Prior to transfection MEFs were cultured to approx. 70-80% confluency. Cells were transfected with plasmids containing GFP-fascin RNA containing constructs for downregulation of *fascin1* gene of human origin (Th) or of mouse

and human origins (Tc). Post 18-20 hours transfection cells were rescued with fresh medium containing FCS and further cultivated for 8-12 hours. Thereafter cells were seeded on coverslips and adhered overnight. Finally cells were fixed with 4% PFA and stained for F-actin using phalloidin alexa-594. Cells were imaged by fluorescence microscopy in 63x magnification. Filopodia were counted at protruding edges of cells. Results were exported for statistical analysis to Sigmaplot 13 software. Statistical analysis was performed using Mann-Whitney Rank Sum Test. Non-Transf: Control MEFs treated with transfection reagent. Error bars show one standard deviation of the mean value form two independent experiments with sample size of 84-118 cells per condition.

The transfection of MEFs with shRNA constructs against fascin mRNA of mouse or human origin, in both cases, leads to a reduction in numbers of filopodia per cell in MEFs as is seen in Figure 16. However, the reduction of filopodia is only statistically significant in cells transfected with the shRNA construct against mouse / human fascin (Tc) and additionally leads to defective formation CDRs.

3.1.8 Effects of formin inhibitor smiFH2 on actin protrusions in MEFs

3.1.8.1 SmiFH2 negatively affects formation filopodia and CDRs

Form the prevous work it was shown that, Cdc42 is essential for the formation of CDRs independent of Rac1. Furthermore, the knockdown of fascin which is enriched in filopodia leads to loss of CDRs reminiscent of Cdc42 knockout phenotype (Schloen, K,. PhD thesis). So, we hypothized that the reduced rate of CDR formation in Cdc42 knockout MEFs might be due to defects in signaling downstream of Cdc42 leading to formation of filopodia. Indeed, Cdc42 knockout MEFs show a 13 % reduction in the number of filopfoia per cell compared to control cells (Figure 10).

The most prominent downstream effectors of the Cdc42 GTPase are WASP / N-WASP and formins (Faix and Rottner 2006a; Chhabra and Higgs 2007a). It was shown that N-WASP was not involved in the formation of CDRs in Cdc42(fl/-) MEFs (Ladwein and Guledani unpublished). On the other hand, formins are involved in generation of filopdoia and are constituents of a tip complex of these structures (Faix and Rottner 2006a). Thus, I wanted to test whether formins were involved in the formation of CDRs, possbily downstream of Cdc42, as nucleators in filopodia. Therefore, I utilized smiFH2, a novel formin inhibitor, to interfere with

formin-mediated actin nucleation in MEFs. I pretreated the cells with smiFH2 inhibitor before stimulation with PDGF-BB and subsequent fixation. The representative images form Figure 17 show control cells that produce normal lamellipodia and filopodia, whereas in smiFH2 treated cells reduced number of filopodia were detected.

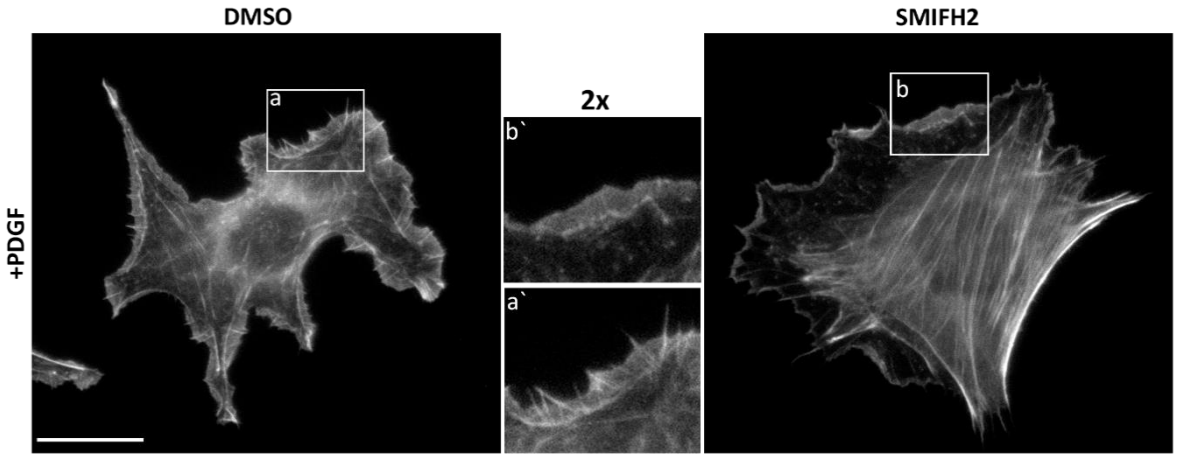

Figure 17: Negative effect of formin inhibitor smiFH2 on the formation of filopodia in MEFs. Cdc42 (fl/-) MEFs (390) were plated on glass coverslips and cultivated for 18-24 hours at 37°C in cell culture incubator. Medium was changed to starvation medium (without FCS) and cells were starved for 16-18 hours. After starvation, cells were pretreated with DMSO or smiFH2 followed by stimulation with 20nM PDGF-BB. Finally, cells were fixed in 4% PFA and stained using Alexa594-conjugated phalloidin. Cells were visualized by fluorescence microscopy. Scale bar 20µm. (a, a'): control treatment with DMSO; (b, b'): Treatment with 15µM smiFH2.

To quantify these results primarily filopodia-like protrusions that were embedded in lamellipodia were counted in treated and control cells. The results are shown in Figure 18.

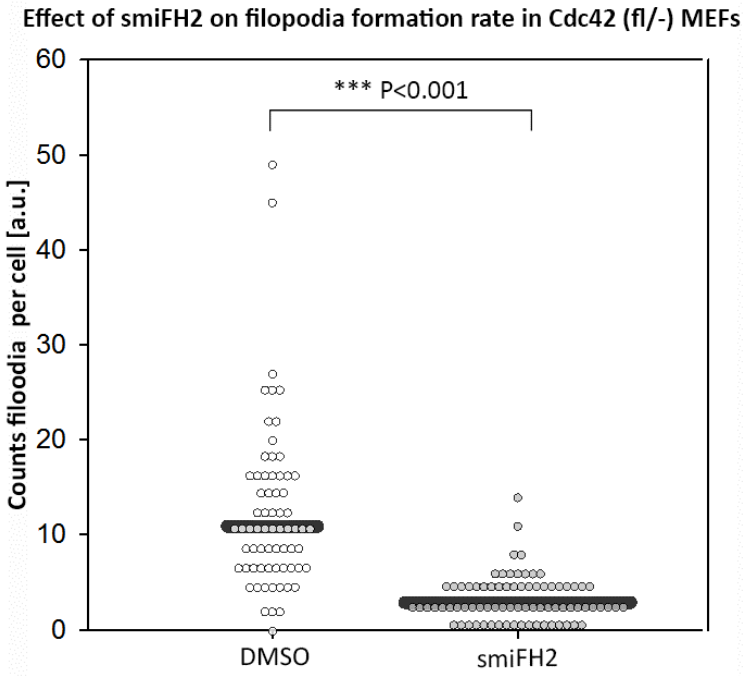

Figure 18: Formin inhibitor smiFH2 leads to reduced formation of filopodia in MEFs. Cdc42 (fl/-) MEFs were pretreated with DMSO or smiFH2 for 30 minutes followed by stimulation by 20nM PDGF-BB. Cells were fixed with 4% PFA and stained using phalloidin alexa-594. Cells were imaged and pictured in fluorescence microscopy. Filopodia were counted at protruding edges of cells. Results were exported for statistical analysis to Sigma plot 13 software. Horizontal bars represent median values from three independent experiments with sample size of n = 73-83 cells per condition. Statistical analysis was performed using Mann-Whitney Rank Sum Test.

As seen in Figures 17 and 18, after smiFH2 treatment, cells produce markedly fewer filopodia compared to the control group when treated with PDGF-BB. I simultaniously monitored the formation of CDRs and lamellipodia under conditions where formins are inhibited and filopodia supressed (Figure 19).

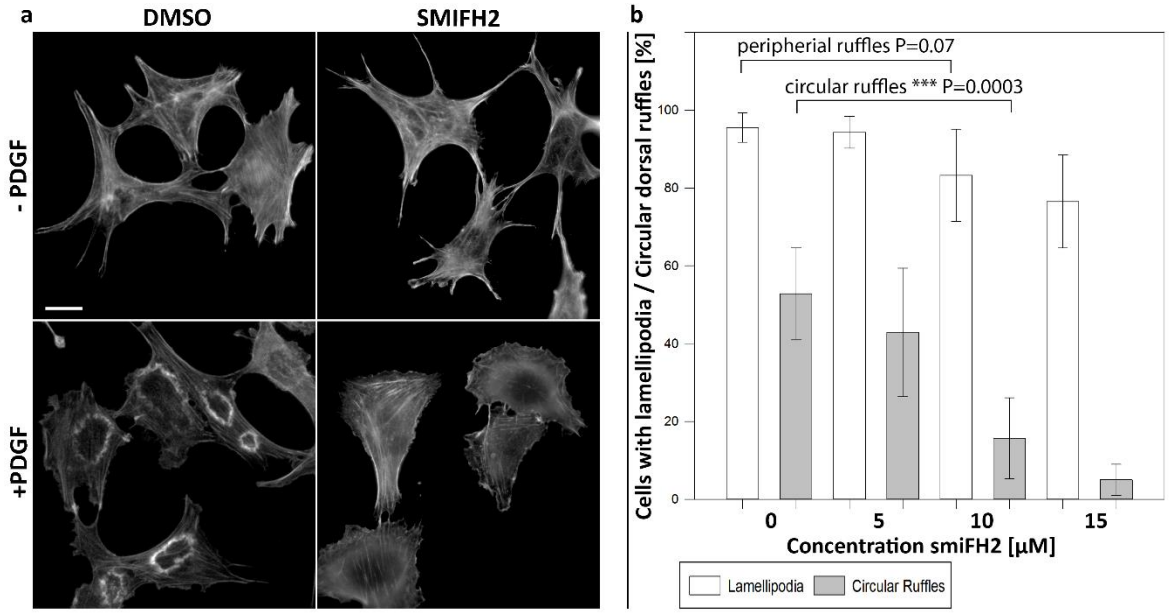

Figure 19: Effects of formin inhibitor smiFH2 on the formation of lamellipodia and CDRs in MEFs. MEFs (390) were plated on glass coverslips and cultivated for 18-24 hours at 37°C in cell culture incubator. Medium was changed to starvation medium (without FCS) and cells were starved for 16-18 hours. After starvation, cells were pretreated with DMSO or smiFH2 in the concentration range of 0-15 µM. This was followed by stimulation of cells with 20nM PDGF-BB. Finally, cells were fixed in 4% PFA and stained using Alexa594-conjugated phalloidin. Cells were visualized by fluorescence microscopy. Scale bar 20µm. (a): Pictures of DMSO and smiFH2 treated cells stimulated or not with PDGF-BB. (b): Statistical analysis of lamellipodia and circular dorsal ruffle formation rate after application of smiFH2 in concentration rage of 0-15µM. Error bars show one standard deviation of the mean value form four independent experiments with sample size of 81-204 cells per condition.

According to results shown in Figure 19 smiFH2 specifically and dose dependently inhibited the formation of CDRs, however did not have a profound effect on the formation of lamellipodia. Cells treated with the formin inhibitor resemble the Cdc42 knockout phenotype of MEFs, showing lost ability to form CDRs and reduced numbers of filopodia after PDGF-BB treatment. This supports our hypothesis that stimulation of MEFs with PDGF-BB activates formins downstream of Cdc42 and formins nucleate filopodia that are essential in the formation of CDRs.

3.1.8.2 SmiFH2 has a negative effect on PDGF-BB induced cell polarity

In our hands, Cdc42 deficiency in MEFs resulted in markedly increased non-polarized formation of lamellipodia all over the cell perimeter, a decreased formation of filopodia and loss of chemo-

taxis. Formins are known as prominent downstream effectors of Cdc42, which nucleate unbranched actin filaments such as in filopodia or invadopodia. The nucleation activity of formins is probably induced by activated Cdc42 (Seth, Otomo, and Rosen 2006; Pellegrin and Mellor 2005; Lizárraga, Poincloux, Romão, et al. 2009). Actin-based protrusions contribute largely to the mitogen induced polarity of the cell. Apparently, intact cell polarity can contribute to directed migration and chemotaxis. As previously assessed, treatment of cells with smiFH2 led to decrease in a number of filopodia and CDRs per cell, whereas lamellipodia were less affected by this treatment.

To test, how inhibition of formins affects the PDGF-bb induced polarization of the cytoskeleton, I utilized the formin inhibitor smiFH2. Cdc42 (fl/-) MEFs were pretreated with smiFH2 or DMSO (s. M/M) followed by the global stimulus of PDGF-BB (Figure 20).

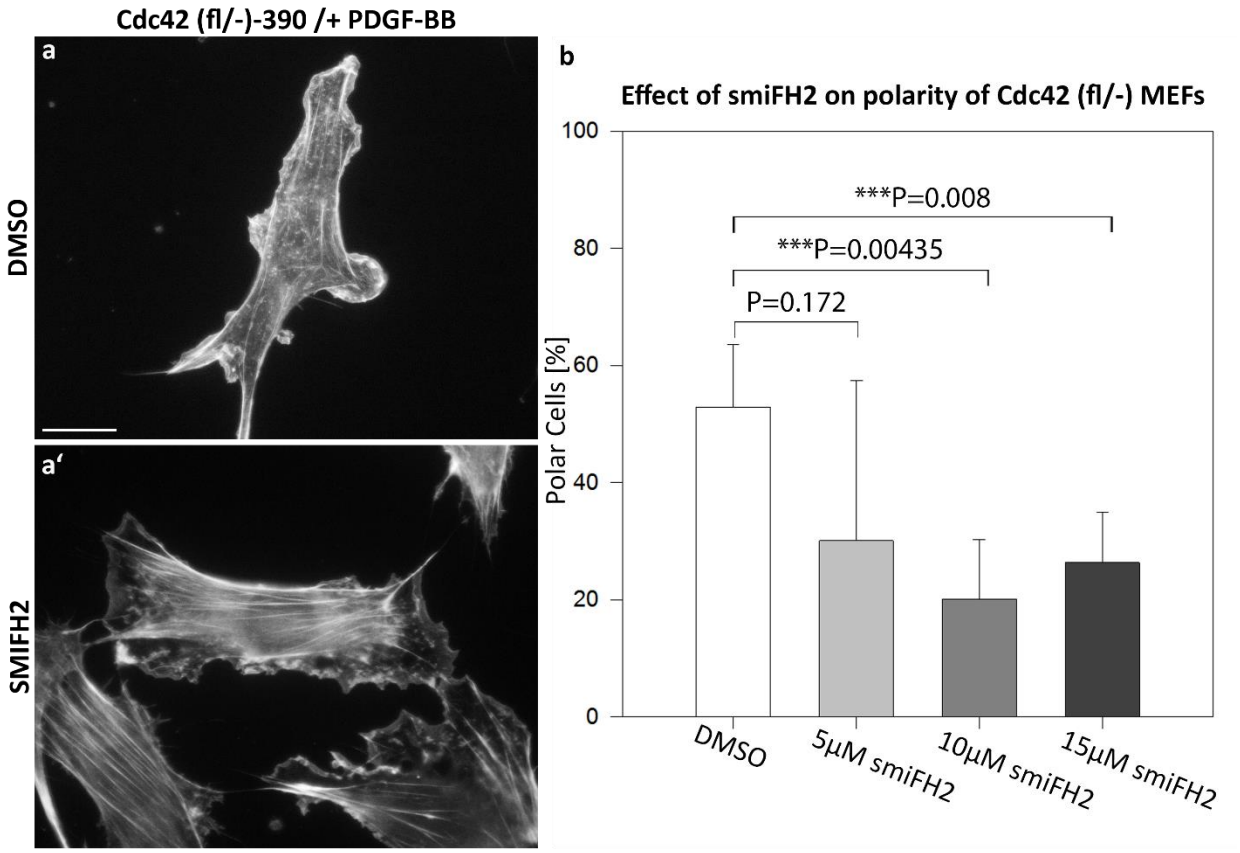

Figure 20: Effects of formin inhibitor smiFH2 on cell polarity in MEFs. MEFs (390) were plated on glass coverslips and cultivated for 18-24 hours at 37°C in cell culture incubator. Medium was changed to starvation medium (without FCS) and cells were starved for 16-18 hours. After starvation, cells were pretreated with DMSO or smiFH2 in the concentration range of 0-15 µM. This was followed by stimulation of cells with 20nM PDGF-BB. Finally, cells were fixed in 4% PFA and stained using

Alexa594-conjugated phalloidin. Cells were visualized by fluorescence microscopy. Scale bar 20µm. (a, a'): Representative pictures of DMSO- and smiFH2-treated cells stimulated with PDGF-BB respectively; (b): Statistical analysis of cell polarity in different treatment groups after application of smiFH2 in concentration rage of 0-15µM. Error bars show one standard deviation of the mean value form three independent experiments with sample size of 243-324 cells per condition.

As seen from quantification (Figure 20b) and representative microscopic images of treated and control cells (Figure 20a), the polarity of MEFs was reduced to 20-35% when cells were pretreated with smiFH2 concentrations in the range of 5-15 µM. With higher smiFH2 concentrations the standard deviation of mean values of polar cell population decreases.

3.1.8.3 Cdc42 knockout MEFs show reduced velocity in wound healing assay

Next, I tested whether the differences in the cell velocity between Cdc42 (fl/-) and Cdc42 (-/-) cells in chemotaxis assays also occur in a wound healing assays. In this assay, an artificial scratch is introduced in a confluent grown cell layer, and the closure of the artificial wound is monitored via time lapse microscopy. Furthermore, the role of formins was assessed in the wound healing assay by using smiFH2. In this way it was tested how cells respond to inhibition of formin-mediated nucleation of unbranched actin filaments in a wound healing assay (Figure 21).

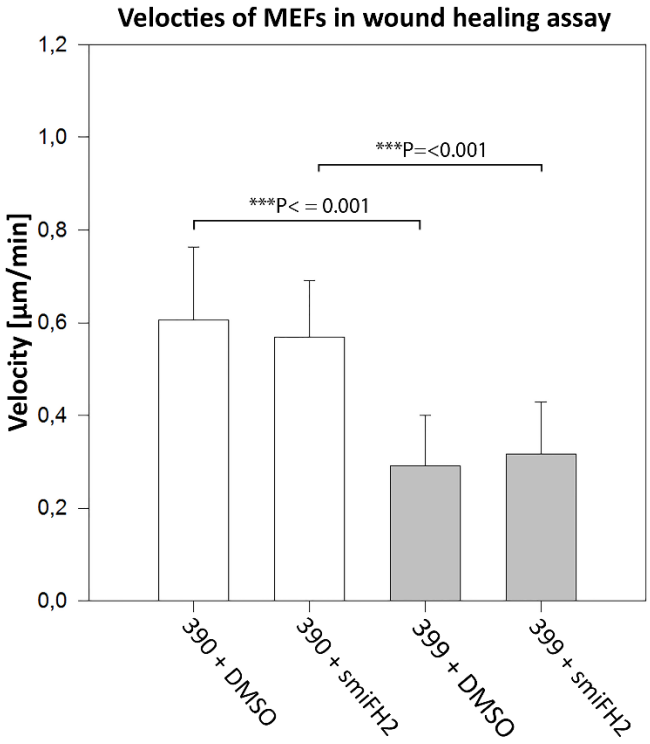

Figure 21: Wound healing assay of Cdc42 (fl/-) and Cdc42 (-/-) MEFs w/o smiFH2. MEFs were plated on wells of Ibidi 24-well µslide chamber (Ibidi) and grown to confluence. A scrape was generated in a cell monolayer using pipet tip, and µslide was placed in an environmental chamber (Ibidi). Wound closure was monitored in brightfield microscopy using motorized xy-table and VisiView software for 12-16 hours. Pictures were taken every 5 minutes at 5x magnification using brightfield illumination. Videos of different treatments were imported and tracked using ImageJ manual tracking plugin. These XY coordinates of cells were imported to chemotaxis tool 2.0 (Ibidi), and the velocities cells in each well were calculated. The results were exported for statistical analysis to Sigma plot 13 software. Statistical analysis was performed using Mann-Whitney Rank Sum Test. Error bars show one standard deviation of the mean value form three replicates with sample size of 66-92 cells per condition.

As seen from the Figure 21 Cdc42 (-/-) MEFs are approx. 50 % slower than Cdc42 (fl/-) cells in the wound healing assay. In 2D chemotaxis assays Cdc42 (-/-) MEFs migrate approx. 20 % slower than Cdc42 (fl/-) cells (Figure 12c). Also in a random migration assay, Cdc42 knockout MEFs migrate approx. 20 % slower than Cdc42 (fl/-) MEFs (Figure 14). This reduced velocity of Cdc42 knockout cells is in line with previous findings. (Czuchra et al. 2005).

As shown above the inhibition of formins by smiFH2 had similar effects on filopodia, dorsal ruffle formation and cell polarity in MEFs as the loss of Cdc42. Additionally, Cdc42 (-/-) MEFs migrate with approx. 10-20 % reduced velocity as control MEFs. To test if smiFH2 also negatively

affects cell velocity in MEFs, Cdc42 (fl/-) MEFs were treated with this inhibitor in a wound healing assay. The treatment of CDC42 (fl/-) cells with smiFH2 did not have a significant effect on cell velocity in the wound healing assay.

3.1.8.4 SmiFH2 has a negative effect on adhesion to ECM

Formins are major actin nucleators of unbranched actin filaments that facilitate formation of cell protrusions such as filopodia and invadopodia (D. Vignjevic 2006; Peng et al. 2003; Mellor 2010b; Faix and Rottner 2006c).

I showed that smiFH2 negatively affects the formation of filopodia and CDRs in MEFs. To test if smiFH2 mediated suppression of filopodia has a negative effect on adhesion of Cdc42 (fl/-) MEFs to ECM, I pretreated cells with smiFH2 before performing an adhesion assay.

Formins are apparently involved in the formation of both, filopodia and invadopodia. By using GM6001, I wanted to test whether or not matrix degradation by invadopodia plays a role in initial adhesion of MEFs to ECM. Inhibitor GM6001 effectively blocks the majority of extracellular MMPs and thus ECM degradation by cells (Figure 22) (Sahai and Marshall 2003)

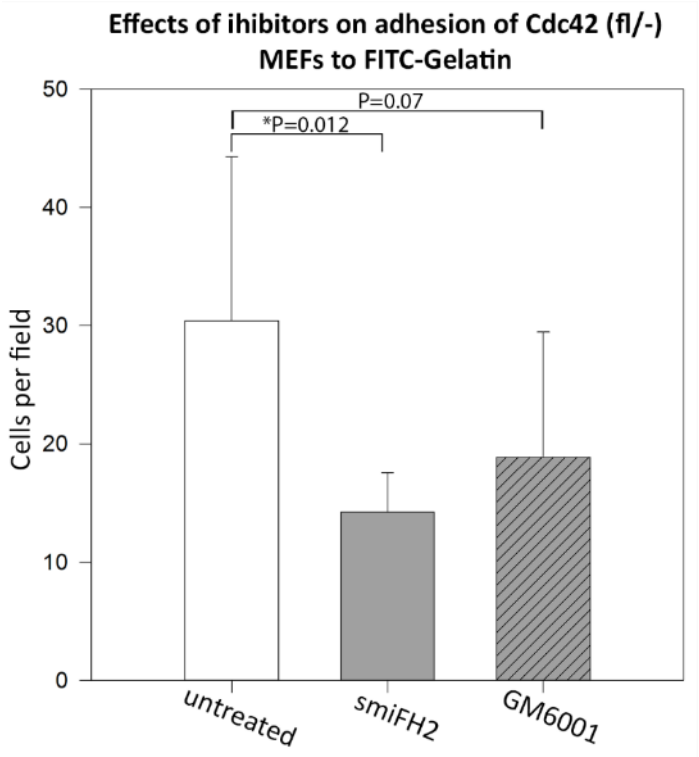

Figure 22: Effect of smiFH2 or GM6001 on the initial adhesion of MEFs on FITC-gelatin. Cdc42 (fl/-) MEFs adhered on FITC-gelatin coated coverslips for 40 min. in the presence of 25µM GM6001, 10µM smiFH2 or DMSO. Subsequently, cells were washed two times with PBS, followed by fixation with 4% PFA. After fixation step, coverslips were stained with phalloidin alexa-594 and visualized in fluorescence microscopy. Numbers of adhered cells per treatment were counted and statistically analyzed using Sigma plot 13 software. Statistical analysis was performed using Mann-Whitney Rank Sum Test. Error bars show one standard deviation of the mean value form two replicates with sample size of 132-217 cells.

In Figure 22, the adhesion assay of MEF cells on FITC-gelatin shows that adhesion of MEFs to ECM is significantly sensitive to formin inhibitor smiFH2. The average number of smiFH2 treated cells that could adhere to ECM is markedly decreased to approx. 40% of that of untreated cells. MEFs treated with GM6001 show no significant decrease in adhesion to ECM.

3.1.8.5 Degradation of ECM by MEFs

When seeded on 2D collagen or embedded in 3D collagen gels, Cdc42 (fl/-) MEFs were not able to adhere to effectively to ECM or migrate efficiently in 3D collagen matrix compared to other

cell types such as B16, C2C12 or HT1080 cells (not shown here). To move in 3D ECM, fibroblasts that usually use mesenchymal mode of migration probably need to degrade and modify the surrounding matrix. For this purpose, cells form invadopodia or invadosomes on 2D or in 3D ECM. Formation of these structures involves the activity of formins and is associated with secretion of MMPs to modify and degrade the ECM. To assess the ability of MEFs to degrade ECM via Invadopodia and secreted MMPs cells were cultivated on FITC-gelatin matrix (Figure 22). Matrix degradation by cells should result in degraded areas of ECM beneath cells. To suppress the extracellular proteinase activity, cells were treated with MMP inhibitor GM6001. To test if formins and thus invadopodia are involved in ECM degradation of MEFs, we applied formin inhibitor smiFH2 to cells prior degradation assay.

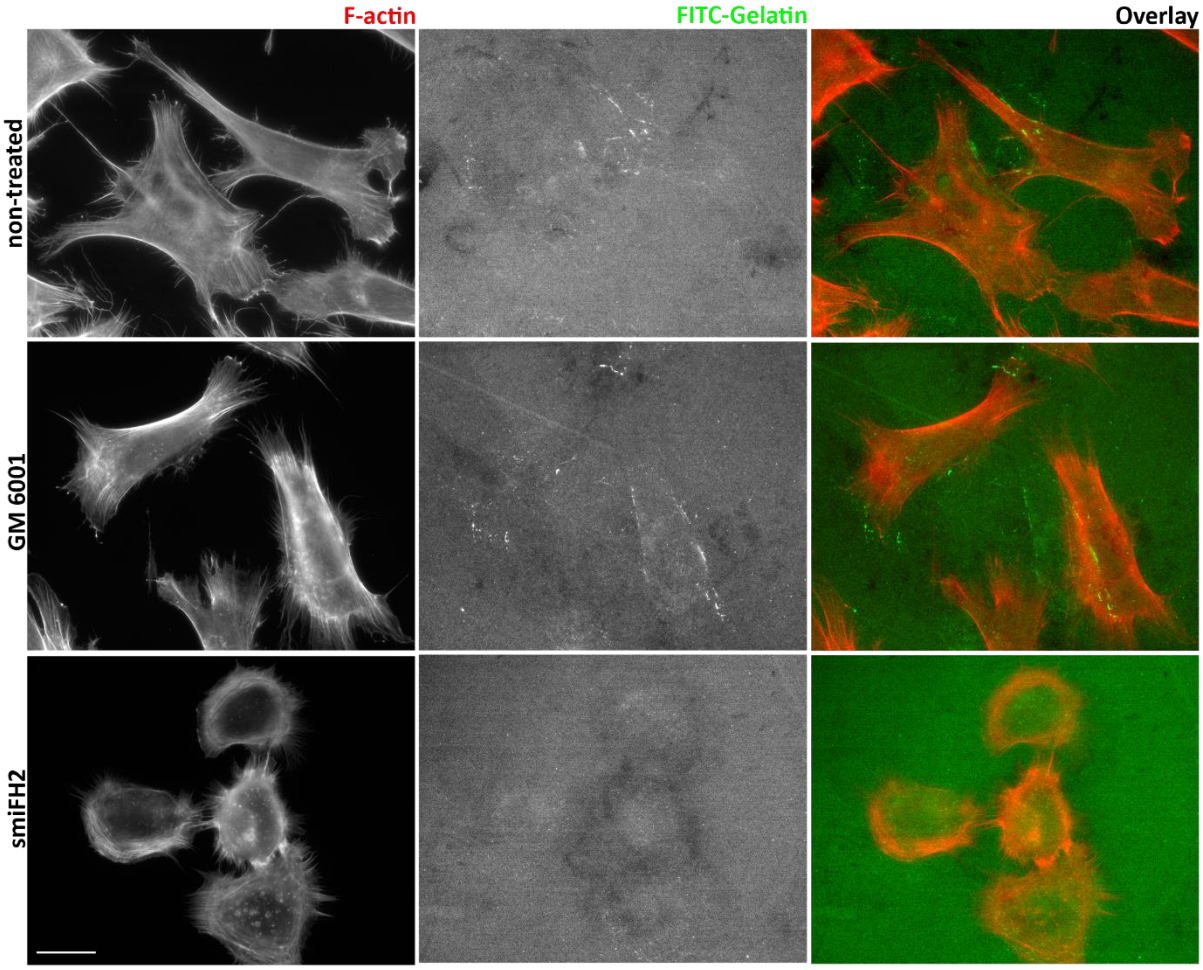

Figure 23: Matrix degradation assay of MEFs in presence of GM6001- or smiFH2. Cells were cultivated on FITC-gelatin coated coverslips for 5 hours in the presence of 25µM GM6001, 10µM smiFH2 or DMSO. Inhibitor treatment was followed by fixation of cells with 4% PFA. After fixation,

coverslips were stained with phalloidin alexa-594 and visualized in fluorescence microscopy. Scale: 20µm.

In Figure 23, neither control- nor MEFs pretreated with inhibitors do show typical matrix degradation, which are seen as non-fluorescent dark dots in green (FITC) channel beneath cells (compare matrix degradation of HT1080 cells (Figure 39; Figure 40). To quantify the results of degradation assay, the relative fluorescence beneath cells in green channel was assessed for each treatment group (Figure 24; for more details see methods section).

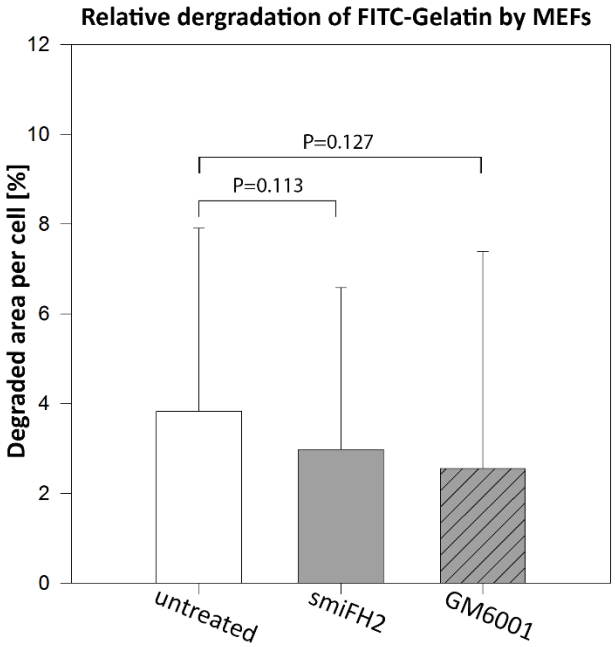

Figure 24: Quantitative analysis of matrix degradation by inhibitor treated MEFs. Cells were cultivated on FITC-gelatin coated coverslips for 5 hours in the presence of 25µM GM6001, 30µM smiFH2 or DMSO. Inhibitor treatment was followed by fixation of cells with 4% PFA. After fixation, coverslips were stained with phalloidin alexa-594 and visualized in fluorescence microscopy. Intensities of FITC-gelatin images beneath cells were measured and quantified for each treatment group in Metamorph 5 software. Statistical analysis was performed using Mann-Whitney Rank Sum Test using Sigma plot 13 software. Error bars show one standard deviation of the mean value form three replicates with sample size of 32-41 cells.

As Figure 24 shows, neither treatment of MEFs with smiFH2 nor GM6001 had a significant negative effect on degradation of FITC-gelatin. Generally, MEFs did not degrade FITC-gelatin at extent comparable to that of HT1080 cells (Figure 39; Figure 40). The minor ECM degradation by MEFs was also not significantly altered when inhibitors of formins or MMPs were applied to cells. Possibly, these cells cannot degrade the ECM such as HT1080 cells can do (Figure 38).

3.2 Effects of *Hem1* knockout in macrophage chemotaxis

3.2.1 Hem1 knockout macrophages lack lamellipodia but can form podosomes

Nap1 is a component of WAVE complex, which is critically involved in the formation of lamellipodia in many cell types. Nap1l also termed as Hematopoietic protein 1 (Hem1) is a variant of Nap1 which is expressed specifically in hematopoietic cells. In the present work, effects of Hem1 depletion on actin-based protrusion and chemotaxis of macrophages were analyzed. C5a was utilized as chemoattractant, which also induces formation actin-based protrusions such as lamellipodia and filopodia in these cells. Application of C5a induced formation of actin-based protrusions and chemotaxis in mouse BM macrophages. The cells were fixed and stained for F-actin to visualize podosomes and/or lamellipodia (Figure 25 a; b.). It is widely accepted that in macrophages podosomes are formed downstream of Cdc42 due to WASP- and not WAVE mediated activation of the Arp2/3 complex (Jones et al. 2002b; S Linder et al. 1999a; Giri et al. 2013b; Stefan Linder, Wiesner, and Himmel 2011).To test if WAVE complex deficiency caused by *Hem1* knockout effects podosome formation BM macrophages the Hem1 knockout cells were stained with antibodies against vinculin besides of F-Actin visualization.

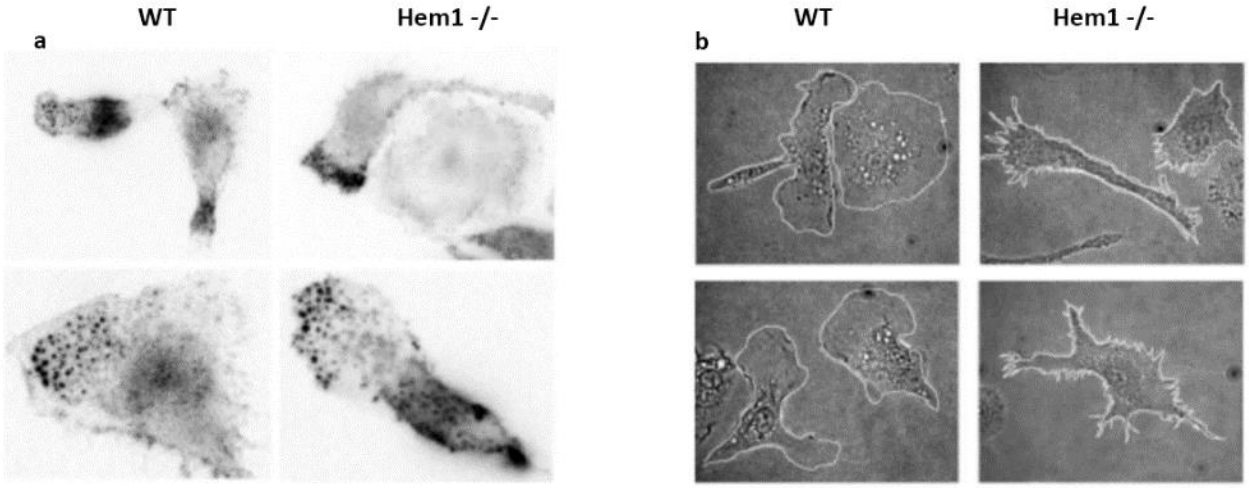

Figure 25: Podosomes and cell morphologies in WT- and Hem1 (-/-) macrophages. (Adopted form de Gorter et al.). (a) Formation of podosomes is not affected in Hem -/- macrophages. Hem1(-/-) cells were plated on fibronectin-coated coverslips. After adhesion cells were fixed and stained for vinculin and visualized in fluorescence microscopy. (b) Cell edges of BM-derived macrophages deficient in Hem1 show filopodia-like protrusions but no lamellipodia after adhesion and spreading on fibronectin covered coverslips.

Macrophages deficient in Hem1 still can form podosomes (Figure 25a), but apparently, lack lamellipodia (Figure 25b). Next, I stained BM-derived macrophages stimulated with chemoattractant C5a to visualize which actin structures are formed during cell protrusion in WT and Hem1 (-/-) cells (Figure 26).

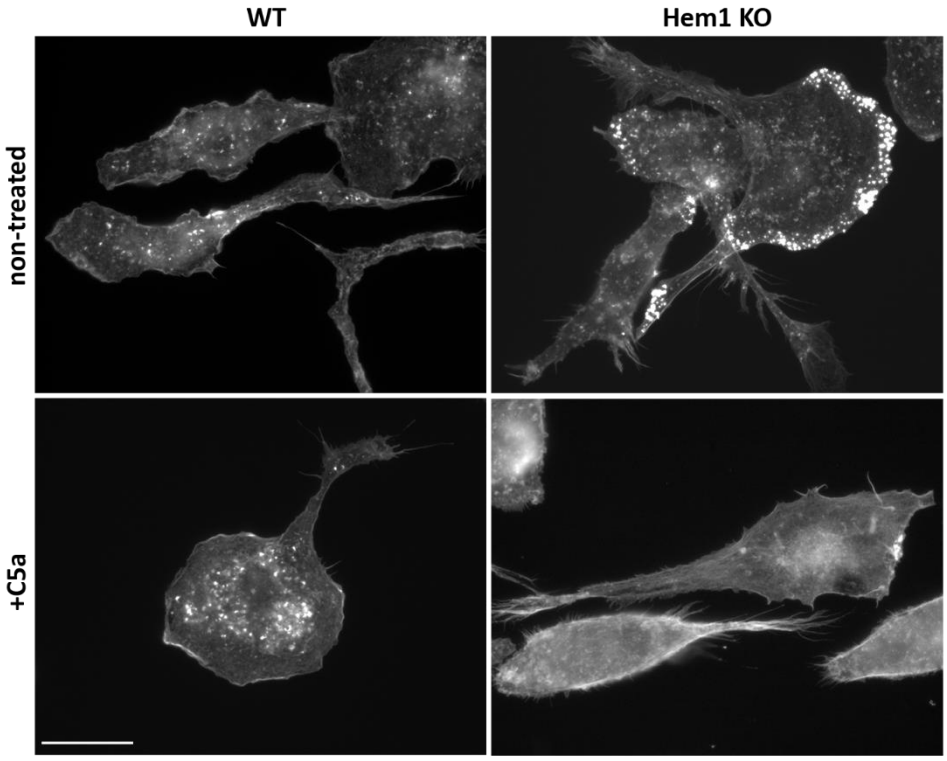

Figure 26: C5a stimulated Hem1 (-/-) macrophages cannot form lamellipodia. Wild-type and Hem1 knockout cells were plated on glass coverslips and incubated overnight in growth medium. Cells were stimulated with 30 nM C5a for 20min. Finally, control and C5a-treated cells were permeabilized and fixed. Cells were stained with Alexa-594-phalloidin.

Contrary to wildtype cells, in Hem1 knockout cells, C5α could not induce typical lamellipodia at the cell periphery. This could be seen in both brightfield- and fluorescent microscopy (Figure 26). Also distinct from WT cells, Hem1-null macrophages showed overproportionally long filopodia-like protrusions at the cell periphery. The podosomes in Hem1-null cells were primarily located at the cell periphery, presumably at the leading edge of cells. The number of podosome-forming Hem1-null cells was generally reduced. However, Hem1 knockout cells formed more podosomes per cell (unpublished data).

3.2.2 Hem1 knockout macrophages show impaired chemotaxis towards C5a.

The Rac- and WAVE mediated activation of Arp2/3 complex is thought to represent the major signaling axis leading to the formation of lamellipodia in many cell types including macrophages. In macrophages, activation of Rac1 leads to complex formation between WAVE2-Hem1 and Abi, which activates Arp2/3 complex leading to formation of actin-based protrusions (Weiner et al. 2006; Kheir et al. 2005). On the other hand, activated Cdc42 is thought to activate WASP and subsequently induce Arp2/3 mediated formation of podosomes in macrophages (Jones et al. 2002b; Theresia E. Stradal and Scita 2006).

The video microscopy-based analysis of chemotaxis of macrophages from WAS patients towards CSF-1 revealed impaired chemotaxis in these cells, expressed by haphazard cell trajectories in a gradient of chemoattractant. Furthermore, these cells were not able to form podosomes and filopodia (Jones et al. 2002b). Studies on Hem1 deficient macrophages revealed defective polarization of these cells and approx. up to 80 % reduced chemotaxis towards fMLP in a transwell assay (Heon Park et al. 2008c; Weiner et al. 2006). However, how lamellipodia, induced by WAVE complex, contribute to chemotaxis of primary BM macrophages is still not clear.

The present work shows that the Hem1 is critical for the formation of lamellipodia, but not podosomes or filopodia in BM-derived macrophages of mice (unpublished data). To shed more light on how Hem1 deficiency and the consequent absence of lamellipodia affects 2D chemotaxis of macrophages towards C5a, I performed chemotaxis assay 2D µslide chemotaxis chambers. I compared the chemotactic performance of wildtype, Hem1- and Wasp KO BM macrophages. In this way I could compare and assess specific parameters of migration, i.e. are FMI, velocity, and directness of cell movement. Representative images of chemotaxis assay, migration plots and analysis of FMI, velocity, and directness are shown in Figure 27.

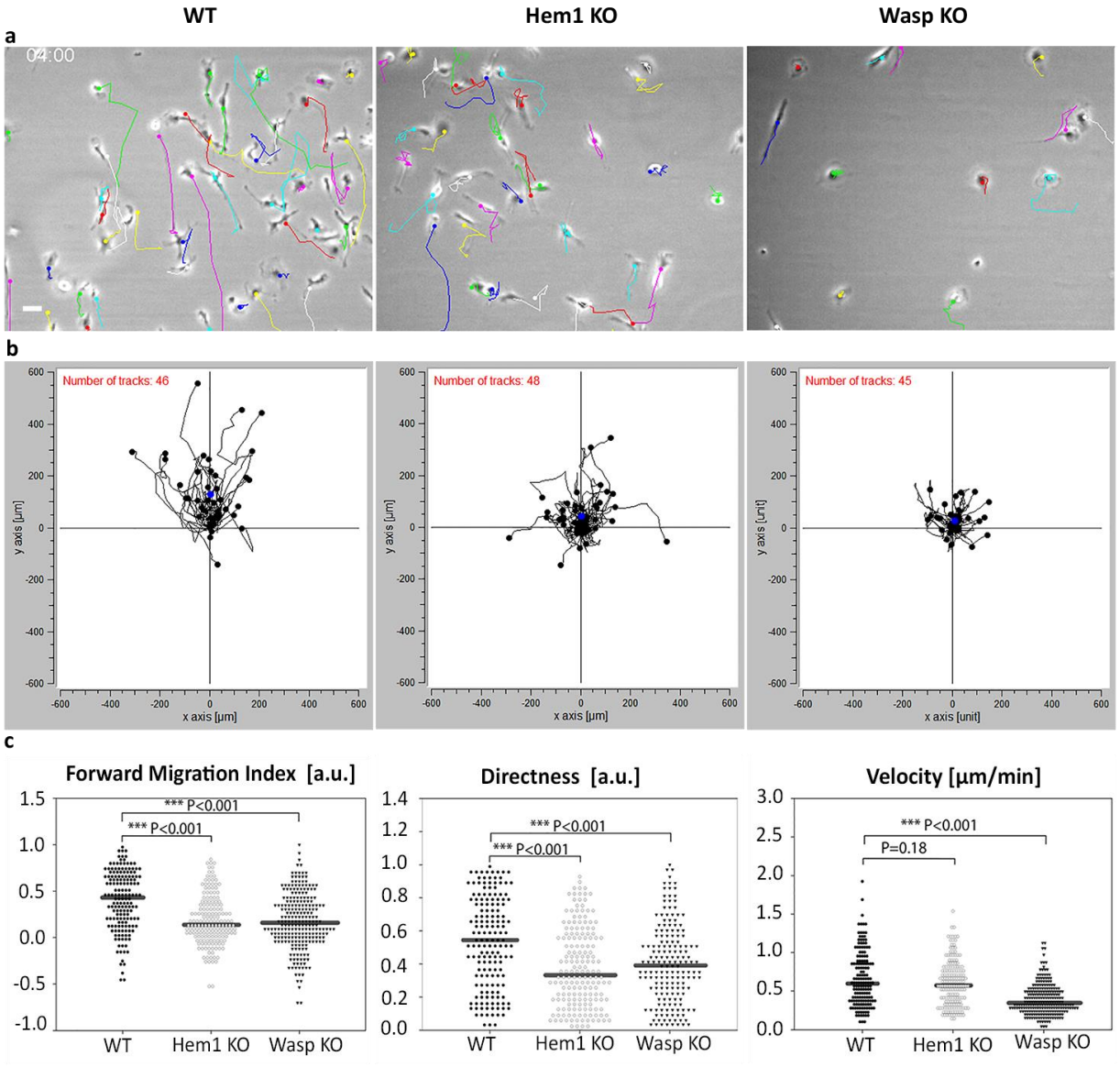

Figure 27: Hem1 knockout macrophages show impaired chemotaxis towards the gradient of C5a. Chemotaxis was evaluated using Ibidi 2D chemotaxis chamber. Chemoattractant was added into one of the reservoirs. Wild-type and Hem1 knockout cells were seeded in a channel of µ-Slide Chemotaxis 2D chamber (Ibidi) which is connected to 40 µl reservoirs on each side. Cells were incubated overnight in a growth medium. On the next day, C5a was added to one of the reservoirs. For live imaging video microscopy, µ-slides with cells were placed on pre-heated chamber on a microscope equipped with motorized XY-stage. Images were recorded every 3 minutes for 8-16h. (a): Videos of different treatment groups were imported and tracked using ImageJ manual tracking plugin. (b): The resulting Datasets of XY coordinates of migrating cells were imported into chemotaxis tool 2.0 (Ibidi) and plotted on an XY coordinate system representing each individual chemotaxis chamber. (c): The forward migration index (FMI), directness and velocities of cells in chemotaxis chamber were calculated. The results were exported for statistical analysis to Sigma plot 13 software. Statistical analysis was performed using Mann-Whitney Rank Sum Test. Horizontal bars represent median values from four independent experiments with sample sizes of n = 177-250 cells per condition.

In 2D chemotaxis experiments both, Hem1- and Wasp-null cells showed approx. 70 % reduced median values of FMI (Figure 27 c). FMI is to date one of the most sensitive readouts for the chemotactic performance of cells (Foxman, Kunkel, and Butcher 1999; Monypenny, Zicha, Higashida, Oceguera-yanez, et al. 2009). Furthermore, both, Hem1 knockout and Wasp KO cells show approx. 50% reduced directness compared to WT cells. Interestingly, the third parameter of cell migration, the cell velocity is markedly reduced specifically in Wasp-null cells. It is also notable that both Hem1- and Wasp KO cells can form cell front and rear, but are not able to polarize durably and follow the C5α gradient. Whereas Wasp deficiency affects all three parameters of cell migration, the Hem1 deficiency specifically affects FMI and directionality of cells but not the velocity as severely as loss of Wasp does.

3.3 Migration and actin protrusions of HT1080 cells in 3D collagen

Not all cell types that can migrate on 2D substrates can also translocate in 3D environments. Additionally, cells in 3D tend to have different morphologies compared to their morphology on 2D substrates (Even-Ram and Yamada 2005b; Katarina Wolf et al. 2003; Sixt 2012; Petrie and Yamada 2012).

The present work focuses on HT1080 cells which, compared to fibroblasts, can quickly adhere and efficiently migrate in 3D collagen scaffolds. In previous studies, HT1080 cells have been used to characterize adhesion and degradation in 3D cell migration (K. Wolf 2003; Katarina Wolf et al. 2007). HT1080 fibrosarcoma cells, like many other cell types, change their morphology and migration pattern in 3D collagen in contrast to their morphology and migration on 2D surfaces. The morphological change in 3D goes together with the formation of morphologically different kinds of actin-based protrusions which are termed as pseudopodia. (Greenberg, Burridge, and Silverstein 1990; Yamazaki, Kurisu, and Takenawa 2009b; Heath and Peachey 1989).

The leading edge of a cell plated on 2D consists of actin-based protrusions termed filopodia and lamellipodia. Actin-based protrusions of cells plated on 2D surfaces in contrast to those of cells in 3D are well studied and possess defined morphologies. Thus, the biochemical composition, assembly and functional genetics regarding filopodia and lamellipodia are well understood (Rottner

and Stradal 2011a). In the course of their migration cells on 2D substrates *in vitro* display spindle-shaped morphology and form broad and flat leading edges. Cells seeded in 3D collagen often drastically change their morphology from spindle shaped with flat leading edges to round- or wedge-shaped morphology with narrow leading edges (Katarina Wolf et al. 2003; Even-Ram and Yamada 2005b; Van Goethem et al. 2010).

It has been a challenge to visualize in detail the much narrower leading edge of migrating cells in 3D scaffolds compared to that of cells cultivated on 2D surfaces. Due to this different and more complex morphology, actin-based protrusions in 3D are often termed pseudopodia. These pseudopodia are not fully characterized due to more complex cell behavior compared to cells on 2D substrates. Merely pseudopodia are described to have a cylindrical form and can be at least morphologically divided into two regions. A shaft supported by thick cortical actin bundles and a tip region which is densely packed with F-actin (Yamazaki, Kurisu, and Takenawa 2009a; Kurisu and Takenawa 2010c).

3.3.1 HT1080 cells show typical wedge shaped morphology in 3D cell migration

To study and compare morphologies of cells in 2D and 3D HT1080 cells were plated on 2D coverslips or embedded in 3D collagen matrix respectivly. Cells were visualized in brightfield microscopy after 3-5 days of cultivation (Figure 28).

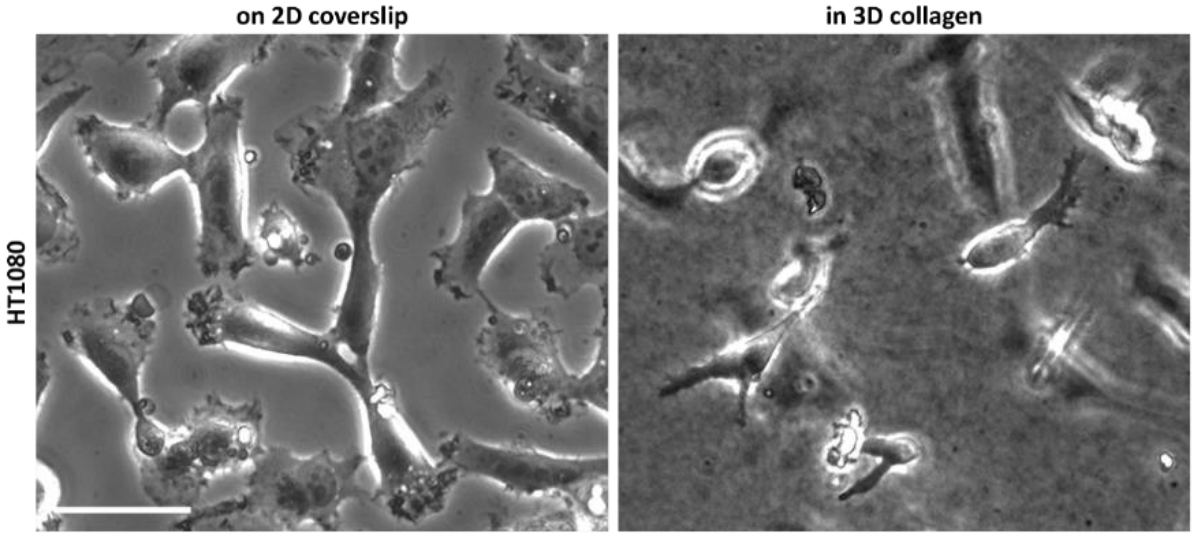

Figure 28: HT1080 cells change morphology in 3D collagen. HT1080 cells were embedded in 1.0 mg/ml 3D collagen scaffolds and cultured in an incubator for 1-5 days. To visualize HT1080 cells in 3D collagen, cells from Day3 were photographed at 20x magnification on brightfield microscope. Scale bar: 50µm.

Figure 28 shows typical morphologies of 2D spindle-shaped adherent cells on coverslips and 3D wedge-shaped elongated morphologies of HT1080 cells in the 3D collagen matrix.

During their migration in a 3D environment, some cells have a wedge shape and possess narrow leading edges; others show rather rounded morphologies accompanied with frequent shape-changes (K. Wolf 2003). To analyze the common migration morphology of HT1080 cells in 3D environments cells were cultivated in 3D collagen scaffolds and live cell migration was recorded in an environmental chamber. Figure 29 shows representative images at succeeding time points of HT1080 cells migrating in 3D collagen.

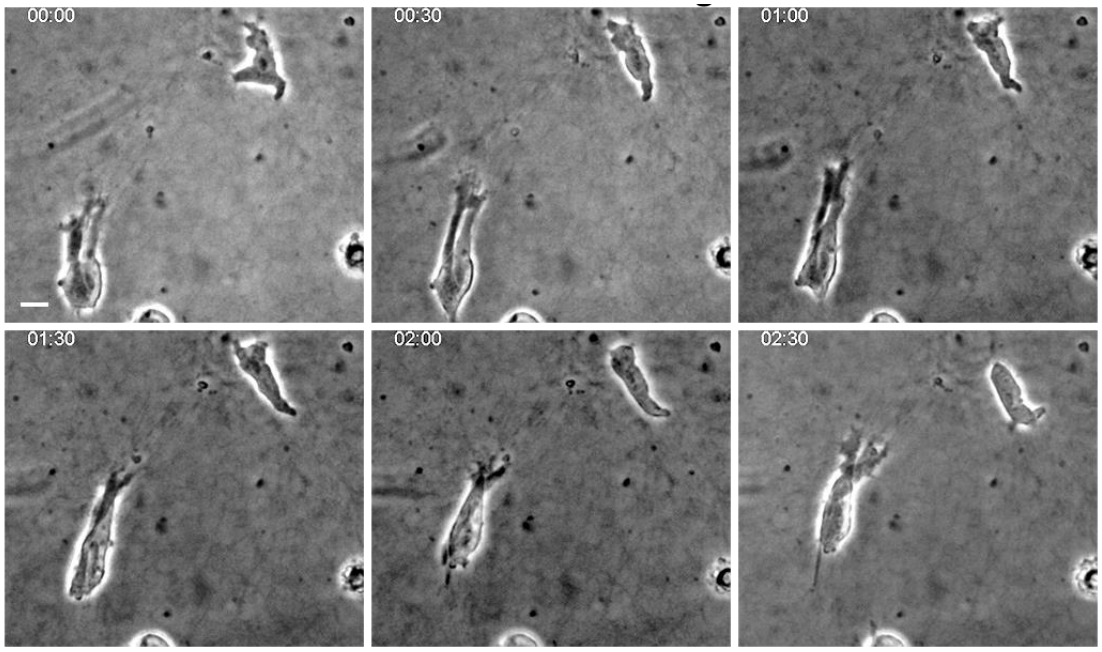

Figure 29: HT1080 cells show typical wedge shaped migratory morphology in 3D collagen. HT1080 cells were cultivated in 1.0mg/ml 3D collagen scaffold for 48 hours. Before live cell imaging, growth medium was replaced with medium containing HEPES. Cells were placed in the environmental chamber on the microscope under brightfield illumination PH1 and 20x. Pictures were taken every 2 minutes. Pictures from every 30 minute of live cell imaging were chosen to represent cell migration in this figure. Scale bar: 50µm.

The bottom left side of Figure 29 shows a typical HT1080 cell which is embedded in a 3D collagen matrix and performs one migration cycle composed of protrusion, attachment, and retraction of the cell body.

3.3.2 HT1080 cells show increased formation of finger-like protrusions in 3D vs. on 2D

Next, I compared actin-based protrusions and leading edges of cells plated on 2D surfaces *versus* those of cells embedded in 3D collagen. Therefore, 2D cultured cells and cells embedded in collagen were fixed and stained for F-actin (Figure 30).

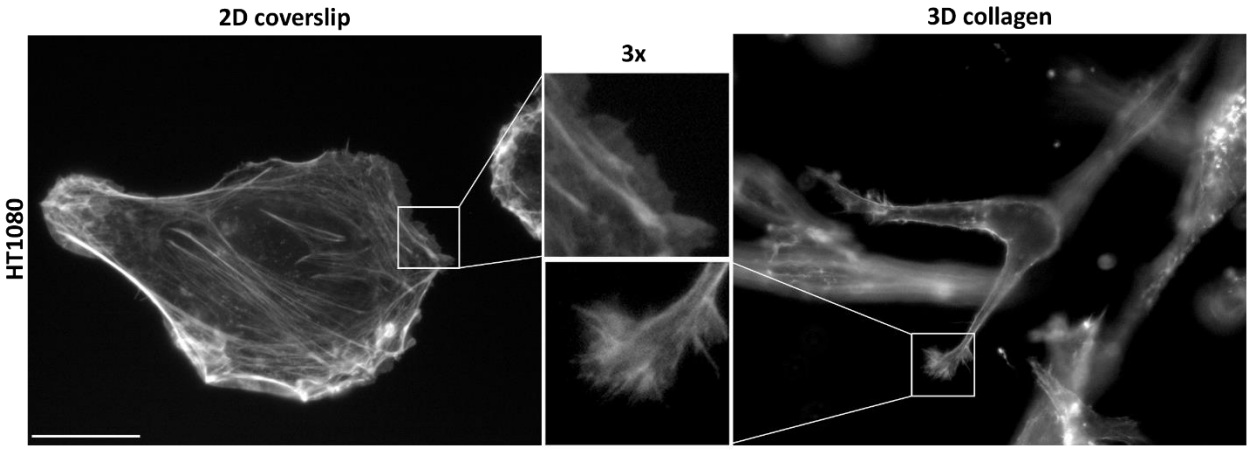

Figure 30: Morphology of the leading edge of HT1080 cells on 2D *vs.* 3D. HT1080 cells were either seeded on coverslips or embedded in 1.0 mg/ml 3D collagen scaffolds and incubated in an incubator for 24 hours. 18-24 hours post incubation cells were fixed, stained with phalloidin Alexa-594 and visualized in fluorescence microscopy. Scale bar 20µm.

HT1080 cells that are cultured on 2D surface show a spindle shape and a broadly formed leading edge consisting of lamellipodia and filopodia. In contrast, cells embedded in 3D collagen matrix are wedge-shaped and form a narrow cylindrical protrusion. At the tip of this protrusion filopodia-like protrusions- but not typical flat sheet formed lamellipodia are visible (Figure 30).

3.3.3 HT1080 cells show narrow lamellipodia, but similar filopodia in 3D *vs* 2D

To date, there is a very sparse amount of live-imaging data regarding cell morphology and cell migration in 3D. Especially morphology of the leading edge during 3D migration is not as clearly defined as for the cells grown on 2D substrates. Thus, some reports even question the existence of lamellipodia and filopodia in 3D (Beningo, Dembo, and Wang 2004).

To gain more insight into the morphology of the leading egde of cells in 3D, I transfected HT1080 cells with a GFP-Lifeact, placed them in collagen and visualized in live spinning disk laser confocal microscopy. The typical wedge-shaped cell was chosen to monitor its migration in 3D. Figure 31 shows representative 2D and 3D rendered images of the protruding cell and its leading edge in collagen.

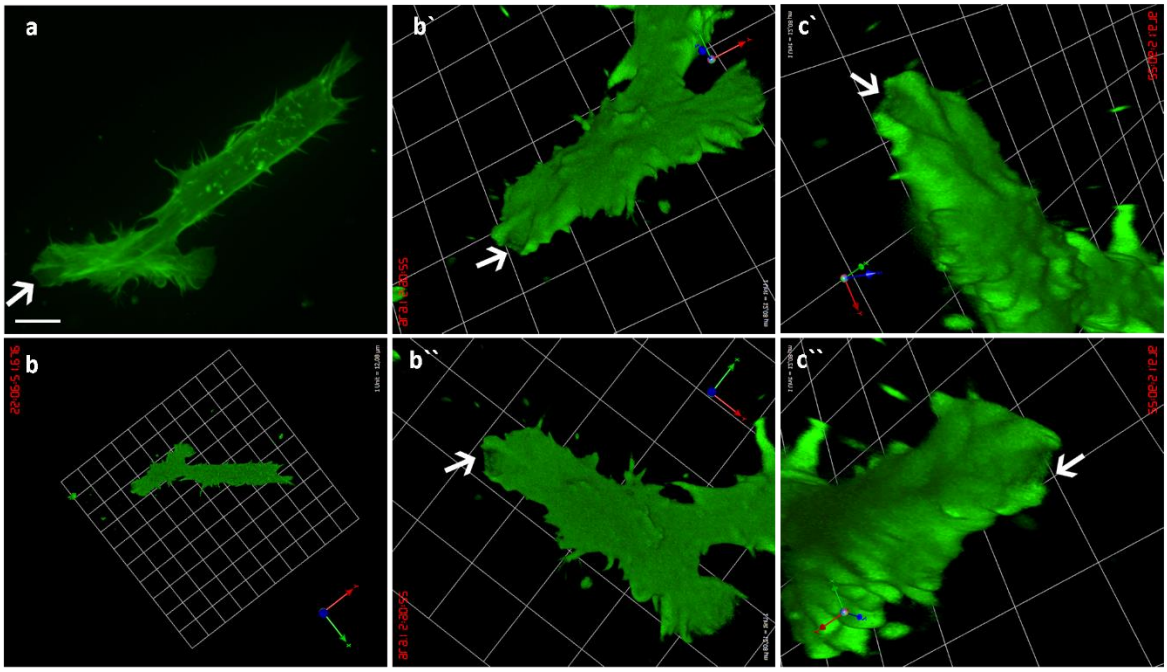

Figure 31: HT1080 cells display lamellipodia at the leading edge during protrusion in 3D collagen. HT1080 cells were transiently transfected with the GFP-lifeact construct and cultivated overnight. On the second day, cells were seeded in 1.0mg/ml 3D collagen scaffold for 24 hours. Before live cell imaging, growth medium was replaced with medium containing HEPES. Cells were placed in Ibidi environmental chamber (37° C) on motorized XYZ stage on the laser spinning disc confocal microscope. Cells were visualized with laser illumination of a 488nm wavelength at 60x magnification. Scans were taken every 2 minutes at 0.4µm steps (Z-axis). (**a)**: merged image of all Z-sections. (**b)**: 3D rendered image of (a). (**b`-c``)**: 3D rendered leading edge of the cell form different viewing angles. Arrow indicates sheet-like thin actin protrusion. Scale bar: 10µm.

Figure 31 shows leading edge of HT1080 cell which is embedded in 3D collagen, from 2D (a) and 3D perspectives (b`- c``). 3D reconstitution of the images of the leading edge shows thin flat sheet-like lamellipodia between apparently ruffling sections of protruding cell edge (arrows).

Reportedly, it is necessary to monitor live cells as filopodia are generated to identify finger-like protrusions as filopodia. Filopodia have typical finger-like morphology with approx. the diameter of up to 1µm (in fluorescence microscopy) (D. Vignjevic 2006).

To test if these finger-like protrusions in 3D observed in fluorescence microscopy (Figure 31) are possibly filopodia, GFP-lifeact transfected HT1080 living cells in 3D collagen were monitored in live laser spinning disc confocal microscopy. Figure 32 shows representative images of GFP-Lifeact transfected HT1080 cells in 3D collagen.

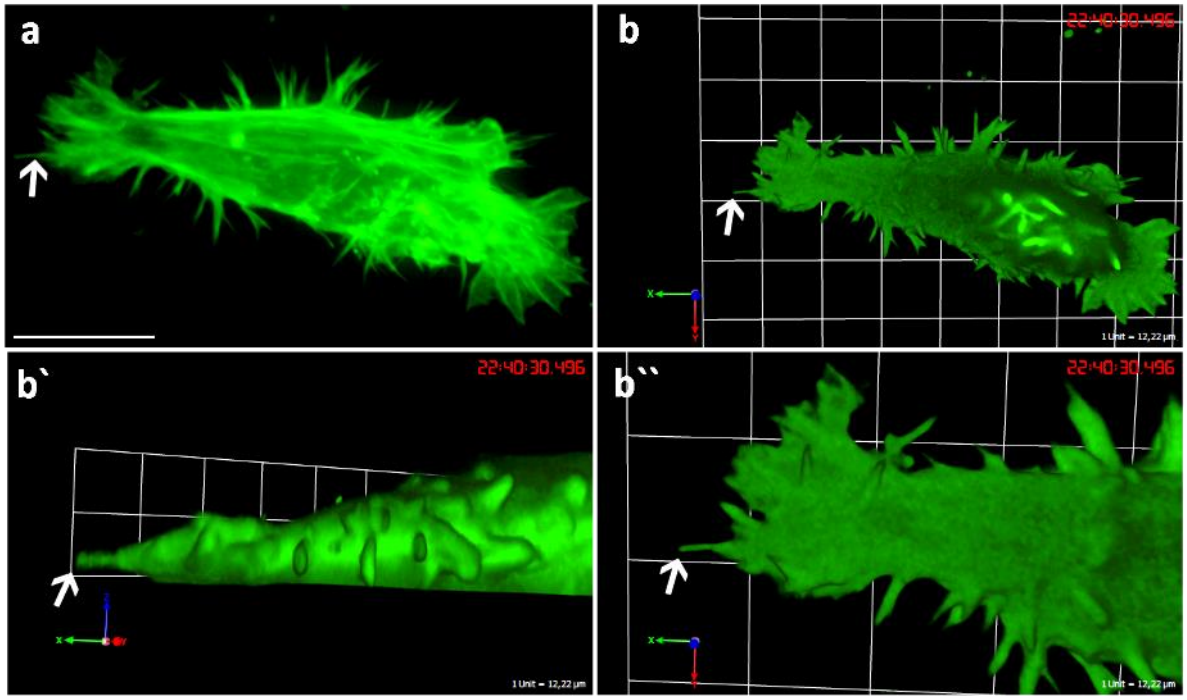

Figure 32: HT1080 cells display filopodia at the leading edge in 3D collagen. HT1080 cells were transiently transfected with the GFP-lifeact construct and cultivated overnight. On the second day, cells were seeded in 1.0mg/ml 3D collagen scaffold for 24 hours. Before live cell imaging, growth medium was replaced with medium containing HEPES. Cells were placed in Ibidi environmental chamber (37° C) on motorized XYZ stage on the laser spinning disc confocal microscope. Cells were visualized with laser illumination of a 488nm wavelength at 60x magnification. Scans were taken every 20 seconds at 0.2µm steps (Z-axis). (**a)**: a merged image of all Z-sections of a cell. (**b)**: 3D rendered image of a. (**b`- b``)**: 3D rendered leading edge of the cell form different viewing angles. Arrow indicates finger-like thin actin protrusion.

Figure 32 shows spinning disc confocal images of HT1080 cell embedded in 3D collagen. Image (a) represents 2D view followed by 3D rendered images with the enlarged leading edge of the cell using velocity 6 imaging software. In the corresponding movie (s. supplemental data) the cell actively protrudes at the leading edge. This leading edge shows embedded actin-based protrusions which show similar protrusion dynamics to filopodia and have a thickness of approx. 1µm. Thus apparently these structures could be indeed filopodia.

Furthermore, the same cell showed distinct type of actin protrusions on dorsal and ventral surfaces which are more static compared to protrusions at the leading edge and in general to filopodia and lamellipodia.

3.3.4 VASP localizes at the tips of filopodia-like protrusions in 3D collagen

According to our results, actin-rich protrusions at the leading edge of HT1080 cells during in 3D collagen were reminiscent of 2D filopodia regarding their morphology and dynamics (see Figure 32, suppl. video). One of the characteristics of filopodia besides faster dynamics than invadopodia is the presence of VASP at their tips (Lai et al. 2008; Rottner and Stradal 2011b; Rottner et al. 1999b) (D. A. Murphy and Courtneidge 2011b).

I wandered whether ectopically expressed VASP localized at the tips of filopodia-like structures at the leading edge of HT1080 cells in 3D collagen. Thus, I double transfected cells with GFP-VASP and Ruby-lifeact plasmids to visualize both proteins simultaneously and thus VASP and actin-rich filopodia-like protrusions in 3D. Further, I subjected cells to live spinning disc confocal microscopy. A representative image including time series of protrusion formation by the cell is shown in Figure 33.

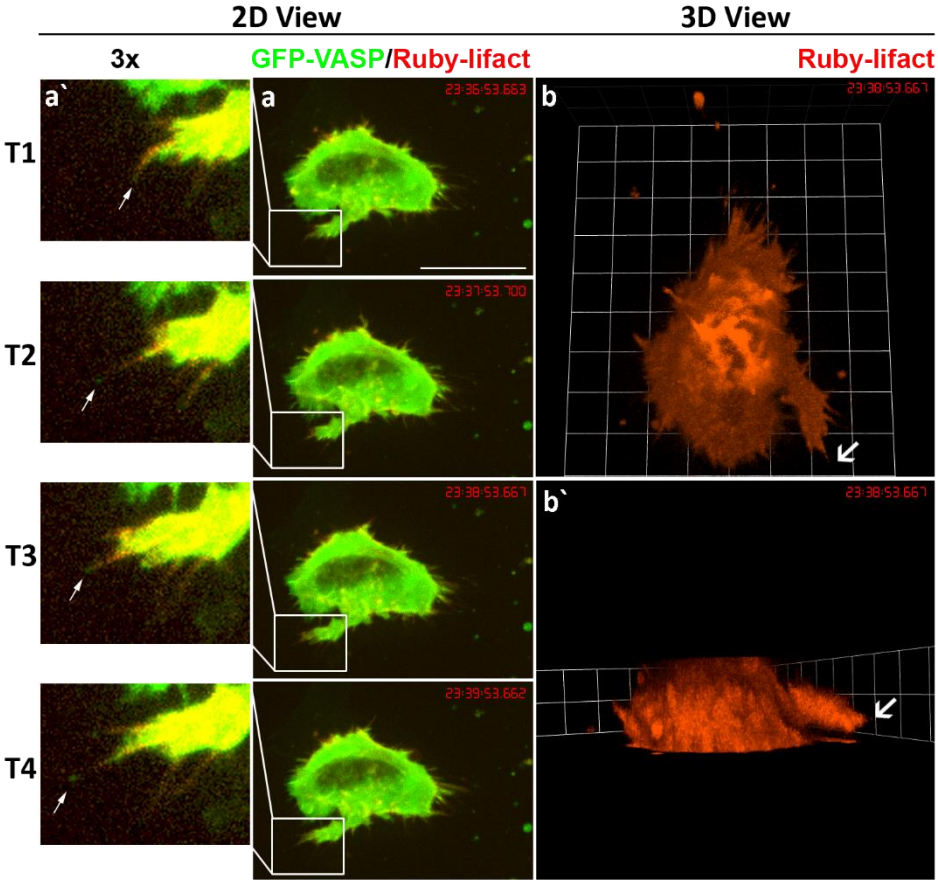

Figure 33: VASP is enriched at the tips of filopodia-like protrusions of HT1080 cells in 3D collagen. HT1080 cells were transiently double-transfected with GFP-lifeact and Ruby-lifeact plasmids and cultivated for 24h. On the next day, cells were seeded in 1.0mg/ml 3D collagen scaffold for 24 hours. Before live cell imaging, growth medium was replaced with medium containing HEPES. Cells were placed in Ibidi environmental chamber (37° C) on motorized XY stage on the laser spinning disc confocal microscope. Living cells were visualized with laser illuminations of 488nm and 561nm wavelengths at 60x magnification. Scans were taken once a minute at 0.2µm steps (Z-axis) for 1.5 hours. The picture shows 2D-and 3D views of the cell. The region where filopodia protrudes is marked and 3x enlarged. The arrow shows GFP-VASP at the tips of protruding filopodia at four succeeding time points (minutes). The same cell is rendered in 3D to show that the depicted protrusion is not attached to 2D. The images were combined to show dorsal/ventral protrusions in 2D and 3D. (**a)**: 2D view; (**a`)**: boxed region in a, 3x enlarged; (**b)**: 3D rendered cell shown in (a), arrow corresponds to arrows in T1-T4; (**b**`): xz view of (b).

Figure 33 shows images of formation of filopodium at the leading edge of HT1080 cells embedded in 3D collagen. With succeeding time points (T1-T4), putative filopodium elongates. At the same time, GFP-VASP is enriched at the tip of elongating filopodium. Furthermore, this structure is embedded in 3D as the rendering of cell shows. The arrow in Figure 33 b` shows that protrusion visible in T1-T4 series is not attached to any surface. The presence of VASP at the tip of finger-like protrusion during the elongation phase and its dynamics is supportive of that finger-like protrusions at the leading edge of cells in 3D in Figure 32 collagen are filopodia.

3.3.5 Dorsal and ventral actin-based protrusions in 3D migration

In contrast to 2D environments where the movement and protrusion of a cell are limited to XY space or lateral, frontal and backward directions (such as cell culture plastics) in 3D there are also ventral and dorsal directions available for protrusion formation and cell translocation. Accordingly, it can be speculated that cells use dorsal / ventral actin-based protrusions to move in this directions.

Live confocal imaging data of representatively translocating HT1080 cell in 3D collagen (Figure 32) was displayed and analyzed in xyz view (Figure 34). This allows visualization of the dorsal and ventral protrusions and their dynamics in 3D. Corresponding actin protrusions on the cell surface were tracked (using ImageJ manual tracking plugin) relative to translocation of leading and trailing edges of the cell. The resulting image represents the overlay of translocation paths of ventral protrusions and of leading and trailing edges.

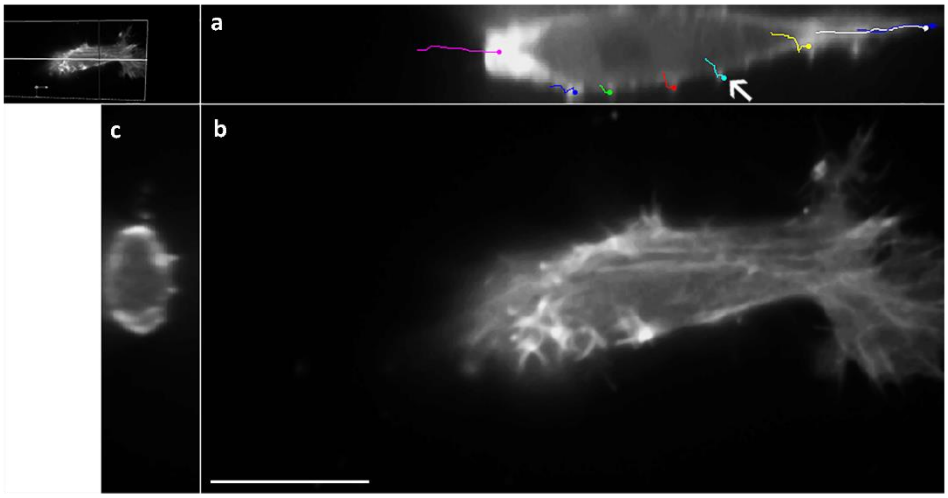

Figure 34: Tracking of dorsal / ventral actin-based protrusions during 3D migration. HT1080 cells were transiently transfected with the GFP-lifeact construct and cultivated overnight. On the second day, cells were seeded in 1.0mg/ml 3D collagen scaffold for 24 hours. Before live cell imaging, growth medium was replaced with medium containing HEPES. Cells were placed in Ibidi environmental chamber (37° C) on motorized XYZ stage on the laser spinning disc confocal microscope. Cells were visualized with laser illumination of a 488nm wavelength at 60x magnification. Scans were taken every 20 seconds at 0.2µm steps (Z-axis) for 10min. The XYZ view most well representing the cell periphery was chosen to export to ImageJ manual tracking plugin. The corresponding points at the cell periphery were tracked, and the video was overlaid with these tracks. The last frame of video is shown. Scale 50µm. (**a)**: xz section; (**b)**: xy section; (**c)**: yz section.

In Figure 34, pictures **(a)** and **(c)** show longitudinal and cross-sectional profile views of the cell. The tracked ventral protrusions, cell rear, and leading edge protrusions are represented in Figure 34 (a). According to results from the motion tracking, the ventral protrusions show much slower translocation relatively to the cell body and of leading- and trailing edges. Furthermore, these protrusions are apparently anchored in collagen network during retraction of cell rear and protrusion of cells leading edge. This is also apparent when distances traveled by dorsal protrusions (colored lines) are compared to those showing translocation of leading and trailing edges (Figure 34 (a).

For visualization of Dorsal/ventral protrusions in more detail, the confocal imaging data of 3D migration were rendered using Volocity 6.1 software, and corresponding ventral/dorsal actin protrusions were visualized in 3D (Figure 35).

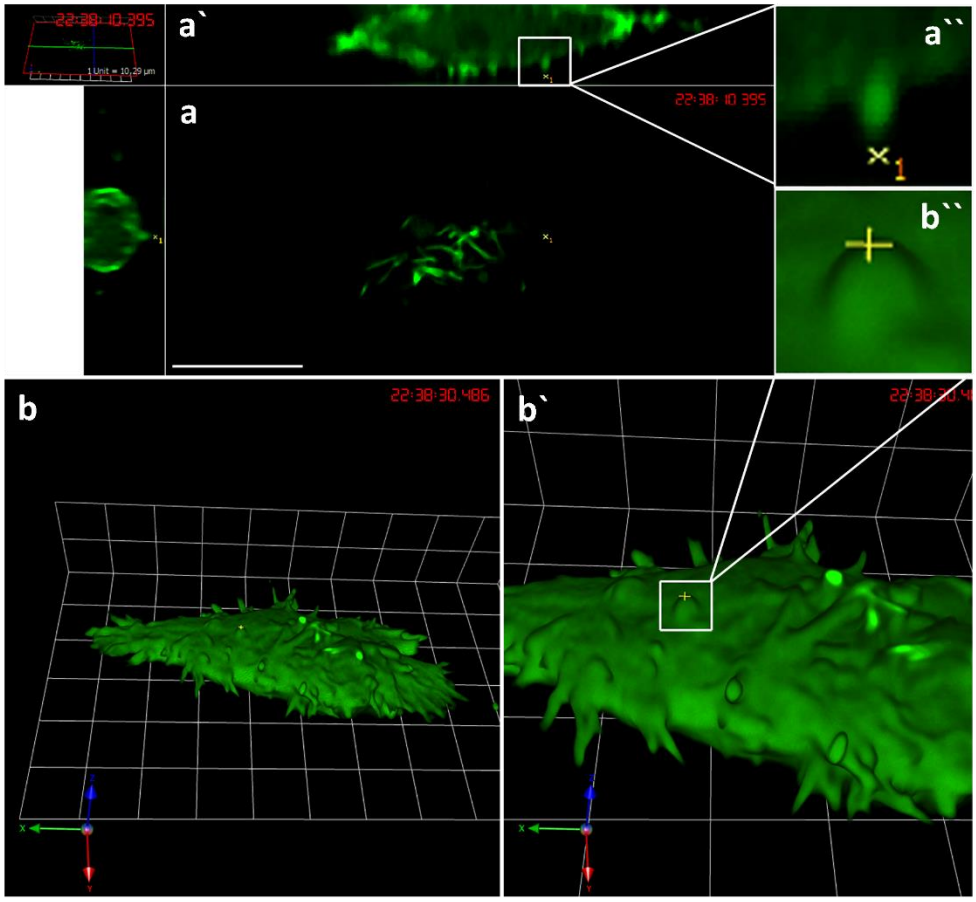

Figure 35: Morphological analysis of dorsal/ventral actin-based protrusions. HT1080 cells were transiently transfected with the GFP-lifeact construct and cultivated overnight. On the second day, cells were seeded in 1.0mg/ml 3D collagen scaffold for 24 hours. Before live cell imaging, growth medium was replaced with medium containing HEPES. Cells were placed in Ibidi environmental chamber (37° C) on motorized XYZ stage on the laser spinning disc confocal microscope. Cells were visualized with laser illumination of a 488nm wavelength at 60x magnification. Scans were taken every 20 seconds at 0.2µm steps (Z-axis). The migration Data were 3D rendered and visualized from different viewpoints in velocity 6 software. One of the ventral protrusions was marked and visualized in 3D. **(a)**: xy plane; **(a`)**: xz plane; **(a``)**: 3x digital zoom of boxed region in (a`); **(b)**: 3D rendered image of the cell in (a-a`). **(b`-b``)**: 3D rendered image and 3x digital zoom of protrusion from images (a-a`-a``).

Analysis of 2D and 3D rendered pictures, and videos representing the cell in Figure 35 reveal that these dorsal/ventral actin-based protrusions have a different shape and show slower dynamics compared to lamellipodia or filopodia (s. supplemental video). Particularly, these protrusions had rounded appearance and their lifetime lasts approx. 10 minutes.

Apart from the rounded dorsal/ventral protrusions, HT1080 cells in 3D collagen occasionally showed more dynamic dorsal /ventral protrusions that had the spiked appearance (Figure 36 a; b).

The morphology of these protrusions was studied by applying 3D rendering of velocity 6.1 software on recorded live confocal data of HT1080 cell embedded in 3D collagen.

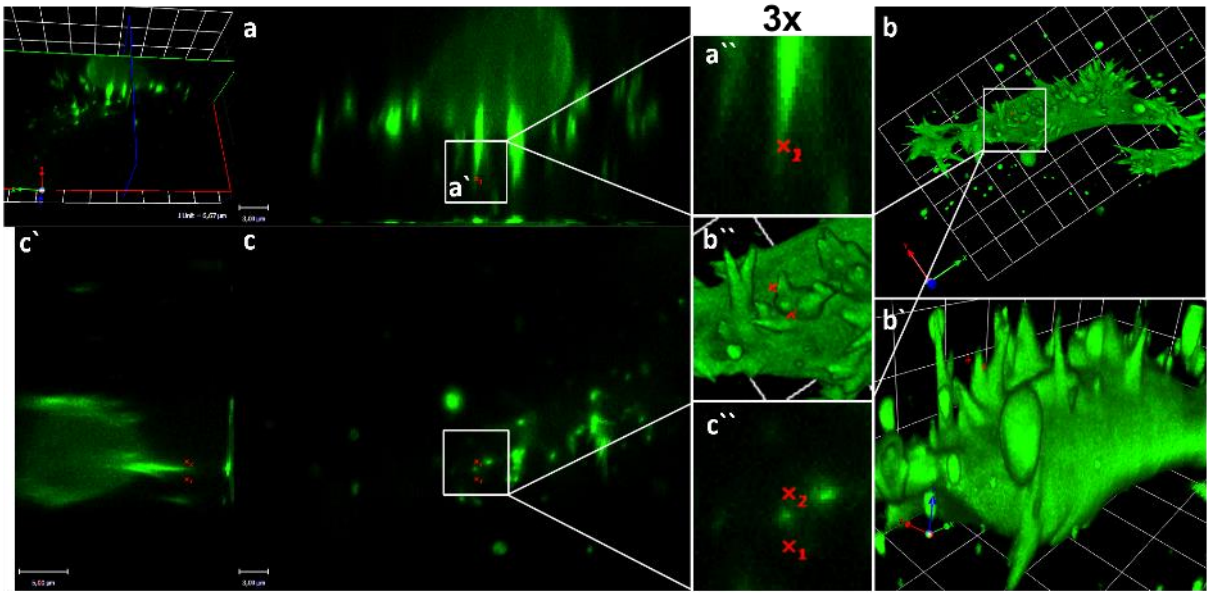

Figure 36: HT1080 cells show spiked dorsal/ventral protrusions besides rounded dorsal /ventral protrusions in 3D collagen. HT1080 cells were transiently transfected with GFP-lifeact construct and cultivated overnight. On the second day, cells were seeded in 1.0mg/ml 3D collagen scaffold for 24 hours. Before live cell imaging, growth medium was replaced with medium containing HEPES. Cells were placed in Ibidi environmental chamber (37° C) on motorized XYZ stage on the laser spinning disc confocal microscope. Cells were visualized with laser illumination of a 488nm wavelength at 60x magnification. Scans were taken every 20 seconds at 0.2µm steps (Z-axis) for 8 minutes. The picture shows XYZ view of the cell and rendering of migration data from Volocity-6 software form the same timepoints. The images were combined, and 3D rendered to illustrate same dorsal/ventral protrusions in 2D and 3D. (**a)**: xz plane; (**a`)**: boxed regions showing ventral protrusions; (**a``)**: 3x digital zoom of boxed region in (a); (**b)**: 3D rendered image of the cell in a, b and c form dorsal view. (**b`)**: Different dorsal view of (b); (**b``)**: 3x digital zoom of protrusion from boxed regions of images (a-c). (**c)**: 2D view of ventral protrusions from the top confocal plane. **(c´)**: yz view of the cell; **(c``)**: 3x digital zoom of boxed region in (c).

According to 3D rendered images in Figure 36 these GPF-lifeact enriched protrusions are formed on the dorsal/ventral side of the cell and show "spiky" morphology reminiscent of filopodia. However, these protrusions appear thicker than filopodia (in Figure 32 b``). As the corresponding video of Figure 36 was observed form the top xy-view, this cell did not translocate significantly in 3D collagen. However, as the viewing perspective was changed from xy (top) to yz or to xz (profile view) the same cell showed significant movement in vertical direction. Therefore, the cell from Figure 36 and its protrusions were tracked in the corresponding video using ImageJ and manual tracking tool (Ibidi). Figure 37 shows the end frame of the tracked video.

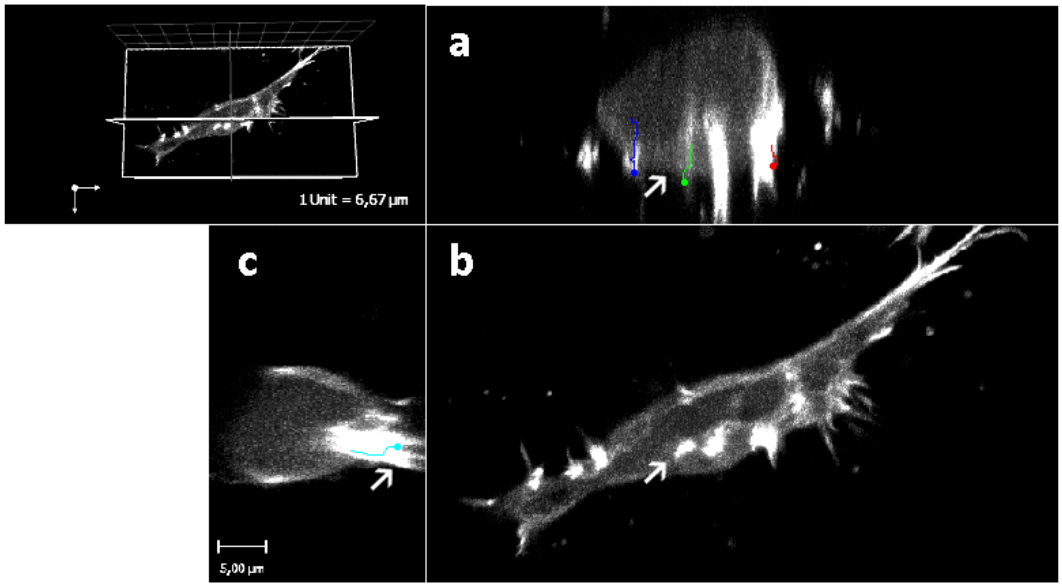

Figure 37: Spiked dorsal/ventral actin-based protrusions in vertical movement of HT1080 cells in 3D collagen. HT1080 cells were transiently transfected with the GFP-lifeact construct and cultivated overnight. On the second day, cells were seeded in 1.0mg/ml 3D collagen scaffold for 24 hours. Prior to live cell imaging, growth medium was replaced with medium containing HEPES. Cells were placed in Ibidi environmental chamber (37° C) on motorized XY stage on the laser spinning disc confocal microscope. Cells were visualized with laser illumination of a 488nm wavelength at 60x magnification. Scans were taken every 20 seconds at 0.2µm steps (Z-axis) for 8 minutes. The XYZ view representing the cell periphery and cross-section was chosen to export to ImageJ manual tracking plugin. The corresponding points located at the central regions of protrusions were tracked, and the video was overlaid with these tracks. The last frame of video is shown. Scale 5 µm. (**a)**: xz section. (**b)**: xy section; **(c)**: zy section.

Figure 37 shows an overlay of tracks which were generated by tracking the corresponding points from the central area of protrusions visible at the side view of the cell. These protrusions together with the cell body translocate in vertical direction demonstrated by an overlay of colored paths of translocation (See supplemental video). This indicates that spike formed dorsal/ventral protrusions could be used for (or are involved) in vertical movements by HT1080 cells in 3D environments.

3.3.6 VASP is enriched in dorsal / ventral protrusions

Mena, a member of Ena/VASP family proteins, also has been shown to co-localise with cortactin in invadopodia of breast cancer cell line plated on fibronectin-gelatin matrix. Furthermore, These

proteins co-localized in protrusions during the invasion into collagen I matrix. Overexpression of Mena leads to increased degradation activity and liftime of invadopodia in these cells (Philippar et al. 2008b). The dorsal and venrtal protrions of HT1080 cell in 3D collagen are reminiscent of invadopodia (due to their dynamics and morphology). Therefore it was tempting to test if VASP is enriched in these strucktures. For this purpose, GFP-VASP and Ruby-Lifact constructs were expressed in HT1080 cells to visualize the distribution of VASP and F-actin simultaneously. Transfected cells were embedded in 3D collagen, and the migration was monitored using live confocal spinning disc microscopy (Figure 38).

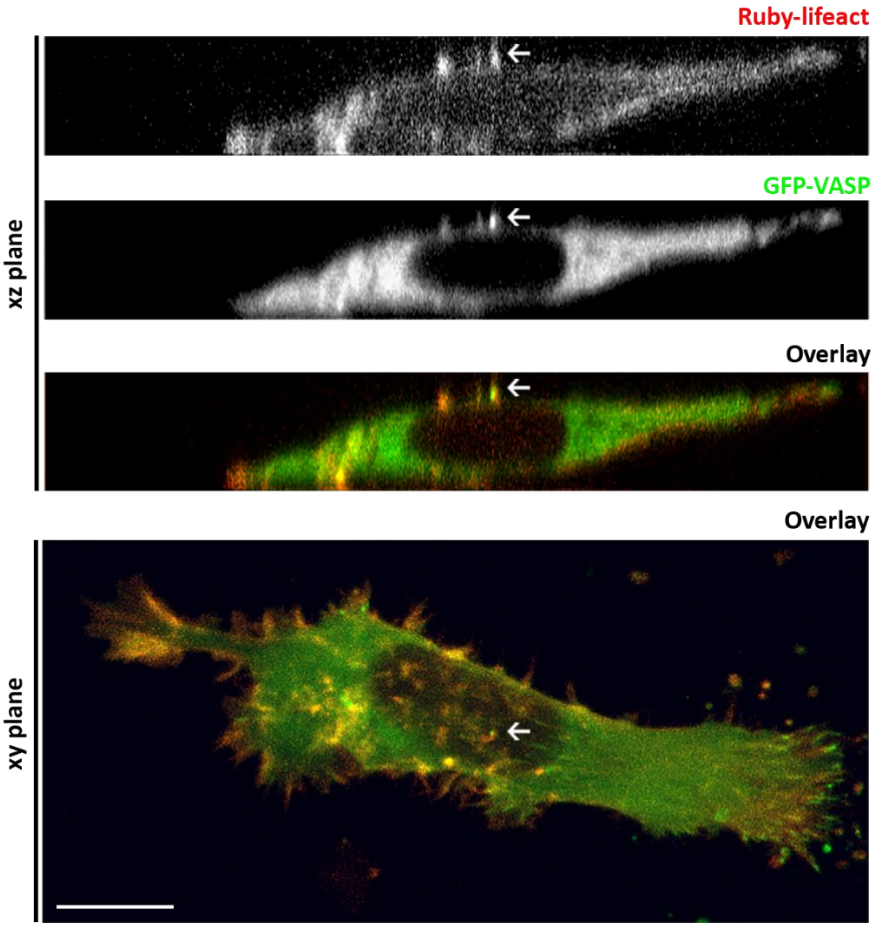

Figure 38: VASP is enriched at the dorsal/ventral protrusions of HT1080 cells in 3D collagen. HT1080 cells were transiently double-transfected with GFP-VASP and Ruby-lifeact plasmids and cultivated for 24h. On the next day, cells were seeded in 1.0mg/ml 3D collagen scaffold for 24 hours. Before live cell imaging, growth medium was replaced with medium containing HEPES. Cells were placed in Ibidi environmental chamber (37° C) on motorized XYZ stage on the laser spinning disc confocal microscope. Living cells were visualized with laser illuminations of 488nm and 561nm wavelengths at 60x magnification. Scans were taken once a minute at 0.2µm steps (Z-axis) for 1 hour. The picture shows xz- and xy sections of the cell in green and red channels and an overlay of both channels. Additionally, the

cells is shown in xy plane (bottom picture). The Arrow indicates representative dorsal dot-like protrusion enriched in ruby-lifeact and GFP-VASP. Scale: 20µm.

Figure 38 shows HT1080 cell that displays typical dot-like ventral and dorsal actin-based protrusions (arrows) enriched in Ruby-lifeact and GFP-VASP. These protrusions show dynamics that are markedly slower than filopodia dynamics (s. supplemental video). Furthermore, the GFP-VASP is not localized at the tip of the dorsal actin protrusion in Figure 38 which on the contrary is the case in filopodia or lamellipodia.

3.3.7 Matrix degradation takes place at central and rear regions of HT1080 cells

Matrix degradation has an important role in fibroblast- and especially cancer cell migration in 3D collagen (K. Wolf 2003; Katarina Wolf et al. 2009). Most prominent degradative structures of these type of cells on 2D ECM substrates are dot-like actin-based protrusions termed invadopodia.These actin protrusions are enriched in MMPs that can be either membrane-associated, or secreted in the extracellular matrix (Poincloux, Lizárraga, and Chavrier 2009). Furthermore, Ena/VASP protein possibly play an important role in the degradative activity of invadopodia (Philippar et al. 2008b). Invadopodia are grouped to actin-based protrusions and are generated reportedly by the activity of both types of actin nucleators: formins and Arp2/3 complex (Yamaguchi et al. 2005; Stefan Linder, Wiesner, and Himmel 2011).

It has been reported that the leading edge and the rear of the cell have degradative properties in the 3D migration of macrophages and several other cell types (Van Goethem et al. 2010; Van Goethem et al. 2011). To test if the leading edge of HT1080 cells is degradative, I cultured HT1080 cells on coverslips coated with FITC-coupled gelatin matrix, fixed and visualized by fluorescence microscopy (Figure 39).

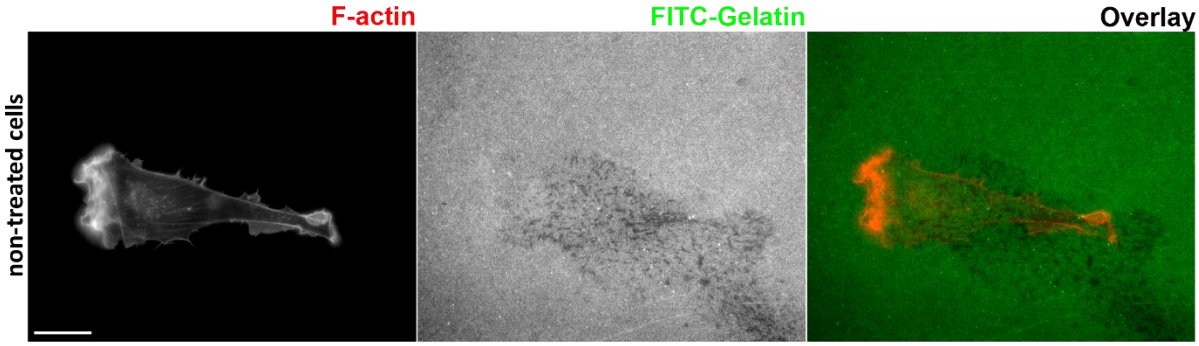

Figure 39: HT1080 cells degrade FITC-gelatin primarily at central and rear regions of the cell but not at the leading edge. HT1080 cells were cultivated on FITC-gelatin-coated coverslips for 5 hours followed by fixation with 4% PFA. After fixation, coverslips were stained with phalloidin Alexa-594 and visualized in fluorescence microscopy. Scale bar 20 µm.

Figure 39 shows a representative image of degradation assay. It is visible that HT 1080 cells degrade gelatin matrix primarily at the central and rear regions of the cell. The degradative activity of cells residing on FITC-gelatin is visible through lack or markedly reduced fluorescence at particular regions beneath the cell.

3.3.8 Inhibition of MMPs but not of formins suppresses ECM degradation by HT1080 cells

As shown above, the degradation of ECM by HT1080 cells on 2D takes place primarily at the center and rear / peripheral regions of the cell, but not at the leading edge. The degradation at the central region of the cell occurs in proximity or beneath actin-rich dots (which represent invadopodia) (García et al. 2014). Besides of MMPs, apparently, formins are also important for effective matrix degradation by cancer cells, because of their involvement in the formation of invadopodia (Lizárraga, Poincloux, Romão, et al. 2009). Formins can generate unbranched F-actin arrays within invadopodia. MMPs, on the other hand, are degradative constituents of invadopodia and can also be secreted by cells (Katarina Wolf et al. 2003; Friedl, Zänker, and Bröcker 1998).

The matrix degradation assay in the presence of formin- or MMP inhibitors was performed to test how the inhibition of either formins or MMPs affects degradation activity of HT1080 cells, (Figure 40).

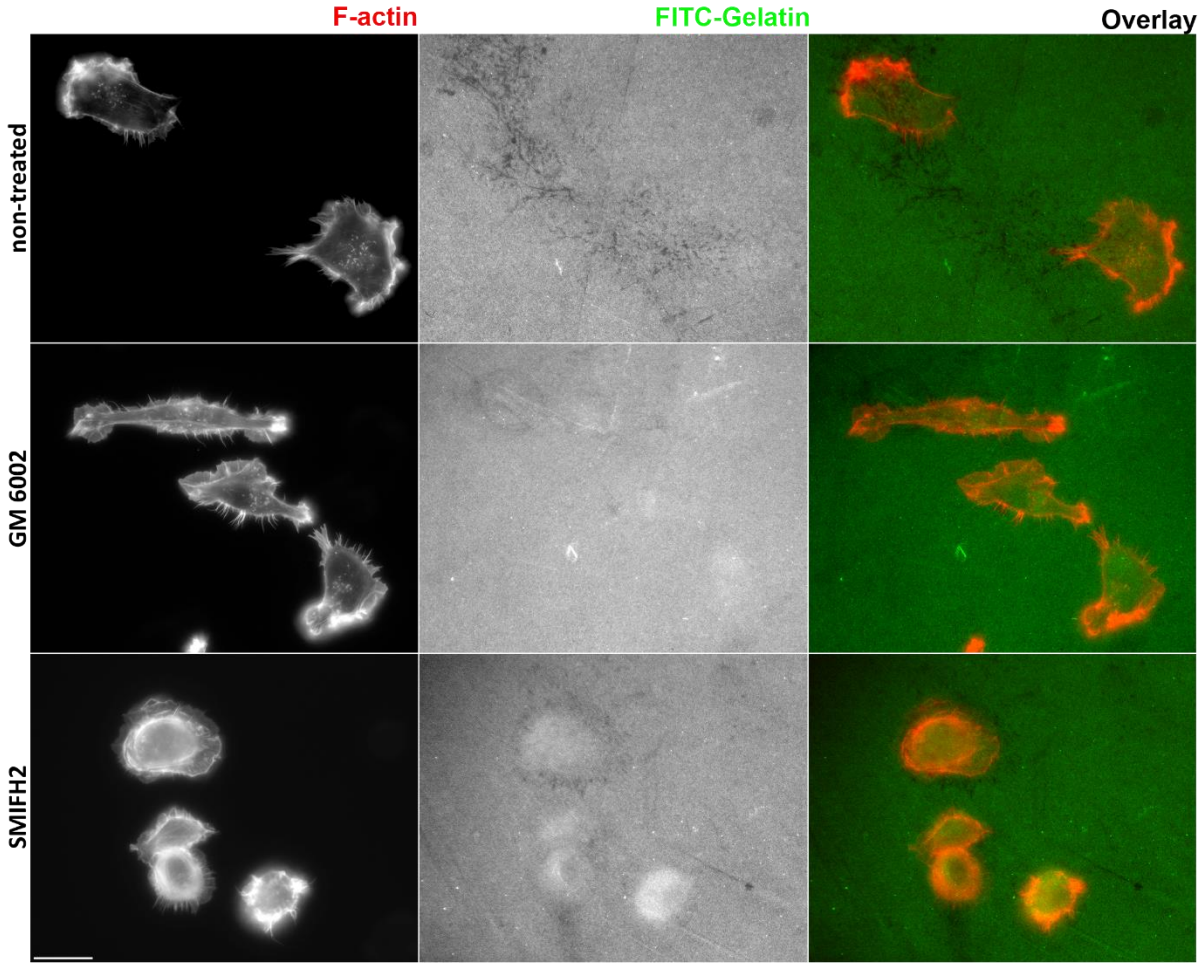

Figure 40: Different inhibition of matrix degradation by MMP- and formin inhibitors. HT1080 cells were cultivated on FITC-gelatin-coated coverslips for 5 hours in the presence of 25µM GM6001, 30µM smiFH2 or DMSO. This was followed by fixation of cells with 4% PFA. After fixation, coverslips were stained with phalloidin Alexa-594 and visualized in fluorescence microscopy. Scale: 20µm.

As it can be observed form the Figure 40 that GM6001 effectively blocks the degradation of FITC-gelatin matrix at both, rear and central regions of the HT1080 cells. Furthermore, the treatment of cells with GM6001caused no visual defects of actin-based protrusions. The GM6001 treated cell population also retained normal cell morphology. Effective inhibition of matrix degradation is visible in Figure 40 as an absence of dark dots on the FITC-gelatin compared to non-treated cells. The representative image in Figure 40 shows that smiFH2 blocks the degradation FITC-gelatin primarily at the central region of the cell, despite that cells still can form actin-rich dots. Cells from smiFH2 treatment group show a qualitative decrease of FITC-gelatin degradation at the center-, but degrade matrix at the periphery of the cell. Furthermore, smiFH2 treated

cells show decreased polarity which is depicted in more rounded morphologies of cells from this treatment group.

To quantify the results of degradation assay and effects of smiFH2 or GM6001 on degradation the relative intensities of FITC-gelatin fluorescence beneath the cells were measured and statistically analyzed using sigma plot software (Figure 41).

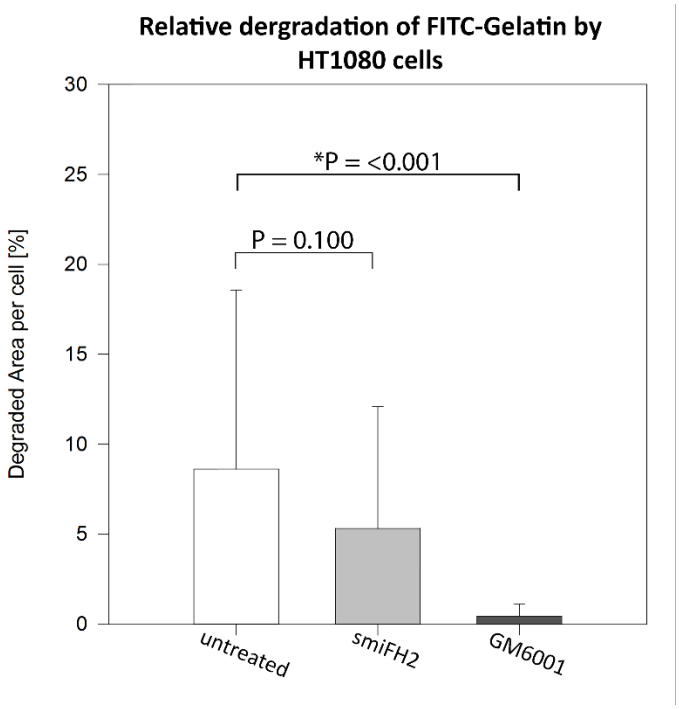

Figure 41: Quantitative analysis of matrix degradation by inhibitor-treated HT1080 cells. HT1080 cells were cultivated on FITC-gelatin-coated coverslips for 5 hours in the presence of 25µM GM6001, 30µM smiFH2 or DMSO. This was followed by fixation of cells with 4% PFA. After fixation, coverslips were stained with phalloidin Alexa-594 and visualized in fluorescence microscopy. Intensities of FITC-gelatin images were measured and quantified for each treatment group in Metamorph 5 software. Statistical analysis was performed using Mann-Whitney Rank Sum Test. Error bars show one standard deviation of the mean value form three replicates with sample sizes of 31-45 cells per condition.

Statistical analysis of matrix degradation assay in Figure 41 shows that application of formin inhibitor smiFH2 reduced relative degraded area per cell approx. to 60 % of untreated cells, but this reduction was not statistically significant. Inhibition of MMPs by applying GM6001 drastically and significantly reduces the degraded area per cell to approx. 5% of untreated cells in both, quantitative and visual/qualitative analysis.

The matrix adhesion assay was performed in the presence of formin inhibitor smiFH2 or GM6001 to test if smiFH2 treatment affects adhesion of HT1080 cells on FITC-gelatin, (Figure 42).

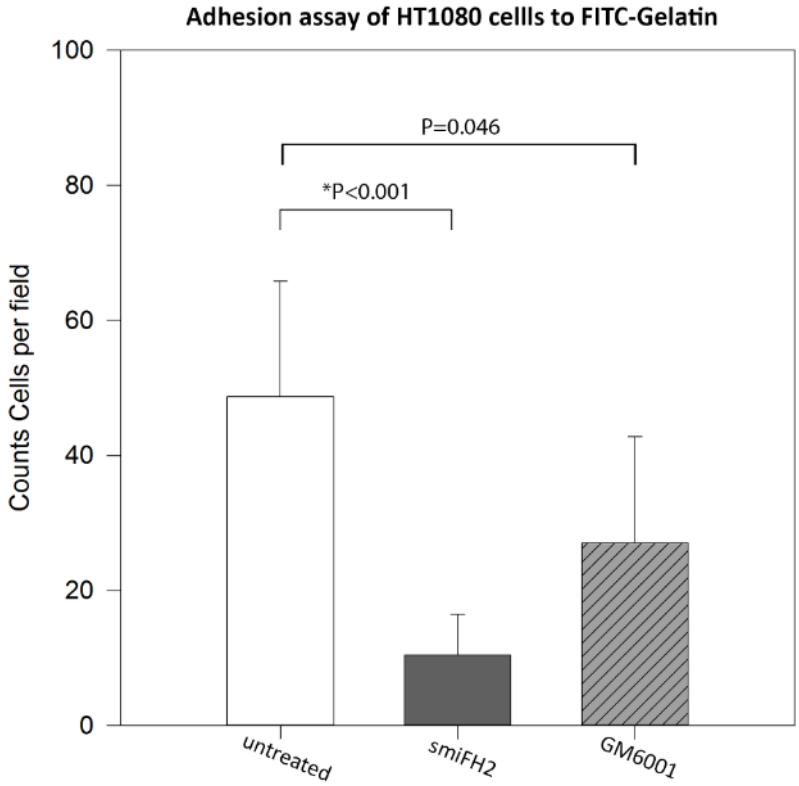

Figure 42: Initial adhesion of HT1080 cells on FITC-gelatin is markedly impaired by application of smiFH2 but not by GM6001. HT1080 cells adhered to FITC-gelatin-coated coverslips for 40 min. in the presence of 25µM GM6001, 30µM smiFH2 or DMSO. Subsequently, cells were washed two times with PBS, followed by fixation with 4% PFA. After fixation, coverslips were stained with phalloidin Alexa-594 and visualized in fluorescence microscopy. Numbers of adhered cells per treatment were counted and statistically analyzed using Sigma plot 13 software. Statistical analysis was performed using Mann-Whitney Rank Sum Test. Error bars show one standard deviation of the mean value form three replicates with sample sizes of 98-267 cells per condition.

The statistical analysis of adhesion assay shows that smiFH2 treated cells are markedly negatively affected by their ability to form initial adhesions to ECM substrate resulting in approx. 75% reduced adhesion rate of HT1080 cells. GM6001 treatment also led to approx. 45 % reduced adhesion rate of HT1080 cells.

3.3.9 Inhibitors of MMPs, formins and Arp2/3 complex in 3D migration

In previous chapters of this work, I showed that HT1080 cells use filopodia, lamellipodia and dorsal/ventral actin-based protrusions in 3D migration. Furthermore, these cells apparently degrade ECM at central and rear regions of the cell on a 2D substrate. Further, when compared to HT1080 cells on 2D (glass or plastic) substrates, cells in 3D collagen showed qualitatively more filopodia (or filopodia-like protrusions) than sheet-like broad lamellipodia at their leading edges (representative Figure 30 2D *vs.* 3D). GFP-VASP was enriched at the tips of these filopodia-like structures at the leading edge in 3D. Furthermore, dynamics of these structures are similar to filopodia dynamics observed in 2D (Figure 32 b``).

Formin inhibitor smiFH2 led to inhibition of formins and thereby reduced the formation rate of filopodia and dorsal circular ruffles without effecting lamellipodia formation in MEFs (Figure 18 and Figure 19 respectively). In degradation assay treatment of cells with smiFH2 had no significant effect on cell degradation, but negatively affected cell adhesions such as in MEFs, probably affecting the formation of filopodia during cell spreading (Figure 21). Thus, I applied smiFH2 to study the formation of filopodia and dorsal /ventral protrusions in 3D. I used CK-666 (Arp2/3-inhibitor) to suppress actin structures produced majorly by the activity of the Arp2/3 complex. To hinder matrix degradation I used general MMP inhibitor GM6001.

3.3.9.1 Effects of formin, Arp2/3 and MMP inhibitors on actin-based protrusions in 3D

SmiFH2 is a formin inhibitor, which can inhibit formins in yeast and mammalian cells (mDia family 1 and 2), apparently due to its specific interaction with an FH2 domain of formins (S. a Rizvi et al. 2009b). A Recent study indicated specific downregulation of mDia2, but not mDia1 or mDia3 formins in cancer cells and MEFs treated with smiFH2 (Isogai, Kammen, and Innocenti 2015).

SmiFH2 treated MEFs from the present work showed 80 % decrease in filopodia numbers and markedly interfered formation of circular dorsal ruffles downstream of CDC42 and formins (Figure 17-18; Figure 19). Furthermore, smiFH2 treatment led to reduced cell velocities on 2D in MEFs.

Thus, I applied smiFH2 to monitor its effects on the formation of filopodia of HT1080 cells embedded in 3D collagen. Noteworthy, DRF1 (mDia1) and FMNL2 show relatively high expression profile of known formins in HT1080 cells (Kitzing et al. 2010). Additionally, I wanted to evaluate if this inhibitor affects the formation invadopodia which are dependent on both, formin- and Arp2/3 complex activity. Invadopodia are visible as actin-rich dots on the cell surface. Similarly, an inhibitor of Ap2/3 complex or MMP inhibitor GM6001 was applied to monitor the effects on protrusions that are dependent on Arp2/3 complex- or MMP activity such as lamellipodia or invadopodia respectively (Figure 43).

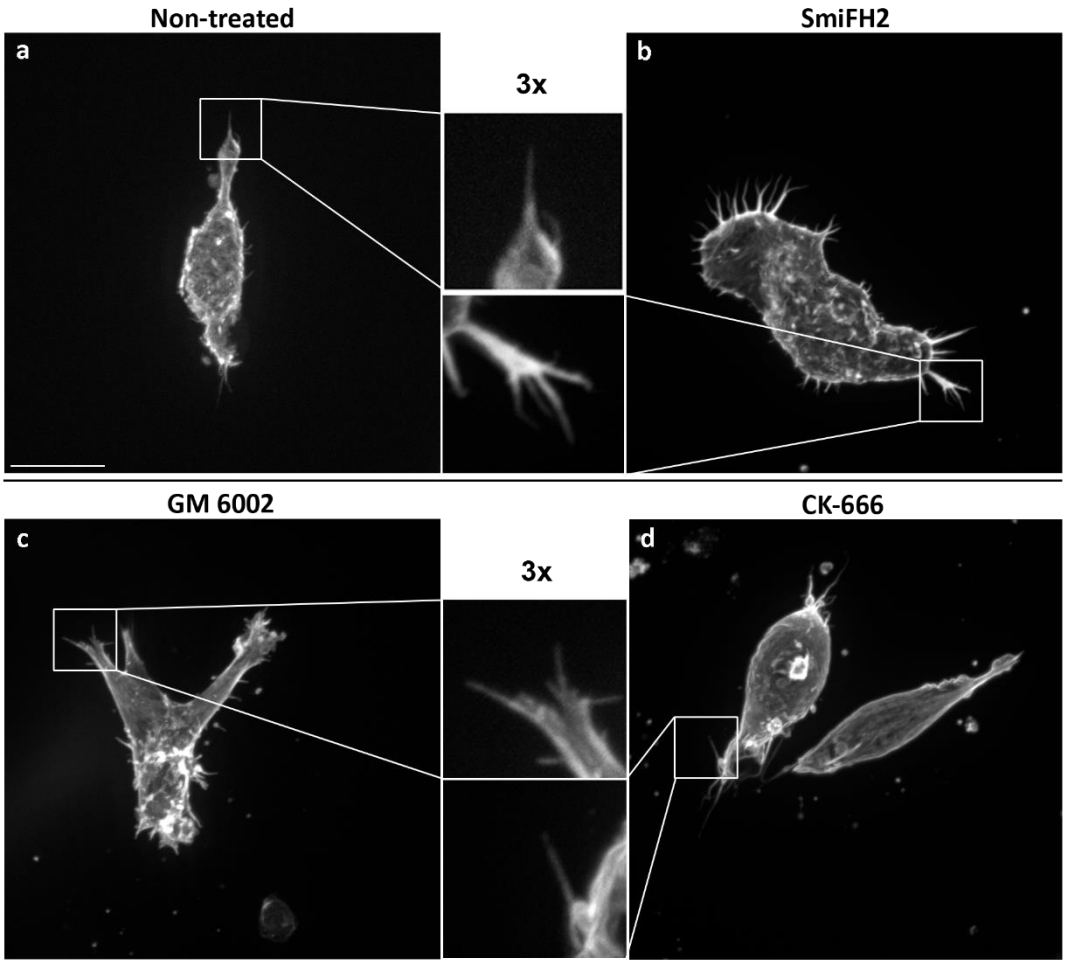

Figure 43: Effects of formin-, Arp2/3- or MMP inhibitor on actin-based protrusions in 3D collagen. HT1080 cells were embedded in 1.0 mg/ml 3D collagen scaffolds and incubated in presence of inhibitors: 30µM smiFH2; 25µM GM6001; 100µM CK666 or DMSO for 24-36 hours. Post incubation cells were fixed, stained with phalloidin Alexa-594 and visualized in spinning disc confocal microscopy. Slices were merged and exported form velocity 6.0 imaging software. Scale bar 20µm. (a): DMSO-treated cell; (b): 30µm smiFH2; (c): 25µM GM6001; (d): 100µM CK-666.

Images in Figure 43 show representative non-treated HT1080 cells and HT1080 cells treated with either smiFH2, CK-666 or GM6001. The smiFH2 treated cells (Figure 43 b) show reduced numbers of filopodia, and increased blebbing at the leading edge and dorsal/ventral surfaces (supplemental Figures). Furthermore, the cell shows spike like actin structures at the cell periphery apparently representing retraction fibers. Of note, smiFH2 treated cells have less polar morphology than cells from other treatment groups. Cells treated with GM6001 in Figure 43c have no apparent defects of the actin cytoskeleton at the leading edge, forming "normal" 3D leading edge with embedded filopodia. However, GM6001 treated cells display less dorsal/ventral protrusions and therefore have smoother dorsal/ventral surface compared to control cells (s. supplemental Figures). Cells treated with CK-666 (Figure 43 d) show also smoother cell surface with less dorsal/ventral spiked protrusions compared to control. Treated Cells show increased blebbing at dorsal /ventral surfaces and leading edge. CK-666 treated cells have no visible lamellipodia, whereas filopodia are still detectable at the leading edge in confocal fluorescence microscopy. Apparently, affected actin structures in CK-666 and smiFH2 treated cells are substituted either by blebbing or are absent from the cell surface.

3.3.9.2 Inhibitors of MMPs and formins reduce velocity of cell migration in 3D collagen

HT1080 cells migrate in 3D collagen using different modes of cell migration and apparently switch between migration modes (Katarina Wolf et al. 2003). However, as common in adhesion dependent migration, to project cell body forward, cells use actin-based protrusions. Furthermore, migration of HT1080 cells in 3D collagen is accompanied by matrix degradation (Katarina Wolf et al. 2003; Katarina Wolf et al. 2007).

Results from degradation assay suggest that on 2D substrates matrix degradation by HT1080 cells takes place at central- and rear regions of the cell, but not at the leading edge during migration as

shown in Figure 39. Inhibitor of formins (by smiFH2) which suppresses formation of filopodia did not inhibit the degradation of ECM significantly and at comparable levels to GM6001 (Figure 41). The smiFH2 treated HT1080 cells showed reduced filopodia and impaired cell polarity (Figure 40, Figure 41).

The inhibition of MMPs using MMP inhibitor GM6001 blocked degradation almost completely without affecting the formation of filopodia and lamellipodia, normal morphology and polarity on 2D in HT1080 cells (Figure 40).

The treatment of HT1080 cells with GM6001 in 3D collagen resulted in visually reduced dorsal /ventral actin-based protrusions, whereas filopodia and lamellipodia were still retained. Treatment of cells with CK-666 led to the loss of dorsal /ventral protrusions, but cells still could form filopodia at the leading edge (Figure 43). SmiFH2 treatment of HT1080 cells in 3D collagen led to the loss of filopodia and led to increased formation of blebs.

The sparse amount of previous studies regarding cell migration in the presence of smiFH2 show that treated cancer cells increased their velocity in 2D migration (Isogai, Kammen, and Innocenti 2015). In 3T3 fibroblasts treatment with smiFH2 led to 50 % reduced velocity in 2D migration assay (S. A. Rizvi et al. 2009). Another report showed that in 3D spheroid cultures, smiFH2 mediated inhibition of formins led to the markedly reduced invasiveness of glioblastoma cells (Arden et al. 2015b).

To evaluate how the inhibition of actin structures or MMP mediated degradation effects 3D migration HT1080 cells were treated either with smiFH2, CK-666 or GM6001 in a 3D random migration assay and cell migration was analyzed as described previously. Figure 44 shows the comparison of directionalities of different treatment groups of HT1080 cells.

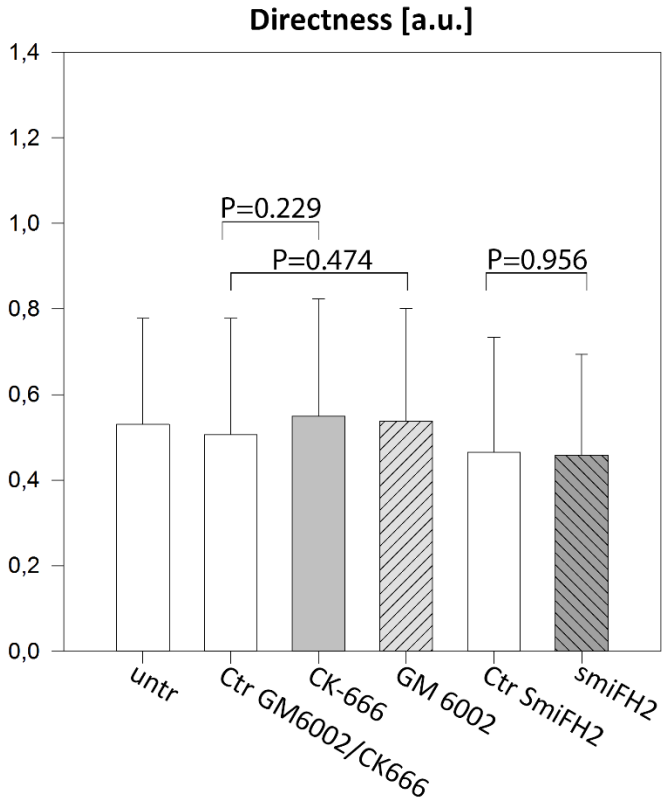

Figure 44: Effect of Arp2/3-, formin- or MMP inhibitor on directionality in a 3D random migration assay. HT1080 cells were embedded in 1.0 mg/ml 3D collagen and injected to µlide6 (Ibidi). After polymerization of collagen, inhibitors were applied: 30µM smiFH2; 25µM GM6001; 100µM CK666 or DMSO for 24 hours. Next, cells were placed in an environmental chamber (Ibidi) and live cell migration from each well was recorded using VisiView software. Pictures were taken every 5 minutes at 5x in brightfield illumination. Videos of different treatments were imported and tracked using ImageJ manual tracking plugin. These XY coordinates of cells were imported to chemotaxis tool 2.0 (Ibidi), and the directness of each migrating cell was calculated. The results were exported for statistical analysis to Sigma plot 13 software. Statistical analysis was performed using Mann-Whitney Rank Sum Test. Error bars show one standard deviation of the mean value form two independent experiments with sample sizes of 72-165 cells per condition.

In random 3D migration assay, the directness of cell movement was not significantly influenced by inhibitors of either Arp2/3 complex, MMPs or formins. Next, I analyzed cell velocities per treatment group (Figure 45).

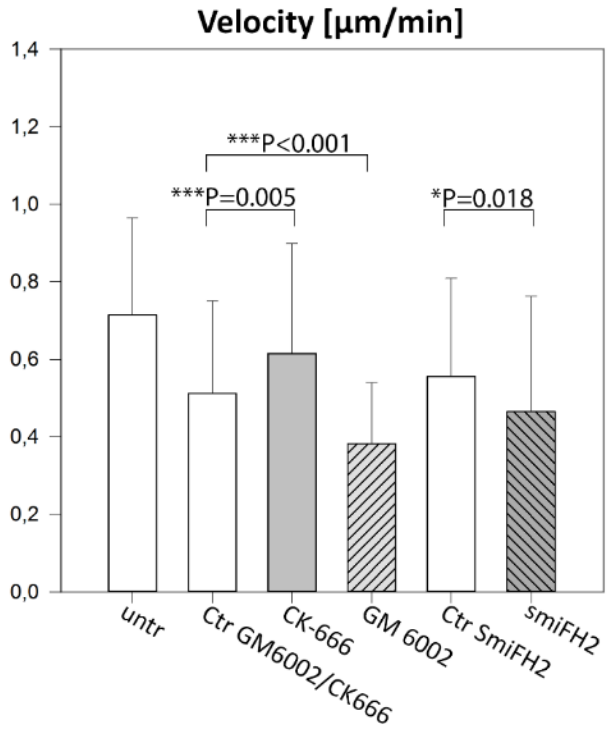

Figure 45: Effect of Arp2/3-, formin- or MMP inhibitor on cell velocity in a 3D random migration assay. HT1080 cells were embedded in 1.0 mg/ml 3D collagen and injected to µlide6 (Ibidi). After polymerization of collagen, inhibitors were applied: 30µM smiFH2; 25µM GM6001; 100µM CK666 or DMSO for 24 hours. Next, cells were placed in an environmental chamber (Ibidi) and live cell migration from each well was recorded using VisiView software on a microscope equipped with motorized XY-table. Pictures were taken every 5 minutes at 5x magnification in brightfield illumination for 8-12 hours. Videos of different treatment groups were imported and tracked using ImageJ manual tracking plugin. These XY coordinates of cells were imported to chemotaxis tool 2.0 (Ibidi), and the directness of each migrating cell was calculated. The results were exported for statistical analysis to Sigma plot 13 software. Statistical analysis was performed using Mann-Whitney Rank Sum Test. (untr): non-treated cells; (Ctr GM6002/CK666): cells treated with same amount of DMSO as used for inhibitor treatments with GM6002 and CK666; (CK-666): cells treated with CK-666; (GM 6002): cells treated with GM6002; (Ctr SmiFH2): Cells treated with same amount of DMSO as used for inhibitor treatments with smiFH2; (smiFH2): cells treated with smiFH2. Error bars show one standard deviation of the mean value form two independent experiments with sample sizes of 71-179 cells per condition.

In contrast to the similar directness values of cells treated with different inhibitors (Figure 44), these inhibitors affect cell velocity during 3D migration markedly. Surprisingly, in the case of CK-666 treatment, the average cell velocity increased to approx. 20 % compared to control group. As visible in representative Figure 43 d, CK-666 treated cells can form filopodia at the leading edge, but fail to produce lamellipodia. On the other hand, the GM6001 treatment, which resulted in smooth cell surfaces and less dorsal/ventral actin protrusions but “normal” leading

edge (Figure 43 c), shows approx. 30% reduced average velocity compared to control group. Finally, smiFH2, which suppresses the formation of filopodia at the leading edge in HT1080 cells, leads to 20 % reduced average cell velocity compared to control group (Figure 45).

3.3.9.3 Inhibition of formins has a negative effect on chemotaxis of HT1080 cells in 3D collagen

In the 3D random migration assay form the present work the suppression of formin dependent actin-based protrusions such as filopodia at the leading edge using smiFH2 coincided with a decreased velocity of these cells. As next, I further studied the effect of smiFH2 on 3D chemotaxis of HT1080 cells. Therefore, chemotaxis assay in a gradient of FCS in 3D collagen in the presence of smiFH2 was performed. The results were processed as described previously (Figure 46).

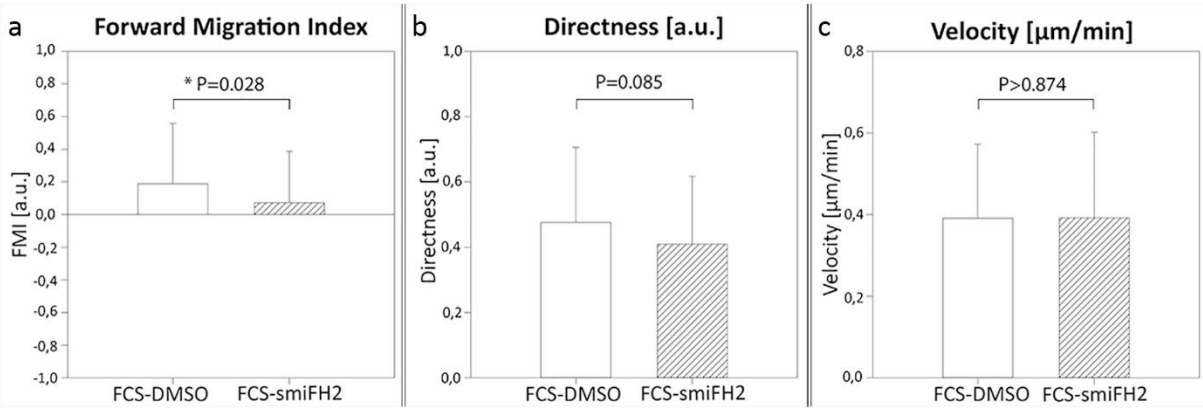

Figure 46: Effect of formin inhibitor smiFH2 on chemotaxis in 3D collagen. HT1080 cells were embedded in 1.0 mg/ml 3D collagen and injected into µslide 3D chemotaxis chamber (Ibidi). After polymerization of the cell-collagen mixture, 30µM smiFH2 (final concentration) together with 10% FCS were applied to the upper well of one the channels. In other channels, DMSO and FCS were applied in upper well as positive control. Next, the chemotaxis slide was placed in an environmental chamber (Ibidi) and live cell migration from each well was recorded using VisiView software on a microscope equipped with motorized XY-table. Pictures were taken every 5 minutes at 5x magnification in brightfield illumination for 8-12 hours. Videos of different treatment groups were imported and tracked using ImageJ manual tracking plugin. The resulting Datasets of XY coordinates of cells were imported to chemotaxis tool 2.0 (Ibidi). The FMI (**a**), directness (**b**) and velocities (**c**) of cells in chemotaxis chamber were calculated. The results were exported for statistical analysis to Sigma plot 13 software. Statistical analysis was performed using Mann-Whitney Rank Sum Test. Error bars show one standard deviation of the mean value form two independent experiments with sample sizes of 77-98 cells per condition.

Figure 46 (a) shows that smiFH2 treatment significantly reduces the chemotactic efficiency (expressed in FMI value) of HT1080 cells towards FCS gradient to approx. 40 % of untreated cells (a). The directness of smiFH2-treated cells is also reduced compared to control, but this reduction is not statistically significant (Figure 46 b). Furthermore, smiFH2 treated, and control cells show similar velocities (Figure 46 c). These results indicate a possible role of smiFH2 inhibited actin structures, such as filopodia and ventral/dorsal protrusions (invadopodia), in 3D chemotaxis.

3.3.10 Effects of fascin knockdown on migration and protrusions of HT1080 cells in collagen

Fascin bundles F-actin filaments *in vitro* and is suggested to be a major actin-bundling protein in filopodia (Otto, Kane, and Bryan 1979) (D. Vignjevic 2006). Downregulation of fascin led to the loss of filopodia in B16 melanoma cells and led to reduced numbers of filopodia and loss of circular dorsal ruffles in MEFs (D. Vignjevic 2006; Ladwein and Guledani unpublished). Fascin is overexpressed in several cancers and is often localized at the invasive front of tumors, suggesting its important role in tissue invasion of cancer (Hashimoto, Skacel, and Adams 2005; Danijela Vignjevic et al. 2007b). Reportedly, fascin localized within invadopodia together with F-actin and Arp2/3 complex and its knockdown had a significant negative effect on actin-rich dot-like protrusions on 2D ECM substrates (Li et al. 2010a).

Based on importance of fascin in the formation of filopodia and possible involvement in the formation of invadpodia, I performed fascin shRNA experiments in HT1080 cells aiming the question if fascin is important in the formation of filopodia in 3D migration.

3.3.10.1 Fascin shRNA leads to downregulation of *fascin1* expression in HT1080 cells

For knockdown of fascin, HT1080 cells were treated with a shRNA-Th construct which targets human *fascin1* mRNA. To analyze the expression of *fascin1* and efficiency of shRNA mediated knockdown of fascin in HT1080 cells western blot was performed (Figure 47).

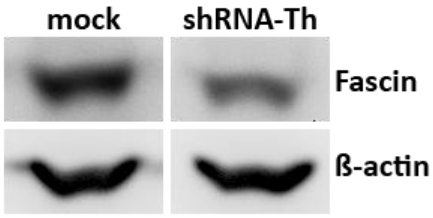

Figure 47: Western blot analysis of fascin knockdown in HT1080 cells. HT1080 cells were transfected with shRNA construct against human fascin. After 48h post transfection, cells were harvested and lysed. Western blotting was performed using antibodies against human fascin and ß-actin.

Figure 47 shows results of western blot analysis of fascin shRNA-Th transfected cells compared to control. Due to Figure 47, the signal intensity of fascin band is approx. 40% of that of mock cells, whereas the signal intensity of ß-actin band is comparable in both probes. The lower intensity of fascin signal in shRNA treated cells indicates the downregulation of fascin synthesis due to shRNA treatment compared to mock control.

3.3.10.2 *Fascin1* shRNA treated cells show less organized filopodia in 3D collagen

Fascin shRNA treated cells embedded in 3D collagen scaffolds were fixed and stained for F-actin to monitor the effect of fascin shRNA on actin-based protrusions, in particular of filopodia at the leading edge and putative invadopodia presented as actin-rich dots at central regions of cells embedded in 3D collagen (Figure 49).

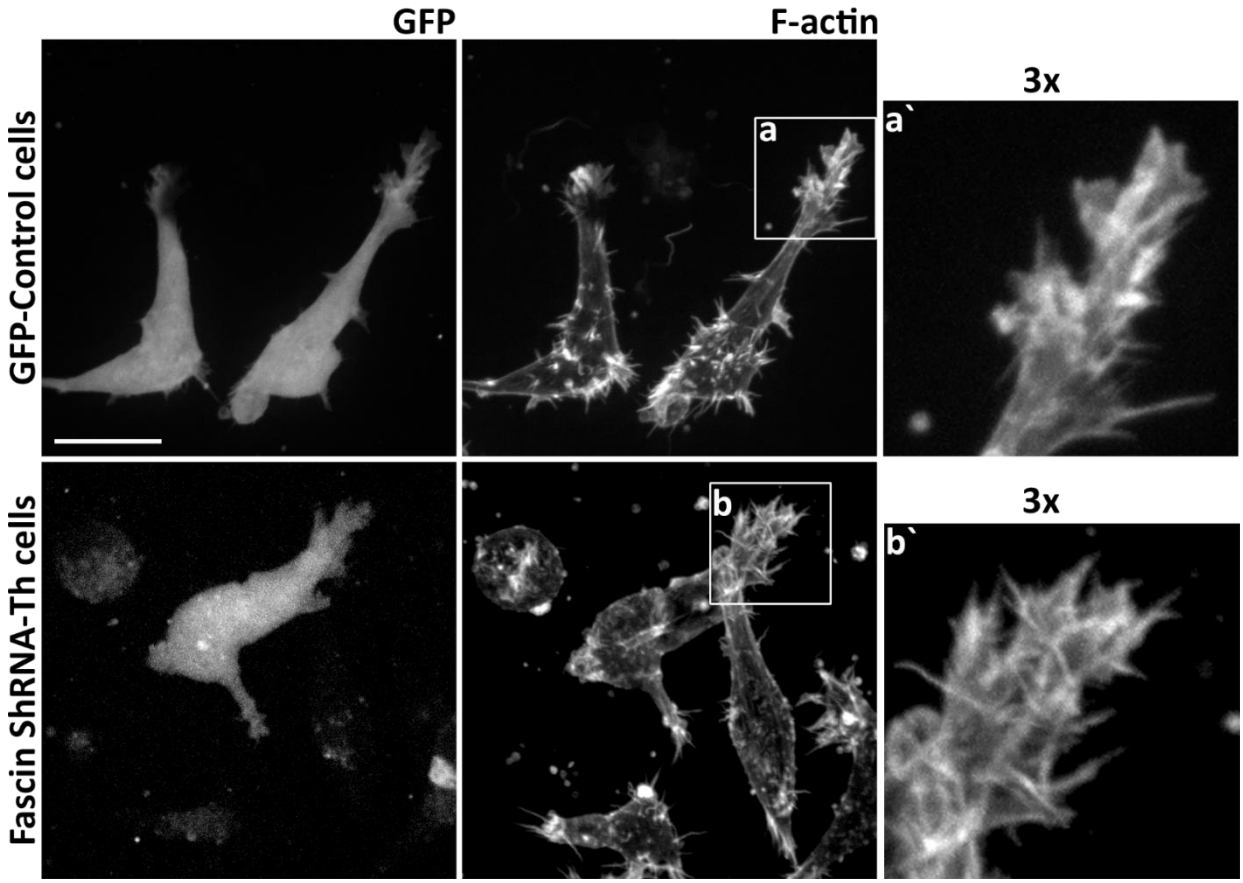

Figure 48: Fascin knockdown cells show disorganized filopodia at the leading edge of HT1080 cells in 3D collagen. HT1080 cells were transfected with shRNA construct against human fascin fused with the sequence for co-expression of GFP. After 48h post transfection, cells were harvested and embedded in 1.0 mg/ml collagen for 18-24 hours. Post incubation cells were fixed, stained with phalloidin Alexa-594 and visualized in spinning disc confocal microscopy. Slices were merged and exported form Volocity 6.0 imaging software. Scale bar 20µm.

Fascin1 shRNA expressing cells in Figure 49b show less dorsal/ventral actin dots in 3D (and form fewer finger-like protrusions. Data not shown here) than control cells. The fascin shRNA treated cells that still can form filopodia show more filopodia-like protrusions per cell which are although, disorganized at the leading edge compared to those of GFP control cells (Figure 49 a' and b'). Also, filopodia formed by fascin shRNA transfected cells are oriented approx. perpendicular relative to the direction of cells leading edge. The disorganized appearance of filopdoia or the reduced grade of the organization of filopodia at the leading edge of HT1080 cells can be caused due to reduced bundling activity of fascin in shRNA treated cells. The reduced grade of organization of filopodia was also reported in another study as a result of fascin depletion in B16 cells (D. Vignjevic 2006).

3.3.10.3 Fascin1 knockdown reduces velocity and directness in random migration of HT1080 cells

HT1080 cells treated with *fascin1* shRNA were subsequently subjected to random migration assay in 3D collagen, to assess their migratory capabilities after downregulation of *fascin1* expression (Figure 48).

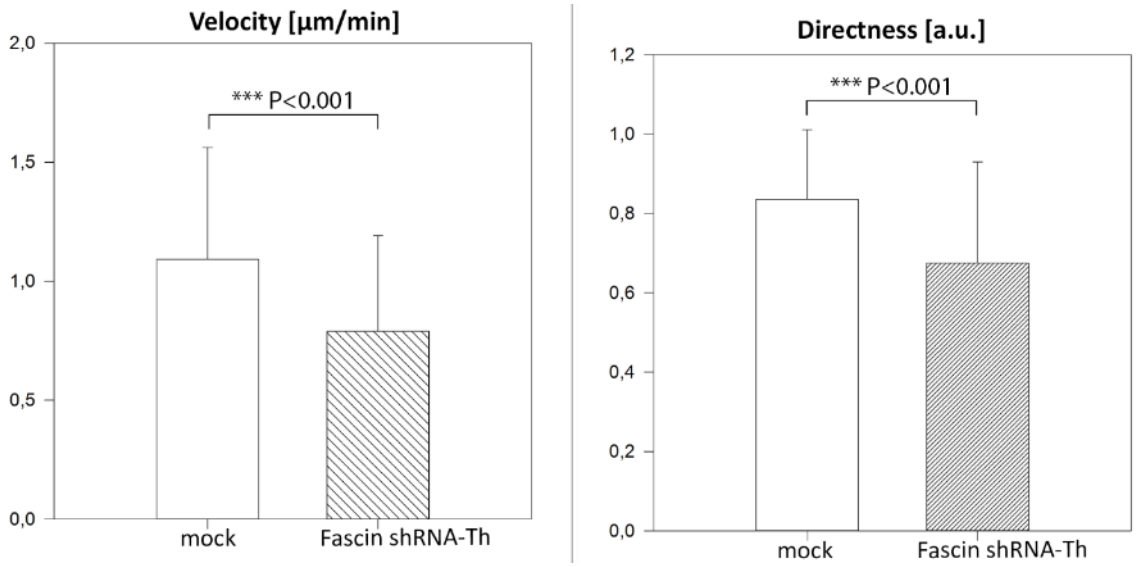

Figure 49: Fascin knockdown in HT1080 cells leads to reduced velocity and directionality in 3D random migration. HT1080 cells were transfected with shRNA construct against human fascin. After 48h post transfection, cells were harvested and embedded in 1.0 mg/ml collagen for 18-24 hours. Before live cell imaging, growth medium was replaced with medium containing HEPES. Cells were placed in an environmental chamber (37° C) on motorized XY stage on the laser spinning disc confocal microscope. Living cells were visualized with laser illuminations of 488nm and brightfield at 10x magnification. Scans were taken every 30 seconds for 1 hour at seven different locations per treatment group. Videos were imported and tracked using ImageJ manual tracking plugin. The XY coordinates of cells were imported to chemotaxis tool 2.0 (Ibidi), and the directness and velocity of each migrating cell were calculated. The results were exported for statistical analysis to Sigma plot 13 software. Statistical analysis was performed using Mann-Whitney Rank Sum Test. Error bars show one standard deviation of the mean value form five replicates per condition with sample size of n = 45-119 cells per condition.

Knockdown of fascin in HT 1080 cells led to approx. 30% reduced directness and 40 % reduced velocity in the 3D random migration of HT1080 cells compared to mock cells. The reduced velocity of fascin knockdown HT1080 cells is comparable to that of smiFH2 treated cells which showed 20% reduced cell velocities compared to control (Figure 45). Apparently, disorganized filopodia and reduced numbers of dorsal/ventral actin-rich dots in fascin shRNA expressing cells

(Figure 48) correlate with reduced velocity and directness of this cells in the 3D migration assay (Figure 49).

4 Discussion

4.1 2D migration

4.1.1 *Cdc42* knockout reduces formation of CDRs and filopodia in MEFs

Cdc42 GTPase and its homologs are one of the central nodes in the regulation of actin cytoskeleton in eukaryotic cells. Activated Cdc42 reportedly is involved in the formation of actin-based protrusions, particularly of filopodia at the cell periphery. Filopodia consist of bundles of unbranched actin filaments, therefore, actin polymerization in these structures is driven by formins and Ena/VASP proteins that can produce such unbranched actin filaments. Actin filaments are bundled within filopodia by bundling proteins such as fascin which also contributes to formation and stability of these structures. The role of filopodia, besides their general function as cell protrusion, has been implicated in establishing of cell polarity and in directional sensing during chemotaxis of cells. Also, filopodia were reported to play a role in cell-substrate adhesion. However, despite well studied biochemical composition and dynamics of formation of filopodia, the role of these structures in cell migration is controversial debated and not well understood.

Fibroblasts are attracted to PDGF during wound healing process. When treated with PDGF-BB, fibroblasts in 2D cell culture reorganize their actin cytoskeleton, develop actin-based protrusions such as filopodia and lamellipodia and begin to migrate (Schneider and Haugh 2005; Stephens, Milne, and Hawkins 2008; Kundra et al. 1994b). Besides lamellipodia and filopodia, fibroblasts form another type of transient actin protrusion at their dorsal surface which are explicitly formed in response to growth factors such as PDGF-BB. These protrusions are termed circular dorsal ruffles (CDRs). Whereas lamellipodia and filopodia apparently enable cells to protrude in a specific direction, the role of CDRs in cell migration is not understood yet. (Orth and McNiven 2006a; Buccione, Orth, and McNiven 2004) Previous work forms our lab has shown that CDRs were composed of lamellipodia and filopodia and were enriched in filopodia. Although, Cdc42 and Rac1 are essential for the formation of these structures, Cdc42 but not Rac1, was explicitly crucial for the formation of CDRs.

Resting Cdc42 (-/-) MEFs showed no visible defects of their actin cytoskeleton in fluorescence microscopy. However, when these cells were treated with PDGF-BB, they could not form CDRs. Formation of lamellipodia was not noticeably affected in these cells (Figure 9). Though, leading edges or lamellipodia in these cells were less "spiky" than that of control cells. It is likely that the spiky appearance of leading edge of cells is a result of the formation of filopodia. Therefore, I quantified and compared filopodia of Cdc42 (-/-) MEFs with that of control cells. The quantification showed that Cdc42 (-/-) cells produce approx. 13 % less filopodia after treatment with PDGF-BB compared to control cells (Figure 10). This result is in line with the study performed by Czuchra and colleagues which reported that in MEFs, Cdc42 was important, but was not essential for the formation of filopodia. They also showed that formation dynamics of filopodia was not altered in Cdc42 knockout MEFs compared to control cells, although they did not quantify numbers of filopodia per cell in their study (Czuchra, Wu, Meyer, van Hengel, et al. 2005).

Cdc42 knockout MEFs with no available Cdc42 GTPase still can produce filopodia, which can be explained by the existence of several mechanisms in cells to these strucktures. Two major proposed models- a tip nucleation- and a convergent elongation model both exist in cells, but are activated differently. Thus, in the absence of Cdc42, the essential GTPase in tip nucleation model, the convergent elongation mechanism could dominate in the formation of filopodia. Accordingly, in this scenario, VASP and not formins are considered to nucleate actin filaments in filopodia (Mellor 2010a; Svitkina et al. 2003).

Another possibility of formation of filopodia in the absence of Cdc42 can be explained by substitution of Cdc42 activity by related Rif GTPase, which can also drive formin dependent formation of filopodia. Reportedly Rif GTPase interacts with Drf3 (mDia2) formin during this process (Pellegrin and Mellor 2005). Also, Rif and mDia1 mediated formation of filopodia has been reported which was independent of Rac1 and Cdc42 (Pellegrin and Mellor 2005; Gorelik et al. 2011). Also supportive of formation of filopodia alternatively either by VASP or mDia formins is the study that used MEFs deficient of Ena/VASP or detectable levels of mDia2, showing that both, ectopically expressed mDia2 or VASP can induce filopodia in these cells. However, filopodia that were induced by VASP were shorter and mechanically more stable than those induced by mDia2 (Barzik et al. 2014).

VASP localizes at the tips of protruding lamellipodia and filopodia, where it can bundle and/or elongate actin filaments in a processive manner (Rottner et al. 1999b; Breitsprecher et al. 2011; Barzik et al. 2005). VASP was shown to be required for formation of filopodia in murine neuronal cells and *Dictyostelium* (Faix and Rottner 2006c; Lebrand et al. 2004; Applewhite et al. 2007; Schirenbeck et al. 2006).

It is likely that in MEFs VASP is activated in response to PDGF-BB by PDGFR mediated and Src kinase dependent activation of the c-Abl kinase (Plattner et al. 1999). The subsequent interaction between c-Abl and Abi1 leads to phosphorylation and activation of VASP at the cell membrane (Tani et al. 2003; Storz, Enabled, and Kinase 2010). Abi1 is a key adaptor protein that is critical in the reorganization of the actin cytoskeleton during formation of protrusions and thus localizes at tips of lamellipodia and filopodia in protruding cells (T. Stradal et al. 2001a). Abi1 is a part of GEF protein complex Eps8-Abi1-Sos1 which activates Rac downstream of PDGF Receptor and PI3 kinase in fibroblasts. This signaling axis is critical for PDGF-BB induced formation circular dorsal ruffles (M Innocenti et al. 2002). Abi1 is was shown to be an integral a part of WAVE complex which can directly interact with Rac1 and mediate activation of WAVE complex to drive the formation of lamellipodia at the leading edge of cells. Additionally, Abi is essential for the stability of this complex (Steffen et al. 2004b; Dubielecka et al. 2011).

VASP reportedly interacts with WAVE complex via Abi1 downstream of Rac1 as reported in studies using s2 cells form *Drosophila*. The disruption of Abi-VASP interaction led to loss of VASP at tips of lamellipodia, whereas VASP still was retained at tips of filopodia in s2 cells (X. J. Chen et al. 2014). So probably, Abi recruits VASP downstream of Rac1 at the leading edge where VASP takes part in the formation of lamellipodia in concert with WAVE-complex. At the leading edge, VASP can be further modified by phosphorylation which might lead to detachment of VASP form Abi- and WAVE complex. After detachement form Abi, VASP can probably form tetramers to facilitate the formation of protrusions such as filopodia. In this regard, Irsp53 was shown to induce clustering of VASP downstream of activated Cdc42 (Disanza, Bisi, Winterhoff, Milanesi, Ushakov, Kast, Marighetti, Romet-lemonne, et al. 2013). On the other hand, at the leading edge of a cell formins and VASP can form a protein complex. The formation of such protein complex was detected between VASP and Diaphanous family of formins during formation of filopodia. Of note, probably recruitment of VASP and mDia to tips of filopodia is independent of

each other (Grosse et al. 2003; Schirenbeck et al. 2006). In this scenario, mDia and VASP possibly capture and bundle barbed ends of actin filaments within lamellipodia. In a further step, the elongation of these filaments is facilitated through EVH2-and FH2 domains of VASP and formins respectively. This activity finally sums up in the formation of filopodia.

It is likely that in Cdc42 knockout MEFs VASP participates in the formation of filopodia independently of formins. Thus, the filopodia that were produced by Cdc42 (-/-) cells from this work in response to PDGF-BB can be formed by the activity of VASP downstream of activated Rac1 GTPase and members of Cdc42 subfamily that also can activate formins.

4.1.2 Cdc42 knockout MEFs are less polar in response to PDGF-BB

Cdc42 GTPase reportedly is an important regulator of cell polarity in many cell types (Catherine D Nobes and Hall 1999; S. Etienne-Manneville 2004; A. E. Adams et al. 1990b). However, the mechanisms that enable Cdc42 to regulate polarization of cell is a matter of controversial debate. The development of polar cell morphology is dependent on polar formation actin-based protrusions at the leading edge, where Cdc42 is supposed to play a key role. On the other hand, Cdc42 reportedly influences the orientation of Golgi apparatus and microtubules towards the direction of migration which is considered an important step in cell polarity (Palazzo et al. 2001; Bartolini et al. 2008).

The assessment of cell polarity after PDGF-BB treatment of Cdc42 (-/-) MEFs showed that these cells produced lamellipodia that were scattered around cell periphery resulting in a non-polar cell morphology. The quantification revealed that population of Cdc42 (-/-) MEFs that showed polar morphology was approx. 50 % reduced compared to control cells (Figure 11). This result fits well with other study showing that Cdc42 deficiency results in defective cell polarity, which was manifested in the formation of several lamellipodia at the cell edges of murine Cdc42 knockout DCs. Also in neuronal cells depleted of Cdc42, polarized formation actin protrusions and thus formation of an axon was lost (Lämmermann et al. 2009; Garvalov et al. 2007). In a previous study Cdc42 (-/-) MEFs were assessed in their ability to polarize during wound healing assay.

The affected cells could form lamellipodia towards wound site and migrate, however, their directionality and mean angle vector of movement were markedly reduced which may indicate partial role for Cdc42 in polarization in these cells (Czuchra, Wu, Meyer, van Hengel, et al. 2005)

The reorientation of microtubules and of a Golgi apparatus apparently directs intracellular transport pathways of a cell to the leading edge, which is probably important for polarization and directional migration (Palazzo et al. 2001). However, reports that assign loss of microtubule and Golgi reorientation to the removal of Cdc42 are based on experiments that utilize re-expression of a dominant negative (dN) Cdc42 or microinjection of dominant negative Cdc42 GTPase. (Catherine D Nobes and Hall 1999; Palazzo et al. 2001). A dominant negative version of Cdc42 can affect additionally other Cdc42 subfamily members or even Rac or Rho GTPases by binding to shared GEFs (Czuchra, Wu, Meyer, van Hengel, et al. 2005).

The orientation of Golgi-apparatus and microtubule filaments of Cdc42 (fl/-) or Cdc42 (-/-) MEFs was not assessed in the present work. However, another study which utilized Cdc42 (-/-) MEFs did not detect deficient Golgi apparatus orientation in wound healing assay in these cells. Apparently, other GTPases of Cdc42 subfamily could have redundant functions for Cdc42 in the reorientation of microtubule and Golgi apparatus in MEFs (Czuchra, Wu, Meyer, van Hengel, et al. 2005).

Probably during polarization cells initially have to form actin-based protrusions in the form of lamellipodia and filopodia on 2D. The polarized actin cytoskeleton then provides a pattern for Golgi apparatus and microtubule network to reorient themselves. So probably, the orientation of Golgi apparatus and of microtubules is not essential for the initial polarization of cells towards chemoattractant, but is probably important to support cell movement over a long distance in a particular direction (Stramer et al. 2005b).

To assess if the orientation of microtubules and Golgi apparatus in response to PDGF-BB is also affected in Cdc42 (-/-) MEFs, a 2D chemotaxis assay can be performed using PDGF-BB as a source. Finally, cells can be fixed and stained for both these structures together with F-actin. This way it is possible to study the orientation of these structures, together with cell morphology, towards the source of chemoattractant.

4.1.3 *Cdc42* knockout reduces cell velocity in MEFs

The removal of Cdc42 can have a negative or a positive effect on cell velocity during 2D migration of cells *in vitro*. However, the extent of this effect is often reliant on a cell type, a method of Cdc42 removal and an environment of migration assay which is used (2D or 3D).

In the previous study knockout of *Cdc42* in MEFs resulted in a slightly less directness, but had no negative effect on cell velocity in a wound healing assay. Re-expression of dNCdc42 led to 30 % reduced velocity and a further decrease of directness in Cdc42 knockout MEFs compared to Cdc42 (fl/-) control cells (Czuchra, Wu, Meyer, van Hengel, et al. 2005). The knockout of *Cdc42* in murine dendritic cells resulted in slightly impaired migration speeds and reduced directness on 2D. Affected cells formed multiple, non-polar protrusions in response to chemoattractant CCL19 indicative of defective polarity. When embedded in 3D collagen or in a dermal tissue of mouse, these cells showed severely decreased migration speed and directionality (Lämmermann et al. 2009). A different study that utilized siRNA mediated knockdown of Cdc42 in MEFs showed 20-30 % reduced cell speeds and slightly reduced directness (6%) in affected cells. Although, knockdown of Rac1 or inhibition of Rho isoforms led to similar results in these cells (Monypenny, Zicha, Higashida, Oceguera-yanez, et al. 2009). In fibroblasts the removal or a dominant negative suppression of Cdc42 is apparently associated with the non-polar formation of lamellipodia, reduction of filopodia numbers and reduced cell velocity. Whereas in immune cells, the dominant negative suppression of Cdc42 led to formation of less filopodia per cell, increased velocity and loss directionality during wound closure (Catherine D Nobes and Hall 1995a; C D Nobes and Hall 1999; Czuchra, Wu, Meyer, Hengel, et al. 2005; Stramer et al. 2005b).

Cdc42 (-/-) MEFs form this work showed slightly (approx. 20-30 % slower than control cells), but significantly reduced cell velocities in a random migration or when globally stimulated with PDGF-BB. Furthermore, the reduced cell velocity was robustly present in 2D migration assays when different conditions were applied (Figure 14). Although, same cells in a wound healing assay showed 30-50 % increased average cell velocities compared cells from random migration assays (Figure 21). The negative effect of Cdc42 depletion on cell migration was in fact indicated by other studies where microinjection of dNCdc42 led to reduced velocity in primary rat fibroblasts and murine SV40 macrophages. Additionally, affected cells formed fewer filopodia and

had lost the ability to perform chemotaxis compared to control cells (C D Nobes and Hall 1999; Allen et al. 1998). In line with this, Cdc42 (-/-) MEFs used in present work also produce approx. 13 % less filopodia per cell. Furthermore, these cells developed less polar morphology when stimulated with PDGF-BB compared to Cdc42 (fl/-) control cells (Figure 11).

Noticeably, the loss of approx. 13 % of filopodia in Cdc42 (-/-) MEFs, does not severely impair the velocities of these cells and is probably partly compensated by Cdc42 subfamily members. Moreover, this loss of filopodia subpopulation may represent the unique contribution of Cdc42 and downstream formins in the formation of filopodia. Of note, at conditions when dominant negative suppression of Cdc42 is applied, other Cdc42 subfamily members or even Rho GTPases are probably also affected (Czuchra, Wu, Meyer, Hengel, et al. 2005). Therefore Cdc42 subfamily members are less available to compensate the loss of filopodia in cells where dN Cdc42 is expressed.

Dependent on the cell type and thus availability of alternative migration mechanisms, some cell types under conditions when Cdc42 is suppressed can change migration mode and even show increased motility and velocity. This is probably the case in immune cells when dN Cdc42 is expressed. These cells showed increased migration speed in response to dominant negative suppression of Cdc42 (Stramer et al. 2005b; Allen et al. 1998). Fibroblasts probably possess no alternative migration mechanisms other than adhesion dependent mesenchymal migration mode. So, in these cells application of dominant negative expression- or microinjection of dn-Cdc42 leads to decreased motility (C D Nobes and Hall 1999; Czuchra, Wu, Meyer, Hengel, et al. 2005). Reduced numbers of filopodia in response to removal of Cdc42 fits well with the reduced velocity of cells (13 % less filopodia *vs*. 20-30 % reduced velocity of cells). This can be probably explained by fact that less filopodia lead to less protrusive force generated by Cdc42 deficient cells leading to reduced velocity. Furthermore, MEFs at least at their current developmental stage (embryonic), are not able to use different migration modes. In their study, Czuchra and colleagues did not detect reduced velocities of Cdc42 knockout MEFs, which probably depend on the mesurement methods of cell velocity (Czuchra, Wu, Meyer, Hengel, et al. 2005).

On the contrary to 2D migration assays where Cdc42 deficient cells showed decreased migration speeds, *in vivo*, the expression of dominant negative Cdc42 in hemocytes of *Drosophila* resulted

in doubled cell velocities during laser induced wound healing assay. However, these cells migrated in haphazard paths towards the wounding site, which is indicative of less directed migration. Furthermore, hemocytes expressing dN Cdc42 formed multiple lamellipodia suggesting negative effect of such treatment on the polarization of cells. Although, the affected cells were still able to migrate towards the wound (Stramer et al. 2005b). The ability of hemocytes to find the wounded site is probably enhanced due to additional physical cue provided when the laser beam creates the wound. Possibly cells can sense changes in the physical tension arising from the wounded site (disrupted tissue).

The knockout of *Cdc42* in murine dendritic cells resulted in cells that formed several lamellipodia and thus showed non-polar morphologies in response to chemoattractant on 2D. In 2D migration assay, these cells migrated with 33 % reduced directional persistence, and 20 % reduced velocities compared to control cells in response to chemoattractant CCL19. Cdc42 knockout DCs that were overlaid with 3D collagen could not invade into the matrix, although were able to form multiple protrusions. When embedded in 3D collagen these cells showed 56 % reduced velocity, and 75 % reduced directness compared to wildtype. Furthermore, directness of Cdc42 knockout DCs dropped 50% when cells were embedded in 3D collagen. On the contrary, directness of WT cells rose to 130% compared to that of 2D migration assays (Lammermann et al. 2009). This study shows that ability of Cdc42 knockout DCs is markedly reduced on 2D and further reduced in 3D collagen. Cdc42 knockout DCs migrated with approx. double velocities on 2D than in 3D towards CCL19. The different velocities of these cells on 2D *vs.* 3D is probably due to less degrees of freedom for cells to move towards a chemical cue on 2D compared to 3D environment. Thus on 2D, the decision where to protrude is made faster by a cell, which may result in increased cell velocity. However, cells on 2D can less efficiently measure the gradient of a chemical cue than cells in 3D. This is due to less contract surface with chemoattractant which is mostly the dorsal side of a cell on 2D. The less efficiency of gradient measurement results in more haphazard paths and decreased directness of cells on 2D. In a 3D environment, cells have more options to move towards chemoattractant and can probably measure and estimate chemical gradient more effectively than on 2D surfaces. The efficient gradient detection in 3D is assumingly due to the increased contact surface of a cell with chemoattractant compared to 2D. In this manner cells

detect steepness of the gradient more efficiently in 3D than on 2D, resulting in less haphazard movements and increased directness in 3D.

Reminiscent of results in murine Cdc42 (-/-) MEFs from the present work (Figure 14), Cdc42 knockout DCs showed 20% reduced cell velocity on 2D towards chemoattractant CCL19 compared to control cells (Lammermann et al. 2009). This fits well with results from the present study showing approx. 20 % reduced velocities in Cdc42 knockout MEFs on 2D in response to PDGF-BB. It is possible that reduced velocity in Cdc42 (-/-) MEFs correlates to reduced numbers of filopodia (Figure 10) which in turn probably leads to less protrusive force in these cells. However, Cdc42 (-/-) MEFs showed reduced polarity by producing multiple lamellipodia. The development of several non-polar distributed lamellipodia also can lead to inefficient cell movement and thus less velocity. On the other hand, loss of up to 13 % of filopodia which is the case in Cdc42 knockout MEFs can lead to loss of cell polarity and thus formation of multiple lamellipodia.

Whereas in Cdc42 knockout cells merely Cdc42 GTPase is removed from cells, a dominant negative expression or microinjection of dN Cdc42 can interfere with other Cdc42 subfamily proteins leading probably to exxgarated assumption of the role of Cdc42 GTPase. Possibly, some functions of Cdc42 are shared and thus can be compensated by Cdc42 subfamily members in case of Cdc42 depletion. Therefore, if removal of Cdc42 leads to slightly fewer filopodia per cell than this might represent the unique contribution of Cdc42 that cannot be fully compensated by other members of Cdc42 subfamily. Consequently, the reduced filopodia numbers probably can be assigned to the removal of Cdc42 and its downstream effectors.

In the present work for the first time, 2D migration of a large number of Cdc42 (-/-) MEFs were analyzed using video microscopy. These cells showed consistently reduced cell velocity when different conditions were applied in 2D migration assays. Furthermore, several studies indicate that removal of activated Cdc42 coincides with slightly reduced velocity and fewer filopodia per cell, whereas others studies are not supportive of this. The results from this work are supportive of negative impact of removal of Cdc42 on cell velocity on 2D and provide quantification which states that Cdc42 (-/-) MEFs produce approx. 13 % less filopodia per cell. This coincides with 20-30 % reduced velocity in 2D migration assays in affected cells. It is also noteworthy that

whereas cells showed different velocities depending on conditions used, still in all performed assays Cdc42 (-/-) MEFs were consistently slower than Cdc42 (fl/-) controls.

In previous studies, the effect of depletion of Cdc42 on the velocity of fibroblasts was either not detected or if detected was regarded negligible (Czuchra, Wu, Meyer, Hengel, et al. 2005; Catherine D Nobes and Hall 1995a). These studies used wound healing assay for evaluation of cell velocity. This assay is although very robust, but still probably not sensitive enough to detect minor differences in cell velocities. In a scratch induced wound healing assay, cells have predefined space to move into. Additionally, cells that reside at the edges of the wound are probably physically pushed form cells growing and proliferating in layers behind. These effects probably cumulate, and thus cells migrate faster in wound healing assay than in other 2D assays.

4.1.4 *Cdc42* knockout diminishes 2D chemotaxis towards PDGF-BB in MEFs

Fibroblasts *in vivo* are usually attracted to gradient of PDGF-BB. This process is important in wound healing in mammals where the PDGF-BB is accumulated in a wounded site. It is thought that the gradient of PDGF-BB attracts fibroblasts from deeper layers of tissue to the wound. Fibroblasts migrate to into the wound and contribute to a wound closure and healing. It was shown at a cellular and a molecular level, that PDGF-BB binds and activates its transmembrane receptors which transduce the signal into the cytoplasm of fibroblasts which in response prepare for migration. Therefore, the actin cytoskeleton has to be reorganized in a way that cells can produce protrusions. Rac1 and Cdc42 GTPases are known to orchestrate this process (Catherine D Nobes and Hall 1999; Kundra et al. 1994b). The role of Cdc42 was thought to support and induce the formation of filopodia, but the role of Cdc42 in cell migration is not well understood. Cells depleted of Cdc42 showed slightly reduced velocities, but were able to migrate on 2D surface in wound healing assays. Several studies indicated the importance of Cdc42 in cell polarity. Additionally, the genetic knockout of *Cdc42* led to reduced velocities and directionality in immune cells (C D Nobes and Hall 1995; Catherine D Nobes and Hall 1999; Stramer et al. 2005; Lämmermann et al. 2009).

Despite several studies, the role of Cdc42 in chemotaxis and generally in cell migration is still controversially discussed. Dominant negative suppression of Cdc42 was associated with loss of cell polarity and defective directionality in rat primary fibroblasts (Catherine D Nobes and Hall 1999). The conditional knockout of *Cdc42* in MEFs led to similar effects, but in less extent. These effects were markedly enhanced when the dominant negative Cdc42 was expressed in Cdc42 knockout cells (Czuchra, Wu, Meyer, van Hengel, et al. 2005). Both studies used wound healing assay to measure cell directionality or velocity. A dominant negative suppression of Cdc42 in hemocytes from *Drosophila* led to haphazard migratory paths of these cells during *in vivo* wound healing process. This process was induced by a laser beam based wounding of the *Drosophila* tissue. Interestingly, Cdc42 depleted immune cells showed markedly increased velocities that their wildtype counterparts and thus could reach the wound site at similar times as wildtype cells (Stramer et al. 2005a). The decreased directness of cell migration and increased velocity indicate that loss of Cdc42 in hemocytes of *Drosophila* led to defective sensing of the wound site. Likewise, in mouse SV-40 macrophages the depletion of Cdc42 led to increased cell speed, loss of polarity and defective chemotaxis (Allen et al. 1998). In contrast to these findings knockdown of Cdc42 in MEFs had although a negative effect on PDGF induced chemotaxis, but this effect was of qualitative nature and not measured regarding reduced FMI of effected cells. Based on this, authors suggest that shRNA mediated knockdown of either Cdc42, Rac1 or inhibition of Rho one at a time had no negative effects on PDGF induced chemotaxis of MEFs in Dunn-chamber assay. Although, mean speed of cells was 20% reduced in case of Cdc42 knockdown cells, 30% reduced in case of Rac1 KD and approx. 60% reduced when all three GTPases were knocked down simultaneously. Therefore, the defective chemotaxis of Cdc42 knockdowns MEFs was assigned to reduced velocity of these cells (Monypenny, Zicha, Higashida, Oceguera-Yanez, et al. 2009).

To better characterize the migration of Cdc42 (-/-) MEFs I performed 2D chemotaxis assay towards the gradient of PDGF-BB. In this assay, Cdc42 deficient cells showed slightly reduced velocity compared to control, which is reminiscent of random migration assays, and almost completely lost ability to follow the gradient of PDGF-BB in contrast to control cells.

These results from the present work demonstrate that Cdc42 is essential for chemotaxis of MEFs towards PDGF-BB. This result complements other studies that indicated the importance of Cdc42

for directional movements such as of immune cells during *in vivo* wound healing of *Drosophila* embryos or chemotaxis of murine dendritic cells towards CCL19 (Stramer et al. 2005a; Lämmermann et al. 2009). However, results from this work also partly contradicts report which implies that knockdown of Cdc42 in MEFs did not cause defective chemotaxis in MEFs (Monypenny, Zicha, Higashida, Oceguera-Yanez, et al. 2009). In 2D chemotaxis assay, cells migrate with slower velocities than in wound healing or random migration assays (Figure12; Figure14; Figure 21). The reduced velocity in the chemotaxis assay compared to random migration- or wound healing assays, can be explained by the assumption that during chemotaxis cells do not have to move fast and therefore spend much energy to reach a chemoattractant source. In a random migration, assay cells move with higher velocities because no clear chemoattractant cue is presented but instead only a global stimulus is applied. Therefore cells probably are continuously are "searching" for a gradient or source of the chemical cue.

Taken together, the present work demontrates that Cdc42 knockout MEFs produce 13 % less filopodia than control cells and show less polarity in response to PDGF-BB. Furthermore, knockout of *Cdc42* in MEFs resulted in reduced cell velocity and directionality on 2D which supports studies that report the negative role of Cdc42 removal on cell velocity on 2D (Lammermann et al. 2009; Monypenny, Zicha, Higashida, Oceguera-Yanez, et al. 2009). In experiments perfomed during the present work, Cdc42 knockout MEFs cells migrated with approx. 15-30 % reduced velocity in various setups on 2D. The reduced number of filopodia downstream of Cdc42 which results in reduced cell polarity and reduced velocity during cell migration probably sum up in the reduced ability of Cdc42 knockout MEFs to follow chemical gradient of PDGF-BB.

An important aspect when studying effects of Cdc42 removal on cell migration is the consideration of Rac1 activity in affected cells because of an apparent cell type- or mitogen-dependent degree of cross-talk between Rac1 and Cdc42. Reportedly, removal of Cdc42 is associated with up to 50 % reduced activation level of Rac1 in MEFs (Czuchra, Wu, Meyer, van Hengel, et al. 2005; Bosse et al. 2007). Moreover, Rac1 is a prominent inducer of lamellipodia formation and lamellipodia are important in cell migration and chemotaxis in MEFs on 2D (Pankov et al. 2005). Genetic removal of all Rac isoforms in MEFs resulted in loss of lamellipodia in cells and severe reduction of motility and chemotaxis on 2D in response to HGF. Although, Rac KO cells still could form filopodia and migrate at 70-80 % reduced velocities compared to control cells. The residual

migration velocity of Rac depleted cells was thought to be filopodia driven (Steffen, Ladwein, Dimchev, Hein, Schwenkmezger, Arens, Ladwein, Holleboom, et al. 2013). In line with this, Cdc42 knockout cells, in present work, migrated with 20-30 % reduced velocities compared to control cells on 2D. The reduction of cell velocity in Cdc42 or Rac depleted cells could represent individual contributions of these GTPases to cell velocities during migration on 2D. In this scenario, Rac activity would provide 70-80 percent- and Cdc42 consequently approx. 20-30 percent of cell velocity during migration on 2D. Therefore, the contributions to cell velocity of lamellipodia and filopodia respectively would lie within this ranges at least in MEFs migrating on 2D. Furthermore, due to results of present work, the removal of Cdc42 does not markedly affect the velocity of cell migration, but severely affects the ability of MEFs to perform chemotaxis towards PDGF-BB. In case of Rac KO cells apparently both, the velocity and chemotaxis are severely affected. Thus, it can be speculated that Cdc42 is responsible for maintaining the correct direction towards PDGF-BB by facilitating production of filopodia in that specific direction, whereas Rac provides, the main force of the protrusion in the form of lamellipodia on 2D.

Due to other report Rac1 KO cells showed suppressed formation of lamellipodia and 50 % reduced velocity in wound healing assay. However, affected cells showed no significant difference in chemotaxis towards PDGF-BB (Vidali et al. 2006). The reason for such a contradicting results regarding chemotaxis of Rac depleted cells could be the use of different chemoattractants (HGF vs. PDGF-BB) and different chemotaxis assays (2D chemotaxis assay vs. transmigration assay). Transmigration assay has a disadvantage that additionally to a chemotactic cue it provides a physical cue as a physical sink which leads to probably less sensitivity than a 2D chemotaxis assay. Of note, in 2D chemotaxis assay, mainly a chemical cue is provided.

However, the Cdc42 knockout MEFs form our lab showed similar activation level of Rac1 in response to PDGF-BB compared to control cells. Consequently, the Cdc42 knockout cells were able to form lamellipodia at comparable levels to control cells (Schloen K., PhD thesis). The altered activation levels of Rac1 GTPase form our studies compared to others is supposedly caused by the use of different mitogens in Rac activation assays or can be a cultivation dependent effect.

It is also possible that there is a degree of a cross-talk between Cdc42 and Rac1 GTPases. The occurrence and intensity of this cross-talk probably depends on the membrane receptor that is activated by an incoming signal. How this cross-signaling is achieved in not known to date. It is

likely that cross-talk between Rac1 and Cdc42 is mediated via shared GEFs of these GTPases. To do so, a shared GEF probably recruits Cdc42 and Rac simultaneously (or stepwise one after the other) at the adjacent loci at the cell membrane, were both GTPases are activated. If this activation is dependent of recruitment of both Cdc42 and Rac1, this would imply the formation of protein complex encompassing both of these GTPases. In this case, the removal of Cdc42 would lead to situation where Rac1 cannot be activated at these sites. Such a mechanism could be achieved by formation of a transient protein complex at the membrane involving a shared GEF, Rac and Cdc42. A recent report showed that such interaction is possible and was detected in response to VEGF endothelial cells during formation of lateral filopodia in the process of cell sprouting and angiogenesis (Abraham et al. 2015).

Several key events have to take place before GTPases such as Rac or Cdc42 can localize to the sites of a cell membrane that faces the PDGF-BB gradient. In fibroblasts the activation of RTKs by growth factors such as PFGF-BB leads to activation of PI3 kinase at the cytosolic side of the cell membrane and local generation of its products prominently of PIP_3. PIP_3 recruits GEFs to the cell membrane. Additionally, prenylated GTPases first need to be dissociated from their GDIs to associate to the membrane by inserting their lipid moiety into the membrane. The dissociation of GTPase form GDI can be initiated by phosphorylation of GDI by PKA or Src-Kinases. Also, GDI displacement factors are supposedly involved in dissociation of GDI-GTPase complex. At the membrane, GEFs bind to PIP_3 and are activated revealing their catalytic domain which can bind and activate Rho GTPases.

GEFs of Dbl subfamily are in an inactive state due to auto-inhibition which is enabled by the interaction of C-and N-terminal domains of GEF. Both termini of a GEF are flanking its catalytic domain (Cherfils and Zeghouf 2013). Reportedly, the interaction of second messengers such as cAMP or phosphatidylinositides with specific sites within domain of GEF activates the GEF protein and unmasks its catalytic domain (de Rooij et al. 1998; Rossman, Der, and Sondek 2005)). In this manner, the Vav1 GEF is recruited and activated by binding to PIP_3. Reportedly, the interaction between PIP_3 and Vav1 enhances the GEF activity of Dbl homology domain (DH) of this GEF (J. Han et al. 1998b). Vav2, a shared GEF, is tyrosine phosphorylated and activated in response to PDGF-BB. Vav2 can activate RhoA, Rac1, and Cdc42, whereas Cdc42 showed the strongest activation by this GEF compared to RhoA or Rac1 (B. P. Liu and Burridge 2000). The

PIP_3 is not selective for different families of GEFs and is able to bind and activate GEFs from different subfamilies such as Pix, Swap70, and P-rex1 as well (H. C. E. Welch et al. 2002; J. Han et al. 1998b; Shinohara et al. 2002). Activated GEFs reportedly can act as protein complexes which are bound to other adaptor proteins. An example of this is an assembly of Sos1 GEF complex in response to PDGF-BB. The esp8-abi1-sos1 complex is essential for PDGF induced membrane ruffling in MEFs. Probably the binding of this complex to the p85 subunit of PI3 kinase was also essential for circular dorsal ruffling in MEFs. This complex signals probably to Rac1 in MEFs leading to the formation of lamellipodia (M Innocenti et al. 2002).

GEFs form Dock family comprise of eleven members in mammals and reportedly exclusively activate only Rac and Cdc42 GTPases but not RhoA (Laurin and Côté 2014; Côté and Vuori 2002). Whereas Dock 180 (Dock1) and Dock2 were shown to be specific for Rac, zizimin1 (Dock9) and zizimin2 (Dock11) were selective for Cdc42 (Kwofie and Skowronski 2008; Kulkarni et al. 2011; Côté and Vuori 2002; Meller et al. 2002b). In case of PDGF-BB stimulated fibroblasts probably Dock family of GEFs such as Dock9 and Dock11 activate Cdc42 and localize Cdc42 at membrane site that faces chemoattractant. Active Cdc42 can bind and activate formin and mediate formation of filopodia. In the absence of Cdc42, these GEFs are probably still activated, but cannot recruit and activate Cdc42 in MEFs. To test if the interaction between Dock proteins and Cdc42 exists in MEFs a pulldown assay could be performed after stimulation of Cdc42 (fl/-) cells with PDGF-BB. Dock proteins could be precipitated using immobilized Cdc42 or Rac GTPases and analyzed in western blot. Furthermore, siRNA experiments to knockdown the Dock 9 and Dock 11 can be performed to test if cells show similar to Cdc42 knockout phenotype regarding the loss of CRs and reduced number of filopodia in affected cells.

As a consequence of enrichment of PIPs and activation of GEFs at the cell membrane section that faces chemoattractant, Cdc42 and Rac are recruited and activated at these sites. In a further step actin nucleators such as Arp2/3 complex, VASP and formins are recruited and initiate actin polymerization. This leads to the formation of filopodia and lamellipodia and emergence of the leading edge of a cell. Rho is mostly localized to the sites where cell retraction takes place. In this manner Cdc42 and Rac orchestrate protrusion and Rho regulates retraction of a cell during its movements (Hall 1998; J. F. Cote and Vuori 2007). Cdc42 and Rac mediated recruitment of actin nucleators such as Arp2/3 complex, formins, and VASP leads probably to the recruitment of G-

actin pool at the cell membrane and nucleation of G-actin to F-actin thereby removing the G-actin form the polymerization reaction.

How does the knockout of *Cdc42* affect chemotaxis of cells? The Tip nucleation model suggests that filopodia that are formed downstream of Cdc42 are probably induced and elongated by formin that is activated by active Cdc42 at the cell membrane (Mellor 2010a). In Cdc42 knockout cells, Cdc42 specific GEFs cannot encounter and recruit Cdc42 at the membrane loci that faces chemoattractant. Thus appropriate formin cannot be activated at these sites. Therefore, less filopodia are produced at loci where cell faces chemoattractant, whereas Rac1 can be still activated and induce lamellipodia formation. The absence of Cdc42 activated formins leads to fewer filopodia and accordingly less protrusion force at these sites. Therefore, PDGF-BB mediated activation of Rac1, and thus Arp2/3 complex is probably not enough to generate sufficient protrusion (or protrusive force generated within lamellipodia) to form stable and persistent leading edge. Therefore, cell loses its ability to follow PDGF-BB gradient efficiently. In support of this the recent study showed that formins play an important role in force generation during protrusion of lamellipodia (Kage et al. 2017a).

Supposedly, lamellipodia and filopodia, both induced and localized at membrane site that faces chemoattractant by Rac1 and Cdc42 respectively, are essential for chemotaxis towards PDGF-BB. When Cdc42 is not available in cells, there are consequently insufficient filopodia produced to form a leading edge that can persist over time. It is likely that Cdc42 knockout cells move in Rac1 dependent manner which accounts for approx. 80 % of cell velocity whereas Cdc42 activity probably provides approx. 20 % of cell velocity on 2D. Nonetheless, formins can be activated also by other Cdc42 subfamily members. These processes cumulatively contribute to cell migration without Cdc42. However, in absence of Cdc42 formins are not activated at the specific loci where Cdc42 would usually locate these in response to PDGF-BB to induce the formation of filopodia. It can be speculated that the correct localization of Cdc42 is a prerequisite to direct specific formin (s) to the leading edge during chemotaxis. In case of availability of Cdc42, filopodia are formed at these sites probably in higher intensity than at other loci, so the cell consequently protrudes with more force at sites where it faces chemoattractant compared to rest of cell periphery. In this way cell movement probably can be directed to the chemoattractant.

In this study for the first time cell migration of large number of Cdc42 (-/-) MEFs was studied in a 2D chemotaxis assay using PDGF-BB. Additionally to migration analysis the actin based protrusions of Cdc42 deficient cells were assessed to identify possible link between loss of Cdc42 and formation of actin-based protrusions and the effect on cell migration. This link is probably the reduced the formation of filopodia, caused by defective activation of formins by Cdc42 which supposedly leads to loss of chemotaxis towards PDGF-BB in MEFs.

4.1.5 Knockdown of fascin leads to reduced CDR-and filopodia formation

The activation of fascin by phosphorylation leads to fascin mediated actin filament bundling (Yamakita et al. 1996; J C Adams et al. 1999). Besides formins, fascin is suggested to be essential for the formation of filopodia. Downregulation of this protein by RNAi leads to reduced numbers of filopodia in B16 melanoma cells to approx. of 25% of that of wildtype cells. Expression of constitutively active dephosphorylated fascin (S39A) coincided with markedly increased number and length of filopodia, whereas the expression of inactive, a phosphorylated mutant of fascin (S39E) reduced filopodia frequency per cell 2.5 fold. Thus, it was proposed that fascin is a specific actin cross-linker in filopodia providing the stiffness of these structures. The shRNA constructs were designed by D. Vignjevic and colleagues to achieve the knockdown of fascin. Fascin shRNA-Th construct, bearing two base pair mismatches to mouse specific Tm-construct, targets human *fascin1* and serves as a negative control in MEFs. Fascin shRNA-Tm construct targets mouse *fascin1* whereas Fascin shRNA-Tc targets conserved sequence in human and mouse f*ascin1* (Danijela Vignjevic et al. 2006a).

In the present work, the knockdown of fascin in MEFs was achieved by transfecting cells with the shRNA-Tc construct. The shRNA-Tc construct was slightly effective than shRNA-Tm construct in knockdown of fascin in B16 cells from the previous study. Moreover, the transfection efficiency of MEFs with shRNA-Tc construct was higher than that of shRNA-Tm construct in the present study. The treatment of MEFs with shRNA-Tc construct led to approx. 50 % decreased the formation of CDRs whereas shRNA-Th which was specific to human *fascin1* showed no effect on the formation of CDRs (Figure 15). Furthermore, downregulation of *fascin1* led to

approx. 50 % decrease in the formation of filopodia in MEFs which is in line with the previous study that showed 25 % decrease in filopodia numbers in treated cells (D. Vignjevic 2006). Present study shows the similar tendency of the shRNA-Tc construct being effective in reducing filopodia numbers per cell compared with the study done by D.Vignjevic and colleagues. The variation in effectivity of filopdia suppresstion between both studies is probably due to different cell lines utilized in the mentioned study and in the present work. B16 cells that were used in the pervious study are highly aggressive cancer cells that show increased motility and increased filopodia formation than non-cancer cell lines. Therefore, these cells have probably more mechanisms available to support (over)production of filopodia. Thus, higher amount of fascin specific shRNA is needed to achieve higher rates of filopodia suppression in B16 cells as shown in MEFs form this study. The reduction of CDRs and filopodia numbers due to fascin RNAi is in line with results obtained from Cdc42 knockout MEFs and MEFs treated with smiFH2 that show similar effects on the formation of these structures (Figure 17,18; Figure 19; Figure 20). Suppression of filopodia apparently leads to the defective formation of CDRs indicating that filopodia are essential for formation these structures.

4.1.6 Effect of formin inhibition in MEFs

Formins are, besides Arp2/3 complex, the major nucleators of actin filaments during formation of actin-based protrusions in mammalian cells (Schönichen and Geyer 2010; Seth, Otomo, and Rosen 2006). Rho GTPases activate formins, which nucleate unbranched actin filaments that are found in protrusions such as filopodia or invadopodia (Mellor 2010b; Lizárraga, Poincloux, Romão, et al. 2009). However, recent work form our lab showed that also PDGF-BB induced circular dorsal ruffles in MEFs are enriched in filopodia. Further, it was shown that Cdc42 is essential for the formation of CDRs independent form active Rac1 in MEFs. In line with this, the knockdown of fascin, which as an actin-bundling protein important for the formation of filopodia, performed in present and previous works form our lab, led to the loss of CDRs reminiscent that of Cdc42 knockout phenotype in MEFs (Figure 15).

In this work Cdc42 (-/-) MEFs show slightly, but significantly reduced numbers of filopodia and loss of CDR formation in response to PDGF-BB. In line with previous findings, in present work Cdc42 (-/-) MEFs showed normal formation of lamellipodia. This supports the assumption that Rac1 and Cdc42 activate distinct actin nucleators such as Arp2/3 complex and formins respectivly. The activation of distinct nucleators leads to formation of branched network in lamellipodia by Arp2/3 complex and formation of unbranched filaments by formins within protrusions such as filopodia or invadopodia, respectively (Steffen et al. 2004a; Le Clainche and Carlier 2008b). The fact that activated Cdc42 induces filopodia in cells (Allen et al. 1998) and filopodia being enriched in CDRs together with finding that loss of either fascin or Cdc42 leads to loss of CDRs, suggest that probably filopodia that are induced downstream of activated Cdc42 are essential components in formation of CDRs. Therefore, it may be possible that loss of CDRs in Cdc42 (-/-) MEFs is due to defective signaling downstream of PDGF receptor and Cdc42 GTPase. One of two majorly supported mechanisms of formation of filopodia involves formins that can be activated by active Cdc42 and nucleate actin at the tip of these structures (J. Block et al. 2008; Lammers et al. 2008; Kühn and Geyer 2014; M Evangelista 1997). Consequently, the inactivation of formins in MEFs should lead to comparable effects that were observed on filopodia of Cdc42 knockout MEFs. To test this, cells were treated with formin inhibitor smiFH2 and assessed if inhibition of formins leads to similar effects on filopodia and cytoskeleton in MEFs as it was observed for Cdc42 (-/-) cells.

The formin inhibitor smiFH2 effectivly inhibits formins from diverse organisms possibly by targeting concerved FH2 domain and thereby decreasing the affinity of formins to barebed ends of actin filaments. This results in loss of ability of formins to polymerize unbranched actin filaments. 3T3 fibroblasts showed initially reduced stress fibres when treated with smiFH2. Furthermore, affected cells showed 50% reduced velocity during 2D migration. However, the binding of smiFH2 to formins is reversible, and the molecule appears to undergo cellular brakedown after several hours (S. A. Rizvi et al. 2009). Therefore, some of the smiFH2 treated cells show recovery from the effects caused by appilcation of this inibitor or they switch to blebbing based motility if this mechanism is available. Inhibitor smiFH2 shows selectivity towards distinct formin subtypes. Reportadly, treatment of cells with smiFH2 led to selective

downregulation of mDia2, but not mDia1 or mDia3 in MEFs and cancer cells (Isogai, Kammen, and Innocenti 2015).

In this work, treatment of MEFs with increasing doses (0-15 µM) of smiFH2 resulted in dose dependent decrease of CDR formation, but not of lamellipdoia (Figure 19 (b)). The highest dose applied to cells (15 µM) reduced the ability of MEFs to prodcue CDRs to 5 % of control cells. As a working solution for MEFs, 10µM smiFH2 was applied, because at this concentration of smiFH2 MEFs showed reduced filopodia and were still viable. The induction of Cdc42 knockout phenotype in Cdc42 (fl/-) cells by treatmenot of cells with smiFH2 indicates that formins probably act downstream of Cdc42 being the nucleators of actin flaments, such as filopodia in CDRs. Reminicent of Cdc42 knockout cells, cells treated with smiFH2 formed less spiky leading edges than control cells. The quantification of filopodia per cell revealed that number of filopodia per cell was approx. 80 % reduced in smiFH2 tereated cells (Figure 18). This indicates that formins are essentailly involved in the formation of filopdoia in MEFs. However, the effect of 10 µM smiFH2 on the formation of CDRs and especially on the formation of filopodia was more profound than the effect of Cdc42 removal in MEFs. This is probably because in case of smiFH2 treatment also the subfamily members of Cdc42 cannot be used to activate smiFH2 bound formins leading to more efficient suppression of formation of filopodia compared to Cdc42 removal. In this case apparently the activity of VASP can not compensate the formin mediated formation of filopodia. In turn, in Cdc42 (-/-) MEFs probably causes formins that are usually specifically activated by Cdc42 remain inactive leading to reduced filopodia numbers and markdly reduced CDR formation.

Interstingly, MEFs treated with smiFH2 showed 40%-60% reduced polarity in response to PDGF-BB stimulus compared to control, reminicent of Cdc42 knockout MEFs and other reports showing reduced polarity in cells caused by depletion of Cdc42 (C D Nobes and Hall 1999; Stramer et al. 2005b; Lämmermann et al. 2009). The reduced polarity in Cdc42 knockout cells could be probably due to the lost ability of afftected cells to activate distinct formins that lead to the formation of protruisons such as filopodia towards the source of chemoattractant. However, activated formins are still recruited to the leading edge in the absence of active Cdc42 (Jennifer Block et al. 2012; Kühn et al. 2015). Nevertheless, under such circumstances, formins are not distributed in a polar manner, but are rather spread all over the cells egde leading to a non-polar

formation of protrusions. Therefore, active Cdc42 probably both, activates and directs formins to specific sites via GEFs to the indcue formation of polarized protruisons leading to polariation of the cell. A possible experiment to test this would be generation of formin knockdown or knockout cells and assessing their ability to polarize towards PDGF-BB gradient. Furthermore, it would be interesting to test if re-expressed or microijected const. active formin shows polarized distribution in Cdc42 knockout MEFs when these are confronted with PDGF-BB gradient.

The role of formins in cell polarity is majorly discussed regarding their function in controlling the spacial orientation of Golgi apparatus and microtubuli towards the leading edge during cell migration. This reorientaton of Golgi and microtubuli is reportadly also an important process during cell polarisation (Sandrine Etienne-Manneville 2004). However, the role of filopodia or other actin-based protruions in developing of cell polarity is less understood. Of note, it is likely that filopodia and lamellipodia are formed as an earlier response to chemtical cue than the reorientation of Golgi or microtubuli network is achieved (Czuchra, Wu, Meyer, van Hengel, et al. 2005). This issue can be adressed by stimulating MEFs with PDGF-BB and monitoring these processes simultaneously in live cell imaging experiments. Actin protruisons, Golgi and microtubuli can be simulataniously co stained within a same cell. On the other hand, after several timepoints, cells can be fixed, and Golgi and microtubuli orientation can be assassed and compared to filopdia and lamellipodia orientation towards chemoattractant.

Taken together this work shows for the first time that the inhibition of formins by smiFH2 has a profound negative effect on the formation of filopodia and CDRs in MEFs, which is reminiscent of the Cdc42 knockout phenotype of MEFs regadring formation these strucktures. This corroborates the existance of the signaling axis from PDGF receptor to active Cdc42 and formins leading to the formation of filopodia and CDRs in reponce to PDGF.

However, which formins, out of fifteen known mammalian isoforms are activated in response to PDGF-BB downstream of Cdc42 and induce the formation of filopodia? A certain cell type espresses few formins at a time, at least at detectable levels. From these probably one or two subfamily members are involved in the generation of filopodia. Cdc42 reportadly interacts and activates mDia2 (DRF3) in murine ES-derived cells leading to the formation of filopodia. The interaction of mDia2 with Cdc42 probably faciliates localization of mDia2 at tips of filopodia (Peng et al. 2003; J. Block et al. 2008). However, also Rac1 besides Cdc42 was reported to

activate mDia2 (Lammers et al. 2008). Furthermore, DRFs were reportadly localised at tips of filopodia and lamellipodia and involved in the formation of these stucktures, whereas activated DRFs induce the formation of filopodia (Peng et al. 2003; Pellegrin and Mellor 2005; J. Block et al. 2008; Pruyne et al. 2007). This filopodia-rich phenotype of cells is reminiscent of overexpression of activated Cdc42 in many cell types and supports signaling axis form Cdc42 to formins leading to the formation of filopodia. Of note, proteins harbouring SH3-domains such as tyrosine kinases can interact with DRFs. This trait probably could also link DRFs with PDGF receptor signalling (Young and Copeland 2010b).

Another subfamily of formins that is a downstream target of Cdc42 GTPase is FMNL. FMNL2 was shown to be upregulated compared to FMNL1 or FMNL3 in murine fibroblasts. Whereas, in same cells, mDia2 was not expressed at detectable levels. Cdc42 was reported to interact and activate FMNL2 *in vivo* which led to translocation of FMNL2 form cytoplasm to the cell periphery (Steffen et al. 2006). Moreover, FMNL2 was reported to be activated by Cdc42 leading to the formation of filopodia and lamellipodia during cell migration (Jennifer Block et al. 2012). Also, being activated downstream of Cdc42, FMNL2 and FMNL3 were reportadly essential for the force generation in lamellipdoia during protrusion of this struckture (Kühn et al. 2015; Kage et al. 2017a). Supportive of the role for FMNLs in the formation of protruisons, the activation of these proteins leads to relocation of FMNL from the cytoplasm to cell the cell membrane and to phagoyctic cups (Steffen et al. 2006; Seth, Otomo, and Rosen 2006). Furthermore, the activation event itself is apparnetly enough for the translocation of FMNL2 to the cell memnrane (Jennifer Block et al. 2012).

Based on these data probably formins of DRF- and FMNL families such as mDia2 (DRF3) and FMNL2/3 are involved in the formation of filopodia downstream of Cdc42 in several cell types. Furthermore, DRF and FMNL formins are also utilized by cancer cells to form protrusions. In line with this, B16 mouse melanoma cell line siRNA mediated depletion of FMNL2, which is activated downstream of Cdc42, led to reduced protusion rates of lamellipodia and slightly reduced cell velocities in affected cells (Jennifer Block et al. 2012). In MDA-MB-231 cells downregulation of one of DRF (DRF1-3) family formins led to decreased of invadpodia and matrix dergadation (Sakurai-Yageta et al. 2008).

However, which formins are expressed in a certain cell line and are involved in the formation of filopodia in these cells is most likly dependent on idividual cell type. To adress this issue for MEFs or generally other cell types it has to be assessed which of fifteen mammalian formins are expressed in these cells. Form there it can be tested which of expressed formins are involved in fomation of filopodia. This can be achieved by tagging of formin with GFP or other flourescent proteins to visualize their cellular localisation.

4.1.7 Software based docking of smiFH2 with FH2 domain of formin

The binding of smiFH2 to formins is supposedly achieved by reversible attachement of smiFH2 to the FH2 domain of formins (S. A. Rizvi et al. 2009). For a better understanding of this interaction, I perforemd software based docking (SwissDock website) of smiFH2 to the FH2 domain of FMNL3, the cristal struckture of which was already avalabile (Thompson et al. 2012a). Form the strucktural data of FMNL3-actin complex I choosed the 401AA chain, which contains the FH2 domain of this formin, for the sofware docking expriment. The docking analsys showed that most likly smiFH2 binds to an a-helix within the FH2 domain of FMNL3 which is located between Met766 and Met777 (s. suppl. Data). On the other hand, it is also possible that smiFH2 is captured between two a-helices that are located opposite of each other (Met 766 –Met 777 and Leu 790-Leu 795) within the FH2 domain. The proposed binding region of smiFH2 to the FH2 domain of FMNL3 is termed as post region of formin and is rerpotadly improtant for dimerisation of fromin (Thompson et al. 2012b). Therefore, the interaction of smiFH2 with an FH2 domain of formin probably interfers the dimerisation of formins and thereby the binding of formin dimer to the barbed end of the actin filament.

To gain more persice data about how smiFH2 inhibits activity of formins it could be investigated if incubation of smiFH2 with formins disrupts the dimerisation of FMNLs. This probably can be analysed by coimmunoprecipitation of smiFH2 treated formins and/or isothermic calorimerty of formin / smiFH2 interation. In cytoplasm, inactive formins are present in soluble form. Binding of Cdc42 to CRIB doamin of formins leads to unfolding of formin and revieling of its hydrphobic regions. This probably leads to transition of formin to insoluble form, which might faciliate its

reqruitment to the cell membrane (Gorelik et al. 2011). Thus, formins are apparnetly soluble in an inactive conformation under physiological conditions. Probably, in an inactive state no dimerisation of formins occures. However, constitutivly activated formins probably form dimers. Thus the const. activated formins (with deleted DAD domains) can be reesxpressed and purified. When recostituted in physiological buffers they probably form activated dimers. These putative dimers can be in next step pretreated with smiFH2 and subjected to a size exlucion chromatography to detect whether dimerisation of formins is affected by pretreatement with smiFH2. If so, the transition from a dimeric to monomeric form can be visible in form of UV-peak that is eluted at markdly later timepoints than UV-peak representing dimeric proteins.

4.1.8 Inhibition of formins in a wound healing assay

The formation of protrusions is one of three basic steps of cell migration on 2D substrates together with adhesion and cell retraction. As shown above, the inhibition of formins by smiFH2 almost diminished CDR formation and drastically decreased the filopodia numbers per cell in Cdc42 (fl/-) MEFs (Figure 18; Figure 19). To date, there is a relativly sparse amount of data avalable on effects of smiFH2 on cell migration. Stil, initial studies utilizing 10µM smiFH2 report 50% reduced cell velocity in 3T3 fibroblasts and the switch to blebbing associated cell migrtaion in a subpopulation of treated cells (S. A. Rizvi et al. 2009). However, another study using comparable conditions reproted increased velocity of osteosarcoma cells after treatment with smiFH2, despite defects in stress fibre formation, microtubuli network- and golgi apparatus organisation of smiFH2 treated cells (Isogai, Kammen, and Innocenti 2015). This indicates that those organells or stress fibres are not essential in maintaining the velocity of cell migration, at least in utilized cancer cell type. Another report showed that in a wound healing assay, velocity of glioblastoma cells is not affected, but persistance of migration (directionality) is drastically reduced. This result was reminiscent of siRNA mediated downregulation of mDia1 or mDia2 in these cells, indicating that these formins are involved in diectional sensing during migraton of cells (Arden et al. 2015b).

To test if the loss of filopodia and CDRs by the inhibition of formins has a similar effect on velocity as loss of Cdc42 in MEFs the wound healing assay of MEFs using smiFH2 was performed (Figure 21). In this work, the wound healing assay was the most robust assay, from tested 2D migration assays where smiFH2 treated cells could survive on the microscope stage conditions for long periods of time (>8h). Interestingly, smiFH2 had no significant effect on velocity or directness of Cdc42 (fl/-) or Cdc42 (-/-) MEFs in a wound healing assay. This could be explained due to higher density of cells in this assay compared to previous 2D migration assays form this work (Figure 12; Figure 14). Therefore, for the future wound healing experiments the concentration of smiFH2 should be adjusted to high cell density in this assay to achieve the effects on cytoskeleton that were shown in previous chapters.

The different responses of cells to smiFH2 treatment and thereby caused inhibition of formins probably reflects their ability to use different migratory mechanisms. Cancer cells can reportedly switch between different migration strategies (Katarina Wolf et al. 2003). Therefore, these cells probably switch to blebbing based motility when treated with smiFH2. In case of fibroblasts, smiFH2 treatment leads to reduced filopodia formation, which also reportedly reduces the protrusion rate and force which is generated within lamellipodia (Kage et al. 2017b). These cells are probably less efficient in blebbing based motility compared to cancer cells and thus show reduced motility as this was shown in smiFH2 treated 3T3 fibroblasts (S. A. Rizvi et al. 2009).

Still there are more studies needed to address the issue of different responses of cells to smiFH2 regarding their migratory behavior. Probably the comparative analysis of cancer cells vs. fibroblasts, using similar conditions, would give a better picture of this issue. It would be interesting to test how various cancer cells- or cancers cells *vs.* fibroblasts differ in responses to smiFH2 and which of these cell types can switch migration modes. This might represent important data for understanding behavior metastatic cancers, because in this stage cancer cells are highly motile and are often very resistant to typical chemotherapy treatments that usually target DNA and induce apoptosis (Hanahan and Weinberg 2011).

4.1.9 MEFs cannot degrade ECM effectively

Cells interact with ECM in numerous ways. In cultured cells, this interaction is typically visible by adhesion of cells to- and/or degradation of the ECM. Cell adhesion can be accomplished by macromolecular F-actin-rich structures such as focal adhesions or podosomes. Podosomes can additionally degrade ECM, whereas focal adhesions usually don't. Fibroblasts reportedly don't form podosomes, but can form podosome related invadopodia which are known as degradative actin-based protrusions in cancer cells (W. -T Chen 1989). Besides their essential role in the formation of filopodia, formins are most likely involved in assambly of invadopodia (Schoumacher, Louvard, and Vignjevic 2011; Lizárraga, Poincloux, Romão, et al. 2009; Young and Copeland 2010b). Additionally, some reports also indicate the involvement of formins in formation/turnover of focal adhesions (Dettenhofer, Zhou, and Leder 2008; Gupton et al. 2007; Young and Copeland 2010b). However, a clear evidence of the involvement of formins in formation of focal adhesions is still missing.

In present work Cdc42 knockout MEFs and smiFH2 treated control MEFs both showed a reduced rate of the formation of filopodia and reduced velocity in migration assays. Decreased filopodia formation in Cdc42 knockout or smiFH2 treated cells was probably due to decreased activity of formins and was assumingly the reason of reduced velocity of MEFs in migration assays. However, because of the putative role of formins in nucleation of F-actin during adhesion formation, adhesions could also be affected in smiFH2 treated cells, which also can lead to defective migration. To study putative effects of smiFH2 on focal adhesions and/or invadopodia, adhesion and degradation assays were performed and analyzed.

On the other hand, this work compares interaction of MEFs and HT1080 with ECM in adhesion and matrix degradation assays. This way cell-matrix interaction of highly invasive HT1080 cells versus non-invasive MEFs can be assessed to identify possible requirements for effective migration on 2D and in 3D ECM.

In adhesion assay both cell types (MEFs and HT1080) showed similar adhesion pattern when treated with smiFH2 or GM6001 (Figure 22; Figure 42). Whereas the treatment of cells with

MMP inhibitor GM6001 had no significant effect on adhesion, in smiFH2 treated cells number of adhered cells was decreased in both cell types.

In degradation assay, however, MEFs and HT1080 cells showed different behaviors (Figure 24; Figure 41). Compared to HT1080 cells MEFs did not degrade FITC-gelatin at significant levels and showed no signs of matrix degradation, such as the presence of typical non-fluorescent areas beneath cells. Additionally, no actin dot-like structures where could be observed in these cells which corroborates this assumption and thus GM6001 had no effect on matrix degradation in these cells. HT1080 cells, on the other hand, degraded FITC-gelatin and showed drastic sensitivity to GM6001 by seizing their degradative activity (Figure 40; 41).

Because MEFs used in this work do not form invadopodia, adhesive structures that hypothetically could be affected by smiFH2 treatment are focal contacts / focal adhesions (Gupton et al. 2007; Young and Copeland 2010b). Therefore, smiFH2 induced defective adhesion to ECM in MEFs can be assigned to defective formation of adhesive structures in smiFH2 treated cells. However, previously it has been shown that filopodia were also important in the process of initial adhesion and spreading of cells to the substrate (Partridge and Marcantonio 2006). Furthermore, filopodia were shown to mediate spreading of Rac (-/-) cells on 2D substrates (Steffen, Ladwein, Dimchev, Hein, Schwenkmezger, Arens, Ladwein, Margit Holleboom, et al. 2013).

To fully adhere to substrate cells need to contact, spread and form focal adhesions to substrate. This implies that adhesion and spreading of the cell on the substrate are essential for completion of the cell to substrate adhesion. Adhesion in MEFs is accomplished by focal contacts that further can evolve to focal adhesions. Spreading is accomplished by the formation of actin-based protrusions such as lamellipodia and filopodia.

Of note, the adhesion of a cell to the substrate involves initial adhesion of cell, followed by spreading of the cell on the substrate. By spreading on the 2D surface, the cell increases its contact area to a substrate which then facilitates the formation of more adhesions and thus leads to firm attachment of the cell to the substrate. The spreading of cells to the 2D substrate is reminiscent of cell migration and requires protrusions, thus formation of filopodia and lamellipodia. Consequently, by inhibition of formins and thereby filopodia by smiFH2, cell spreading is likely to be negatively affected regarding effectivity of this process. Therefore, during spreading cell

protrusion rate could be similarly affected. This can lead to less contact area of cells to substrate in given time of adhesion assay (see Methods) and therefore less adhesiveness than the non-treated cells. Thus, the washing step after adhesion assay could wash away more of cells that are not fully spread on the substrate which apparently is the case in smiFH2 treated cells. So the inhibitory effect of smiFH2 on the formation of filopodia and thus cell spreading could be the reason for the defective cell to substrate adhesion.

In further experiments the smiFH2 treated cells, and a control group could be stained for adhesion protein vinculin and F-actin to visualize the actin content in adhesions. If formins are involved in adhesion formation and sensitive to smiFH2, treated cells would show less F-actin in adhesions. Given the focal adhesions show less F-actin content in adhesion sites this would suggest that formins are indeed involved in the formation of adhesions and at least partly contribute in the cell to substrate adhesion this way. Furthermore, the diameter or perimeter of spread cells could be monitored for determination of spreading behaviors of treated versus control cells.

4.1.10 Protrusions and chemotaxis in Hem1 knockout macrophages

The Rac- and WAVE mediated activation of Arp2/3 complex is thought to represent the main signaling axis leading to the formation of lamellipodia in many cell types including cells from the hematopoietic lineage. In neutrophils, activation of Rac1 leads to the formation of a protein complex including WAVE2, Hem1 and Abi1, which activates Arp2/3 complex leading to formation of actin-based protrusions (Weiner et al. 2006; Kheir et al. 2005). On the other hand, activated Cdc42 can activate WASP, which is thought to induce the Arp2/3 complex-dependent formation of podosomes in hematopoietic cells (Jones et al. 2002b; Thrasher et al. 2000).

The video microscopy-based analysis of chemotaxis of macrophages from WAS patients towards CSF-1 revealed impaired chemotaxis in this cells, expressed by haphazard cell trajectories. Furthermore, these cells were not able to form podosomes (Jones et al. 2002b). Studies on Hem1 deficient neutrophils revealed defective polarization of these cells and approx. up to 80 % reduced chemotaxis towards fMLP in a transwell assay (Heon Park et al. 2008c; Weiner et al. 2006).

In this work I analyzed whether the removal of Hem1 affects the formation of lamellipodia or other actin protrusions and how this affects chemotaxis of mouse BM-derived macrophages towards chemoattractant C5a. The results of Hem1 KO macrophages were compared to that of Wasp KO cells.

Due to western blot analysis the constituents of WAVE-complex are degraded in Hem1 deficient neutrophils and T-lymphocytes (Heon Park et al. 2008a). Unpublished data from our group also suggest partial degradation of WAVE-complex in Hem1 knockout BM-derived macrophages. The present work shows that Hem1 KO macrophages lack lamellipodia (Figure 25b; Figure 26). Supposedly, the presence of WAVE-complex is a prerequisite for recruitment of Arp2/3 complex at the leading edge and subsequent formation of lamellipodia**.**

Moreover, Hem1-null macrophages were shown to form podosomes that contained vinculin and F-actin (Figure 25a, kindly provided by David de Gorter). Whereas podosomes are formed in Hem1-null cells, their formation is severely affected in Wasp KO cells. This is supportive of the different regulation of Arp2/3 complex by WASP and WAVE –complexes and their non-redundant function considering the activation of Arp2/3 in hematopoietic cells. Podosomes were majorly detected at the leading edge of Hem1-null macrophages in contrast to WT cells, where these structures are distributed in the central region of cells. (Figure 25; Figure 26). Furthermore, in Wasp-deficient macrophages, number of podosomes per cell was markedly decreased (unpublished observation) which is in line with prior reports (Jones et al. 2002a). Probably, WASP is targeted explicitly to podosomes when activated, whereas activated WAVE relocates to tips of lamellipodia. The open, activated conformations of these proteins apparently reveal motifs that target them to specific cellular locations.

Reportedly, lamellipodia are formed exclusively downstream of WAVE complex (T. Stradal et al. 2001b; Small et al. 2002a; Steffen et al. 2004b). In line with this, Hem1 knockout macrophages cannot form lamellipodia when stimulated with C5a (Figure 26). Moreover, in contrast to WT cells, Wasp- and Hem1 KO cells, both showed severely impaired chemotaxis and directionality towards C5a in 2D chemotaxis assays (Figure 27). This is in line with previous results regarding the chemotaxis of Hem1 deficient neutrophils towards fMLP in a transwell assay (Heon

Park et al. 2008b), or 2D chemotaxis of macrophages from WAS patients towards CSF1 in a direct viewing chamber (Jones et al. 2002b). These results support that two distinct (Wave- and Wasp-dependent) mechanisms of Arp2/3 complex activation cannot compensate each other in chemotaxis to C5a. However, supposedly, coordinated activation of Arp2/3, by WAVE and WASP together, is essential for an effective chemotactic response (Rougerie 2013), which is apparently also true for chemotaxis of macrophage towards C5a.

Furthermore, in the present work the Hem1 KO macrophages did not show decreased cell velocity besides decreased chemotaxis (FMI and directionality). In contrast, in Wasp KO macrophages both, velocity and chemotaxis (FMI and directionality) were reduced. Thus, possibly in Wasp KO cells, overall cell motility, including cell velocity and chemotaxis, was severely impaired, whereas in Hem1 KO cells chemotaxis was diminished, but cells were able to migrate at almost same speed as WT macrophages (Figure 26). Therefore, it is tempting to speculate that Hem1 is more specifically involved in chemotaxis towards C5a than WASP in macrophages. This putative specific impact of the loss of Hem1 on macrophage chemotaxis would indicate the importance of activation of Arp2/3 complex by WAVE and subsequent formation of lamellipodia to achieve the efficient chemotaxis towards C5a. The formation of oversized filopodia in Hem1 KO cells is probably caused by the effort to compensate the loss of lamellipodia (or Arp2/3 mediated protrusion) using formin-mediated protrusions (Figure 25b; Figure 26). In this case apparently formins are the most dominant nucleating machines at the leading edge of macrophages whereas Arp2/3 complex is not able to compete for actin nucleation. Therefore, the majority of G-actin subunits are captured and polymerized by formins at the leading edge, and this may contribute to the formation of oversized filopodia in affected cells. Formin-mediated formation of protrusions, supported by normal podosome formation, probably enables Hem1 KO cells to move with comparable velocity as WT cells. The Presence of intact WASP enables the formation of podosomes in Hem1 KO cells. Therefore, the formation of podosomes and cell adhesion are probably not affected in these cells.

Hem1 KO cells lack functional WAVE complex and thus cannot target Arp2/3 complex to the leading edge to form lamellipodia. Surprisingly these cells did not show reduced velocity in the chemotaxis assay (Figure 27c). On the other hand, Wasp KO macrophages show reduced velocity

additionally to their lost ability to form podosomes. Furthermore, these cells can still form filopodia and lamellipodia (unpublished data). So, WASP is in some way involved in the generation of cell speed, perhaps as a result of WASP-mediated formation of podosomes, but this needs still to be corroborated. The essential role of WASP in cell speed could explain why Hem1 knockout cells (which still express WASP) don't show reduced cell velocity *vs.* WT cells. Alternatively, the formin-mediated formation of filopodia could compensate the potential loss of velocity in the Hem1-null cells. The observation of over-proportionally long filopodia in Hem1-null *vs.* WT- and Wasp-null cells supports this assumption. The severe chemotaxis defect in Hem1-null macrophages can also be explained by lack of gradient sensing mechanism which is provided by lamellipodia besides its protrusive role.

Further experiments could address the inhibition of formation of lamellipodia by inhibitors of Arp2/3 complex such as CK-666 and assessment of chemotactic performance of wildtype BM-derived macrophages towards C5a. Furthermore, it is also interesting to test how formin depletion or inhibition affects the migration of Hem1 KO macrophages. In this case the effect formin inhibitor smiFH2 could be assessed in chemotaxis and formation of filopodia in these cells. In this manner the effect of putative compensatory mechanism, to loss of *Hem1* and lamellipodia on migration, by formin mediated induction of filopodia could be estimated.

4.1.11 Protrusions and chemotaxis in Wasp knockout macrophages

The Wasp KO macrophages showed defects in adhesion on glass and plastic 2D surfaces and couldn't form podosomes as effectively as WT- and Hem1 KO cells did (unpublished observation). Although, Wasp KO cells could still develop lamellipodia in contrast to Hem1 KO macrophages. Wasp KO cells showed markedly reduced velocity compared to WT and Hem1 KO cells. It is possible that the reduced adhesion is caused by the lost ability to form podosomes as the consequence of *Wasp* knockout. Adhesions have to form beneath protrusions to perform chemotaxis efficiently on 2D, which is apparently impaired in Wasp KO cells. This adhesion defect probably is responsible for loss of velocity and reduced FMI in these cells. Reportedly, the absence of

WASP leads to the defective formation of podosomes and probably impaired adhesion of leading edge in macrophages on 2D (Monypenny et al. 2011).

In the present work Wasp KO BM macrophages showed severely impaired chemotaxis (Figure 27). However, these cells form morphologically normal filopodia and lamellipodia (not shown). Reportedly, the formation of filopodia does not require WASP or Arp2/3 complex (Faix and Rottner 2006a). Thus, presumably normal formation of lamellipodia and filopodia, which is apparently intact in Wasp KO macrophages, cannot provide efficient chemotaxis towards C5a (Figure 27). Supposedly, formation of filopodia and lamellipodia without support of podosomes, cannot rescue chemotaxis towards C5a in Wasp KO cells. This may point to the important role of podosomes in a full scale chemotactic response of macrophages towards C5a. Assumingly, at least two of actin-based protrusions have to be presented by cells (either lamellipodia or filopodia) together with podosomes for cells to be able to perform chemotaxis on 2D.

The observation of actin puncta reminiscent of podosomes in Wasp KO macrophages was surprising, because the WASP is a specific Arp2/3 activator in hematopoietic cells which is essential for podosome formation. Furthermore, loss of WASP can be only slightly compensated by N-WASP in macrophages (Isaac et al. 2010). In the process of formation of podosomes in macrophages, WASP localizes and activates Arp2/3 complex at the core region of podosome to induce local actin polymerization. Presumably, the WASP activated Arp2/3 complex is recruited by vinculin at podosomes such as in focal adhesions (DeMali, Barlow, and Burridge 2002). This leads to enhanced actin polymerization, strengthening, and maturation of these structures. In Wasp KO cells Arp2/3 complex cannot be recruited and activated at podosomes, so the formation of the core region of podosome can only be performed by formins in these cells. Therefore, the absence of WASP, and thus Arp2/3 complex-mediated actin nucleation, could lead to functional defects in podosomes while the actin-puncta still can be observed. In Wasp KO cells Arp2/3 mediated nucleation in podosomes does not take place and apparently nor N-WASP or WAVE complex seem to be able to compensate it. For a functional test of podosomes, a matrix degradation assay can be considered. On the other hand, staining with anti Arp2/3 monoclonal antibody should show if Arp2/3 complex is localized in podosomes of Wasp KO cells.

Taken together, actin-based protrusions such as lamellipodia and podosomes are both involved in chemotaxis and required for the full chemotactic response of the macrophages to C5a. Depletion of either structure (lamellipodia or podosomes) by genetic knockout of *Hem*1 or *Wasp* in mice results over 50% reduced the effectiveness of chemotaxis in macrophages. This suggests that these both Arp2/3 dependent structures are somehow in concert involved in macrophage chemotaxis on 2D substrates. It is still to determine how exactly these both structures cooperate in chemotaxis. The experiments form this work regarding the motility and formation of actin based protrusions in macrophages from the bone marrow of Hem1 KO mice revealed the critical role of Hem1 in the formation of lamellipodia, but not of podosomes or filopodia (unpublished data).Furthermore, the loss of Hem1 results in the absence of lamellipodia in macrophages. Whereas, removal of WASP selectively affects podosomes in macrophages. Both structures (lamellipodia and podosomes) probably act together in concert during macrophage chemotaxis. Thus removal of either structure results in defective chemotaxis. Probably, lamellipodia provide protrusive and sensory functions whereas podosomes adhere behind lamellipodia and manifest the direction of cell protrusion. This probably provides durability of direction which is essential for chemotaxis.

4.2 3D cell migration

4.2.1 Cell migration in 3D collagen

The cell migration on planar 2D substrates involves cell to substrate adhesion, formation of cell protrusion and retraction of cell body for all studied mammalian cell types so far (Raftopoulou and Hall 2004b). Cell migration in 3D environments is a more complicated process compared to 2D motility, which not necessarily involves cell to substrate adhesion (Katarina Wolf et al. 2003; Renkawitz et al. 2009a; Lämmermann and Sixt 2009). Additionally, some cells have to degrade ECM to pass through matrix pores. Thus, the degradation of ECM by cell surface-bound or secreted degradative enzymes plays a significant role in cell migration when cells are surrounded by the ECM. Furthermore, dependent on cell type, cells can adjust their migratory behavior to their environment by changing their migration mode. This change is often observed in cancer cell

types. These cancer cells can switch between adhesion-dependent and independent modes of migration (Katarina Wolf et al. 2003).
Almost all types of adherent mammalian cells can migrate on 2D *in vitro* surfaces. When the same cells are placed in 3D scaffolds of ECM, they might adopt rounded cell morphology and seize cell migration. Some cell types show rounded morphology and perform blebbing associated movement. Cells that migrate in 3D show different morphology and migratory behavior in contrast to that on 2D surfaces (Even-Ram and Yamada 2005b; Katarina Wolf et al. 2003; Sixt 2012; Petrie and Yamada 2012). Moreover, the actin based protrusions that are produced by cells on 2D are often difficult to visualize in 3D environments (Beningo, Dembo, and Wang 2004; Lakshman et al. 2007).

The cell morphology in 3D is apparently dependent on both, the migration mode of cells and the local architecture of the physical barrier (such as collagen network) that cells encounter (Katarina Wolf and Friedl 2009; Katarina Wolf et al. 2009). Probably cells that move in adhesion-dependent manner in 3D display increased interactions with ECM compared with same cells on 2D substrates. Therefore, during the movement across 3D ECM these cells supposedly encounter higher physical resistance compared with that of on the 2D surface. Moreover, in certain situations cells additionally degrade the ECM. Accordingly, cells adopt different migratory patterns during movement in 3D compared to that on 2D and have to adopt their actin based protrusions to 3D environments. Thus, actin based protrusions in 3D are morphologically different to those formed by cells on 2D sufaces and are often termed as pseudopodia.

4.2.2 HT1080 cells change morphology in 3D

As shown in Figures 28/29 when HT1080 cells are embedded in 3D collagen they change their morphology form flat, spindle-shaped on 2D, to more rounded, cylindrical and wedge-shaped presenting narrow leading edge in 3D. This change of cell morphology probably is due to an adaptation of the cell to the porous architecture of collagen. The narrow leading edge of cells in 3D probably represents the pathfinding process of cells when protrusions are finding their way

through the narrow matrix pores. At a certain stage, the cell body behind protrusion possibly attaches to the substrate (Figure 29 s. supplemental video), and the cell begins to retract its body to a new location. After retraction, the protrusion-adhesion-retraction cycle reinitiates. To visualize protrusions in 3D this typical wedge-shaped and therefore migrating cells were considered to be surrounded by 3D matrix and have no contact with the 2D substrate. The tips of protrusions of such cells were monitored in fluorescence microscopy to study actin-based protrusions (Figure 30). Because of the narrowness of the leading edge of cells in 3D compared to 2D, the protrusions such as lamellipodia and filopodia that are well observable on 2D are probably more tightly packed in a narrow space when cells are embedded in 3D environments. Therefore, these structures are difficult to recognize. Some researchers even question the existence of filopodia and lamellipodia during 3D migration (Beningo, Dembo, and Wang 2004).

Figures 28 and 29 show typical wedge-shaped morphology of cells that migrate in 3D collagen. This morphology is also presented by cells that migrate *in vivo* such as when implanted in the dermis of mice (Katarina Wolf et al. 2003; Katarina Wolf et al. 2007). Thus this wedge-shaped morphology appears to be one of the typical cell morphologies in 3D *in vivo* tissues.

Why do the cells adopt this wedge shape during migration in 3D tissue? Probably because of the leading edge of a cell has to move through narrow pores of the 3D matrix. The leading edge does not need to degrade ECM, because filopodia and lamellipodia are narrow enough to pass through collagen pores of up to 20 µm of 1mg/ml collagen (Helary et al. 2012). However, cells probably need to degrade matrix behind the leading edge so that the cell nucleus can pass through pores of collagen network. Once the gap produced by the degradative activity of cell becomes wide enough, the thicker part of the cell passes through, and the leading edge protrudes ahead. Probably the morphology of cells in 3D is defined by these processes.

4.2.3 HT1080 cells form lamellipodia and filopodia at the leading edge in 3D cell migration

To date, there is no data available showing lamellipodia and filopodia during 3D migration. Some researchers even suggest that these structures as such are not produced by cells in 3D

environments, because of the absence of clear evidence showing these structures during 3D migration. Instead, protrusions formed by cells in 3D ECM are often termed pseudopodia, which are thought to be morphologically and biochemically distinct form lamellipodia and filopodia (Petrie and Yamada 2012) (Giri et al. 2013b) (Beningo, Dembo, and Wang 2004). Another type of actin protrusions termed lobopodia were newly described as actin-based protrusions representative for lamellipodia in dense 3D ECM (Petrie et al. 2012). Due to another report HT1080 cells adhered and degraded ECM posterior the leading edge. Therefore, the leading edge of migrating cells in 3D collagen was classified in regions: anterior pseudopods that are engaged with collagen fibers, followed by an expanding cell body with branched pseudopods and a region of maximal cell diameter behind it (Katarina Wolf et al. 2007). Although, in a study using electron microscopy small lamellipodia-like protrusions were detected at the tips of pseudopodia (Heath and Peachey 1989; Even-Ram and Yamada 2005b). However, still, the existence and contribution of lamellipodia and filopodia in 3D migration are controversially discussed not well understood.

Here I addressed, the existence and formation of typical 2D protrusions such as filopodia and lamellipodia in migration of HT1080 cells in 3D collagen. To assess the typical 3D cell morphology, cells were embedded in a collagen matrix (1 mg/ml). This concentration of collagen represents the approximate physiological collagen concentration of loose connective tissue and should be a close approximation to physiological conditions of these cells. In line with this, HT1080 cells that are injected into loose connective tissue within footpads of mice adopt similar morphology to that of HT1080 cells in gels of 1-1.5mg/ml collagen (Katarina Wolf et al. 2003).

When embedded in a 3D collagen gel, HT1080 cells adopt wedge-shaped morphology presenting a narrow cylindrical leading edge termed pseudopodium (Figure 28). Fluorescence microscopy of the leading edge of phalloidin-stained cells in 3D ECM revealed that the tip of leading edge (or so-called pseudopodia) was enriched with filopodia-like protrusions whereas sheet-like lamellipodia not clearly visible (Figure 30). This supports the work of Heath and colleagues that also detected such structures using electron microscopy (Heath and Peachey 1989; Even-Ram and Yamada 2005b). To elucidate the composition of the leading edge in 3D cells were transfected using the GFP-lifeact construct, which is an established F-actin marker in living cells (Riedl 2010). Transfected cells were embedded in collagen and imaged in live spinning disc confocal microscopy (Figure 31; see supplemental video). The representative cell in the Figure 31 shows

small lamellipodia during protrusion phase which is located between two probably ruffling regions of the leading edge. This lamellipodium is morphologically similar to that produced by cells on 2D surfaces. However, it is markedly narrower than the lamellipodia observed on 2D substrates. The lamellipodia in 3D in Figure 31 is approx. 5µm broad as opposed to broader lamellipodia of cells on 2D substrates that can reach 50 µm in width. The narrow lamellipodia in 3D are possibly due to less space available in 3D *vs.* 2D, for lamellipodia to spread.

Reportedly, treatment of HT-1080 cells with siRNA targeted to Rac1, WAVE2 or Arp2/3 complex can severely affect the tip structure of pseudopodia in these cells. Notably, this treatment led to the shrinking of the lamellipodia-like protrusions, while leaving filopodia-like protrusions and shaft of pseudopodia intact. In glioblastoma cells (U87MG), which are thought to be unable to switch from the mesenchymal to the amoeboid mode of migration, the disruption of the tip-structure of pseudopodia using siRNA constructs against Rac1-3, WAVE2 or Arp3 was accompanied with a marked reduction of the invasive capability of these cells in collagen gels. In contrast, in HT1080 cells, which can switch between migration modes, the depletion of these proteins, one at a time using RNAi, had no significant adverse effect on 3D invasion. Although, these treatments induced shifting of cell morphologies from spindle to more rounded shapes. So by depleting proteins which are essential in formation of lamellipodia cells might switch to adhesion-independent mode of migration. The treatment of cells with ROCK inhibitor Y27632 did not affect the invasion of these cells in 3D. Finally, the combination treatment of ROCK inhibitor together with one of the previous siRNA treatments led to significant reduction of invasion into the collagen gel in HT1080 cells. This probably indicates that ROCK inhibitor suppresses amoeboid migration whereas siRNA that targets mRNA of key proteins in lamellipodia suppresses mesenchymal migration. (Yamazaki, Kurisu, and Takenawa 2009b; Kurisu and Takenawa 2010c).

The spike-like protrusions at the tip of pseudopodium of HT1080 cells in 3D culture were morphologically reminiscent of filopodia form 2D cultures (Figure 30; 32). Moreover, these structures show similar thickness as filopodia of approx. 1µm (Figure 32 b``) as shown in reconstituted image form spinning disc microscopy. Additionally, the dynamics of this finger-like structure resembled of that of filopodia on 2D (see supplemental. video).

VASP is enriched within tips of filopodia and lamellipodia, and its presence at the tip of finger-like protrusions is a marker, which can dissect filopodia from retraction fibers. Besides it polymerase activity, VASP apparently can cluster actin filaments thus enhancing formation of filopodia (Rottner and Stradal 2011b; Rottner et al. 1999b) (Steffen et al. 2006; Y. H. Han et al. 2002; Kwiatkowski et al. 2007). (Breitsprecher et al. 2011).

For further characterization of filopodia-like protrusions in 3D, the localization of GFP-VASP was studied relative to these structures in the present work. As shown in Figure 33 GFP-VASP localizes at the tip of such protrusion of the HT1080 cell in collagen during its protrusion phase. This is solid indication that these protrusion is a filopodium. Moreover, the analysis of migration speed of these cells in 3D collagen suggested that suppression of lamellipodia and filopodia by shRNA of Arp2/3, CDC42, and WAVE1 more efficiently reduced cell speed than targeting of lamellipodia and invadopodia by the treatment of these cells with shRNA of N-WASP, cortactin or with Arp2/3 inhibitor CK636 (Giri et al. 2013a). This also indicates importance of filopodia in 3D migration of HT1080 cells.

4.2.4 The role of dorsal and ventral actin-based protrusions in 3D migration

Besides formation of lamellipodia and filopodia, HT1080 cells also form dorsal and ventral actin protrusions during migration in 3D collagen. The software-based motion tracking of these protrusions revealed that the protrusions are formed almost perpendicular to the direction of cell migration such as in case of formation of invadopodia on 2D. The morphology of these protrusions was somewhat rounded showing lifetime of approx. 10 min which is alike of lifetime of podosomes (Stefan Linder and Kopp 2005) (Figure 34; s. supplemental movie). However, podosomes usually were viewed on 2D substrates and were not assigned to protrusions (Yamaguchi et al. 2005). Reportedly invadopodia show lifetime form several minutes to hours (Li et al. 2010a; Stefan Linder, Wiesner, and Himmel 2011).

The present work shows that GFP-VASP co-localized with F-actin within these dot-like dorsal/ventral protrusions, (Figure 38). However, VASP is localized not at the tip of these structure such as in filopodia (Figure 34), but instead is concentrated short behind the F-actin-rich tip of

the protrusion. Furthermore, VASP does not localize at podosomes. These observations are supportive that these structures are invadopodia (Philippar et al. 2008a). In addition, because of their protrusive nature, similar lifetime as invadopodia and localization of VASP within these structures these dorsal / ventral structures probably are invadopodia. One function of these protrusions in 3D migration could be to anchor the central cell region of the cell during the protrusion of the leading edge and retraction of the rear (Figure 34, s. supplemental movie).

To classify these F-actin dot-like structures as invadopodia in cancer cells, additionally to co-localization of Arp2/3 complex, fascin, and cortactin, matrix degradation by these structures can be addressed (Yamaguchi et al. 2005; Buccione, Orth, and McNiven 2004).

Probably the third distinct type of protrusions in 3D was observed at the dorsal /ventral surface of HT1080 cells which appeared as stationary cells in 3D live confocal microscopy (Figure 36). These protrusions had spiky appearance and showed a markedly higher fluorescence intensity than the rounded protrusions indicating higher F-actin content of these structures compared with rounded protrusions. Furthermore, the spiked dorsal/ventral protrusions were apparently thicker than filopodia and showed fast dynamics of formation compared to rounded dorsal protrusions (Figure 35 a``; b``). Interestingly, this apparently stationary cell as viewed from the top view in live spinning disc confocal microscopy was, in fact, translocating in the vertical direction (Figure 37). This movement became first visible as the ZY scans of the cell were combined into a movie. The formation of spiked protrusions form (Figure 36) coincided with the direction of cell movement (Figure 37a). Based on their dynamics, occurrence and the role, these structures are not defined yet according to state of research form the present work. Therefore, further studies are necessary to dissect and define these structures in more detail.

4.2.5 The degradation of ECM takes place at rear and central regions-, not at the leading edge of cells

During migration in 3D cells show typical wedge shaped morphology. Several publications suggest that cells degrade ECM at, or in the proximity of their leading edge which was reported during migration of macrophages in 3D collagen (Van Goethem et al. 2010; Van Goethem et al.

2011). HT1080 cells behave differently and apparently degrade matrix several microns behind their leading edges and at lateral actin spikes enriched with MMPs during 3D migration (Katarina Wolf et al. 2009). Highly invasive MDA-MB-31 cancer cells reportedly form finger-like actin-rich protrusions as they invade into the underlying substrate. These protrusions are accompanied by matrix degradation via MT1-MMP on their surface (Lizárraga, Poincloux, Romao, et al. 2009; Poincloux, Lizárraga, and Chavrier 2009).

To shed more light on matrix degradation during 3D movement its is helpful to screen where the degradation takes place during 2D movement on the ECM. Reportedly, cells degrade ECM at central regions beneath actin-rich dots which are assigned to invadopodia. The matrix degradation assay form present work showed that the degradation takes place at the cell-center, which coincides with the location of doral/ventral protrusions of cells in 3D collagen (Figure 36). The similar localisation of the dedgradation loci and the formation of dorsal/ventral protrusions may indicate degradative nature of dorsal/venrtal protrusions in 3D. However, results from this work also suggest that dorsal/ventral protrusions are anchoring the cell, as the rear retracts and leading edge protrudes, during 3D migration (Figure 32 s. supplemental movie). This raises the question if these cells adhere to and degrade collagen at same locations? Of note, dynamics of dorsal/ventral protrusions form Figure 34 suggests that these structures protrude and then retract back to the cell body. Possibly, the degradation (by MMPs) can loosen the adhesion of a cell to collagen fibers, so that this adhesive structure can lose grip for the cell to move further. In this case, the treatment of cells with MMP-inhibitor should block the cell movement. GM6001 treated HT1080 cells show elongated morphology in 3D collagen after long-term treatment with GM6001 (Data not shown. see suppl. Data). This morphology is partly reminiscent of the phenotype of MEFs in collagen that cannot degrade matrix. One explanation of elongated morphology of GM6001 treated cells in 3D collagen could be that cells which cannot degrade collagen are not able to detach from collagen during retraction. So these cells merely protrude, but fail to detach from the matrix, which might lead to elongated cell morphology. This implies that probably adhesions have to be cleaved by MMPs for cells to detach, retract and move further. The cleavage of adhesions by MMPs can be a possible link between adhesion and degradation during cell migration.

It is also possible that ventral structures shown in Figure 34 only mechanically interact with collagen fibers and anchor the cell during movement. On the other hand, MMPs could be released at contact sites to degrade collagen fibers and enable thicker parts of the cell to move through collagen fibers.

To further clarify this question 3D degradation assay involving confocal microscopy should be adopted which can detect matrix degradation in 3D such as on 2D (Katarina Wolf et al. 2003). The HT1080 cells can be transfected with Ruby-lifact construct and embedded cells in 3D FITC labelled collagen can be visulized in confocal microscopy to detect if degradation takes place at dorsal / ventral protruions of HT1080 cells in 3D collagen.

4.2.6 Inhibition of MMPs, but not of formins suppresses matrix degradation by HT1080 cells

The degradation of ECM is apparently one of the integral parts of cancer cell migration in 3D environments (K. Wolf 2003; Katarina Wolf et al. 2009). To degrade and adjust ECM to their requirements invasive cancer cells use invadopodia. In cells plated on 2D ECM substrates such as on gelatin, these structures are visible as F-actin rich dots at a ventral surface of cell that degrades the substrate. Invadopodia are enriched with ECM degrading enzymes that can be secreted into the extracellular space (Poincloux, Lizárraga, and Chavrier 2009). Polymerization of F-actin and thus protrusion of invadopodia is apparently accomplished by formins and Arp2/3 complex (Yamaguchi et al. 2005; Stefan Linder, Wiesner, and Himmel 2011). Additionally, Ena/VASP proteins besides MMPs, are important for degrading activity of these structures (Philippar et al. 2008b).

In this work I addressed the issue how the inhibition of formins or MMPs affects the functionality of invadopodia in HT1080 cells. Furthermore, I assessed if adhesion and degradation of ECM occur independently from each other in HT1080 cells.

The matrix degradation assay from the present work shows that HT1080 cells degrade ECM at central and rear regions of the cell (Figure 39; Figure 40, non-treated cells).The Treatment of cells with MMP inhibitor GM6001 suppressed degradation of ECM by HT1080 cells almost

completely (Figure 40, Figure 41). To target formins and thus invadopodia-mediated degradation, the smiFH2 inhibitor was utilized. SmiFH2 treated cells showed no significant defect in matrix degradation (Figure 40 Figure 41). However, visually, less degradative activity was observed at central areas of cells. Apparently, these cells degraded matrix at the periphery at high rates so that in the sum no significant defects of matrix degradation could be detected. The degradation of ECM at the cell periphery could be performed by other structures than invadopodia without involvement of formins. Otherwise, the cell could mechanically remove ECM by cell retraction process. However, if this is the case than MMP inhibitor should not affect ECM degradation at the cell periphery. Instead the treatment with MMP-inhibitor completely seized degradation activity of cells (Figure 40, Figure 41). This also indicates enzymatic- and not solely mechanical degradation at the rear, which can mean that degradative structures such as invadopodia are also present at the cell-rear.

Formins at the cape of invadopodia can push the actin core beneath them during their actin-polymerizing activity. Together with the activity of Arp2/3 complex formins generate the force that can push invadopodium outwards from the cell membrane. Therefore, smiFH2 as the formin inhibitor, could affect protrusion phase during formation of invadopodia, but not the degradation activity of these actin protrusions.

Adhesion and degradation assays form present work also intend to compare interaction of non-invasive MEFs and highly invasive HT1080 cells with the ECM. In contrast to highly invasive HT1080 cell line, MEFs does not invade into collagen. These cells need several days to spread in 3D collagen. MEFs can produce filopodia and actin-rich protrusions in 3D when stimulated with growth factor PDGF. However, these cells still cannot migrate efficiently in 3D collagen. On the contrary to MEFs, related HT1080- or C2C12 cells, can adhere and spread within hours in the 3D collagen matrix.

Similar to MEFs, smiFH2 treated HT1080 cells showed decreased cell to matrix adhesion (Figure 22, Figure 42). The decreased cell numbers in adhesion assay were probably due to inhibition of filopodia formation during spreading of cells. However, the effect of smiFH2 on the formation of focal adhesions cannot be excluded.

Degradation assay confirmed that MEFs degraded FITC-gelatin at a much lower rate than HT1080 cells, which reflects the difference of these cell types in adaptation to the 3D collagen matrix. Furthermore, MEFs did not produce dot-like degradation defects known for the invadopodia based degradation (Figure 23 non-treated; Figure 40 non-treated). The virtual absence of matrix degradation in MEFs was confirmed by the fact that inhibition of MMPs had no significant effect on degradation in MEFs (Figure 24). Conversly, the same treatment in HT1080 cells using MMP inhibitor GM6001 led to approx. 90-95 % drop in degradation activity of these cells (Figure 41). Of note, both cell types can form actin protrusions and can adhere to ECM matrix. However, MEFs cannot degrade ECM as effectively and probably via invadopodia, as HT1080 cells can do. Thus, based on these results it can be speculated that degradative activity is essential for efficient migration of large cells such as, fibroblasts or cancer cells in 3D ECM. Further, because of abscecne of matrix degradation in MEFs it can be assumed that these cells lack functional invadopodia, which is the main reason for their inability to efficently migrate in 3D collagen.

4.2.7 Effects of formin-, Arp2/3- and MMP inhibitors on actin-based protrusions in 3D

Formins of mDia subfamily are involved in the formation of filopodia in numerous cell types (Pellegrin and Mellor 2005; J. Block et al. 2008; C. Yang et al. 2007). Reportedly, HT1080 cells express high levels of mDia1 together with FMNL2 (Kitzing et al. 2010). Therefore, this cell line appears suitable to study effects of smiFH2 on formins and how the inhibition formins affects actin-based protrusions and cell migration in 3D.

The present work shows negative effects of smiFH2 on the formation of filopodia in MEFs downstream of Cdc42. Similar to MEFs, the application of smiFH2 on HT1080 cells on 2D resulted in reduced filopodia and defective cell polarity on 2D substrates (not shown, see suppl. Data). The adhesion and degradation assays showed that cell adhesion, caused by defective spreading, was affected in smiFH2 treated cells supportive of effects of smiFH2 on filopodia and probably invadopodia (Figure 41, 42). In addition, data obtained from the live spinning disc con-

focal microscopy after treatments of HT1080 cells with smiFH2 are supportive of that this inhibitor acts specifically on filopodia-like protrusions of HT1080 cells in 3D collagen (Figure 43 s. suppl. videos).

GM6001 probably does not inhibit formation actin-based protrusions of cells in 3D directly, but inhibits matrix degradation which is associated with invadopodia. Thus, this treatment probably cancels out degradative effects of invadopodia in 3D migration. Probably combined treatment of HT1080 cells with smiFH2 and GM6001 should provide more insight on the role of filopodia in 3D migration. In this kind of experiment GM6001 would merely inhibit invadopodia mediated degradation leaving filopodia and lamellipodia intact. However, cells probably switch migration mode to bleb based migration in this case.

The inhibitor of Arp2/3 complex CK666 inhibits the formation of Arp2/3 dependent protrusions at the leading edge and on dorsal/ventral sides of the cells, but doesn't affect the formation of filopodia at the leading edge of HT1080 cells in 3D collagen (Figure 43, CK-666 s. suppl. video).

4.2.8 Inhibition of formins or MMPs reduces the cell velocity during random migration in 3D

The mesenchymal cell migration in 3D ECM involves the formation of actin-based protrusions, cell to matrix adhesion and matrix degradation by MMPs. Cell migration in 3D environments has been studied regarding the role of matrix degradation (Katarina Wolf et al. 2003; Katarina Wolf et al. 2007), or the role of proteins involved in the formation of actin-based protrusions such as formins, Arp2/3, WAVE/WASP-proteins, or GTPases Rho, Rac1 and Cdc42. The final products of activity of these proteins in cell migration are actin-based protrusions. However, to date, there is no consensus about types of actin-based protrusions that are formed in 3D cell migration. Clear evidence provided by live cell imaging of that lamellipodia and filopodia were still formed in 3D environments was missing. Thus the existence of these structures in 3D cell migration is controversially discussed. On the other hand, the degradation of ECM and invadopodia have been identified as important in 3D migration. Therefore, the majority of reports considering 3D cell

migration focus on invasion of cells in 3D ECM and the role of matrix degradation and invadopodia in this process. Moreover, several groups suggest that cells from other kinds of the actin-based protrusion in 3D instead of filopodia and lamellipodia. Giri and colleagues termed these as mother and daughter protrusions as they did not detect lamellipodia or formation of filopodia in HT1080 cells in 3D (Giri et al. 2013a). Their study however used phase contrast brightfield microscopy to detect lamellipodia in 3D which is probably less suitable for visualization of such fine structures of cells embedded in the 3D environment full of collagen fibers. On the other hand, they did not focus at the tips of protrusions, but rather at branching points of protrusions where filopodia usually are not formed. The measurements of the cell speed in 3D showed that shRNA Cdc42 was the most potent suppressor of speed compared to of that of WASP, WAVE1, cortactin or Arp2/3, suggesting the importance of filopodia in 3D migration.

Conversely, another report showed that downregulation of Rac1, WAVE2 or constituents of the Arp2/3 complex that are essential for formation of lamellipodia led to shrinking of the tip structure of pseudopodia in 3D, whereas filopodia-like spikes on the tip of pseudopodia were not affected. These cells also showed a reduction of invasive capacity into collagen ECM. In HT1080 cells, this treatment did not lead to reduced invasiveness probably because these cells can switch to the amoeboid mode of migration when lamellipodia are suppressed (Yamazaki, Kurisu, and Takenawa 2009b; Kurisu and Takenawa 2010c). This fits partly with results obtained in the present work where the application of Arp2/3 inhibitor CK666 to 20 % increased cell velocity in 3D random migration (Figure 45). When visualized in confocal microscopy these cells show blebs and putative filopodia at the leading edge of these cells (Figure 43). Thus, HT1080 cells probably switch to amoeboid or mixed migration mode when Arp2/3 inhibitor CK666 is applied (visible on blebbing associated cell morphology in 3D after treatment of cells with CK666) (Figure 43 s. suppl. Figures). Probably the activity of the Arp2/3 complex is so crucial for mesenchymal migration mode that cells change the mode of migration when this actin nucleator seizes its activity. Amoeboid migration mode in 3D generates more speed in cells than any other studied type of migration. Additionally, probably matrix degradation and filopodia formation are still available in CK666 in treated cells. Thus this positive effects sum up and probably result in an increased velocity of cells in random migration. However, in 3D chemotaxis, this could turn out to be a disadvantage and cells possibly are not able to follow gradients well. Thus, 3D migration assay using

chemoattractant such as FCS would provide more insight whether amoeboid migration mode can be efficient in 3D chemotaxis.

Reportedly, also the inhibition of matrix degradation in HT1080 cells either by MMP inhibitor GM6001 or by downregulation of MT1-MMP impairs invasiveness and leads to switch from mesenchymal to amoeboid migration mode, but cells still can migrate in 3D using amoeboid mode of migration. Same cells showed this change of morphology also when they were implanted in mouse dermis. Based on these results authors proposed the compensatory migration mode to bypass physical resistance of ECM by the change from adhesion and degradation dependent mesenchymal to adhesion and degradation independent- amoeboid migration mode termed as mesenchymal-amoeboid -transition (MAT) (Katarina Wolf et al. 2003; Katarina Wolf et al. 2007).

MMPs are apparently transported in vesicles and released at sites of matrix degradation in MDA-MB-231 cells. This process was shown to be dependent on Arp2/3 activator N-WASP (Steffen et al. 2008). Thus either depletion of N-WASP or treatment of cells with MMP inhibitor GM6001 both led to reduces invasiveness 10 % and speed of cells approx. 40-50 % of control in 3D ECM. Furthermore, the affected cells apparently switch to the amoeboid mode of migration. Also, depletion of N-WASP was associated with loss of invadopodia (Steffen et al. 2008; DesMarais et al. 2009; Yu and Machesky 2012). Thus, the reduced velocity of cells under GM6001 treatment in previous studies is consistent with results from present work where GM6001 treated cells showed approx. 95 % reduced degradation in 2D degradation assay and approx. 50 % reduced velocity in 3D migration assay (Figure 40; 41;45).

The Present work shows, that at least on 2D substrates, matrix degradation takes place at central- and rear regions of the cell, but not at the leading edge during migration which is apparently also the case during 3D migration in collagen (Katarina Wolf et al. 2007). The inhibition of MMPs using MMP inhibitor GM6001 blocked degradation almost entirely on the 2D substrate without affecting the formation of filopodia and lamellipodia, normal morphology and polarity of HT1080 cells on 2D. This treatment had no apparent effect on the formation of the actin-based protrusions at the leading edge of cells in 3D (Figure 43). Thus the reduced velocity of GM6001 treated HT1080 cells possibly can be assigned to diminished matrix degradation due to inhibition

of MMPs. This inhibitory effect of GM6001 on degradation was also demonstrated in 2D degradation assay (Figure 40; Figure 41). However, GM6001 treated cells are apparently still able to move in 3D collagen. This movement is probably supported at least by lamellipodia and filopodia, and likely does not involve matrix degradation. Because GM6001 treated cells still form dorsal/ventral actin protrusions reminiscent of invadopodia, the role of invadopodia should be considered. However, without their degradative activity, when MMPs are inhibited, invadopodia probably can physically anchor cell in the 3D fibrous matrix and provide a prop for translocation of the cell body (Figures 34; 35). It is also possible that cells use mixed mode of migration which additionally involves myosin type II-dependent blebbing. However, there is no sign of switch of migration mode when cells are treated with GM6001, because treated cells still form actin protrusions and don't show extensive blebbing which is the case during amoeboid migration (Figure 43, suppl. Figures).

Excellent studies were done to gain more understanding of how cells use matrix degradation and switch between modes of migration to surpass tissue barriers. However, the primary challenge, to establish relationships between proteins involved in actin polymerization, actin protrusions that are formed as consequence of the activity of these proteins and their effects on cell migration in 3D, is still not well understood. The present work shows, for the first time using live confocal microscopy, that filopodia and lamellipodia are formed during cell migration in 3D collagen (Figures 31; 32; 33). Especially, filopodia are apparently enriched at tips of pseudopodia in 3D (Figures 30; 32). The inhibition of formins reduces formation these filopodia, and this is probably translated into less cell velocity during random migration in 3D (Figure 45). Moreover, inhibition of Arp2/3 complex leads to loss of lamellipodia and formation of bleb like protrusions at the leading edge of cells (Figure 43). However, affected cells can still migrate with 20 % increased velocities in 3D (Figure 45). The inhibition of matrix degradation has no apparent effect on the formation of actin-based protrusions in 3D (Figure 43). Whereas, treatment of cells with MMP-inhibitor diminishes matrix degradation (Figure 40, 41). These cells can migrate in 3D collagen but show approx. 50% reduced velocities in 3D (Figure 45).

In present work, the effect of suppression of filopodia, lamellipodia and matrix degradation by specific inhibitors was studies in 3D migration assay in collagen. These experiments revealed commonly reduced cell velocity in GM6001, and smiFH2 treated HT1080 cells. The GM6001

treated cells showed approx. 50 % reduced velocity, whereas the effect of smiFH2 was of less impact, showing approx. 30 % reduced velocity. The directness of cell migration for all treatment groups was not significantly altered (Figure 45).

To date, there is a sparse amount of data available that describe effects of formin inhibitor smiFH2 on cell motility. Besides suppression of MMPs, the invasive capability of cells in 3D matrices was addressed by interfering formin activity revealing a significant role of formins in the 3D invasion of cancer cells. Regarding cell migration, treatment of cells with smiFH2 led to increased velocity in 2D migration assay in cancer cells (Isogai, Kammen, and Innocenti 2015). On the other hand, in 3D spheroid cultures, smiFH2 mediated inhibition of formins or downregulation of mDia2 via siRNA mediated knockdown led to markedly reduced invasiveness of glioblastoma cells (Arden et al. 2015b). In a comprehensive study, formins form three cancer cell lines were analyzed in their role in invasiveness of these cells. Targeting of either Daam2, Dia1, FMN1 or INF2 by shRNA reduced invasiveness of HT1080 cells at 80 %, 70 %, 30 % and 90 % respectively in inverted invasion assay (Kitzing et al. 2010). Thus, formins apparently play a significant role in the invasion of cancer cell into 3D collagen.

Nonetheless, it is not entirely clear which actin-based protrusions are suppressed by application of smiFH2 in the 3D migration cells. Formins are involved in the formation of both, invadopodia and filopodia. Because there was less evidence of formation of filopodia in 3D, the motility of cells during the 3D invasion was associated with the activity of invadopodia and MMPs. However, the involvement of formins in the formation of filopodia as well as of invadopodia points to the important role of both of these structures in 3D migration.

The effect of interfering formation of invadopodia on invasive capacity of cells is apparently dependent on the ability of cells to switch between migration modes during invasion or 3D migration. The downregulation of actin-bundling protein fascin was shown to reduce the formation of invadopodia (represented as actin-rich dot-like structures containing Arp2/3 complex) and invasion of cells at approx. 40 %. Whereas in cells, that can switch to amoeboid (blebbing) dependent migration, downregulation of fascin had no significant effect on 3D invasion (Li et al. 2010a). Probably in this case cells degraded ECM which was accompanied by the amoeboid mode of migration. Thus cells showed no defective invasion.

In the present work treatment of HT1080 cells with formin inhibitor smiFH2 led to reduced migration velocity of cells which is probably caused by the loss of filopodia and thus reduced rates of cell protrusion (Figure 45). This is reminiscent of negative effects on MEFs caused by genetic removal of *Cdc42* on filopodia and cell velocity in 2D migration (Figures 12; 14). Also, smiFH2 treated HT1080 cells showed reduced numbers of filopodia without apparent effects on the formation of lamellipodia on 2D. SmiFH2 treated HT1080 cells showed loss of filopodia in 3D collagen. This was accompanied with extensive blebbing of treated cells. However, the matrix degradation was not affected by smiFH2 treatment as shown in matrix degradation assay (Figure 41). Thus inhibition of formins by smiFH2 probably leads to loss of filopodia, but cells can migrate using mixed mode consisting of blebbing and matrix degradation. However, when matrix degradation is inhibited, cells apparently maintain characteristics of mesenchymal migration mode such as cell to matrix adhesion and formation of actin protrusions (Figure 43).

Approx. 20 % reduced cell velocity in filopodia suppressed cells may reflect the relative contribution of filopodia in cell protrusion and thus velocity in a given environment. In MEFs on 2D and HT1080 cells in 3D, the contribution of filopodia to cell velocity is similar. The reason for the reduced velocity is probably reduced formation of filopodia, which in case of Cdc42 knockout MEFs is also approx. 13 % decreased. The affected cells migrate with approx. 20 % reduced velocity, which coincides with reduced filopodia numbers. In 3D migration of HT1080 cells, this kind of quantification was not performed but can be done in future experiments.

4.2.9 The inhibition formins negatively affects chemotaxis of HT1080 cells in 3D collagen

Reportedly, several subfamilies of formins are activated by Cdc42 GTPase. The interaction of Cdc42 with formins is important for formation of filopodia, the polarization of cell and chemotaxis(Peng et al. 2003; Jennifer Block et al. 2012). The Cdc42 GTPase prominently induces the formation of filopodia in fibroblasts, and its removal causes defective polarization and reduced cell velocity during 2D migration (Catherine D Nobes and Hall 1995b; C D Nobes and Hall 1999; Czuchra, Wu, Meyer, van Hengel, et al. 2005; Kozma et al. 1995). Loss of Cdc42 GTPase

is associated with reduced filopodia numbers, less polarity and reduced cell velocity in macrophages (Allen et al. 1998). Also in hemocytes (equivalent of macrophage in mammals) of *Drosophila* loss of Cdc42 led to defective cell migration showing haphazard migration during wound closure (Stramer et al. 2005b). Filopodia, one of the major end products of formin activity, were implicated to be involved in chemotaxis in *Dictyostelium* (Schirenbeck et al. 2006). However, the role of filopodia in cell migration is still not well understood.

In the present work HT1080 cells showed extensive formation of filopodia in 3D that could be suppressed by smiFH2. This treatment resulted in a reduced velocity of cells during 3D random migration. Therefore, it was interesting to test how inhibition of filopodia affects 3D chemotaxis in these cells. The 3D chemotaxis assay in the presence of smiFH2 indeed led to reduced chemotaxis of cells expressed in reduction of FMI of the treated cell population (Figure 46a). In contrast to random migration assay (Figure 45), in 3D chemotaxis, smiFH2 treatment did not result in a decreased velocity of cells (Figure 46c). This probably can be explained by the use of a mixture of chemoattractant (FCS) and smiFH2 in the chemotaxis assay which was not the case in a random migration assay. In the random migration assay smiFH2 without FCS was added to cells.

To perform the 3D chemotaxis assay I used FCS as the source of chemoattractant providing a gradient of growth factors such as PDGF or EGF. These growth factors activate their specific tyrosine kinase receptors in HT1080 cells. This signaling probably leads to activation of Cdc42 and Rac1 at the cell membrane which in turn activate nucleators such as Arp2/3 and formins thus inducing the formation of lamellipodia and filopodia respectively. The Cdc42 GTPase binds and activates formins that lead to the formation of filopodia. Cdc42 together with GEF facilitates recruitment and activation of formins at the cell membrane. In cells treated with smiFH2 formins are inhibited, because of binding of smiFH2 to FH2 domains of formins. This probably suppresses the dimerization of formins. Dimerization of formins is essential for binding of these to the barbed ends of actin filaments and thus their recruitment and activity as actin nucleators. Thus, when dimerization of formins is disabled by smiFH2, filopodia cannot be formed at specific loci, which apparently play an essential role in chemotaxis of HT1080 cells towards growth factors. Filopodia, besides their contribution in cell protrusion, are probably directing or providing directional cues for the protrusion of lamellipodia towards chemoattractant ensuring that the cell maintains an accurate path over the time course of the directional migration.

In the present work, HT1080 showed the prominent formation of filopodia when embedded- and during their migration 3D collagen (Figure; 32). Similar to MEFs on 2D, treatment of HT1080 cells with smiFH2 caused reduced filopodia formation in 3D (Figure 43) which was accompanied with the reduced spreading of cells on ECM corroborating negative effect of smiFH2 on the formation of filopodia in these cells. In 3D random migration assay, smiFH2 treated cells showed reduced velocity (Figure 45), reminiscent of MEFs depleted of Cdc42.

Reportedly, formin mDia2 (Dfr3) is activated by Cdc42 leading to the relocation of this formin to tips of filopodia (Peng et al. 2003; Pellegrin and Mellor 2005). During the writing of present work, another report emerged indicating selectivity of smiFH2 towards mDia2 (Isogai, Kammen, and Innocenti 2015). Whereas inhibition of both, mDia1 and mDia2, could be achieved using smiFH2 or siRNA approaches in glioblastoma cells which decreased invasion of these cells in 3D (Arden et al. 2015a). However, also FMNL1-3 are associated with the formation of filopodia downstream of Cdc42. Interaction of Cdc42 with FMNL2 leads to recruitment of this formin to the leading edge of cells (Steffen et al. 2006) (Jennifer Block et al. 2012; Kühn et al. 2015; Kage et al. 2017a). MEFs apparently express FMNL family of formins whereas mDia2 was not detectable in these cells (Steffen et al. 2006). In HT1080 cells mDia1, FMNL2, and FMNL3 are upregulated (Kitzing et al. 2010). Formin mDia1 was shown to be important in chemotaxis and polarization of immune cells (Gupton et al. 2007; Sakata et al. 2007).

Accordingly to dissect which formins exactly are targeted by smiFH2 future work should involve testing of smiFH2 treatments on HT1080 cells and examine the effects of smiFH2 treatment on expression of these formins via western blot or qPCR approaches.

4.2.10 Fascin1 shRNA negatively affects filopodia and motility of HT1080 cells in 3D collagen

Another way to interfere formation of filopodia is a knockdown of fascin by using a siRNA approach. Fascin specifically localizes within filopodia and is apparently essential in their formation in B16 cells (D. Vignjevic 2006). Besides its critical role in the formation of filopodia fascin is

important for the formation of invadopodia (Danijela Vignjevic et al. 2006a; Li et al. 2010a; Svitkina et al. 2003; Yu and Machesky 2012).

In the present work, fascin knockdown HT1080 cells showed apparently normal morphology and protrusions when embedded in 3D. However, confocal spinning disc microscopy revealed differences within the leading edges of fascin knockdown cells compared with untreated control cells. In control cells, filopodia at the leading edge are more aligned with the direction of leading edge of the cell. Whereas filopodia in fascin knockdown cells show criss-crossed distribution (and are not well aligned with the direction of leading edge (Figure 48). The similar defect was also observed in B16 cells depleted of fascin by shRNA treatment. This is possibly due to the reduction of fascin mediated bundling of actin filaments within filopodia due to knockdown of this protein. Bundling activity of fascin in filopodia leads typically to structural strengthening so that these structures can withstand and overcome the pressure opposed by the cell membrane. If filopodia are not rigid enough, they might not be able to protrude over the edge of the cell (D. Vignjevic 2006). The destabilized inner structure of filopodia caused by fascin depletion probably leads to the disorganized appearance of filopodia at the leading edge in 3D, which possibly affects the stability and persistence of the leading edge. The last is reportedly essential in maintaining cell orientation during migration (Giri et al. 2013b). The unstable leading edge could also lead to reduced velocity and directness of cells when filopodia are suppressed in HT1080 cells (Figure 49). Additionally, knockdown of fascin led to qualitatively reduced numbers of dorsal/ventral actin-rich dots in treated cells which probably are invadopodia. However, further experiments are required to address this issue.

Fascin knockdown HT1080 cells showed significantly reduced directness and velocity in 3D random migration assay in collagen (Figure 49). This reduced motility further corroborates that filopodia are important for efficient migration in HT1080 cells in 3D environments. However, fascin knockdown might also affect the formation of invadopodia that are also important in 3D migration, particularly for anchoring of cells as shown in previous results from this work (Figure 34).

Defects in the bundling of filopodia by knockdown of f*ascin1* and the possible effect of this treatment on invadopodia are likely the cause of reduced velocity and directness of these cells in the 3D migration assay (Figure 49).

The 3D random migration assay of fascin shRNA treated cells was performed for approx. one hour because of the reduced vitality of transfected cells when exposed to fluorescence illumination compared to other 3D migration assays that were performed in brightfield microscopy. These factors could influence the velocity and directness of cells negatively. Thus, the longer illumination times can provide more reliable data on cell migration such as in brightfield illumination microscopy approach. For further experiments, removal of fascin can be considered using CRISPR/cas9 technique which does not require fluorescent labeling of cells during microscopy. This way fascin depleted cells can be monitored using brightfield microscopy which is less toxic for and can applied for over duration of 5 hours without affecting much the cell vitality.

In the present work, knockdown of fascin reduced filopodia and CDR formation in MEFs on 2D substrate. In HT1080 cells depletion of fascin by siRNA led probably to decrease in rigidity of filopodia reminiscent of B16 cells from another work (D. Vignjevic 2006). Moreover, this treatment leads to reduced formation of dorsal /ventral protrusions in HT1080 cells that possibly represent invadopodia. Same treatment leads to decrease in the formation of CDRs in MEFs thus it can be speculated that dorsal/ventral structures of HT1080 cells are reminiscent of CDRs observed in MEFs.

Taken together our results support the involvement of both filopodia and invadopodia in 3D random migration and chemotaxis of HT1080 cells. Apparently, invadopodia are anchoring cell during migration. Filopodia are used to protrude in a porous environment such as in 3D collagen and probably preferred over lamellipodia in such environments. In this regard inhibition of filopodia by smiFH2 coincided with reduced cell velocities during random migration of HT1080 cells in 3D collagen and markedly reduced 3D chemotaxis of this cells in a 3D chemotaxis assay (Figure 46).

5 Concluding remarks

The present work demonstrates that the removal of Cdc42 in MEFs leads to reduced filopodia numbers, impaired cell polarity and loss of chemotaxis towards PDGF-BB. The loss of chemotaxis towards PDGF-BB is apparently due to reduced numbers of filopodia. Additionally, Cdc42 knockout MEFs show decreased cell velocity, which is probably due to reduced decreased, filopodia dependent protrusion rate in these cells. Furthermore, the effects of loss of Cdc42 regarding reduced filopodia numbers, loss of cell polarity and reduced cell velocity could be reproduced by inhibition of formins by smiFH2. Thus, supposedly a subpopulation of filopodia is formed downstream of Cdc42 and a specific formin in MEFs. These filopodia contribute to a certain degree in the generation of cell velocity and are essential for chemotaxis towards PDGF-BB in MEFs on 2D. Based on studies on MEFs, formin inhibitor smiFH2 leads to loss of filopodia downstream of Cdc42 without affecting the formation of lamellipodia that are reportedly formed downstream of Rac1. This provides crucial support of studies that argue that formation of filopodia and lamellipodia are independent of each other.

The chemotaxis of macrophages towards C5a is one of the initial steps of innate immune response. To crawl towards chemoattractants, macrophages form actin-based protrusions such as lamellipodia and filopodia. This work shows that Hem1 knockout BM-derived macrophages cannot form lamellipodia which result in loss of chemotaxis towards C5a. This suggests an important role of lamellipodia in sensing of pathogen entry and thus the innate immune response by macrophages.

Furthermore, this work shows that highly motile cancer cells such as HT1080 cells use lamellipodia, filopodia, and dorsal/ventral protrusions, which are probably invadopodia, in 3D migration. In 3D collagen, cells are confronted with small pores which are more suitable for filopodia dominated protrusion and leading edge. Thus, when embedded in 3D collagen HT1080 cells showed prominent filopodia. However, lamellipodia are also formed in 3D, but they are smaller in size and width compared to their 2D counterparts.

HT1080 cells showed qualitatively fewer filopodia in 3D when treated with smiFH2. Furthermore, Inhibition formins negatively affected cell velocity and chemotaxis of HT1080 cells in 3D collagen. This suggests that filopodia are important in 3D chemotaxis such as on 2D in MEFs.

Taken together, the negative effects of removal of Cdc42, depletion of VASP or formin depletion on fibroblastoid cell migration are similar and of note, negatively affect the formation of filopodia. This further strengthens the argument that filopodia are important in chemotaxis and are formed downstream of Cdc42 and formins in fibroblasts and fibroblast related cancer cells.

6 Abbreviations

Abi	Abelson interactor
ActA	Actin assembly-Inducing protein
ADF	Actin-depolymerizing factor
Arp	Actin related Protein
ATP	adenosine triphosphate
ADP	Adenosine diphosphate
APS	Ammonium persulfate
Approx.	Approximately
BM	Bone marrow
BSA	bovine serum albumin
CAAX motif	C stands for Cysteine, A is aliphatic, X can be one of amino acids.
cAMP	cyclic Adenosinmonophosphate
°C	degree Celsius
CapG	Capping Protein Gelsolin like (Also Macrophage capping protein, MCP).
CC	coiled coil
CCD	charge-coupled-device
CDR	Circular dorsal ruffles
Cdc42	Cell division cycle42
CO_2	carbon dioxide
CP	Capping protein
CR	Circular Ruffles
CRIB	Cdc42/Rac interactive binding
DAD	Diaphanous autoregulatory domain
DD	Dimerization domain

DH	Dbl homology
DID	Diaphanous inhibitory domain
DMSO	Dimethyl sulfoxide
DMEM	Dulbecco´s modified eagle´s medium
DNA	Deoxyribonucleic acid
DRF	Diaphanous-related formin
DTE	Dithioerythrol
ECM	Extracellular matrix
EDTA	Ethylendiamintetraactetic acid
EGFR	EGF-receptor
FMNL	Formin like protein
EGF	epidermal growth factor
EGFP	Enhanced green fluorescent protein
ER	endoplasmic reticulum
ES	embryonic stem cell
Eps8	epidermal growth factor receptor pathway substrate 8
EVL	Ena/VASP-like protein
et al.	and others (et alii)
FAK	focal adhesion kinase
F-Actin	filamentous actin
FCS	fetal calf serum
FHOD	Fh1/Fh2 domain containing protein
FITC	fluorescein isothiocyanate
FMN	formin
FMNL	formin-like protein
FMI	Forward migration index
g	gram
G-actin	globular actin

GAP	GTPase activating protein
GBD	GTPase binding domain
GDI	Guanine nucleotide dissociation inhibitor
GDP	Guanosindiphosphate
GEF	Guanine exchange factors
GFP	green fluorescent protein
GPCR	G-protein coupled receptors
GTP	Guanosintriphosphate
HCl	hydrochloric acid
HEPES	4-(2-hydroxyethyl)-1-piperazineethanesulfonic acid
HGF	hepatocyte growth factor
IgG	Immunoglobulin class g
INF	Inverted formin
KCl	potassium chloride
kDa	kilo Dalton
K.O.	Knockout
m	Meter
M	Molar (mol/L)
µ	micro
mA	milliampere
MAT	mesenchymal-amoeboid transition
MEF	mouse embryonic fibroblast
Min	Minute
Mg^{2+}	Magnesium ion
Mm	Millimeter
MMP	matrix metalloproteinase
Ms	millisecond
MTOC	microtubule organizing center

mV	millivolt
µm	micrometer
Nap	Nck associated protein
ng	Nano gram
nm	Nanometer
NPF	nucleation-promoting factor
N-WASP	neuronal Wiskott-Aldrich syndrome protein
o/n	over night
PDGF	Platelet-derived growth factor
p.a.	pro analysii
PBS	Phosphate Buffered Saline
PCR	polymerase chain reaction
PFA	paraformaldehyde
PH	Pleckstrin homology
pH	potential of hydrogen
PKA	Protein kinase A
P_i	inorganic phosphate
PAK	Serine/threonine protein kinase
p85	regulatory subunit of PI3K
p110	catalytic subunit of PI3K
PI3K	Phosphatidylinositol 3-Kinase
PIP_2	Phosphatidylinositol (4,5)-diphosphate
PIP_3	Phosphatidylinositol (3,4,5)-triphosphate
PKB	Protein Kinase B (also Akt)
PKC	Protein Kinase C
P/S	Penicillin/Streptomycin
PVDF	Polyvinylidendifluoride
PAK	Serine/threonine protein kinase

PDGFR	Platelet-derived growth factor receptor
PDZ	Postsynaptic density 95, Discs large, Zonula occldens-1
PPP	polyproline motif
PTEN	phosphatase and tensin homolog
QPCR	quantitative PCR
Rac	Ras-associated C3 botulinum toxin substrate
Rho	Ras homology protein
RhoA	Ras homolog gene family member A
RhoB	Ras homolog gene family member B
RhoBTB	Ras homolog gene family member broad-complex, tramtrack, bric à brac
RhoD	Ras homolog gene family member D
RhoG	Ras homolog gene family member
RhoGDI	Rho GDP-dissociation inhibitor
ROS	Reactive oxygen species
RT	Room temperature
RTK	Receptor tyrosine kinases
RNA	ribonucleic acid
Rpm.	Rounds per minute
ROCK	Rho associated protein kinase
SCIT	single cell invasion tunnels
shRNA	short hairpin RNA
siRNA	short interfering RNA
smiFH2	small molecule inhibitor of formin homology 2 domains
s	second
s.	see
SCAR	suppressor of cyclic AMP repressor
SDS	Sodium dodecyl sulfate
SDS-PAGE	SDS- Polyacrylamidgelelectrophoresis

SH2-Domain	Src-Homology domain 2
SH3-Domain	Src-Homology domain 3
Sos1	son of sevenless 1
Sra	specific Rac associated protein
SF	Stress fiber
TBS-T	Tris Buffered Saline +Tween20
TEMED	N,N,N,N-Tetramethylethylendiamine
VASP	Vasodilator-stimulated phosphoprotein
v/v	Volume per Volume
VCA	V: C-terminal verprolin-homology domain; C: cofilin homology domain; A: acidic domain
VEGF	Vascular endothelial growth factor
VVCA	VV (two veroprolin motifs)
WAVE	WASP family verprolin-homologous
WIP	WASP-interacting Protein
WT	Wild type
w/v	weight per volume
WAS	Wiskott-Aldrich syndrome
WASP	Wiskott-Aldrich syndrome protein
WHD	WAVE homology domain
WIP	WASP interacting protein

7 Literature

Abraham, Sabu, Margherita Scarcia, Richard D Bagshaw, Kathryn McMahon, Gary Grant, Tracey Harvey, Maggie Yeo, et al. 2015. “A Rac/Cdc42 Exchange Factor Complex Promotes Formation of Lateral Filopodia and Blood Vessel Lumen Morphogenesis.” *Nature Communications* 6. Nature Publishing Group: 7286. doi:10.1038/ncomms8286.

Adams, A E, Douglas I. Johnson, Richard M. Longnecker, Barbara F. Sloat, and John R. Pringle. 1990a. “CDC42 and CDC43, Two Additional Genes Involved in Budding and the Establishment of Cell Polarity in the Yeast Saccharomyces Cerevisiae.” *The Journal of Cell Biology* 111 (1): 131–42. doi:10.1083/jcb.111.1.131.

———. 1990b. “CDC42 and CDC43, Two Additional Genes Involved in Budding and the Establishment of Cell Polarity in the Yeast Saccharomyces Cerevisiae.” *The Journal of Cell Biology* 111 (1): 131–42. doi:10.1083/jcb.111.1.131.

Adams, J C, J D Clelland, G D Collett, F Matsumura, S Yamashiro, and L Zhang. 1999. “Cell-Matrix Adhesions Differentially Regulate Fascin Phosphorylation.” *Molecular Biology of the Cell* 10 (12): 4177–90. doi:10.1091/mbc.10.12.4177.

Adams, Josephine C, N Kureishy, A L Taylor, J Breivik, G Gaudernack, K M Carr, K Rosenblatt, et al. 2004a. “Roles of Fascin in Human Carcinoma Motility and Signaling: Prospects for a Novel Biomarker?” *Clin Cancer Res* 9 (1): 1–11. doi:10.1038/nature03799.

———. 2004b. “Roles of Fascin in Human Carcinoma Motility and Signaling: Prospects for a Novel Biomarker?” *Clin Cancer Res* 9 (1): 1–11. doi:10.1038/nature03799.

Adra, C N, D Manor, J L Ko, S Zhu, T Horiuchi, L Van Aelst, R A Cerione, and B Lim. 1997. “RhoGDIgamma: A GDP-Dissociation Inhibitor for Rho Proteins with Preferential Expression in Brain and Pancreas.” *Proceedings of the National Academy of Sciences of the United States of America* 94 (9): 4279–84. doi:10.1073/pnas.94.9.4279.

Alberts, Bruce, Alexander Johnson, Julian Lewis, Martin Raff, Keith Roberts, and Peter Walter. 2002a. *Molecular Biology of the Cell. 4th Edition, New York.*

———. 2002b. “Transport into the Cell from the Plasma Membrane: Endocytosis.” Garland Science. http://www.ncbi.nlm.nih.gov/books/NBK26870/.

Allen, William E, Daniel Zicha, Anne J Ridley, and Gareth E Jones. 1998. “A Role for Cdc42 in Macrophage Chemotaxis” 141 (5): 1147–57.

Anderl, Janet, Jun Ma, and Luke Armstrong. n.d. “Fluorescent Gelatin Degradation Assays for Investigating Invadopodia Formation,” 1–5.

Andrianantoandro, Ernesto, and Thomas D. Pollard. 2006. “Mechanism of Actin Filament Turnover by Severing and Nucleation at Different Concentrations of ADF/Cofilin.” *Molecular Cell* 24 (1): 13–23. doi:10.1016/j.molcel.2006.08.006.

Applewhite, Derek a, Melanie Barzik, Shin-Ichiro Kojima, Tatyana M Svitkina, Frank B Gertler, and Gary G Borisy. 2007. “Ena/VASP Proteins Have an Anti-Capping Independent

Function in Filopodia Formation." *Molecular Biology of the Cell* 18 (7): 2579–91. doi:10.1091/mbc.E06-11-0990.

Arber, S, F A Barbayannis, H Hanser, C Schneider, C A Stanyon, O Bernard, and P Caroni. 1998. "Regulation of Actin Dynamics through Phosphorylation of Cofilin by LIM- Kinase [See Comments]." *Nature* 393 (6687): 805–9. doi:10.1038/31729.

Arden, Jessica D, Kari I Lavik, Kaitlin A Rubinic, Nicolas Chiaia, Sadik A Khuder, Marthe J Howard, Andrea L Nestor-Kalinoski, Arthur S Alberts, and Kathryn M Eisenmann. 2015a. "Small-Molecule Agonists of Mammalian Diaphanous-Related (MDia) Formins Reveal an Effective Glioblastoma Anti-Invasion Strategy." *Molecular Biology of the Cell* 26 (21): 3704–18. doi:10.1091/mbc.E14-11-1502.

———. 2015b. "Small-Molecule Agonists of Mammalian Diaphanous-Related (MDia) Formins Reveal an Effective Glioblastoma Anti-Invasion Strategy." *Molecular Biology of the Cell* 26 (21): 3704–18. doi:10.1091/mbc.E14-11-1502.

Artym, Vira V., Ying Zhang, Françoise Seillier-Moiseiwitsch, Kenneth M. Yamada, and Susette C. Mueller. 2006. "Dynamic Interactions of Cortactin and Membrane Type 1 Matrix Metalloproteinase at Invadopodia: Defining the Stages of Invadopodia Formation and Function." *Cancer Research* 66: 3034–43. doi:10.1158/0008-5472.CAN-05-2177.

Asakura T., Sasaki T Nagano F Satoh A Obaishi H Nishioka H Imamura H Hotta K Tanaka K Nakanishi H Takai Y. 1998. "Isolation and Characterization of a Novel Actin Filament-Binding Protein from Saccharomyces Cerevisiae." *Oncogene* 16 (1): 121–30. http://www.scopus.com/inward/record.url?eid=2-s2.0-15644379785&partnerID=40&md5=0fabb275fdce721d1689184efab4610a.

Aspenstrom, P, A Fransson, and J Saras. 2004. "Rho GTPases Have Diverse Effects on the Organization of the Actin Filament System." *The Biochemical Journal* 377: 327–37. doi:10.1042/BJ20031041.

Aspenström, Pontus, Uno Lindberg, and Alan Hall. 1996. "Two GTPases, Cdc42 and Rac, Bind Directly to a Protein Implicated in the Immunodeficiency Disorder Wiskott–Aldrich Syndrome." *Current Biology*. doi:10.1016/S0960-9822(02)00423-2.

Bachmann, Christiane, Lieselore Fischer, Ulrich Walter, and Matthias Reinhard. 1999. "The EVH2 Domain of the Vasodilator-Stimulated Phosphoprotein Mediates Tetramerization, F-Actin Binding, and Actin Bundle Formation." *Journal of Biological Chemistry* 274 (33): 23549–57. doi:10.1074/jbc.274.33.23549.

Baggett, Andrew W., Zoe Cournia, Min Suk Han, George Patargias, Adam C. Glass, Shih Yuan Liu, and Brad J. Nolen. 2012. "Structural Characterization and Computer-Aided Optimization of a Small-Molecule Inhibitor of the Arp2/3 Complex, a Key Regulator of the Actin Cytoskeleton." *ChemMedChem* 7 (7): 1286–94. doi:10.1002/cmdc.201200104.

Bailly, Maryse, Ilia Ichetovkin, Wayne Grant, Noureddine Zebda, Laura M. Machesky, Jeffrey E. Segall, and John Condeelis. 2001. "The F-Actin Side Binding Activity of the Arp2/3 Complex Is Essential for Actin Nucleation and Lamellipod Extension." *Current Biology* 11 (8): 620–25. doi:10.1016/S0960-9822(01)00152-X.

Bartolini, Francesca, James B. Moseley, Jan Schmoranzer, Lynne Cassimeris, Bruce L. Goode, and Gregg G. Gundersen. 2008. “The Formin MDia2 Stabilizes Microtubules Independently of Its Actin Nucleation Activity.” *Journal of Cell Biology* 181 (3): 523–36. doi:10.1083/jcb.200709029.

Barzik, Melanie, Tatyana I. Kotova, Henry N. Higgs, Larnele Hazelwood, Dorit Hanein, Frank B. Gertler, and Dorothy A. Schafer. 2005. “Ena/VASP Proteins Enhance Actin Polymerization in the Presence of Barbed End Capping Proteins.” *Journal of Biological Chemistry* 280 (31): 28653–62. doi:10.1074/jbc.M503957200.

Barzik, Melanie, Leslie M. McClain, Stephanie L. Gupton, and Frank B. Gertler. 2014. “Ena/VASP Regulates MDia2-Initiated Filopodial Length, Dynamics, and Function.” *Molecular Biology of the Cell* 25 (17): 2604–19. doi:10.1091/mbc.E14-02-0712.

Bear, James E, Joseph J Loureiro, Irina Libova, Reinhard Fa, and D- Braunschweig. 2000. “Negative Regulation of Fibroblast Motility by Ena / VASP Proteins” 101: 717–28.

Behnia, Rudy, and Sean Munro. 2005. “Organelle Identity and the Signposts for Membrane Traffic.” *Nature* 438 (7068): 597–604. doi:10.1038/nature04397.

Benesch, Stefanie, Simona Polo, Frank P L Lai, Kurt I Anderson, Theresia E B Stradal, Juergen Wehland, and Klemens Rottner. 2005. “N-WASP Deficiency Impairs EGF Internalization and Actin Assembly at Clathrin-Coated Pits.” *Journal of Cell Science* 118 (Pt 14): 3103–15. doi:10.1242/jcs.02444.

Beningo, Karen a, Micah Dembo, and Yu-li Wang. 2004. “Responses of Fibroblasts to Anchorage of Dorsal Extracellular Matrix Receptors.” *Proceedings of the National Academy of Sciences of the United States of America* 101 (52): 18024–29. doi:10.1073/pnas.0405747102.

Binks, Michael, Gareth E. Jones, Paul M. Brickell, Christine Kinnon, David R. Katz, and Adrian J. Thrasher. 1998. “Intrinsic Dendritic Cell Abnormalities in Wiskott-Aldrich Syndrome.” *European Journal of Immunology* 28 (10): 3259–67. doi:10.1002/(SICI)1521-4141(199810)28:10<3259::AID-IMMU3259>3.0.CO;2-B.

Blain, Emma J. 2009. “Involvement of the Cytoskeletal Elements in Articular Cartilage Homeostasis and Pathology.” *International Journal of Experimental Pathology* 90 (1): 1–15. doi:10.1111/j.1365-2613.2008.00625.x.

Blanchoin, Laurent, Kurt J. Amann, Henry Higgs, Jean-Baptiste Marchand, Donald A. Kaiser, and Thomas D. Pollard. 2000. “Direct Observation of Dendritic Actin Filament Networks Nucleated by Arp2/3 Complex and WASP/Scar Proteins.” *Nature* 404 (1994): 1007–11. doi:10.1038/35010008.

Blaser, Heiko, Michal Reichman-Fried, Irinka Castanon, Karin Dumstrei, Florence L Marlow, Koichi Kawakami, Lilianna Solnica-Krezel, Carl Philipp Heisenberg, and Erez Raz. 2006. “Migration of Zebrafish Primordial Germ Cells: A Role for Myosin Contraction and Cytoplasmic Flow.” *Developmental Cell* 11 (5): 613–27. doi:10.1016/j.devcel.2006.09.023.

Block, J., T. E B Stradal, J. Hänisch, R. Geffers, S. A. Köstler, E. Urban, J. V. Small, K. Rottner, and J. Faix. 2008. “Filopodia Formation Induced by Active MDia2/Drf3.” In *Journal of*

Microscopy, 231:506–17. doi:10.1111/j.1365-2818.2008.02063.x.

Block, Jennifer, Dennis Breitsprecher, Sonja Kühn, Moritz Winterhoff, Frieda Kage, Robert Geffers, Patrick Duwe, et al. 2012. "FMNL2 Drives Actin-Based Protrusion and Migration Downstream of Cdc42." *Current Biology* 22 (11): 1005–12. doi:10.1016/j.cub.2012.03.064.

Bosse, Tanja, Julia Ehinger, Aleksandra Czuchra, Stefanie Benesch, Anika Steffen, Xunwei Wu, Kathrin Schloen, et al. 2007. "Cdc42 and Phosphoinositide 3-Kinase Drive Rac-Mediated Actin Polymerization Downstream of c-Met in Distinct and Common Pathways." *Molecular and Cellular Biology* 27 (19): 6615–28. doi:10.1128/MCB.00367-07.

Boujemaa-Paterski, R., E. Gouin, G. Hansen, S. Samarin, C. Le Clainche, D. Didry, P. Dehoux, et al. 2001. "Listeria Protein ActA Mimics WASP Family Proteins: It Activates Filament Barbed End Branching by Arp2/3 Complex." *Biochemistry* 40 (38): 11390–404. doi:10.1021/bi010486b.

Brakebusch, Cord, and Reinhard Fa. 2003. "NEW EMBO MEMBER ' S REVIEW The Integrin ± Actin Connection , an Eternal Love Affair" 22 (10).

Brandt, Dominique T., Sabrina Marion, Gareth Griffiths, Takashi Watanabe, Kozo Kaibuchi, and Robert Grosse. 2007. "Dia1 and IQGAP1 Interact in Cell Migration and Phagocytic Cup Formation." *Journal of Cell Biology* 178 (2): 193–200. doi:10.1083/jcb.200612071.

Breitsprecher, Dennis, and Bruce L Goode. 2013. "Formins at a Glance." *Journal of Cell Science* 126 (Pt 1): 1–7. doi:10.1242/jcs.107250.

Breitsprecher, Dennis, Antje K Kiesewetter, Joern Linkner, Marlene Vinzenz, Theresia E B Stradal, John Victor Small, Ute Curth, Richard B Dickinson, and Jan Faix. 2011. "Molecular Mechanism of Ena / VASP-Mediated" 30 (3): 456–67. doi:10.1038/emboj.2010.348.

Brummelkamp, Thijn R, René Bernards, and Reuven Agami. 2002. "A System for Stable Expression of Short Interfering RNAs in Mammalian Cells." *Science (New York, N.Y.)* 296 (5567): 550–53. doi:10.1126/science.1068999.

Buccione, Roberto, James D Orth, and Mark a McNiven. 2004. "Foot and Mouth: Podosomes, Invadopodia and Circular Dorsal Ruffles." *Nature Reviews. Molecular Cell Biology* 5 (8): 647–57. doi:10.1038/nrm1436.

Burridge, Keith, and Erika S Wittchen. 2012. "Stress Fibers Get a Makeover." *Biophysical Journal* 103 (10). Biophysical Society: 2045–46. doi:10.1016/j.bpj.2012.09.039.

Caldieri, Giusi, Inmaculada Ayala, Francesca Attanasio, and Roberto Buccione. 2009. "Cell and Molecular Biology of Invadopodia." *International Review of Cell and Molecular Biology* 275 (09): 1–34. doi:10.1016/S1937-6448(09)75001-4.

Campellone, Kenneth G, and Matthew D Welch. 2010. *NIH Public Access*. *Molecular Cell*. Vol. 11. doi:10.1038/nrm2867.A.

Cantrell, D A. 2001. "Phosphoinositide 3-Kinase Signalling Pathways." *Journal of Cell Science* 114 (Pt 8): 1439–45.

Carl, Uwe D., Marc Pollmann, Elisha Orr, Frank B. Gertler, Trinad Chakraborty, and Juergen Wehland. 1999. "Aromatic and Basic Residues within the EVH1 Domain of VASP Specify

Its Interaction with Proline-Rich Ligands." *Current Biology* 9 (13): 715–18. doi:10.1016/S0960-9822(99)80315-7.

Carlier, Marie France, Valérie Laurent, Jérôme Santolini, Ronald Melki, Dominique Didry, Gui Xian Xia, Yan Hong, Nam Hai Chua, and Dominique Pantaloni. 1997. "Actin Depolymerizing Factor (ADF/Cofilin) Enhances the Rate of Filament Turnover: Implication in Actin-Based Motility." *Journal of Cell Biology* 136 (6): 1307–22. doi:10.1083/jcb.136.6.1307.

Carpenter, Christopher L., and Lewis C. Cantley. 1996. "Phosphoinositide Kinases." *Current Opinion in Cell Biology*. doi:10.1016/S0955-0674(96)80060-3.

Castrillon, D H, and S a Wasserman. 1994. "Diaphanous Is Required for Cytokinesis in Drosophila and Shares Domains of Similarity with the Products of the Limb Deformity Gene." *Development (Cambridge, England)* 120 (12): 3367–77. doi:7821209.

Chao, Wei Ting, and Jeannette Kunz. 2009. "Focal Adhesion Disassembly Requires Clathrin-Dependent Endocytosis of Integrins." *FEBS Letters* 583 (8): 1337–43. doi:10.1016/j.febslet.2009.03.037.

Chen, Wen-Tien -T. 1989. "Proteolytic Activity of Specialized Surface Protrusions Formed at Rosette Contact Sites of Transformed Cells." *Journal of Experimental Zoology* 251 (2): 167–85. doi:10.1002/jez.1402510206.

Chen, Xing Judy, Anna Julia Squarr, Raiko Stephan, Baoyu Chen, Theresa E Higgins, David J Barry, Morag C Martin, Michael K Rosen, Sven Bogdan, and Michael Way. 2014. "Article Ena / VASP Proteins Cooperate with the WAVE Complex to Regulate the Actin Cytoskeleton." *Developmental Cell* 30 (5). The Authors: 569–84. doi:10.1016/j.devcel.2014.08.001.

Chereau, David, and Roberto Dominguez. 2006. "Understanding the Role of the G-Actin-Binding Domain of Ena/VASP in Actin Assembly." *Journal of Structural Biology* 155 (2): 195–201. doi:10.1016/j.jsb.2006.01.012.

Cherfils, Jacqueline, and Mahel Zeghouf. 2013. "Regulation of Small GTPases by GEFs, GAPs, and GDIs." *Physiological Reviews* 93 (1): 269–309. doi:10.1152/physrev.00003.2012.

Chesarone, Melissa A., and Bruce L. Goode. 2009. "Actin Nucleation and Elongation Factors: Mechanisms and Interplay." *Current Opinion in Cell Biology*. doi:10.1016/j.ceb.2008.12.001.

Chhabra, Ekta Seth, and Henry N. Higgs. 2006. "INF2 Is a WASP Homology 2 Motif-Containing Formin That Severs Actin Filaments and Accelerates Both Polymerization and Depolymerization." *Journal of Biological Chemistry* 281 (36): 26754–67. doi:10.1074/jbc.M604666200.

Chhabra, Ekta Seth, and Henry N Higgs. 2007a. "The Many Faces of Actin: Matching Assembly Factors with Cellular Structures." *Nature Cell Biology* 9 (10): 1110–21. doi:10.1038/ncb1007-1110.

———. 2007b. "The Many Faces of Actin: Matching Assembly Factors with Cellular Structures." *Nature Cell Biology* 9 (10): 1110–21. doi:10.1038/ncb1007-1110.

Chrzanowska-wodnicka, Magdalena, and Keith Burridge. 1996. “Rho-Stimulated Contractility Drives the Formation of Stress Fibers and Focal Adhesions” 133 (6): 1403–15.

Chun, Tae Hwa, Farideh Sabeh, Ichiro Ota, Hedwig Murphy, Kevin T. McDonagh, Kenn Holmbeck, Henning Birkedal-Hansen, Edward D. Allen, and Stephen J. Weiss. 2004. “MT1-MMP-Dependent Neovessel Formation within the Confines of the Three-Dimensional Extracellular Matrix.” *Journal of Cell Biology* 167 (4): 757–67. doi:10.1083/jcb.200405001.

Chung, Chang Y., and Richard A. Firtel. 1999. “PAKa, a Putative PAK Family Member, Is Required for Cytokinesis and the Regulation of the Cytoskeleton in Dictyostelium Discoideum Cells during Chemotaxis.” *Journal of Cell Biology* 147 (3): 559–75. doi:10.1083/jcb.147.3.559.

Condeelis, John, and Jeffrey E Segall. 2003. “Intravital Imaging of Cell Movement in Tumours.” *Nature Reviews. Cancer* 3 (12): 921–30. doi:10.1038/nrc1231.

Contraction, Wound, and Frederick Grinnell. 1994. “Mini-Review on the Cellular Mechanisms of Disease” 124 (4): 401–4.

Cory, Giles O C, Rainer Cramer, Laurent Blanchoin, and Anne J. Ridley. 2003. “Phosphorylation of the WASP-VCA Domain Increases Its Affinity for the Arp2/3 Complex and Enhances Actin Polymerization by WASP.” *Molecular Cell* 11 (5): 1229–39. doi:10.1016/S1097-2765(03)00172-2.

Cote, J F, and K Vuori. 2007. “GEF What? Dock 180 and Related Proteins Help Rac to Polarize Cells in New Ways.” *Trends in Cell Biology* 17 (8): 383–93. doi:Doi 10.1016/J.Tcb.2007.05.001.

Cote, Jean-Francois. 2006. “A Novel and Evolutionary Conserved Pip3 Binding Domain Is Necessary for Dock180 Signaling.” *Nature Cell Biology* 7 (8): 797–807. doi:10.1038/ncb1280.

Côté, Jean-François, and Kristiina Vuori. 2002. “Identification of an Evolutionarily Conserved Superfamily of DOCK180-Related Proteins with Guanine Nucleotide Exchange Activity.” *Journal of Cell Science* 115 (Pt 24): 4901–13. doi:10.1242/jcs.00219.

Cougoule Véronique Poincloux, Renaud Al Saati, Talal Mège, Jean-Louis Tabouret, Guillaume Lowell, Clifford A. Laviolette-Malirat, Nathalie Maridonneau-Parini, Isabelle, Céline Le Cabec. 2009. “Three-Dimensional Migration of Macrophages Requires Hck for Podosome Organization and Extracellular Matrix Proteolysis.” *Blood* 115 (7): 1444–52. http://www.bloodjournal.org/content/115/7/1444.abstract.

Croce, Assunta, Giuseppe Cassata, Andrea Disanza, Maria Cristina Gagliani, Carlo Tacchetti, Maria Grazia Malabarba, Marie-France Carlier, Giorgio Scita, Ralf Baumeister, and Pier Paolo Di Fiore. 2004. “A Novel Actin Barbed-End-Capping Activity in EPS-8 Regulates Apical Morphogenesis in Intestinal Cells of Caenorhabditis Elegans.” *Nature Cell Biology* 6 (12): 1173–79. doi:10.1038/ncb1198.

Crowley, Eileen, and Alan F Horwitz. 1995. “Tyrosine Phosphorylation and Cytoskeletal Tension Regulate the Release of Fibroblast Adhesions” 131 (2): 525–37.

Czuchra, Aleksandra, Xunwei Wu, Hannelore Meyer, Jolanda Van Hengel, Timm Schroeder, Robert Geffers, Klemens Rottner, and Cord Brakebusch. 2005. “Cdc42 Is Not Essential for Filopodium Formation , Directed Migration , Cell Polarization , and Mitosis in Fibroblastoid” 16 (October): 4473–84. doi:10.1091/mbc.E05.

Czuchra, Aleksandra, Xunwei Wu, Hannelore Meyer, Jolanda van Hengel, Timm Schroeder, Robert Geffers, Klemens Rottner, and Cord Brakebusch. 2005. “Cdc42 Is Not Essential for Filopodium Formation, Directed Migration, Cell Polarization, and Mitosis in Fibroblastoid Cells.” *Molecular Biology of the Cell* 16 (10): 4473–84. doi:10.1091/mbc.E05.

de Rooij, J, F J Zwartkruis, M H Verheijen, R H Cool, S M Nijman, a Wittinghofer, and J L Bos. 1998. “Epac Is a Rap1 Guanine-Nucleotide-Exchange Factor Directly Activated by Cyclic AMP.” *Nature* 396 (6710): 474–77. doi:10.1038/24884.

DeMali, Kris a, Christy a Barlow, and Keith Burridge. 2002. “Recruitment of the Arp2/3 Complex to Vinculin: Coupling Membrane Protrusion to Matrix Adhesion.” *The Journal of Cell Biology* 159 (5): 881–91. doi:10.1083/jcb.200206043.

DerMardirossian, Céline, and Gary M. Bokoch. 2005. “GDIs: Central Regulatory Molecules in Rho GTPase Activation.” *Trends in Cell Biology* 15 (7): 356–63. doi:10.1016/j.tcb.2005.05.001.

DesMarais, Vera, Hideki Yamaguchi, Matthew Oser, Lilian Soon, Ghassan Mouneimne, Corina Sarmiento, Robert Eddy, and John Condeelis. 2009. “N-WASP and Cortactin Are Involved in Invadopodium-Dependent Chemotaxis to EGF in Breast Tumor Cells.” *Cell Motility and the Cytoskeleton* 66 (6): 303–16. doi:10.1002/cm.20361.

Dettenhofer, Markus, Fen Zhou, and Philip Leder. 2008. “Formin 1-Isoform IV Deficient Cells Exhibit Defects in Cell Spreading and Focal Adhesion Formation.” *PLoS ONE* 3 (6): 1–8. doi:10.1371/journal.pone.0002497.

Di Modugno, Francesca, Giovanna Bronzi, Matthew J. Scanlan, Duilia Del Bello, Simona Cascioli, Irene Venturo, Claudio Botti, et al. 2004. “Human Mena Protein, a Serex-Defined Antigen Overexpressed in Breast Cancer Eliciting Both Humoral and CD8+ T-Cell Immune Response.” *International Journal of Cancer* 109 (6): 909–18. doi:10.1002/ijc.20094.

Didsbury, J., R. F. Weber, G. M. Bokoch, T. Evans, and R. Snyderman. 1989. “Rac, a Novel Ras-Related Family of Proteins That Are Botulinum Toxin Substrates.” *Journal of Biological Chemistry* 264 (28): 16378–82. doi:10.1002/(SICI)1097-0320(19970801)28:4<289::AID-CYTO3>3.0.CO;2-7.

Disanza, Andrea, Sara Bisi, Moritz Winterhoff, Francesca Milanesi, Dmitry S Ushakov, David Kast, Paola Marighetti, Guillaume Romet-Lemonne, et al. 2013. “CDC42 Switches IRSp53 from Inhibition of Actin Growth to Elongation by Clustering of VASP.” *The EMBO Journal* 32 (20): 2735–50. doi:10.1038/emboj.2013.208.

Disanza, Andrea, Sara Bisi, Moritz Winterhoff, Francesca Milanesi, Dmitry S Ushakov, David Kast, Paola Marighetti, Guillaume Romet-lemonne, et al. 2013. “CDC42 Switches IRSp53 from Inhibition of Actin Growth to Elongation by Clustering of VASP,” no. March: 2735–50. doi:10.1038/emboj.2013.208.

Disanza, Andrea, Marie-France Carlier, Theresia E B Stradal, Dominique Didry, Emanuela Frittoli, Stefano Confalonieri, Assunta Croce, Jurgen Wehland, Pier Paolo Di Fiore, and Giorgio Scita. 2004. “Eps8 Controls Actin-Based Motility by Capping the Barbed Ends of Actin Filaments.” *Nature Cell Biology* 6 (12): 1180–88. doi:10.1038/ncb1199.

Donnelly, Sara Katherine, Jose Javier Bravo-Cordero, and Louis Hodgson. 2014. “Rho GTPase Isoforms in Cell Motility: Don’t Fret, We Have FRET.” *Cell Adhesion & Migration* 8 (4): 37–41. doi:10.4161/cam.29712.

Dubielecka, Patrycja M, Kathrin I Ladwein, Xiaoling Xiong, Isabelle Migeotte, Anna Chorzalska, Kathryn V Anderson, Janet a Sawicki, Klemens Rottner, Theresia E Stradal, and Leszek Kotula. 2011. “Essential Role for Abi1 in Embryonic Survival and WAVE2 Complex Integrity.” *Proceedings of the National Academy of Sciences of the United States of America* 108 (17): 7022–27. doi:10.1073/pnas.1016811108.

E, Brugnera, Brugnera E, Haney L, Haney L, Grimsley C, Grimsley C, Lu M, et al. 2002. “Unconventional Rac-GEF Activity Is Mediated through the Dock180 ELMO Complex.” *Nat Cell Biol* 4: 574–82. doi:10.1038/ncb824.

Eden, Sharon, Rajat Rohatgi, Alexandre V Podtelejnikov, Matthias Mann, and Marc W Kirschner. 2002. “Mechanism of Regulation of WAVE1-Induced Actin Nucleation by Rac1 and Nck.” *Nature* 418 (6899): 790–93. doi:10.1038/nature00859.

Elbashir, Sayda M, Jens Harborth, Winfried Lendeckel, A Yalcin, K Weber, and T Tuschl. 2001. “Duplexes of 21 ± Nucleotide RNAs Mediate RNA Interference in Cultured Mammalian Cells.” *Nature* 411 (6836): 494–98. doi:10.1038/35078107.

Elkhal, Abdallah, Maria D Gallego, Miguel A De Fuente, Yoji Sasahara, Marco Calamito, Koduru Suresh, Katherine Siminovitch, et al. 2007. “WIP Is a Chaperone for Wiskott – Aldrich Syndrome Protein (WASP) WASP” 104 (3): 3–8.

Eriksson, John E., Thomas Dechat, Boris Grin, Brian Helfand, Melissa Mendez, Hanna Mari Pallari, and Robert D. Goldman. 2009. “Introducing Intermediate Filaments: From Discovery to Disease.” *Journal of Clinical Investigation*. doi:10.1172/JCI38339.

Etienne-Manneville, S. 2004. “Cdc42 - the Centre of Polarity.” *Journal of Cell Science* 117 (8): 1291–1300. doi:10.1242/jcs.01115.

Etienne-Manneville, Sandrine. 2004. “Cdc42--the Centre of Polarity.” *Journal of Cell Science* 117 (Pt 8): 1291–1300. doi:10.1242/jcs.01115.

———. 2006. “In Vitro Assay of Primary Astrocyte Migration as a Tool to Study Rho GTPase Function in Cell Polarization.” *Methods in Enzymology* 406: 565–78. doi:10.1016/S0076-6879(06)06044-7.

Eva, A, G Vecchio, C D Rao, S R Tronick, and S A Aaronson. 1988. “The Predicted DBL Oncogene Product Defines a Distinct Class of Transforming Proteins.” *Proceedings of the National Academy of Sciences of the United States of America* 85 (7): 2061–65. doi:10.1073/pnas.85.7.2061.

Evangelista, M. 1997. “Bni1p, a Yeast Formin Linking Cdc42p and the Actin Cytoskeleton During Polarized Morphogenesis.” *Science* 276 (5309): 118–22.

doi:10.1126/science.276.5309.118.

Evangelista, Marie, Sally Zigmond, and Charles Boone. 2003. “Formins: Signaling Effectors for Assembly and Polarization of Actin Filaments.” *Journal of Cell Science* 116 (Pt 13): 2603–11. doi:10.1242/jcs.00611.

Even-Ram, Sharona, and Kenneth M Yamada. 2005a. “Cell Migration in 3D Matrix.” *Current Opinion in Cell Biology* 17 (5): 524–32. doi:10.1016/j.ceb.2005.08.015.

———. 2005b. “Cell Migration in 3D Matrix.” *Current Opinion in Cell Biology* 17 (5): 524–32. doi:10.1016/j.ceb.2005.08.015.

Ezratty, Ellen J., Claire Bertaux, Eugene E. Marcantonio, and Gregg G. Gundersen. 2009. “Clathrin Mediates Integrin Endocytosis for Focal Adhesion Disassembly in Migrating Cells.” *Journal of Cell Biology* 187 (5): 733–47. doi:10.1083/jcb.200904054.

Faix, Jan, and Klemens Rottner. 2006a. “The Making of Filopodia.” *Current Opinion in Cell Biology* 18 (1): 18–25. doi:10.1016/j.ceb.2005.11.002.

———. 2006b. “The Making of Filopodia.” *Current Opinion in Cell Biology* 18 (1): 18–25. doi:10.1016/j.ceb.2005.11.002.

———. 2006c. “The Making of Filopodia.” *Current Opinion in Cell Biology* 18 (1): 18–25. doi:10.1016/j.ceb.2005.11.002.

Feb, Kees Straatman, Olympus Cell, and Normally Nikon. 2008. “Wound Healing Assay.”

Ferguson, G John, Laura Milne, Suhasini Kulkarni, Takehiko Sasaki, Simon Walker, Simon Andrews, Tom Crabbe, et al. 2007. “PI(3)Kgamma Has an Important Context-Dependent Role in Neutrophil Chemokinesis.” *Nature Cell Biology* 9 (1): 86–91. doi:10.1038/ncb1517.

Fire, A., S. Xu, M. K. Montgomery, S. A. Kostas, S. E. Driver, and C. C. Mello. 1998. “Potent and Specific Genetic Interference by Double-Stranded RNA in Caenorhabditis Elegans.” *Nature* 391 (6669): 806–11. doi:10.1038/35888.

Fischer, Markus, Ilka Haase, Sebastian Wiesner, and Annette Müller-Taubenberger. 2006. “Visualizing Cytoskeleton Dynamics in Mammalian Cells Using a Humanized Variant of Monomeric Red Fluorescent Protein.” *FEBS Letters* 580 (10): 2495–2502. doi:10.1016/j.febslet.2006.03.082.

Foxman, E F, E J Kunkel, and E C Butcher. 1999. “Integrating Conflicting Chemotactic Signals. The Role of Memory in Leukocyte Navigation.” *The Journal of Cell Biology* 147 (3): 577–88. doi:10.1083/jcb.147.3.577.

Franke, Werner W. 2004. “Actin ’ s Many Actions Start at the Genes” 6 (11): 1013–17.

Friedl, P, and E B Bröcker. 2000. “The Biology of Cell Locomotion within Three-Dimensional Extracellular Matrix.” *Cellular and Molecular Life Sciences : CMLS* 57 (1): 41–64. http://www.ncbi.nlm.nih.gov/pubmed/10949580.

Friedl, P, K S Zänker, and E B Bröcker. 1998. “Cell Migration Strategies in 3-D Extracellular Matrix: Differences in Morphology, Cell Matrix Interactions, and Integrin Function.” *Microscopy Research and Technique* 43 (5): 369–78. doi:10.1002/(SICI)1097-

0029(19981201)43:5<369::AID-JEMT3>3.0.CO;2-6.

Funamoto, Satoru, Kristina Milan, Ruedi Meili, and Richard A. Firtel. 2001. “Role of Phosphatidylinositol 3??? Kinase and a Downstream Pleckstrin Homology Domain-Containing Protein in Controlling Chemotaxis in Dictyostelium.” *Journal of Cell Biology* 153 (4): 795–809. doi:10.1083/jcb.153.4.795.

García, Esther, Laura M Machesky, Gareth E Jones, and Inés M Antón. 2014. “WIP Is Necessary for Matrix Invasion by Breast Cancer Cells.” *European Journal of Cell Biology*. Elsevier GmbH. doi:10.1016/j.ejcb.2014.07.008.

Garvalov, Boyan K, Kevin C Flynn, Dorothee Neukirchen, Liane Meyn, Nicole Teusch, Xunwei Wu, Cord Brakebusch, James R Bamburg, and Frank Bradke. 2007. “Cdc42 Regulates Cofilin during the Establishment of Neuronal Polarity.” *The Journal of Neuroscience : The Official Journal of the Society for Neuroscience* 27 (48): 13117–29. doi:10.1523/JNEUROSCI.3322-07.2007.

Gasteier, J E, R Madrid, E Krautkramer, S Schroder, W Muranyi, S Benichou, and O T Fackler. 2003. “Activation of the Rac Binding Partner Formin Homology 2 Domain Containing 1 Induces Actin Stress Fibers via a ROCK Dependent Mechanism.” *J Biol Chem*. http://www.ncbi.nlm.nih.gov/entrez/query.fcgi?cmd=Retrieve&db=PubMed&dopt=Citation&list_uids=12857739.

Gautreau, Alexis, Hsin-yi H Ho, Jiaxu Li, Hanno Steen, Steven P Gygi, and Marc W Kirschner. 2004. “Purification and Architecture of the Ubiquitous Wave Complex.” *Proceedings of the National Academy of Sciences of the United States of America* 101 (13): 4379–83. doi:10.1073/pnas.0400628101.

Gauvin, Timothy J, Lorna E Young, and Henry N Higgs. 2014. “The Formin FMNL3 Assembles Plasma Membrane Protrusions That Participate in Cell-Cell Adhesion.”

“Gelatin Degradation Assay – Buccione Lab .” 2003. *Molecular Biology of the Cell* 7: 2003.

Gelfand, V I, and A D Bershadsky. 1991. “Microtubule Dynamics: Mechanism, Regulation, and Function.” *Annual Review of Cell Biology* 7 (1): 93–116. doi:10.1146/annurev.cb.07.110191.000521.

Gertler, Frank B., Kirsten Niebuhr, Matthias Reinhard, Jürgen Wehland, and Philippe Soriano. 1996. “Mena, a Relative of VASP and Drosophila Enabled, Is Implicated in the Control of Microfilament Dynamics.” *Cell* 87 (2): 227–39. doi:10.1016/S0092-8674(00)81341-0.

Ghosh, Mousumi, Xiaoyan Song, Ghassan Mouneimne, Mazen Sidani, David S Lawrence, and John S Condeelis. 2004. “Cofilin Promotes Actin Polymerization and Defines the Direction of Cell Motility.” *Science (New York, N.Y.)* 304 (5671): 743–46. doi:10.1126/science.1094561.

Giri, Anjil, Saumendra Bajpai, Nicholaus Trenton, Hasini Jayatilaka, Gregory D Longmore, and Denis Wirtz. 2013a. “The Arp2 / 3 Complex Mediates Multigeneration Dendritic Protrusions for Efficient 3-Dimensional Cancer Cell Migration,” 1–11. doi:10.1096/fj.12-224352.

———. 2013b. “The Arp2/3 Complex Mediates Multigeneration Dendritic Protrusions for

Efficient 3-Dimensional Cancer Cell Migration." *FASEB Journal : Official Publication of the Federation of American Societies for Experimental Biology* 27 (10): 4089–99. doi:10.1096/fj.12-224352.

Goldman, D W, F H Chang, L A Gifford, E J Goetzl, and H R Bourne. 1985. "Pertussis Toxin Inhibition of Chemotactic Factor-Induced Calcium Mobilization and Function in Human Polymorphonuclear Leukocytes." *J Exp Med* 162 (1): 145–56. doi:10.1084/jem.162.1.145.

Goley, Erin D, and Matthew D Welch. 2006. "The ARP2/3 Complex: An Actin Nucleator Comes of Age." *Nature Reviews. Molecular Cell Biology* 7 (10): 713–26. doi:10.1038/nrm2026.

Gomez-Cambronero, Julian. 2011. "The Exquisite Regulation of PLD2 by a Wealth of Interacting Proteins: S6K, Grb2, Sos, WASp and Rac2 (And a Surprise Discovery: PLD2 Is a GEF)." *Cellular Signalling*. doi:10.1016/j.cellsig.2011.06.017.

Gorelik, Roman, Changsong Yang, Vasumathi Kameswaran, Roberto Dominguez, and Tatyana Svitkina. 2011. "Mechanisms of Plasma Membrane Targeting of Formin MDia2 through Its Amino Terminal Domains." *Molecular Biology of the Cell* 22 (2): 189–201. doi:10.1091/mbc.E10-03-0256.

Greenberg, S, K Burridge, and S C Silverstein. 1990. "Colocalization of F-Actin and Talin during Fc Receptor-Mediated Phagocytosis in Mouse Macrophages." *The Journal of Experimental Medicine* 172 (6): 1853–56. doi:10.1084/jem.172.6.1853.

Grosse, Robert, John W. Copeland, Timothy P. Newsome, Michael Way, and Richard Treisman. 2003. "A Role for VASP in RhoA-Diaphanous Signalling to Actin Dynamics and SRF Activity." *EMBO Journal* 22 (12): 3050–61. doi:10.1093/emboj/cdg287.

Gu, Zhizhan, Erika H. Noss, Victor W. Hsu, and Michael B. Brenner. 2011. "Integrins Traffic Rapidly via Circular Dorsal Ruffles and Macropinocytosis during Stimulated Cell Migration." *Journal of Cell Biology* 193 (1): 61–70. doi:10.1083/jcb.201007003.

Gupton, Stephanie L, Kathryn Eisenmann, Arthur S Alberts, and Clare M Waterman-Storer. 2007. "MDia2 Regulates Actin and Focal Adhesion Dynamics and Organization in the Lamella for Efficient Epithelial Cell Migration." *Journal of Cell Science* 120 (Pt 19): 3475–87. doi:10.1242/jcs.006049.

Hall, a. 1998. "Rho GTPases and the Actin Cytoskeleton." *Science* 279 (5350): 509–14. doi:10.1126/science.279.5350.509.

Hall, a. 1992. "Ras-Related GTPases and the Cytoskeleton." *Molecular Biology of the Cell* 3 (5): 475–79. doi:10.1091/mbc.3.5.475.

Han, J, K Luby-Phelps, B Das, X Shu, Y Xia, R D Mosteller, U M Krishna, J R Falck, M A White, and D Broek. 1998a. "Role of Substrates and Products of PI 3-Kinase in Regulating Activation of Rac-Related Guanosine Triphosphatases by Vav." *Science* 279 (5350): 558–60. doi:10.1126/science.279.5350.558.

———. 1998b. "Role of Substrates and Products of PI 3-Kinase in Regulating Activation of Rac-Related Guanosine Triphosphatases by Vav." *Science* 279 (5350): 558–60. doi:10.1126/science.279.5350.558.

Han, Young Hoon, Chang Y. Chung, Deborah Wessels, Stephen Stephens, Margaret A. Titus, David R. Soll, and Richard A. Firtel. 2002. “Requirement of a Vasodilator-Stimulated Phosphoprotein Family Member for Cell Adhesion, the Formation of Filopodia, and Chemotaxis in Dictyostelium.” *Journal of Biological Chemistry* 277 (51): 49877–87. doi:10.1074/jbc.M209107200.

Hanahan, Douglas, and Robert a. Weinberg. 2011. “Hallmarks of Cancer: The next Generation.” *Cell* 144 (5). Elsevier Inc.: 646–74. doi:10.1016/j.cell.2011.02.013.

Harris, B Z, and W a Lim. 2001. “Mechanism and Role of PDZ Domains in Signaling Complex Assembly.” *Journal of Cell Science* 114 (Pt 18): 3219–31. http://jcs.biologists.org/content/114/18/3219.full.pdf.

Harris, Elizabeth S., Timothy J. Gauvin, Ernest G. Heimsath, and Henry N. Higgs. 2010. “Assembly of Filopodia by the Formin FRL2 (FMNL3).” *Cytoskeleton* 67 (12): 755–72. doi:10.1002/cm.20485.

Hart, M J, A. Eva, T Evans, S A Aaronson, and R A Cerione. 1991. “Catalysis of Guanine Nucleotide Exchange on the CDC42Hs Protein by the Dbl Oncogene Product.” *Nature* 354 (6351): 311–14. doi:10.1038/354311a0.

Hashimoto, Yosuke, Marek Skacel, and Josephine C. Adams. 2005. “Roles of Fascin in Human Carcinoma Motility and Signaling: Prospects for a Novel Biomarker?” *International Journal of Biochemistry and Cell Biology*. doi:10.1016/j.biocel.2005.05.004.

Heath, J. P., and L. D. Peachey. 1989. “Morphology of Fibroblasts in Collagen Gels: A Study Using 400 KeV Electron Microscopy and Computer Graphics.” *Cell Motility and the Cytoskeleton* 14: 382–92. doi:10.1002/cm.970140308.

Helary, C, B Rodriguez-Sanchez, B Rodrigues-Sanchez, S Vigier, and M-M Giraud Guill. 2012. “Dense Fibrillar Collagen Matrices to Analyse Extracellular Matrix Receptor Function.” *Pathologie-Biologie* 60 (1). Elsevier Masson SAS: 7–14. doi:10.1016/j.patbio.2011.10.007.

Higgs, Henry N, and Kevin J Peterson. 2005. “Phylogenetic Analysis of the Formin Homology 2 Domain.” *Molecular Biology of the Cell* 16 (1): 1–13. doi:10.1091/mbc.E04.

Hofmann, Uta B., Johan R. Westphal, Albert J. W. Zendman, Jürgen C. Becker, Dirk J. Ruiter, and Goos N. P. van Muijen. 2000. “Expression and Activation of Matrix Metalloproteinase-2 (MMP-2) and Its Co-Localization with Membrane-Type 1 Matrix Metalloproteinase (MT1-MMP) Correlate with Melanoma Progression.” *The Journal of Pathology* 191 (3): 245–256. doi:10.1002/1096-9896(2000)9999:9999<::AID-PATH632>3.0.CO;2-#.

Hotulainen, Pirta, and Pekka Lappalainen. 2006. “JCB : ARTICLE” 173 (3): 383–94. doi:10.1083/jcb.200511093.

Hrycyna, Christine A., and Steven Clarke. 1993. “Modification of Eukaryotic Signaling Proteins by C-Terminal Methylation Reactions.” *Pharmacology and Therapeutics* 59 (3): 281–300. doi:10.1016/0163-7258(93)90071-K.

Hu, Stefan, Birgit Harbeck, Nils Ole, Tania Me M, Susanne Illenberger, and Brigitte M Jockusch. 1999. “Characterization of the Actin Binding Properties of the Vasodilator-Stimulated Phosphoprotein VASP” 451: 68–74.

Huttelmaier, S, O Mayboroda, B Harbeck, T Jarchau, B M Jockusch, and M Rudiger. 1998. “The Interaction of the Cell-Contact Proteins VASP and Vinculin Is Regulated by Phosphatidylinositol-4,5-Bisphosphate.” *Curr Biol* 8 (9): 479–88. doi:10.1016/S0960-9822(98)70199-X.

Hynes, Richard O. 2002. “Integrins : Bidirectional , Allosteric Signaling Machines In Their Roles as Major Adhesion Receptors , Integrins” 110 (Table 1): 673–87.

Ingley, Evan, and Brian A. Hemmings. 1994. “Pleckstrin Homology (PH) Domains in Signal Transducton.” *Journal of Cellular Biochemistry* 56 (4): 436–43. doi:10.1002/jcb.240560403.

Innocenti, M, P Tenca, E Frittoli, M Faretta, A Tocchetti, P P Di Fiore, and G Scita. 2002. “Mechanisms through Which Sos-1 Coordinates the Activation of Ras and Rac.” *The Journal of Cell Biology* 156 (1): 125–36. doi:10.1083/jcb.200108035.

Innocenti, Metello, Emanuela Frittoli, Isabella Ponzanelli, John R. Falck, Saskia M. Brachmann, Pier Paolo Di Fiore, and Giorgio Scita. 2003. “Phosphoinositide 3-Kinase Activates Rac by Entering in a Complex with Eps8, Abi1, and Sos-1.” *Journal of Cell Biology* 160 (1): 17–23. doi:10.1083/jcb.200206079.

Insall, Robert H., and Orion D. Weiner. 2001. “PIP3, PIP2, and Cell Movement - Similar Messages, Different Meanings?” *Developmental Cell* 1 (6): 743–47. doi:10.1016/S1534-5807(01)00086-7.

Isaac, Beth M, Dan Ishihara, Leora M Nusblat, Jean-Claude Gevrey, Athanassios Dovas, John Condeelis, and Dianne Cox. 2010. “N-WASP Has the Ability to Compensate for the Loss of WASP in Macrophage Podosome Formation and Chemotaxis.” *Experimental Cell Research* 316 (20). Elsevier Inc.: 3406–16. doi:10.1016/j.yexcr.2010.06.011.

Isfort, Katrin, Franziska Ebert, Julia Bornhorst, Sarah Sargin, Rozina Kardakaris, Manolis Pasparakis, Martin Bähler, Tanja Schwerdtle, Albrecht Schwab, and Peter J Hanley. 2011a. “Real-Time Imaging Reveals That P2Y2 and P2Y12 Receptor Agonists Are Not Chemoattractants and Macrophage Chemotaxis to Complement C5a Is Phosphatidylinositol 3-Kinase (PI3K)- and P38 Mitogen-Activated Protein Kinase (MAPK)-Independent.” *The Journal of Biological Chemistry* 286 (52): 44776–87. doi:10.1074/jbc.M111.289793.

———. 2011b. “Real-Time Imaging Reveals That P2Y2 and P2Y12 Receptor Agonists Are Not Chemoattractants and Macrophage Chemotaxis to Complement C5a Is Phosphatidylinositol 3-Kinase (PI3K)- and P38 Mitogen-Activated Protein Kinase (MAPK)-Independent.” *The Journal of Biological Chemistry* 286 (52): 44776–87. doi:10.1074/jbc.M111.289793.

Isogai, Tadamoto, Rob Van Der Kammen, and Metello Innocenti. 2015. “SMIFH2 Has Effects on Formins and P53 That Perturb the Cell Cytoskeleton.” doi:10.1038/srep09802.

Jackson, Trevor R, Leonard R Stephens, and Phillip T Hawkinsq. 1992. “Receptor Specificity of Growth Factor-Stimulated Synthesis of 3-Phosphorylated Inositol Lipids in Swiss.”

Jayo, Asier, and Maddy Parsons. 2010. “Fascin: A Key Regulator of Cytoskeletal Dynamics.” *The International Journal of Biochemistry & Cell Biology* 42 (10). Elsevier Ltd: 1614–17. doi:10.1016/j.biocel.2010.06.019.

Jockuschb, Brigitte M, and Ulrich Walter. 1996. “VASP Interaction with Vinculin : A Recurring

Theme of Interactions with Proline-Rich Motifs I $ Domain Organization" 399: 103–7.

Johnson, Douglas I. 1999. "Cdc42: An Essential Rho-Type GTPase Controlling Eukaryotic Cell Polarity." *Microbiology and Molecular Biology Reviews : MMBR* 63 (1): 54–105. doi:citeulike-article-id:13113720.

Johnson, Douglas I (University of Michigan), and John R (University of Michigan Pringle. 1990. "Gene Involved in the Development of Cell Polarity" 111 (July): 143–52.

Jones, Gareth E., Daniel Zicha, Graham A. Dunn, Mike Blundell, and Adrian Thrasher. 2002a. "Restoration of Podosomes and Chemotaxis in Wiskott-Aldrich Syndrome Macrophages Following Induced Expression of WASp." *International Journal of Biochemistry and Cell Biology* 34 (7): 806–15. doi:10.1016/S1357-2725(01)00162-5.

Jones, Gareth E, Daniel Zicha, Graham A Dunn, Mike Blundell, and Adrian Thrasher. 2002b. "Restoration of Podosomes and Chemotaxis in Wiskott – Aldrich Syndrome Macrophages Following Induced Expression of WASp" 34: 806–15.

Kage, Frieda, Moritz Winterhoff, Vanessa Dimchev, Jan Mueller, Tobias Thalheim, Anika Freise, Stefan Brühmann, et al. 2017a. "FMNL Formins Boost Lamellipodial Force Generation." *Nature Communications* 8: 14832. doi:10.1038/ncomms14832.

———. 2017b. "FMNL Formins Boost Lamellipodial Force Generation." *Nature Communications* 8: 14832. doi:10.1038/ncomms14832.

Kajiwara, Mlchiko, Sliigeaki Nonoyama, Mltsuoki Ecuchi, Tomohiro Morio, Kohsuke Imai, Hiroji Okawa, Masafumi Kaneko, et al. 1999. "WASP Is Involved in Proliferation and Differentiation of Human Haemopoietic Progenitors in Vitro." *British Journal of Haematology* 107 (2): 254–62. doi:10.1046/j.1365-2141.1999.01694.x.

Kawamura, Kazuhiro, Kazunori Takano, Shiro Suetsugu, Shusaku Kurisu, Daisuke Yamazaki, Hiroaki Miki, Tadaomi Takenawa, and Takeshi Endo. 2004. "N-WASP and WAVE2 Acting Downstream of Phosphatidylinositol 3-Kinase Are Required for Myogenic Cell Migration Induced by Hepatocyte Growth Factor." *Journal of Biological Chemistry* 279 (52): 54862–71. doi:10.1074/jbc.M408057200.

Kelleher, Joseph F., Simon J. Atkinson, and Thomas D. Pollard. 1995. "Sequences, Structural Models, and Cellular Localization of the Actin-Related Proteins Arp2 and Arp3 from Acanthamoeba." *Journal of Cell Biology* 131 (2): 385–97. doi:10.1083/jcb.131.2.385.

Kenney, D, L Cairns, E Remold-O'Donnell, J Peterson, F S Rosen, and R Parkman. 1986. "Morphological Abnormalities in the Lymphocytes of Patients with the Wiskott-Aldrich Syndrome." *Blood* 68 (6): 1329–32. doi:10.1097/MAO.0b013e31827de304.

Kheir, Wassim Abou, Jean-Claude Gevrey, Hideki Yamaguchi, Beth Isaac, and Dianne Cox. 2005. "A WAVE2-Abi1 Complex Mediates CSF-1-Induced F-Actin-Rich Membrane Protrusions and Migration in Macrophages." *Journal of Cell Science* 118 (Pt 22): 5369–79. doi:10.1242/jcs.02638.

Kirchhausen, T, and F S Rosen. 1996. "Disease Mechanism: Unravelling Wiskott-Aldrich Syndrome." *Current Biology : CB* 6 (6): 676–78. doi:10.1016/S0960-9822(09)00447-3.

Kitzing, T M, Y Wang, O Pertz, J W Copeland, and R Grosse. 2010. “Formin-like 2 Drives Amoeboid Invasive Cell Motility Downstream of RhoC.” *Oncogene* 29 (16). Nature Publishing Group: 2441–48. doi:10.1038/onc.2009.515.

Kojima, Shin-ichiro, Danijela Vignjevic, and Gary G Borisy. 2004. “Improved Silencing Vector Co-Expressing GFP and Small Hairpin RNA.”

Kojima, Shin Ichiro, Danijela Vignjevic, and Gary G. Borisy. 2004. “Improved Silencing Vector Co-Expressing GFP and Small Hairpin RNA.” *BioTechniques* 36 (1): 74–79.

Kovar, David R, and Thomas D Pollard. 2004a. “Insertional Assembly of Actin Filament Barbed Ends in Association with Formins Produces Piconewton Forces.” *Proceedings of the National Academy of Sciences* 101 (41): 14725–30. doi:10.1073/pnas.0405902101.

———. 2004b. “Insertional Assembly of Actin Filament Barbed Ends in Association with Formins Produces Piconewton Forces.” *Proceedings of the National Academy of Sciences* 101 (41): 14725–30. doi:10.1073/pnas.0405902101.

Kozma, R, S Ahmed, A Best, L Lim, Robert Kozma, Sohail Ahmed, and Anthony Best. 1995. “The Ras-Related Protein Cdc42Hs and Bradykinin Promote Formation of Peripheral Actin Microspikes and Filopodia in Swiss 3T3 Fibroblasts . The Ras-Related Protein Cdc42Hs and Bradykinin Promote Formation of Peripheral Actin Microspikes and Filopodia in Swi.”

Krueger, Eugene W, James D Orth, Hong Cao, and Mark a McNiven. 2003. “A Dynamin-Cortactin-Arp2/3 Complex Mediates Actin Reorganization in Growth Factor-Stimulated Cells.” *Molecular Biology of the Cell* 14 (3): 1085–96. doi:10.1091/mbc.E02-08-0466.

Kühn, Sonja, Constanze Erdmann, Frieda Kage, Jennifer Block, Lisa Schwenkmezger, Anika Steffen, Klemens Rottner, and Matthias Geyer. 2015. “The Structure of FMNL2-Cdc42 Yields Insights into the Mechanism of Lamellipodia and Filopodia Formation.” *Nature Communications* 6 (May): 7088. doi:10.1038/ncomms8088.

Kühn, Sonja, and Matthias Geyer. 2014. “Formins as Effector Proteins of Rho GTPases.” *Small GTPases* 5 (June): 1–16. doi:10.4161/sgtp.29513.

Kulkarni, Kiran, Jing Yang, Ziguo Zhang, and David Barford. 2011. “Multiple Factors Confer Specific Cdc42 and Rac Protein Activation by Dedicator of Cytokinesis (DOCK) Nucleotide Exchange Factors.” *Journal of Biological Chemistry* 286 (28): 25341–51. doi:10.1074/jbc.M111.236455.

Kundra, V, J A Escobedo, A Kazlauskas, H K Kim, S G Rhee, L T Williams, and B R Zetter. 1994a. “Regulation of Chemotaxis by the Platelet-Derived Growth Factor Receptor-Beta.” *Nature* 367 (6462): 474–76. doi:10.1038/367474a0.

———. 1994b. “Regulation of Chemotaxis by the Platelet-Derived Growth Factor Receptor-Beta.” *Nature* 367 (6462): 474–76. doi:10.1038/367474a0.

Kurisu, Shusaku, and Tadaomi Takenawa. 2010a. “WASP and WAVE Family Proteins: Friends or Foes in Cancer Invasion?” *Cancer Science* 101 (10): 2093–2104. doi:10.1111/j.1349-7006.2010.01654.x.

———. 2010b. “WASP and WAVE Family Proteins: Friends or Foes in Cancer Invasion?”

Cancer Science 101 (10): 2093–2104. doi:10.1111/j.1349-7006.2010.01654.x.

———. 2010c. "WASP and WAVE Family Proteins: Friends or Foes in Cancer Invasion?" *Cancer Science* 101 (10): 2093–2104. doi:10.1111/j.1349-7006.2010.01654.x.

Kwiatkowski, Adam V., Douglas A. Rubinson, Erik W. Dent, J. Edward van Veen, Jonathan D. Leslie, Jiangyang Zhang, Leslie M. Mebane, et al. 2007. "Ena/VASP Is Required for Neuritogenesis in the Developing Cortex." *Neuron* 56 (3): 441–55. doi:10.1016/j.neuron.2007.09.008.

Kwofie, Michael A., and Jacek Skowronski. 2008. "Specific Recognition of Rac2 and Cdc42 by DOCK2 and DOCK9 Guanine Nucleotide Exchange Factors." *Journal of Biological Chemistry* 283 (6): 3088–96. doi:10.1074/jbc.M705170200.

Ladwein, Kathrin, Aleks Guledani, Tanja Bosse, Manfred Rohde, Cord Brakebusch, Nir Gov, Klemens Rottner, Theresia E.B. Stradal. "Differential Contribution of Filopodia to Circular Dorsal Ruffling versus Peripheral Membrane Protrusion," 1–15.

Lai, Frank P L, Malgorzata Szczodrak, Jennifer Block, Jan Faix, Dennis Breitsprecher, Hans G Mannherz, Theresia E B Stradal, Graham a Dunn, J Victor Small, and Klemens Rottner. 2008. "Arp2/3 Complex Interactions and Actin Network Turnover in Lamellipodia." *The EMBO Journal* 27 (7): 982–92. doi:10.1038/emboj.2008.34.

Lakshman, N, a Kim, K J Bayless, G E Davis, and W M Petroll. 2007. "Rho Plays a Central Role in Regulating Local Cell-Matrix Mechanical Interactions in 3D Culture." *Cell Motility and the Cytoskeleton* 64 (6): 434–45. doi:10.1002/cm.20194.

Lammermann, T, J Renkawitz, X Wu, K Hirsch, C Brakebusch, and M Sixt. 2009. "Cdc42-Dependent Leading Edge Coordination Is Essential for Interstitial Dendritic Cell Migration." *Blood* 113 (23): 5703–10. doi:10.1182/blood-2008-11-191882\rblood-2008-11-191882 [pii].

Lämmermann, Tim, Jörg Renkawitz, Xunwei Wu, Karin Hirsch, Cord Brakebusch, and Michael Sixt. 2009. "Cdc42-Dependent Leading Edge Coordination Is Essential for Interstitial Dendritic Cell Migration." *Blood* 113 (23): 5703–10. doi:10.1182/blood-2008-11-191882.

Lämmermann, Tim, and Michael Sixt. 2009. "Mechanical Modes of 'amoeboid' Cell Migration." *Current Opinion in Cell Biology* 21 (5): 636–44. doi:10.1016/j.ceb.2009.05.003.

Lammers, Michael, Simon Meyer, Dorothee Kühlmann, and Alfred Wittinghofer. 2008. "Specificity of Interactions between MDia Isoforms and Rho Proteins." *Journal of Biological Chemistry* 283 (50): 35236–46. doi:10.1074/jbc.M805634200.

Lammers, Michael, Rolf Rose, Andrea Scrima, and Alfred Wittinghofer. 2005. "The Regulation of MDia1 by Autoinhibition and Its Release by Rho*GTP." *The EMBO Journal* 24 (23): 4176–87. doi:10.1038/sj.emboj.7600879.

Laurent, Valérie, Thomas P. Loisel, Birgit Harbeck, Ann Wehman, Lothar Gröbe, Brigitte M. Jockusch, Jürgen Wehland, Frank B. Gertler, and Marie France Carlier. 1999. "Role of Proteins of the Ena/VASP Family in Actin-Based Motility of Listeria Monocytogenes." *Journal of Cell Biology* 144 (6): 1245–58. doi:10.1083/jcb.144.6.1245.

Laurin, Mélanie, and Jean François Côté. 2014. "Insights into the Biological Functions of Dock

Family Guanine Nucleotide Exchange Factors.” *Genes and Development*. doi:10.1101/gad.236349.113.

Le Clainche, Christophe, and Marie-France Carlier. 2008a. “Regulation of Actin Assembly Associated with Protrusion and Adhesion in Cell Migration.” *Physiological Reviews* 88 (2): 489–513. doi:10.1152/physrev.00021.2007.

———. 2008b. “Regulation of Actin Assembly Associated with Protrusion and Adhesion in Cell Migration.” *Physiological Reviews* 88 (2): 489–513. doi:10.1152/physrev.00021.2007.

Leader, Benjamin, Hyunjung Lim, Mary Jo Carabatsos, Anne Harrington, Jeffrey Ecsedy, David Pellman, Richard Maas, and Philip Leder. 2002. “Formin-2, Polyploidy, Hypofertility and Positioning of the Meiotic Spindle in Mouse Oocytes.” *Nature Cell Biology* 4 (12): 921–28. doi:10.1038/ncb880.

Lebensohn, Andres M., and Marc W. Kirschner. 2009. “Activation of the WAVE Complex by Coincident Signals Controls Actin Assembly.” *Molecular Cell* 36 (3): 512–24. doi:10.1016/j.molcel.2009.10.024.

Lebrand, Cecile, Erik W. Dent, Geraldine A. Strasser, Lorene M. Lanier, Matthias Krause, Tatyana M. Svitkina, Gary G. Borisy, and Frank B. Gertler. 2004. “Critical Role of Ena/VASP Proteins for Filopodia Formation in Neurons and in Function Downstream of Netrin-1.” *Neuron* 42 (1): 37–49. doi:10.1016/S0896-6273(04)00108-4.

Li, Ang, John C. Dawson, Manuel Forero-Vargas, Heather J. Spence, Xinzi Yu, Ireen König, Kurt Anderson, and Laura M. Machesky. 2010a. “The Actin-Bundling Protein Fascin Stabilizes Actin in Invadopodia and Potentiates Protrusive Invasion.” *Current Biology* 20 (4): 339–45. doi:10.1016/j.cub.2009.12.035.

Li, Ang, John C Dawson, Manuel Forero-Vargas, Heather J Spence, Xinzi Yu, Ireen König, Kurt Anderson, and Laura M Machesky. 2010b. “The Actin-Bundling Protein Fascin Stabilizes Actin in Invadopodia and Potentiates Protrusive Invasion.” *Current Biology : CB* 20 (4): 339–45. doi:10.1016/j.cub.2009.12.035.

Linder, S, D Nelson, M Weiss, and M Aepfelbacher. 1999a. “Wiskott-Aldrich Syndrome Protein Regulates Podosomes in Primary Human Macrophages.” *Proceedings of the National Academy of Sciences of the United States of America* 96 (17): 9648–53. doi:10.1073/pnas.96.17.9648.

———. 1999b. “Wiskott-Aldrich Syndrome Protein Regulates Podosomes in Primary Human Macrophages.” *Proceedings of the National Academy of Sciences of the United States of America* 96 (17): 9648–53. http://www.pubmedcentral.nih.gov/articlerender.fcgi?artid=22264&tool=pmcentrez&rendertype=abstract.

Linder, Stefan. 2007. “The Matrix Corroded: Podosomes and Invadopodia in Extracellular Matrix Degradation.” *Trends in Cell Biology*. doi:10.1016/j.tcb.2007.01.002.

———. 2009. “Invadosomes at a Glance.” *Journal of Cell Science* 122: 3009–13. doi:10.1242/jcs.032631.

Linder, Stefan, and Petra Kopp. 2005. “Podosomes at a Glance.” *Journal of Cell Science* 118 (Pt

10): 2079–82. doi:10.1242/jcs.02390.

Linder, Stefan, Christiane Wiesner, and Mirko Himmel. 2011. “Degrading Devices: Invadosomes in Proteolytic Cell Invasion.” *Annual Review of Cell and Developmental Biology* 27 (January): 185–211. doi:10.1146/annurev-cellbio-092910-154216.

Liu, B P, and K Burridge. 2000. “Vav2 Activates Rac1, Cdc42, and RhoA Downstream from Growth Factor Receptors but Not Beta1 Integrins.” *Molecular and Cellular Biology* 20 (19): 7160–69. doi:10.1128/MCB.20.19.7160-7169.2000.Updated.

Liu, Su Ling, Jordan R. May, Luke a. Helgeson, and Brad J. Nolen. 2013. “Insertions within the Actin Core of Actin-Related Protein 3 (Arp3) Modulate Branching Nucleation by Arp2/3 Complex.” *Journal of Biological Chemistry* 288 (1): 487–97. doi:10.1074/jbc.M112.406744.

Lizárraga, Floria, Renaud Poincloux, Maryse Romao, Guillaume Montagnac, Gaëlle Le Dez, Isabelle Bonne, Guillem Rigaill, Graça Raposo, and Philippe Chavrier. 2009. “Diaphanous-Related Formins Are Required for Invadopodia Formation and Invasion of Breast Tumor Cells.” *Cancer Research* 69 (7): 2792–2800. doi:10.1158/0008-5472.CAN-08-3709.

Lizárraga, Floria, Renaud Poincloux, Maryse Romão, Guillaume Montagnac, Gaëlle Le Dez, Isabelle Bonne, Guillem Rigaill, Graça Raposo, and Philippe Chavrier. 2009. “Diaphanous-Related Formins Are Required for Invadopodia Formation and Invasion of Breast Tumor Cells.” *Cancer Research* 69 (7): 2792–2800. doi:10.1158/0008-5472.CAN-08-3709.

Lommel, Silvia, Stefanie Benesch, Klemens Rottner, Thomas Franz, Jürgen Wehland, and Ralf Kühn. 2001. “Actin Pedestal Formation by Enteropathogenic Escherichia Coli and Intracellular Motility of Shigella Flexneri Are Abolished In” 2 (9): 850–57.

Machesky, L M, R D Mullins, H N Higgs, D a Kaiser, L Blanchoin, R C May, M E Hall, and T D Pollard. 1999. “Scar, a WASp-Related Protein, Activates Nucleation of Actin Filaments by the Arp2/3 Complex.” *Proceedings of the National Academy of Sciences of the United States of America* 96 (7): 3739–44. doi:10.1073/pnas.96.7.3739.

Machesky, Laura M., and Robert H. Insall. 1998. “Scar1 and the Related Wiskott–Aldrich Syndrome Protein, WASP, Regulate the Actin Cytoskeleton through the Arp2/3 Complex.” *Current Biology* 8 (25). Elsevier: 1347–56. doi:10.1016/S0960-9822(98)00015-3.

Machesky, Laura M, Simon J Atkinson, Christophe Ampe, and Joel Vandekercldaove. 1994. “Purification of a Cortical Complex Containing Two Unconventional Actins From” 127 (1): 107–15.

Mains, P. E., I. A. Sulston, and W. B. Wood. 1990. “Dominant Maternal-Effect Mutations Causing Embryonic Lethality in Caenorhabditis Elegans.” *Genetics* 125 (2): 351–69. doi:10.1091/mbc.E05.

Mass, R L, R Zeller, R P Woychik, T F Vogt, and P Leder. 1990. “Disruption of Formin-Encoding Transcripts in Two Mutant Limb Deformity Alleles.” *Nature* 346: 853–55. doi:10.1038/346853a0.

Meller, Nahum, Mohammad Irani-Tehrani, William B Kiosses, Miguel a Del Pozo, and Martin a Schwartz. 2002a. “Zizimin1, a Novel Cdc42 Activator, Reveals a New GEF Domain for Rho Proteins.” *Nature Cell Biology* 4 (9): 639–47. doi:10.1038/ncb835.

———. 2002b. “Zizimin1, a Novel Cdc42 Activator, Reveals a New GEF Domain for Rho Proteins.” *Nature Cell Biology* 4 (9): 639–47. doi:10.1038/ncb835.

Mellor, Harry. 2010a. “The Role of Formins in Filopodia Formation.” *Biochimica et Biophysica Acta - Molecular Cell Research* 1803 (2). Elsevier B.V.: 191–200. doi:10.1016/j.bbamcr.2008.12.018.

———. 2010b. “The Role of Formins in Filopodia Formation.” *Biochimica et Biophysica Acta* 1803 (2). Elsevier B.V.: 191–200. doi:10.1016/j.bbamcr.2008.12.018.

Merlot, Sylvain, and Richard a Firtel. 2003. “Leading the Way: Directional Sensing through Phosphatidylinositol 3-Kinase and Other Signaling Pathways.” *Journal of Cell Science* 116 (Pt 17): 3471–78. doi:10.1242/jcs.00703.

Mersich, Akos T., Matthew R. Miller, Halina Chkourko, and Scott D. Blystone. 2010. “The Formin FRL1 (FMNL1) Is an Essential Component of Macrophage Podosomes.” *Cytoskeleton* 67 (9): 573–85. doi:10.1002/cm.20468.

Michaelson, David, Joseph Silletti, Gretchen Murphy, Peter D’Eustachio, Mark Rush, and Mark R. Philips. 2001. “Differential Localization of Rho GTPases in Live Cells: Regulation by Hypervariable Regions and RhoGDI Binding.” *Journal of Cell Biology* 152 (1): 111–26. doi:10.1083/jcb.152.1.111.

Miki, H, K Miura, and T Takenawa. 1996. “N-WASP, a Novel Actin-Depolymerizing Protein, Regulates the Cortical Cytoskeletal Rearrangement in a PIP2-Dependent Manner Downstream of Tyrosine Kinases.” *The EMBO Journal* 15 (19): 5326–35.

Miki, H, S Suetsugu, and T Takenawa. 1998. “WAVE, a Novel WASP-Family Protein Involved in Actin Reorganization Induced by Rac.” *The EMBO Journal* 17 (23): 6932–41. doi:10.1093/emboj/17.23.6932.

Mogilner, Alex. 2006. “On the Edge: Modeling Protrusion.” *Current Opinion in Cell Biology*. doi:10.1016/j.ceb.2005.11.001.

Mogilner, Alexander, and B Rubinstein. 2005. “The Physics of Filopodial Protrusion.” *Biophysical Journal* 89 (2): 782–95. doi:10.1529/biophysj.104.056515.

Monypenny, James, Hsiu Chuan Chou, Inmaculada Bañón-Rodríguez, Adrian J. Thrasher, Inés M. Antón, Gareth E. Jones, and Yolanda Calle. 2011. “Role of WASP in Cell Polarity and Podosome Dynamics of Myeloid Cells.” *European Journal of Cell Biology*. doi:10.1016/j.ejcb.2010.05.009.

Monypenny, James, Daniel Zicha, Chiharu Higashida, Fabian Oceguera-yanez, Shuh Narumiya, and Naoki Watanabe. 2009. “Cdc42 and Rac Family GTPases Regulate Mode and Speed but Not Direction of Primary Fibroblast Migration during Platelet-Derived” 29 (10): 2730–47. doi:10.1128/MCB.01285-08.

Monypenny, James, Daniel Zicha, Chiharu Higashida, Fabian Oceguera-Yanez, Shuh Narumiya, and Naoki Watanabe. 2009. “Cdc42 and Rac Family GTPases Regulate Mode and Speed but Not Direction of Primary Fibroblast Migration during Platelet-Derived Growth Factor-Dependent Chemotaxis.” *Molecular and Cellular Biology* 29 (10): 2730–47. doi:10.1128/MCB.01285-08.

Mullins, R. Dyche, Walter F. Stafford, and Thomas D. Pollard. 1997. “Structure, Subunit Topology, and Actin-Binding Activity of the Arp2/3 Complex from Acanthamoeba.” *Journal of Cell Biology* 136 (2): 331–43. doi:10.1083/jcb.136.2.331.

Mullins, R D, J F Kelleher, J Xu, and Thomas D. Pollard. 1998. “Arp2/3 Complex from Acanthamoeba Binds Profilin and Cross-Links Actin Filaments.” *Molecular Biology of the Cell* 9 (4): 841–52. doi:10.1091/mbc.9.4.841.

Murphy, Danielle A, and Sara A Courtneidge. 2011a. “The ‘ins’ and ‘Outs’ of Podosomes and Invadopodia: Characteristics, Formation and Function.” *Nature Reviews. Molecular Cell Biology* 12 (7): 413–26. doi:10.1038/nrm3141.

———. 2011b. “The ‘ins’ and ‘Outs’ of Podosomes and Invadopodia: Characteristics, Formation and Function.” *Nature Reviews. Molecular Cell Biology* 12 (7): 413–26. doi:10.1038/nrm3141.

Murphy, G a, S a Jillian, D Michaelson, M R Philips, P D’Eustachio, and M G Rush. 2001. “Signaling Mediated by the Closely Related Mammalian Rho Family GTPases TC10 and Cdc42 Suggests Distinct Functional Pathways.” *Cell Growth & Differentiation : The Molecular Biology Journal of the American Association for Cancer Research* 12 (3): 157–67.

Nakahara, H, L Howard, E W Thompson, H Sato, M Seiki, Y Yeh, and W T Chen. 1997. “Transmembrane/Cytoplasmic Domain-Mediated Membrane Type 1-Matrix Metalloprotease Docking to Invadopodia Is Required for Cell Invasion.” *Proceedings of the National Academy of Sciences of the United States of America* 94 (15): 7959–64. doi:10.1073/pnas.94.15.7959.

Nemethova, Maria, Sonja Auinger, and J Victor Small. 2008. “Building the Actin Cytoskeleton: Filopodia Contribute to the Construction of Contractile Bundles in the Lamella.” *The Journal of Cell Biology* 180 (6): 1233–44. doi:10.1083/jcb.200709134.

Neudauer, Cheryl L., Gérard Joberty, Nia Tatsis, and Ian G. Macara. 1998. “Distinct Cellular Effects and Interactions of the Rho-Family GTPase TC10.” *Current Biology* 8 (21): 1151–61. doi:10.1016/S0960-9822(07)00486-1.

Nimnual, A S, B A Yatsula, and D Bar-Sagi. 1998. “Coupling of Ras and Rac Guanosine Triphosphatases through the Ras Exchanger Sos.” *Science (New York, N.Y.)* 279 (5350): 560–63. doi:10.1126/science.279.5350.560.

Niwa, Ryusuke, Kyoko Nagata-Ohashi, Masatoshi Takeichi, Kensaku Mizuno, and Tadashi Uemura. 2002. “Control of Actin Reorganization by Slingshot, a Family of Phosphatases That Dephosphorylate ADF/Cofilin.” *Cell* 108 (2): 233–46. doi:10.1016/S0092-8674(01)00638-9.

Nobes, C D, and a Hall. 1995. “Rho, Rac, and Cdc42 GTPases Regulate the Assembly of Multimolecular Focal Complexes Associated with Actin Stress Fibers, Lamellipodia, and Filopodia.” *Cell* 81 (1): 53–62. doi:10.1016/0092-8674(95)90370-4.

Nobes, C D, and A Hall. 1999. “Rho GTPases Control Polarity, Protrusion, and Adhesion during Cell Movement.” *The Journal of Cell Biology* 144 (6): 1235–44.

doi:10.1083/jcb.144.6.1235.

Nobes, Catherine D, and Alan Hall. 1995a. “Rho , Rac , and Cdc42 GTPases Regulate the Assembly of Multimolecular Focal Complexes Associated with Actin Stress Fibers , Lamellipodia , and Filopodia” 81: 53–62.

———. 1995b. “Rho, Rac, and Cdc42 GTPases Regulate the Assembly of Multimolecular Focal Complexes Associated with Actin Stress Fibers, Lamellipodia, and Filopodia.” *Cell* 81 (1): 53–62. doi:10.1016/0092-8674(95)90370-4.

———. 1999. “Rho GTPases Control Polarity, Protrusion, and Adhesion during Cell Movement” 144 (6): 1235–44.

Nolen, B J, N Tomasevic, A Russell, D W Pierce, Z Jia, C D McCormick, J Hartman, R Sakowicz, and T D Pollard. 2009a. “Characterization of Two Classes of Small Molecule Inhibitors of Arp2/3 Complex.” *Nature* 460 (7258): 1031–34. doi:10.1038/nature08231.

———. 2009b. “Characterization of Two Classes of Small Molecule Inhibitors of Arp2/3 Complex.” *Nature* 460 (7258): 1031–34. doi:10.1038/nature08231.

Oakes, Patrick W, Yvonne Beckham, Jonathan Stricker, and Margaret L Gardel. 2012. “Tension Is Required but Not Sufficient for Focal Adhesion Maturation without a Stress Fiber Template.” *The Journal of Cell Biology* 196 (3): 363–74. doi:10.1083/jcb.201107042.

Ochs, Hans D, and Luigi D Notarangelo. 2005. “Structure and Function of the Wiskott-Aldrich Syndrome Protein.” *Current Opinion in Hematology* 12 (4): 284–91. doi:10.1097/01.moh.0000168520.98990.19.

Olofsson, Birgitta. 1999. “Rho Guanine Dissociation Inhibitors: Pivotal Molecules in Cellular Signalling.” *Cellular Signalling*. doi:10.1016/S0898-6568(98)00063-1.

Orth, James D., and Mark a. McNiven. 2006a. “Get off My Back! Rapid Receptor Internalization through Circular Dorsal Ruffles.” *Cancer Research* 66 (23): 11094–96. doi:10.1158/0008-5472.CAN-06-3397.

Orth, James D, and Mark a McNiven. 2006b. “Get off My Back! Rapid Receptor Internalization through Circular Dorsal Ruffles.” *Cancer Research* 66 (23): 11094–96. doi:10.1158/0008-5472.CAN-06-3397.

Otomo, Takanori, Diana R Tomchick, Chinatsu Otomo, Sanjay C Panchal, Mischa Machius, and Michael K Rosen. 2005. “Structural Basis of Actin Filament Nucleation and Processive Capping by a Formin Homology 2 Domain.” *Nature* 433 (7025): 488–94. doi:10.1107/S0108767305096844.

Otto, Joann J., Robert E. Kane, and Joseph Bryan. 1979. “Formation of Filopodia in Coelomocytes: Localization of Fascin, a 58,000 Dalton Actin Cross-Linking Protein.” *Cell* 17 (2): 285–93. doi:10.1016/0092-8674(79)90154-5.

Palazzo, Alexander F., Hazel L. Joseph, Ying Jiun Chen, Denis L. Dujardin, Arthur S. Alberts, K. Kevin Pfister, Richard B. Vallee, and Gregg G. Gundersen. 2001. “Cdc42, Dynein, and Dynactin Regulate MTOC Reorientation Independent of Rho-Regulated Microtubule Stabilization.” *Current Biology* 11 (19): 1536–41. doi:10.1016/S0960-9822(01)00475-4.

Paluch, Ewa K, and Erez Raz. 2013. “The Role and Regulation of Blebs in Cell Migration.” *Current Opinion in Cell Biology* 25 (5). Elsevier Ltd: 582–90. doi:10.1016/j.ceb.2013.05.005.

Pankov, Roumen, Yukinori Endo, Sharona Even-Ram, Masaru Araki, Katherine Clark, Edna Cukierman, Kazue Matsumoto, and Kenneth M Yamada. 2005. “A Rac Switch Regulates Random versus Directionally Persistent Cell Migration.” *The Journal of Cell Biology* 170 (5): 793–802. doi:10.1083/jcb.200503152.

Parent, Carole A, and Peter N Devreotes. 1999a. “A Cell’s Sense of Direction.” *Science* 284 (5415): 765–70. doi:10.1126/science.284.5415.765.

———. 1999b. “A Cell’s Sense of Direction.” *Science* 284 (5415): 765–70. doi:10.1126/science.284.5415.765.

Park, Haein, and Dianne Cox. 2009. “Cdc42 Regulates Fc ✐ Receptor-Mediated Phagocytosis through the Activation and Phosphorylation of Wiskott-Aldrich Syndrome Protein (WASP) and Neural-WASP” 20: 4500–4508. doi:10.1091/mbc.E09.

Park, Heon, Maia M Chan, and Brian M Iritani. 2010a. “Hem-1: Putting the ‘WAVE’ into Actin Polymerization during an Immune Response.” *FEBS Letters* 584 (24). Federation of European Biochemical Societies: 4923–32. doi:10.1016/j.febslet.2010.10.018.

———. 2010b. “Hem-1: Putting the ‘WAVE’ into Actin Polymerization during an Immune Response.” *FEBS Letters* 584 (24). Federation of European Biochemical Societies: 4923–32. doi:10.1016/j.febslet.2010.10.018.

Park, Heon, Karen Staehling-Hampton, Mark W Appleby, Mary E Brunkow, Tania Habib, Yi Zhang, Fred Ramsdell, et al. 2008a. “A Point Mutation in the Murine Hem1 Gene Reveals an Essential Role for Hematopoietic Protein 1 in Lymphopoiesis and Innate Immunity.” *The Journal of Experimental Medicine* 205 (12): 2899–2913. doi:10.1084/jem.20080340.

———. 2008b. “A Point Mutation in the Murine Hem1 Gene Reveals an Essential Role for Hematopoietic Protein 1 in Lymphopoiesis and Innate Immunity.” *The Journal of Experimental Medicine* 205 (12): 2899–2913. doi:10.1084/jem.20080340.

———. 2008c. “A Point Mutation in the Murine Hem1 Gene Reveals an Essential Role for Hematopoietic Protein 1 in Lymphopoiesis and Innate Immunity.” *The Journal of Experimental Medicine* 205 (12): 2899–2913. doi:10.1084/jem.20080340.

Partridge, M. A., and Eugene E. Marcantonio. 2006. “Initiation of Attachment and Generation of Mature Focal Adhesions by Integrin-Containing Filopodia in Cell Spreading.” *Molecular Biology of the Cell* 17 (10): 4237–48. doi:10.1091/mbc.E06-06-0496.

Pellegrin, Stéphanie, and Harry Mellor. 2005. “The Rho Family GTPase Rif Induces Filopodia through MDia2.” *Current Biology* 15: 129–33. doi:10.1016/j.cub.2005.01.011.

———. 2007. “Actin Stress Fibres.” *Journal of Cell Science* 120 (Pt 20): 3491–99. doi:10.1242/jcs.018473.

Peng, Jun, Bradley J Wallar, Akiko Flanders, Pamela J Swiatek, Arthur S Alberts, and Grand Rapids. 2003. “Disruption of the Diaphanous-Related Formin Drf1 Gene Encoding MDia1

Reveals a Role for Drf3 as an Effector for Cdc42" 13: 534–45. doi:10.1016/S.

Pertz, Olivier, Louis Hodgson, Richard L Klemke, and Klaus M Hahn. 2006. "Spatiotemporal Dynamics of RhoA Activity in Migrating Cells." *Nature* 440 (7087): 1069–72. doi:10.1038/nature04665.

Peskin, C S, G M Odell, and G F Oster. 1993. "Cellular Motions and Thermal Fluctuations: The Brownian Ratchet." *Biophysical Journal* 65 (1): 316–24. doi:10.1016/S0006-3495(93)81035-X.

Petrie, Ryan J, Núria Gavara, Richard S Chadwick, and Kenneth M Yamada. 2012. "Nonpolarized Signaling Reveals Two Distinct Modes of 3D Cell Migration." *The Journal of Cell Biology* 197 (3): 439–55. doi:10.1083/jcb.201201124.

Petrie, Ryan J, and Kenneth M Yamada. 2012. "At the Leading Edge of Three-Dimensional Cell Migration." *Journal of Cell Science* 125 (Pt 24): 5917–26. doi:10.1242/jcs.093732.

Philippar, Ulrike, Evanthia T. Roussos, Matthew Oser, Hideki Yamaguchi, Hyung-Do Kim, Silvia Giampieri, Yarong Wang, et al. 2008a. "A Mena Invasion Isoform Potentiates EGF-Induced Carcinoma Cell Invasion and Metastasis." *Developmental Cell* 15 (6): 813–28. doi:10.1016/j.devcel.2008.09.003.

———. 2008b. "A Mena Invasion Isoform Potentiates EGF-Induced Carcinoma Cell Invasion and Metastasis." *Developmental Cell* 15 (6): 813–28. doi:10.1016/j.devcel.2008.09.003.

Philippar, Ulrike, Evanthia T Roussos, Matthew Oser, Hideki Yamaguchi, Do Kim, Silvia Giampieri, Yarong Wang, et al. 2009. "NIH Public Access" 15 (6): 813–28. doi:10.1016/j.devcel.2008.09.003.A.

Plattner, Rina, Lisa Kadlec, Kris A Demali, Andrius Kazlauskas, and Ann Marie Pendergast. 1999. "Role in the Cellular Response to PDGF C-Abl Is Activated by Growth Factors and Src Family Kinases and Has a Role in the Cellular Response to PDGF," 2400–2411. doi:10.1101/gad.13.18.2400.

Poincloux, Renaud, Floria Lizárraga, and Philippe Chavrier. 2009. "Matrix Invasion by Tumour Cells: A Focus on MT1-MMP Trafficking to Invadopodia." *Journal of Cell Science* 122 (Pt 17): 3015–24. doi:10.1242/jcs.034561.

Pollard, T D, and J a Cooper. 1984. "Quantitative Analysis of the Effect of Acanthamoeba Profilin on Actin Filament Nucleation and Elongation." *Biochemistry* 23 (26): 6631–41. doi:10.1021/bi00321a054.

Pollard, TD. 1986. "Rate Constants for the Reactions of ATP-and ADP-Actin with the Ends of Actin Filaments." *Journal of Cell Biology* 103: 2747.

Pollard, Thomas D., and Gary G. Borisy. 2003. "Cellular Motility Driven by Assembly and Disassembly of Actin Filaments." *Cell*. doi:10.1016/S0092-8674(03)00120-X.

Pollard, Thomas D., and Alan G. Weeds. 1984. "The Rate Constant for ATP Hydrolysis by Polymerized Actin." *FEBS Letters* 170 (1): 94–98. doi:10.1016/0014-5793(84)81376-9.

Pollard, Thomas D, and John a Cooper. 2009. "Actin, a Central Player in Cell Shape and Movement." *Science (New York, N.Y.)* 326 (5957): 1208–12. doi:10.1126/science.1175862.

Pruyne, David, David Pruyne, Marie Evangelista, Changsong Yang, and Erfei Bi. 2007. “Role of Formins in Actin Assembly : Nucleation and Barbed-End Association” 612 (2002). doi:10.1126/science.1072309.

Qiao, Jing, Oksana Holian, Bao-Shiang Lee, Fei Huang, Jihang Zhang, and Hazel Lum. 2008. “Phosphorylation of GTP Dissociation Inhibitor by PKA Negatively Regulates RhoA.” *American Journal of Physiology. Cell Physiology* 295 (5): C1161–68. doi:10.1152/ajpcell.00139.2008.

Quintavalle, Manuela, Leonardo Elia, Gianluigi Condorelli, and Sara a Courtneidge. 2010. “MicroRNA Control of Podosome Formation in Vascular Smooth Muscle Cells in Vivo and in Vitro.” *The Journal of Cell Biology* 189 (1): 13–22. doi:10.1083/jcb.200912096.

Raftopoulou, Myrto, and Alan Hall. 2004a. “Cell Migration: Rho GTPases Lead the Way.” *Dev Biol* 265 (1): 23–32. doi:10.1016/j.ydbio.2003.06.003.

———. 2004b. “Cell Migration: Rho GTPases Lead the Way.” *Dev Biol* 265 (1): 23–32. doi:10.1016/j.ydbio.2003.06.003.

———. 2004c. “Cell Migration: Rho GTPases Lead the Way.” *Developmental Biology* 265 (1): 23–32. doi:10.1016/j.ydbio.2003.06.003.

Reinhard, Matthias, Maria Halbrugge, Ulrich Scheer, Christiane Wiegand, Brigitte M Jockusch, and Ulrich Walter. 1992. “Human Platelets Is a Novel Protein Associated with Actin Filaments and Focal Contacts” 1 (6): 2063–70.

Renkawitz, Jörg, Kathrin Schumann, Michele Weber, Tim Lämmermann, Holger Pflicke, Matthieu Piel, Julien Polleux, Joachim P Spatz, and Michael Sixt. 2009a. “Adaptive Force Transmission in Amoeboid Cell Migration.” *Nature Cell Biology* 11 (12): 1438–43. doi:10.1038/ncb1992.

———. 2009b. “Adaptive Force Transmission in Amoeboid Cell Migration.” *Nature Cell Biology* 11 (12). Nature Publishing Group: 1438–43. doi:10.1038/ncb1992.

Ridley, Anne J. 2001. “Rho Proteins, PI 3-Kinases, and Monocyte/Macrophage Motility.” *FEBS Letters* 498 (2–3): 168–71. doi:10.1016/S0014-5793(01)02481-4.

Riedl, Julia. 2010. “Development and Characterization of Lifeact - a Versatile Marker for the Visualization of F-Actin -.”

Riedl, Julia, Alvaro H Crevenna, Kai Kessenbrock, Jerry Haochen Yu, Dorothee Neukirchen, Michal Bista, Frank Bradke, et al. 2008. “Lifeact: A Versatile Marker to Visualize F-Actin.” *Nature Methods* 5 (7): 605–7. doi:10.1038/nmeth.1220.

Riquelme, Daisy N, Aaron S Meyer, Melanie Barzik, Amy Keating, and Frank B Gertler. 2015. “Selectivity in Subunit Composition of Ena / VASP Tetramers,” 1–15. doi:10.1042/BSR20150149.

Rizvi, Syed a, Erin M Neidt, Jiayue Cui, Zach Feiger, Colleen T Skau, Margaret L Gardel, Sergey a Kozmin, and David R Kovar. 2009a. “Identification and Characterization of a Small Molecule Inhibitor of Formin-Mediated Actin Assembly.” *Chemistry & Biology* 16 (11). Elsevier Ltd: 1158–68. doi:10.1016/j.chembiol.2009.10.006.

———. 2009b. “Identification and Characterization of a Small Molecule Inhibitor of Formin-Mediated Actin Assembly.” *Chemistry & Biology* 16 (11). Elsevier Ltd: 1158–68. doi:10.1016/j.chembiol.2009.10.006.

Rizvi, Syed A, Erin M Neidt, Jiayue Cui, Zach Feiger, Colleen T Skau, Margaret L Gardel, Sergey A Kozmin, and David R Kovar. 2009. “Identification and Characterization of a Small Molecule Inhibitor of Formin-Mediated Actin Assembly.” *Chemistry & Biology* 16 (11). Elsevier Ltd: 1158–68. doi:10.1016/j.chembiol.2009.10.006.

Rohatgi, Rajat, Le Ma, Hiroaki Miki, Marco Lopez, Tomas Kirchhausen, Tadaomi Takenawa, and Marc W Kirschner. 1999a. “The Interaction between N-WASP and the Arp2/3 Complex Links Cdc42-Dependent Signals to Actin Assembly.” *Cell* 97 (2): 221–31. doi:10.1016/S0092-8674(00)80732-1.

———. 1999b. “The Interaction between N-WASP and the Arp2/3 Complex Links Cdc42-Dependent Signals to Actin Assembly.” *Cell* 97 (2): 221–31. doi:10.1016/S0092-8674(00)80732-1.

Rossman, Kent L., Channing J. Der, and John Sondek. 2005. “GEF Means Go: Turning on Rho GTPases with Guanine Nucleotide-Exchange Factors.” *Nature Reviews Molecular Cell Biology* 6 (2): 167–80. doi:10.1038/nrm1587.

Rottner, Klemens, Barbara Behrendt, J.Victor Small, and Jurgen Wehland. 1999a. “VASP Dynamics during Lamellipodia Protrusion .” *Nat Cell Biol* 1 (5). Macmillan Magazines Ltd.: 321–22. http://dx.doi.org/10.1038/13040.

———. 1999b. “VASP Dynamics during Lamellipodia Protrusion .” *Nat Cell Biol* 1 (5). Macmillan Magazines Ltd.: 321–22.

Rottner, Klemens, and Theresia E B Stradal. 2011a. “Actin Dynamics and Turnover in Cell Motility.” *Current Opinion in Cell Biology* 23 (5). Elsevier Ltd: 569–78. doi:10.1016/j.ceb.2011.07.003.

———. 2011b. “Actin Dynamics and Turnover in Cell Motility.” *Current Opinion in Cell Biology* 23 (5). Elsevier Ltd: 569–78. doi:10.1016/j.ceb.2011.07.003.

———. 2011c. “Actin Dynamics and Turnover in Cell Motility.” *Current Opinion in Cell Biology* 23 (5). Elsevier Ltd: 569–78. doi:10.1016/j.ceb.2011.07.003.

Rougerie, Pablo. 2013. “Generation of Membrane Structures during Phagocytosis and Chemotaxis of Macrophages : Role and Regulation of the Actin Cytoskeleton” 256: 222–39.

Rouiller, Isabelle, Xiao Ping Xu, Kurt J. Amann, Coumaran Egile, Stephan Nickell, Daniela Nicastro, Rong Li, Thomas D. Pollard, Niels Volkmann, and Dorit Hanein. 2008. “The Structural Basis of Actin Filament Branching by the Arp2/3 Complex.” *Journal of Cell Biology* 180 (5): 887–95. doi:10.1083/jcb.200709092.

Rudolph, Markus G., Peter Bayer, Arie Abo, Juergen Kuhlmann, Ingrid R. Vetter, and Alfred Wittinghofer. 1998. “The Cdc42/Rac Interactive Binding Region Motif of the Wiskott Aldrich Syndrome Protein (WASP) in Necessary but Not Sufficient for Tight Binding to Cdc42 and Structure Formation.” *Journal of Biological Chemistry* 273 (29): 18067–76. doi:10.1074/jbc.273.29.18067.

Sabeh, Farideh, Ichiro Ota, Kenn Holmbeck, Henning Birkedal-Hansen, Paul Soloway, Milagros Balbin, Carlos Lopez-Otin, et al. 2004. “Tumor Cell Traffic through the Extracellular Matrix Is Controlled by the Membrane-Anchored Collagenase MT1-MMP.” *Journal of Cell Biology* 167 (4): 769–81. doi:10.1083/jcb.200408028.

Sahai, Erik, and Christopher J Marshall. 2003. “Differing Modes of Tumour Cell Invasion Have Distinct Requirements for Rho/ROCK Signalling and Extracellular Proteolysis.” *Nature Cell Biology* 5 (8): 711–19.

Sakata, Daiji, Hiroyuki Taniguchi, Shingo Yasuda, Aki Adachi-Morishima, Yoko Hamazaki, Rika Nakayama, Takashi Miki, Nagahiro Minato, and Shuh Narumiya. 2007. “Impaired T Lymphocyte Trafficking in Mice Deficient in an Actin-Nucleating Protein, MDia1.” *J Exp Med* 204 (9): 2031–38. doi:10.1084/jem.20062647.

Sakurai-Yageta, Mika, Chiara Recchi, Gaëlle Le Dez, Jean Baptiste Sibarita, Laurent Daviet, Jacques Camonis, Crislyn D’Souza-Schorey, and Philippe Chavrier. 2008. “The Interaction of IQGAP1 with the Exocyst Complex Is Required for Tumor Cell Invasion Downstream of Cdc42 and RhoA.” *Journal of Cell Biology* 181 (6): 985–98. doi:10.1083/jcb.200709076.

Sandoval, I. V., J. S. Bonifacino, R. D. Klausner, M. Henkart, and J. Wehland. 1984. “Role of Microtubules in the Organization and Localization of the Golgi Apparatus.” *Journal of Cell Biology* 99 (1 II).

Sasaki, Y, K Hayashi, T Shirao, R Ishikawa, and K Kohama. 1996. “Inhibition by Drebrin of the Actin-Bundling Activity of Brain Fascin, a Protein Localized in Filopodia of Growth Cones.” *J Neurochem* 66 (3): 980–88. doi:10.1046/j.1471-4159.1996.66030980.x.

Schafer, Dorothy A., Phillip B. Jennings, and John A. Cooper. 1996. “Dynamics of Capping Protein and Actin Assembly in Vitro: Uncapping Barbed Ends by Polyphosphoinositides.” *Journal of Cell Biology* 135 (1): 169–79. doi:10.1083/jcb.135.1.169.

Schirenbeck, Antje, Rajesh Arasada, Till Bretschneider, Theresia E B Stradal, Michael Schleicher, and Jan Faix. 2006. “The Bundling Activity of Vasodilator-Stimulated Phosphoprotein Is Required for Filopodium Formation.”

Schmidt, Anja, and Alan Hall. 2002. “Guanine Nucleotide Exchange Factors for Rho GTPases : Turning on the Switch,” 1587–1609. doi:10.1101/gad.1003302.GENES.

Schneider, Ian C, and Jason M Haugh. 2005. “Quantitative Elucidation of a Distinct Spatial Gradient-Sensing Mechanism in Fibroblasts.” *The Journal of Cell Biology* 171 (5): 883–92. doi:10.1083/jcb.200509028.

Schonichen, A., M. Alexander, J. E. Gasteier, F. E. Cuesta, O. T. Fackler, and M. Geyer. 2006. “Biochemical Characterization of the Diaphanous Autoregulatory Interaction in the Formin Homology Protein FHOD1.” *Journal of Biological Chemistry* 281 (8): 5084–93. doi:10.1074/jbc.M509226200.

Schönichen, André, and Matthias Geyer. 2010. “Fifteen Formins for an Actin Filament: A Molecular View on the Regulation of Human Formins.” *Biochimica et Biophysica Acta - Molecular Cell Research* 1803 (2). Elsevier B.V.: 152–63. doi:10.1016/j.bbamcr.2010.01.014.

Schoumacher, Marie, Robert D Goldman, Daniel Louvard, and Danijela M Vignjevic. 2010. "Actin, Microtubules, and Vimentin Intermediate Filaments Cooperate for Elongation of Invadopodia." *The Journal of Cell Biology* 189 (3): 541–56. doi:10.1083/jcb.200909113.

Schoumacher, Marie, Daniel Louvard, and Danijela Vignjevic. 2011. "Cytoskeleton Networks in Basement Membrane Transmigration." *European Journal of Cell Biology* 90 (2–3). Elsevier GmbH.: 93–99. doi:10.1016/j.ejcb.2010.05.010.

Schuh, M. 2011. "An Actin-Dependent Mechanism for Long-Range Vesicle Transport." *Nat Cell Biol* 13 (12): 1431–36. doi:10.1038/ncb2353.

Schwartz, Martin Alexander. 2011. "Super-Resolution Microscopy: A New Dimension in Focal Adhesions." *Current Biology : CB* 21 (3). Elsevier Ltd: R115-6. doi:10.1016/j.cub.2010.12.025.

Schwob, E, and R P Martin. 1992. "New Yeast Actin-like Gene Required Late in the Cell Cycle." *Nature* 355 (6356): 179–82. doi:10.1038/355179a0.

Self-assembly, Collagen. 1981. "N Vitro" 256 (14): 7118–28.

Seth, Abhinav, Chinatsu Otomo, and Michael K. Rosen. 2006. "Autoinhibition Regulates Cellular Localization and Actin Assembly Activity of the Diaphanous-Related Formins FRL?? And MDia1." *Journal of Cell Biology* 174 (5): 701–13. doi:10.1083/jcb.200605006.

Shefcyk, J., R. Yassin, M. Volpi, T. F P Molski, P. H. Naccache, J. J. Munoz, E. L. Becker, M. B. Feinstein, and R. I. Sha'afi. 1985. "Pertussis but Not Cholera Toxin Inhibits the Stimulated Increase in Actin Association with the Cytoskeleton in Rabbit Neutrophils: Role of the 'G Proteins' in Stimulus-Response Coupling." *Biochemical and Biophysical Research Communications* 126 (3): 1174–81. doi:10.1016/0012-1606(82)90376-1.

Shinohara, Masahiro, Yoh Terada, Akihiro Iwamatsu, Azusa Shinohara, Naoki Mochizuki, Maiko Higuchi, Yukiko Gotoh, et al. 2002. "SWAP-70 Is a Guanine-Nucleotide-Exchange Factor That Mediates Signalling of Membrane Ruffling." *Nature* 416 (6882): 759–63. doi:10.1038/416759a.

Sixt, Michael. 2012. "Cell Migration: Fibroblasts Find a New Way to Get Ahead." *The Journal of Cell Biology* 197 (3): 347–49. doi:10.1083/jcb.201204039.

Small, J. Victor, and Guenter P. Resch. 2005. "The Comings and Goings of Actin: Coupling Protrusion and Retraction in Cell Motility." *Current Opinion in Cell Biology*. doi:10.1016/j.ceb.2005.08.004.

Small, J.Victor, Theresia Stradal, Emmanuel Vignal, and Klemens Rottner. 2002a. "The Lamellipodium: Where Motility Begins." *Trends in Cell Biology* 12 (3): 112–20. doi:10.1016/S0962-8924(01)02237-1.

Small, J Victor, and Klemens Rottner. 2010. *Actin-Based Motility*. doi:10.1007/978-90-481-9301-1.

Small, J Victor, Theresia Stradal, Emmanuel Vignal, and Klemens Rottner. 2002b. "The Lamellipodium : Where Motility Begins" 12 (3): 112–20.

Snapper, S B, F Takeshima, I Antón, C H Liu, S M Thomas, D Nguyen, D Dudley, et al. 2001.

"N-WASP Deficiency Reveals Distinct Pathways for Cell Surface Projections and Microbial Actin-Based Motility." *Nature Cell Biology* 3 (10): 897–904. doi:10.1038/ncb1001-897.

Soisson, Stephen M., Anjaruwee S. Nimnual, Marc Uy, Dafna Bar-Sagi, and John Kuriyan. 1998. "Crystal Structure of the Dbl and Pleckstrin Homology Domains from the Human Son of Sevenless Protein." *Cell* 95 (2): 259–68. doi:10.1016/S0092-8674(00)81756-0.

Spiering, Désirée, and Louis Hodgson. 2011. "Dynamics of the Rho-Family Small GTPases in Actin Regulation and Motility." *Cell Adhesion and Migration* 5 (2): 170–80. doi:10.4161/cam.5.2.14403.

Spillane, Mirela, and Gianluca Gallo. 2014. "Involvement of Rho-Family GTPases in Axon Branching." *Small GTPases* 5 (March): e27974. doi:10.4161/sgtp.27974.

Srichai, Manakan Betsy, and Roy Zent. 2010. "Cell-Extracellular Matrix Interactions in Cancer." Edited by Roy Zent and Ambra Pozzi. New York, NY: Springer New York. doi:10.1007/978-1-4419-0814-8.

Steffen, Anika, Jan Faix, Guenter P Resch, Joern Linkner, Juergen Wehland, J Victor Small, Klemens Rottner, and Theresia E B Stradal. 2006. "Filopodia Formation in the Absence of Functional WAVE- and Arp2/3-Complexes." *Molecular Biology of the Cell* 17 (6): 2581–91. doi:10.1091/mbc.E05.

Steffen, Anika, Markus Ladwein, Georgi a Dimchev, Anke Hein, Lisa Schwenkmezger, Stefan Arens, Kathrin I Ladwein, J Margit Holleboom, et al. 2013. "Rac Function Is Crucial for Cell Migration but Is Not Required for Spreading and Focal Adhesion Formation." *Journal of Cell Science* 126 (Pt 20): 4572–88. doi:10.1242/jcs.118232.

Steffen, Anika, Markus Ladwein, Georgi A Dimchev, Anke Hein, Lisa Schwenkmezger, Stefan Arens, Kathrin I Ladwein, J Margit Holleboom, et al. 2013. "Rac Function Is Critical for Cell Migration but Not Required for Spreading and Focal Adhesion Formation," no. July.

Steffen, Anika, Gaëlle Le Dez, Renaud Poincloux, Chiara Recchi, Pierre Nassoy, Klemens Rottner, Thierry Galli, and Philippe Chavrier. 2008. "MT1-MMP-Dependent Invasion Is Regulated by TI-VAMP/VAMP7." *Current Biology : CB* 18 (12): 926–31. doi:10.1016/j.cub.2008.05.044.

Steffen, Anika, Klemens Rottner, Julia Ehinger, Metello Innocenti, Giorgio Scita, Jürgen Wehland, and Theresia E B Stradal. 2004a. "Sra-1 and Nap1 Link Rac to Actin Assembly Driving Lamellipodia Formation." *The EMBO Journal* 23 (4): 749–59. doi:10.1038/sj.emboj.7600084.

———. 2004b. "Sra-1 and Nap1 Link Rac to Actin Assembly Driving Lamellipodia Formation." *The EMBO Journal* 23 (4): 749–59. doi:10.1038/sj.emboj.7600084.

Stephens, Len, Laura Milne, and Phillip Hawkins. 2008. "Moving towards a Better Understanding of Chemotaxis." *Current Biology* 18 (11): 485–94. doi:10.1016/j.cub.2008.04.048.

Storz, Peter, Mammalian Enabled, and Protein Kinase. 2010. "Regulation of VASP by Phosphorylation:" 7 (6): 1–5. http://www.ncbi.nlm.nih.gov/pmc/articles/PMC2889963/pdf/cib0302_0101.pdf%5Cnpapers

3://publication/uuid/89931764-1777-4199-A230-523B6FEF1D33.

Stovold, Craig F, Thomas H Millard, and Laura M Machesky. 2005. “Inclusion of Scar/WAVE3 in a Similar Complex to Scar/WAVE1 and 2.” *BMC Cell Biology* 6: 11. doi:10.1186/1471-2121-6-11.

Stradal, T E B, and J Wehland. 2005. “Aktindynamik Und WASP / WAVE-Proteine.” *BIOspektrum* 11: 283–86.

Stradal, Theresia, Kevin D. Courtney, Klemens Rottner, Penelope Hahne, J. Victor Small, and Ann Marie Pendergast. 2001a. “The Abl Interactor Proteins Localize to Sites of Actin Polymerization at the Tips of Lamellipodia and Filopodia.” *Current Biology* 11 (11): 891–95.

———. 2001b. “The Abl Interactor Proteins Localize to Sites of Actin Polymerization at the Tips of Lamellipodia and Filopodia.” *Current Biology* 11 (11): 891–95. doi:10.1016/S0960-9822(01)00239-1.

Stradal, Theresia E., and Giorgio Scita. 2006. “Protein Complexes Regulating Arp2/3-Mediated Actin Assembly.” *Current Opinion in Cell Biology* 18 (1): 4–10. doi:10.1016/j.ceb.2005.12.003.

Stradal, Theresia EB, and Giorgio Scita. 2006. “Protein Complexes Regulating Arp2/3-Mediated Actin Assembly.” *Current Opinion in Cell Biology* 18 (1): 4–10. doi:10.1016/j.ceb.2005.12.003.

Stramer, Brian, Will Wood, Michael J. Galko, Michael J. Redd, Antonio Jacinto, Susan M. Parkhurst, and Paul Martin. 2005a. “Live Imaging of Wound Inflammation in Drosophila Embryos Reveals Key Roles for Small GTPases during in Vivo Cell Migration.” *Journal of Cell Biology* 168 (4): 567–73. doi:10.1083/jcb.200405120.

Stramer, Brian, Will Wood, Michael J Galko, Michael J Redd, Antonio Jacinto, Susan M Parkhurst, and Paul Martin. 2005b. “Live Imaging of Wound Inflammation in Drosophila Embryos Reveals Key Roles for Small GTPases during in Vivo Cell Migration.” *The Journal of Cell Biology* 168 (4): 567–73. doi:10.1083/jcb.200405120.

Suetsugu, Shiro, Daisuke Yamazaki, Shusaku Kurisu, and Tadaomi Takenawa. 2003. “Differential Roles of WAVE1 and WAVE2 in Dorsal and Peripheral Ruffle Formation for Fibroblast Cell Migration.” *Developmental Cell* 5 (4): 595–609. doi:10.1016/S1534-5807(03)00297-1.

Sung, Kyung Eun, Gui Su, Carolyn Pehlke, Steven M Trier, Kevin W Eliceiri, Patricia J Keely, Andreas Friedl, and David J Beebe. 2009. “Control of 3-Dimensional Collagen Matrix Polymerization for Reproducible Human Mammary Fibroblast Cell Culture in Microfluidic Devices.” *Biomaterials* 30 (27). Elsevier Ltd: 4833–41. doi:10.1016/j.biomaterials.2009.05.043.

Suraneni, Praveen, Boris Rubinstein, Jay R Unruh, Michael Durnin, Dorit Hanein, and Rong Li. 2012. “The Arp2/3 Complex Is Required for Lamellipodia Extension and Directional Fibroblast Cell Migration.” *The Journal of Cell Biology* 197 (2): 239–51. doi:10.1083/jcb.201112113.

Svitkina, Tatyana M., and Gary G. Borisy. 1999a. “Arp2/3 Complex and Actin Depolymerizing Factor/Cofilin in Dendritic Organization and Treadmilling of Actin Filament Array in Lamellipodia.” *Journal of Cell Biology* 145 (5): 1009–26. doi:10.1083/jcb.145.5.1009.

Svitkina, Tatyana M., Elena A. Bulanova, Oleg Y. Chaga, Danijela M. Vignjevic, Shin ichiro Kojima, Jury M. Vasiliev, and Gary G. Borisy. 2003. “Mechanism of Filopodia Initiation by Reorganization of a Dendritic Network.” *Journal of Cell Biology* 160 (3): 409–21. doi:10.1083/jcb.200210174.

Svitkina, Tatyana M, and Gary G Borisy. 1999b. “Progress in Protrusion: The Tell-Tale Scar.” *Trends in Biochemical Sciences* 24 (11): 432–36. doi:10.1016/S0968-0004(99)01461-9.

Takada, Yoshikazu, Xiaojing Ye, and Scott Simon. 2007. “The Integrins.” *Genome Biology* 8 (5): 215. doi:10.1186/gb-2007-8-5-215.

Takeda, Kosuke, Atsuo T. Sasaki, Hyunjung Ha, Hyun A. Seung, and Richard A. Firtel. 2007. “Role of Phosphatidylinositol 3-Kinases in Chemotaxis in Dictyostelium.” *Journal of Biological Chemistry* 282 (16): 11874–84. doi:10.1074/jbc.M610984200.

Takenawa, T, and H Miki. 2001. “WASP and WAVE Family Proteins: Key Molecules for Rapid Rearrangement of Cortical Actin Filaments and Cell Movement.” *Journal of Cell Science* 114 (Pt 10): 1801–9.

Takeya, Ryu, Kenichiro Taniguchi, Shuh Narumiya, and Hideki Sumimoto. 2008. “The Mammalian Formin FHOD1 Is Activated through Phosphorylation by ROCK and Mediates Thrombin-Induced Stress Fibre Formation in Endothelial Cells.” *The EMBO Journal* 27 (4): 618–28. doi:10.1038/emboj.2008.7.

Tani, Katsuko, Seiichi Sato, Taiko Sukezane, Hiroshi Kojima, Hidenori Hirose, Hidesaburo Hanafusa, and Tomoyuki Shishido. 2003. “Abl Interactor 1 Promotes Tyrosine 296 Phosphorylation of Mammalian Enabled (Mena) by c-ABL Kinase.” *Journal of Biological Chemistry* 278 (24): 21685–92. doi:10.1074/jbc.M301447200.

Temm-Grove, C J, B M Jockusch, M Rohde, K Niebuhr, T Chakraborty, and J Wehland. 1994. “Exploitation of Microfilament Proteins by Listeria Monocytogenes: Microvillus-like Composition of the Comet Tails and Vectorial Spreading in Polarized Epithelial Sheets.” *Journal of Cell Science* 107 (Pt 1: 2951–60.

Thompson, Morgan E, Ernest G Heimsath, Timothy J Gauvin, Henry N Higgs, and F Jon Kull. 2012a. “FMNL3 FH2–actin Structure Gives Insight into Formin-Mediated Actin Nucleation and Elongation.” *Nature Structural & Molecular Biology* 20 (1): 111–18. doi:10.1038/nsmb.2462.

———. 2012b. “FMNL3 FH2–actin Structure Gives Insight into Formin-Mediated Actin Nucleation and Elongation.” *Nature Structural & Molecular Biology* 20 (1): 111–18. doi:10.1038/nsmb.2462.

Thrasher, Adrian J, Siobhan Burns, Roberto Lorenzi, and Gareth E Jones. 2000. “The Wiskott-Aldrich Syndrome: Disordered Actin Dynamics in Haematopoietic Cells.” *Immunological Reviews* 178 (5): 118–28.

Tomasek, James J, Giulio Gabbiani, Boris Hinz, Christine Chaponnier, and Robert A Brown.

2002. “MYOFIBROBLASTS AND MECHANO- REGULATION OF CONNECTIVE TISSUE REMODELLING” 3 (May). doi:10.1038/nrm809.

Ulrich, Maria, and J Biochem. 1990. “Stoichiometric and Reversible Phosphorylation of a 46-KDa Protein in Human Platelets in Response to CGMP- and CAMP-Elevating Vasodilators *” 265 (6): 3088–93.

Vale, Ronald D. 2003. “The Molecular Motor Toolbox for Intracellular Transport.” *Cell*. doi:10.1016/S0092-8674(03)00111-9.

Van Goethem, Emeline, Romain Guiet, Stéphanie Balor, Guillaume M Charrière, Renaud Poincloux, Arnaud Labrousse, Isabelle Maridonneau-Parini, and Véronique Le Cabec. 2011. “Macrophage Podosomes Go 3D.” *European Journal of Cell Biology* 90 (2–3). Elsevier GmbH.: 224–36. doi:10.1016/j.ejcb.2010.07.011.

Van Goethem, Emeline, Renaud Poincloux, Fabienne Gauffre, Isabelle Maridonneau-Parini, and Véronique Le Cabec. 2010. “Matrix Architecture Dictates Three-Dimensional Migration Modes of Human Macrophages: Differential Involvement of Proteases and Podosome-like Structures.” *Journal of Immunology (Baltimore, Md. : 1950)* 184 (2): 1049–61. doi:10.4049/jimmunol.0902223.

Van Haastert, P. J M, Ineke Keizer-Gunnink, and Arjan Kortholt. 2007. “Essential Role of PI3-Kinase and Phospholipase A2 in Dictyostelium Discoideum Chemotaxis.” *Journal of Cell Biology* 177 (5): 809–16. doi:10.1083/jcb.200701134.

Vanhaesebroeck, B, and M D Waterfield. 1999. “Signaling by Distinct Classes of Phosphoinositide 3-Kinases.” *Experimental Cell Research* 253 (1): 239–54. doi:10.1006/excr.1999.4701.

Vidali, Luis, Feng Chen, Gregor Cicchetti, Yasutaka Ohta, and David J Kwiatkowski. 2006. “Rac1-Null Mouse Embryonic Fibroblasts Are Motile and Respond to Platelet-Derived Growth Factor □” 17 (May): 2377–90. doi:10.1091/mbc.E05.

Vignjevic, D. 2006. “Role of Fascin in Filopodial Protrusion.” *The Journal of Cell Biology* 174 (6): 863–75. doi:10.1083/jcb.200603013.

Vignjevic, Danijela, Shin-ichiro Kojima, Yvonne Aratyn, Oana Danciu, Tatyana Svitkina, and Gary G Borisy. 2006a. “Role of Fascin in Filopodial Protrusion.” *The Journal of Cell Biology* 174 (6): 863–75. doi:10.1083/jcb.200603013.

———. 2006b. “Role of Fascin in Filopodial Protrusion.” *The Journal of Cell Biology* 174 (6): 863–75. doi:10.1083/jcb.200603013.

Vignjevic, Danijela, Shin Ichiro Kojima, Yvonne Aratyn, Oana Danciu, Tatyana Svitkina, and Gary G. Borisy. 2006c. “Role of Fascin in Filopodial Protrusion.” *Journal of Cell Biology* 174 (6): 863–75. doi:10.1083/jcb.200603013.

Vignjevic, Danijela, Marie Schoumacher, Nancy Gavert, Klaus-Peter Janssen, Gloria Jih, Marick Laé, Daniel Louvard, Avri Ben-Ze’ev, and Sylvie Robine. 2007a. “Fascin, a Novel Target of Beta-Catenin-TCF Signaling, Is Expressed at the Invasive Front of Human Colon Cancer.” *Cancer Research* 67 (14): 6844–53. doi:10.1158/0008-5472.CAN-07-0929.

———. 2007b. “Fascin, a Novel Target of Beta-Catenin-TCF Signaling, Is Expressed at the Invasive Front of Human Colon Cancer.” *Cancer Research* 67 (14): 6844–53. doi:10.1158/0008-5472.CAN-07-0929.

Wade, Richard H., and Anthony A. Hyman. 1997. “Microtubule Structure and Dynamics.” *Current Opinion in Cell Biology*. doi:10.1016/S0955-0674(97)80146-9.

Walter, U, R Waldmann, and M Nieberding. 1988. “Intracellular Mechanism of Action of Vasodilators.” *European Heart Journal* 9 Suppl H: 1–6. doi:10.1093/eurheartj/9.suppl_H.1.

Wang, Fei, Paul Herzmark, Orion D. Weiner, Supriya Srinivasan, Guy Servant, and Henry R. Bourne. 2002. “Lipid Products of PI(3)Ks Maintain Persistent Cell Polarity and Directed Motility in Neutrophils.” *Nature Cell Biology* 4 (7): 513–18. doi:10.1038/ncb810.

Wang, Yu, and Mark A Mcniven. 2012. “Invasive Matrix Degradation at Focal Adhesions Occurs via Protease Recruitment by a FAK–p130Cas Complex” 196 (3). doi:10.1083/jcb.201105153.

Watanabe, N, T Kato, A Fujita, T Ishizaki, and S Narumiya. 1999. “Cooperation between MDia1 and ROCK in Rho-Induced Actin Reorganization.” *Nature Cell Biology* 1 (3): 136–43. doi:10.1038/11056.

Watanabe, Naoki, Pascal Madaule, Tim Reid, Toshimasa Ishizaki, Go Watanabe, Akira Kakizuka, Yuji Saito, Kazuwa Nakao, Brigitte M. Jockusch, and Shuh Narumiya. 1997. “P140mDia, a Mammalian Homolog of Drosophila Diaphanous, Is a Target Protein for Rho Small GTPase and Is a Ligand for Profilin.” *EMBO Journal* 16 (11): 3044–56. doi:10.1093/emboj/16.11.3044.

Weiner, Orion D., Maike C. Rentel, Alex Ott, Glenn E. Brown, Mark Jedrychowski, Michael B. Yaffe, Steven P. Gygi, Lewis C. Cantley, Henry R. Bourne, and Marc W. Kirschner. 2006. “Hem-1 Complexes Are Essential for Rac Activation, Actin Polymerization, and Myosin Regulation during Neutrophil Chemotaxis.” *PLoS Biology* 4 (2): 186–99. doi:10.1371/journal.pbio.0040038.

Weiner, Orion D, Paul O Neilsen, Glenn D Prestwich, Marc W Kirschner, Lewis C Cantley, and Henry R Bourne. 2002. “A PtdInsP(3)- and Rho GTPase-Mediated Positive Feedback Loop Regulates Neutrophil Polarity.” *Nature Cell Biology* 4 (7): 509–13. doi:10.1038/ncb811.

Welch, Heidi C E, W. John Coadwell, Christian D. Ellson, G. John Ferguson, Simon R. Andrews, Hediye Erdjument-Bromage, Paul Tempst, Phillip T. Hawkins, and Len R. Stephens. 2002. “P-Rex1, a PtdIns(3,4,5)P3- and g????-Regulated Guanine-Nucleotide Exchange Factor for Rac.” *Cell* 108 (6): 809–21. doi:10.1016/S0092-8674(02)00663-3.

Welch, M D, a Iwamatsu, and T J Mitchison. 1997. “Actin Polymerization Is Induced by Arp2/3 Protein Complex at the Surface of *Listeria Monocytogenes*.” *Nature*. doi:10.1038/385265a0.

Welch, M D, J Rosenblatt, J Skoble, D A Portnoy, and T J Mitchison. 1998a. “Interaction of Human Arp2/3 Complex and the Listeria Monocytogenes ActA Protein in Actin Filament Nucleation.” *Science* 281 (5373): 105–8. doi:10.1126/science.281.5373.105.

———. 1998b. “Interaction of Human Arp2/3 Complex and the Listeria Monocytogenes ActA Protein in Actin Filament Nucleation.” *Science* 281 (5373): 105–8.

doi:10.1126/science.281.5373.105.

Wennerberg, Krister, and Channing J Der. 2004a. “Rho-Family GTPases : It ’ s Not Only Rac and Rho (and I like It)” 1. doi:10.1242/jcs.01118.

———. 2004b. “Rho-Family GTPases: It’s Not Only Rac and Rho (and I like It).” *Journal of Cell Science* 117 (Pt 8): 1301–12. doi:10.1242/jcs.01118.

Werner, Erica. 2004. “GTPases and Reactive Oxygen Species: Switches for Killing and Signaling.” *Journal of Cell Science* 117 (2): 143–53. doi:10.1242/jcs.00937.

Witke, Walter, Wei Li, David J. Kwiatkowski, and Frederick S. Southwick. 2001. “Comparisons of CapG and Gelsolin-Null Macrophages: Demonstration of a Unique Role for CapG in Receptor-Mediated Ruffling, Phagocytosis, and Vesicle Rocketing.” *Journal of Cell Biology* 154 (4): 775–84. doi:10.1083/jcb.200101113.

Wolf, K. 2003. “Compensation Mechanism in Tumor Cell Migration: Mesenchymal-Amoeboid Transition after Blocking of Pericellular Proteolysis.” *The Journal of Cell Biology* 160 (2): 267–77. doi:10.1083/jcb.200209006.

Wolf, Katarina, Stephanie Alexander, Vivien Schacht, Lisa M Coussens, Ulrich H von Andrian, Jacco van Rheenen, Elena Deryugina, and Peter Friedl. 2009. “Collagen-Based Cell Migration Models in Vitro and in Vivo.” *Seminars in Cell & Developmental Biology* 20 (8): 931–41. doi:10.1016/j.semcdb.2009.08.005.

Wolf, Katarina, and Peter Friedl. 2009. “Mapping Proteolytic Cancer Cell-Extracellular Matrix Interfaces.” *Clinical and Experimental Metastasis* 26 (4): 289–98. doi:10.1007/s10585-008-9190-2.

Wolf, Katarina, Irina Mazo, Harry Leung, Katharina Engelke, Ulrich H von Andrian, Elena I Deryugina, Alex Y Strongin, Eva-B Bröcker, and Peter Friedl. 2003. “Compensation Mechanism in Tumor Cell Migration: Mesenchymal-Amoeboid Transition after Blocking of Pericellular Proteolysis.” *The Journal of Cell Biology* 160 (2): 267–77. doi:10.1083/jcb.200209006.

Wolf, Katarina, Yi I Wu, Yueying Liu, Jörg Geiger, Eric Tam, Christopher Overall, M Sharon Stack, and Peter Friedl. 2007. “Multi-Step Pericellular Proteolysis Controls the Transition from Individual to Collective Cancer Cell Invasion.” *Nature Cell Biology* 9 (8): 893–904. doi:10.1038/ncb1616.

Wu, Congying, Sreeja B Asokan, Matthew E Berginski, Elizabeth M Haynes, Norman E Sharpless, Jack D Griffith, Shawn M Gomez, and James E Bear. 2012. “Arp2 / 3 Is Critical for Lamellipodia and Response to Extracellular Matrix Cues but Is Dispensable for Chemotaxis.” *Cell* 148 (5). Elsevier Inc.: 973–87. doi:10.1016/j.cell.2011.12.034.

Wu, Dianqing. 2005. “Signaling Mechanisms for Regulation of Chemotaxis” 15 (1): 52–56.

Wyckoff, Jeffrey, Weigang Wang, Elaine Y Lin, Yarong Wang, Fiona Pixley, E Richard Stanley, Thomas Graf, Jeffrey W Pollard, Jeffrey Segall, and John Condeelis. 2004. “Wyckoff Condeelis 2004 A Paracrine Loop between Tumor Cells and Macrophages Is Required for Tumor Cell Migration in Mammary Tumors.,” 7022–29. doi:10.1158/0008-5472.CAN-04-1449.

Xu, Jingsong, Fei Wang, Alexandra Van Keymeulen, Paul Herzmark, Aaron Straight, Kathleen Kelly, Yoh Takuwa, Naotoshi Sugimoto, Timothy Mitchison, and Henry R. Bourne. 2003. "Divergent Signals and Cytoskeletal Assemblies Regulate Self-Organizing Polarity in Neutrophils." *Cell* 114 (2): 201–14. doi:10.1016/S0092-8674(03)00555-5.

Xu, Yingwu, James B. Moseley, Isabelle Sagot, Florence Poy, David Pellman, Bruce L. Goode, and Michael J. Eck. 2004. "Crystal Structures of a Formin Homology-2 Domain Reveal a Tethered Dimer Architecture." *Cell* 116 (5): 711–23. doi:10.1016/S0092-8674(04)00210-7.

Yae, Kojiro, Vincent W Keng, Masato Koike, Kosuke Yusa, Michiyoshi Kouno, Yoshihiro Uno, Gen Kondoh, et al. 2006. "Sleeping Beauty Transposon-Based Phenotypic Analysis of Mice: Lack of Arpc3 Results in Defective Trophoblast Outgrowth." *Molecular and Cellular Biology* 26 (16): 6185–96. doi:10.1128/MCB.00018-06.

Yamaguchi, Hideki, Mike Lorenz, Stephan Kempiak, Corina Sarmiento, Salvatore Coniglio, Marc Symons, Jeffrey Segall, et al. 2005. "Molecular Mechanisms of Invadopodium Formation: The Role of the N-WASP-Arp2/3 Complex Pathway and Cofilin." *The Journal of Cell Biology* 168 (3): 441–52. doi:10.1083/jcb.200407076.

Yamaguchi, Hideki, Fiona Pixley, and John Condeelis. 2006. "Invadopodia and Podosomes in Tumor Invasion." *European Journal of Cell Biology* 85 (3–4): 213–18. doi:10.1016/j.ejcb.2005.10.004.

Yamakita, Yoshihiko, Fumio Matsumura, Michael W Lipscomb, Po-chien Chou, Guy Werlen, Janis K Burkhardt, and Shigeko Yamashiro. 2011. "Fascin1 Promotes Cell Migration of Mature Dendritic Cells." *Journal of Immunology (Baltimore, Md. : 1950)* 186 (5): 2850–59. doi:10.4049/jimmunol.1001667.

Yamakita, Yoshihiko, Shoichiro Ono, Fumio Matsumura, and Shigeko Yamashiro. 1996. "Phosphorylation of Human Fascin Inhibits Its Actin Binding and Bundling Activities." *Journal of Biological Chemistry* 271 (21): 12632–38. doi:10.1074/jbc.271.21.12632.

Yamashiro-Matsumura, S., and F. Matsumura. 1986. "Intracellular Localization of the 55-KD Actin-Bundling Protein in Cultured Cells: Spatial Relationships with Actin, Alpha-Actinin, Tropomyosin, and Fimbrin." *Journal of Cell Biology* 103 (2): 631–40. doi:10.1083/jcb.103.2.631.

Yamashiro, S, Y Yamakita, S Ono, and F Matsumura. 1998. "Fascin, an Actin-Bundling Protein, Induces Membrane Protrusions and Increases Cell Motility of Epithelial Cells." *Molecular Biology of the Cell* 9 (5): 993–1006. doi:10.1091/mbc.9.5.993.

Yamazaki, D, S Kurisu, and T Takenawa. 2009a. "Involvement of Rac and Rho Signaling in Cancer Cell Motility in 3D Substrates." *Oncogene* 28 (13): 1570–83. doi:10.1038/onc.2009.2.

———. 2009b. "Involvement of Rac and Rho Signaling in Cancer Cell Motility in 3D Substrates." *Oncogene* 28 (13): 1570–83. doi:10.1038/onc.2009.2.

Yang, Changsong, Lubov Czech, Silke Gerboth, Shin Ichiro Kojima, Giorgio Scita, and Tatyana Svitkina. 2007. "Novel Roles of Formin MDia2 in Lamellipodia and Filopodia Formation in Motile Cells." *PLoS Biology* 5: 2624–45. doi:10.1371/journal.pbio.0050317.

Yang, Hyeong-Cheol, and Liza A Pon. 2002. “Actin Cable Dynamics in Budding Yeast.” *Proceedings of the National Academy of Sciences USA* 99 (2): 751–56. doi:10.1073/pnas.022462899.

Yang, Linda, Lei Wang, and Yi Zheng. 2006. “Gene Targeting of Cdc42 and Cdc42GAP Affirms the Critical Involvement of Cdc42 in Filopodia Induction , Directed Migration , and Proliferation in Primary Mouse Embryonic Fibroblasts □” 17 (November): 4675–85. doi:10.1091/mbc.E06.

Young, Kevin G., and John W. Copeland. 2010a. “Formins in Cell Signaling.” *Biochimica et Biophysica Acta - Molecular Cell Research* 1803 (2). Elsevier B.V.: 183–90. doi:10.1016/j.bbamcr.2008.09.017.

———. 2010b. “Formins in Cell Signaling.” *Biochimica et Biophysica Acta - Molecular Cell Research* 1803 (2). Elsevier B.V.: 183–90. doi:10.1016/j.bbamcr.2008.09.017.

Yu, Xinzi, and Laura M Machesky. 2012. “Cells Assemble Invadopodia-like Structures and Invade into Matrigel in a Matrix Metalloprotease Dependent Manner in the Circular Invasion Assay.” *PloS One* 7 (2): e30605. doi:10.1371/journal.pone.0030605.

Yu, Xinzi, Tobias Zech, Laura McDonald, Esther Garcia Gonzalez, Ang Li, Iain Macpherson, Juliane P Schwarz, et al. 2012. “N-WASP Coordinates the Delivery and F-Actin-Mediated Capture of MT1-MMP at Invasive Pseudopods.” *The Journal of Cell Biology* 199 (3): 527–44. doi:10.1083/jcb.201203025.

Zaki, Mehreen, Jason King, Klaus Fütterer, and Robert H Insall. 2007. “Replacement of the Essential Dictyostelium Arp2 Gene by Its Entamoeba Homologue Using Parasexual Genetics.” *BMC Genetics* 8: 28. doi:10.1186/1471-2156-8-28.

Zalcman, Gérard, Violaine Closson, Jacques Camonis, Nicole Honoré, M. F. Rousseau-Merck, Armand Tavitian, and Birgitta Olofsson. 1996. “RhoGDI-3 Is a New GDP Dissociation Inhibitor (GDI): Identification of a Non-Cytosolic GDI Protein Interacting with the Small GTP-Binding Proteins RhoB and RhoG.” *Journal of Biological Chemistry* 271 (48): 30366–74. doi:10.1074/jbc.271.48.30366.

Zhu, Q, C Watanabe, T Liu, D Hollenbaugh, R M Blaese, S B Kanner, a Aruffo, and H D Ochs. 1997. “Wiskott-Aldrich Syndrome/X-Linked Thrombocytopenia: WASP Gene Mutations, Protein Expression, and Phenotype.” *Blood* 90 (7): 2680–89.

Zicha, D., W. E. Allen, P. M. Brickell, C. Kinnon, G. A. Dunn, G. E. Jones, and A. J. Thrasher. 1998. “Chemotaxis of Macrophages Is Abolished in the Wiskott-Aldrich Syndrome.” *British Journal of Haematology* 101 (4): 659–65. doi:10.1046/j.1365-2141.1998.00767.x.

Zigmond, Sally H. 2004. “Formin-Induced Nucleation of Actin Filaments.” *Current Opinion in Cell Biology* 16 (1): 99–105. doi:10.1016/j.ceb.2003.10.019.

8 Acknowledgements / Danksagung

An dieser Stelle möchte ich mich bei all denjenigen bedanken, die mich während der Anfertigung meiner Doktorarbeit unterstützt haben.

Zuerst gebührt mein großer Dank meiner Mentorin Frau Prof. Dr Theresia Stradal, die meine Doktorarbeit betreut und begutachtet hat. Danke für die herzliche Aufnahme in deiner Arbeitsgruppe und dass du mir die Möglichkeit gegeben hast an diesem außerordentlich interessantem Projekt zu arbeiten. Die vielen Anregungen und Diskussionen bei der Erstellung dieser Arbeit waren sehr hilfreich für mich. Danke, dass du mir viel Freiheit und Selbständigkeit bei meiner Forschung ermöglicht hast und zugleich bei Problemen immer für mich da warst. Des Weiteren möchte ich mich bei Herrn Prof. Dr. Reinhard Köster für die Übernahme des Koreferates sowie bei Herrn Prof. Dr. Martin Korte für die Übernahme des Prüfungsvorsitzes herzlichst bedanken.

Dr. Stefan Arens und Dr. David de Gorter möchte ich fürs Korrekturlesen dieser Arbeit danken. Dr. Daniel Bambach danke ich für die hilfreichen Diskussionen und Tipps rund um die Promotion. Ebenfalls möchte ich mich bei meinen Kollegen aus der Zeit in Münster und in Braunschweig bedanken. Danke an David, Kai, Patrik Stefan und Nadja, die mir mit viel Geduld, Interesse und Hilfsbereitschaft aber auch für die netten Feierabende zur Seite standen. Weiterhin bedanke ich mich bei Annika, Brigitte, Giorgi, Frieda, Sonja und Vanessa am HZI für eine gute Atomsphäre im- und außerhalb des Labors und für eine sehr schöne Zeit in Braunschweig.

Ich möchte ganz besonders meiner Freundin Kati danken. Danke, dass du für mich da bist und an mich geglaubt hast. Deine aufmunternden Worte kamen genau dann, wenn ich es am meisten gebraucht habe. Danke für dein Lächeln;).

Abschließend möchte ich mich bei meinem Bruder für seine bedingungslose Unterstützung in dieser Zeit bedanken. Danke an meine Schwester, für gute Ratschläge und eine gesunde Portion Selbstironie.

Ich bedanke mich recht herzlich bei meinen Eltern, die maßgeblich dazu beigetragen haben mir das Studium in Deutschland zu ermöglichen.